LAPPEENRANTA
UNIVERSITY OF TECHNOLOGY

Jukka Karhula

CARDAN GEAR MECHANISM VERSUS SLIDER-CRANK MECHANISM IN PUMPS AND ENGINES

Thesis for the degree of Doctor of Science (Technology) to be presented with due permission for public examination and criticism in the Auditorium 1383 at Lappeenranta University of Technology, Lappeenranta, Finland on the 29th of February, 2008, at noon.

Acta Universitatis
Lappeenrantaensis
300

Supervisor

Professor Jukka Martikainen
Department of Mechanical Engineering
Faculty of Technology
Lappeenranta University of Technology
Finland

Reviewers

Professor Ettore Pennestrì
Dipartimento di Ingegneria Meccanica
Università di Roma Tor Vergata
Italy

Professor Rosario Sinatra
Dipartimento di Ingegneria Industriale e Meccanica
Facoltà di Ingegneria
Università decli studi di Catania
Italy

Opponents

Professor Ettore Pennestrì
Dipartimento di Ingegneria Meccanica
Università di Roma Tor Vergata
Italy

Dr.Sc. (Tech.) Mika Vartiainen
HAMK University of Applied Sciences
Riihimäki
Finland

ISBN 978-952-214-533-8
ISBN 978-952-214-534-5 (PDF)
ISSN 1456-4491

Lappeenrannan teknillinen yliopisto
Digipaino 2008

Abstract

Jukka Karhula

Cardan Gear Mechanism versus Slider-Crank Mechanism in Pumps and Engines

Lappeenranta 2008
227 p.

Acta Universitatis Lappeenrantaensis 300
Diss. Lappeenranta University of Technology
ISBN 978-952-214-533-8 ISBN 978-952-214-534-5 (PDF)
ISSN 1456-4491

In machine design we always want to save space, save energy and produce as much power as possible. We can often reduce accelerations, inertial loads and energy consumption by changing construction. In this study the old cardan gear mechanism (hypocycloid mechanism) has been compared with the conventional slider-crank mechanism in air pumps and four-stroke engines. Comprehensive Newtonian dynamics has been derived for the both mechanisms. First the slider-crank and the cardan gear machines have been studied as lossless systems. Then the friction losses have been added to the calculations. The calculation results show that the cardan gear machines can be more efficient than the slider-crank machines. The smooth running, low mass inertia, high pressures and small frictional power losses make the cardan gear machines clearly better than the slider-crank machines. The dynamic tooth loads of the original cardan gear construction do not rise very high when the tooth clearances are kept tight. On the other hand the half-size crank length causes high bearing forces in the cardan gear machines. The friction losses of the cardan gear machines are generally quite small. The mechanical efficiencies are much higher in the cardan gear machines than in the slider-crank machines in normal use. Crankshaft torques and power needs are smaller in the cardan gear air pumps than in the equal slider-crank air pumps. The mean crankshaft torque and the mean output power are higher in the cardan gear four-stroke engines than in the slider-crank four-stroke engines in normal use. The cardan gear mechanism is at its best, when we want to build a pump or an engine with a long connecting rod ($\approx 5\cdot$crank length) and a thin piston ($\approx 1.5\cdot$crank length) rotating at high angular velocity and intermittently high angular acceleration. The cardan gear machines can be designed also as slide constructions without gears. Suitable applications of the cardan gear machines are three-cylinder half-radial engines for motorcycles, six-cylinder radial engines for airplanes and six-cylinder double half-radial engines for sport cars. The applied equations of Newtonian dynamics, comparative calculations, calculation results (tables, curves and surface plots) and recommendations presented in this study hold novelty value and are unpublished before. They have been made and written by the author first time in this study.

Keywords: cardan gear mechanism, hypocycloid mechanism, mechanism analysis, mechanism design, pump design, engine design

UDC 621.825.63 : 621.827 : 51.001.57

Preface

This study has been carried out in the Department of Mechanical Engineering at Lappeenranta University of Technology in Finland.

First I thank my supervisor Professor Jukka Martikainen for his encouraging support.

I am also extremely grateful to my reviewers, Professor Ettore Pennestrì and Professor Rosario Sinatra for their valuable suggestions and encouraging attitude.

My deepest respect goes to the memories of Sir Isaac Newton, Professor Leonhard Euler, Monsieur Jean Le Rond d'Alembert, Professor Gaspard-Gustave de Coriolis, Professor Franz Reuleaux, Professor Ludwig Ernst Hans Burmester, Professor Ivan Ivanovich Artobolevsky, Monsieur Sadi Nicolas Léonard Carnot, Professor Rudolf Julius Emmanuel Clausius and their colleagues. Without their mighty life-works all the modern technology and also this minor study would not have been possible.

Finally I thank the Research Foundation of Lappeenranta University of Technology for the financial support.

Lappeenranta, January 2008

Jukka Karhula

Contents

Appendixes 129

List of abbreviations and symbols

General abbreviations and symbols

A	Crank pin
A_0	Main pin
B	Piston pin
BDC	Bottom dead center
b	Joint between the piston and the rod in the cardan gear construction
bmep	Brake mean effective pressure
C	Cardan gear construction (in the appendixes)
fmep	Friction mean effective pressure
S	Slider-crank construction (in the appendixes)
TDC	Top dead center
ZAA0	Crank length (in Mathcad calculations)
ZBA	Length of the connecting rod (in Mathcad calculations)
ωAA00	Initial angular velocity of the crankshaft (in Mathcad calculations)
αAA0	Initial angular acceleration of the crankshaft (in Mathcad calculations)
0	Frame
1	Crank
2	Connecting rod
3	Piston, piston assembly in the cardan gear machine

Main symbols and special symbols of the mathematical theory

A	Area
A	Contact area
a	Acceleration (absolute value)
$\overline{a}$	Acceleration vector
b	Face width of the gear
C_{fill}	Filling coefficient
C_{0b}	Static load rating of the pin bearing
Comp.ratio	Compression ratio
CR_c	Contact ratio
d	Diameter
d_{bm}	Pitch diameter of the pin bearing
d_{1c}	Pitch diameter of the cardan wheel
def_c	Tooth deformation of the gears
E	Modulus of elasticity
e_c	Backlash (gear clearance) at the pitch line of the gears

F	Force (absolute value)
F_{cont}	Contact force of the piston ring
F_{dync}	Dynamic load ofthe gear teeth
F_n	Normal load
F_{stb}	Static equivalent bearing load
F_t	Tangential load
$\bar{F}$	Force vector
$\bar{F}_\mu$	Total friction force
f_{ac}	Acceleration load of the gear teeth
f_0	Bearing lubrication factor
f_{1c}	Force required to accelerate the cardan wheel mass as a rigid body
f_{2c}	Force required to deform gear teeth amount of error (backlash)
H	Auxiliary coefficient
h	Height
h_{cha}	Minimum height of the cylinder chamber
h_{deck}	Deck height
h_f	Central EHD oil film thickness
$h_{pishead}$	Piston head height
I_{p1c}	Polar moment of inertia of the cardan wheel
i	Gear ratio
i	Imaginary unit
J	Mass moment of inertia
L_{i2}	Length from the crank pin to the center of percussion of the connecting rod in the slider-crank machine
$\bar{L}_{i2}$	Relative position vector of the center of percussion of the connecting rod regarding the crank pin in the slider-crank machine
L_{p2}	Length from the center of gravity to the center of percussion of the connecting rod in the slider-crank machine
$\bar{L}_{p2}$	Relative position vector of the center of percussion regarding the center of gravity of the connecting rod in the slider-crank machine
m	Mass
m_c	Gear module
m_{1redc}	Reduced mass of the cardan wheel
n	Rotational speed

P	Power
P_{μ}	Power loss
p	Pressure
p	Contact pressure
R_{eqc}	Equivalent contact radius
r_{g2}	Length from the crank pin to the center of gravity of the connecting rod in the slider-crank machine
$\bar{r}_{g2}$	Relative position vector of the center of gravity of the connecting rod in the slider-crank machine
r_{1c}	Radius of the cardan wheel pitch circle
r_{2c}	Radius of the ring gear pitch circle
Stroke	Stroke
T	Torque
T_{μ}	Torque loss
t	Time
V	Volume
v	Velocity (absolute value)
v_c	Pitch line velocity of the gears
v_r	Rolling velocity
v_s	Sliding velocity
$\bar{v}$	Velocity vector
W	Work
W_{μ}	Work loss
Z	Length of the position vector (absolute value)
$\bar{Z}$	Position vector
z_1	Number of teeth of the cardan wheel
z_2	Number of teeth of the ring gear

α	Angular acceleration (absolute value)
α	Pressure angle of the gears
β_{g2}	Angle of the acceleration of the center of gravity of the connecting rod in the slider-crank machine
γ_{pol}	Polytropic exponent
ε_{α}	Transverse contact ratio
η_{m}	Mechanical efficiency
η_{oil}	Lubrication oil dynamic (absolute) viscosity
θ	Angle of the position vector
μ	Friction coefficient
π	Straight angle in radians (= 180 °)
ρ_{oil}	Lubrication oil density
υ_{oil}	Lubrication oil kinematic viscosity
Σ	Total (summed results)
χ	Angle of the velocity vector
ψ	Angle of the acceleration vector
ω	Angular velocity (absolute value)

Subscript markings

The subscripts can include signs, marks, the source (former) and the receiver (latter). The source and the receiver can be joints, points or links.

Examples:

$\overline{Z}_{BAc}$ = Position vector of B regarding A in the cardan gear construction

$\overline{F}_{2i23}$ = Inertial joint force from the connecting rod to the piston caused by the mass inertia of the connecting rod in the slider-crank machine

$T_{\Sigma eng01c}$ = Total torque (counter torque) from the driven machine to the crankshaft of the cardan gear engine

$T_{\mu Lbc}$ = Load dependent torque loss of the pin bearing in the cardan gear machine

Subscripts of the mathematical theory

A	Crank pin
A_0, A0	Main pin
atm	Atmospheric
B	Piston pin
b	Bearing
b	Joint between the piston and the rod in the cardan gear construction
c	Cardan gear construction (not the first, but mostly the last subscript)
c	Coriolis acceleration (as the first subscript)
co	Compression and combustion (in the figures)
co	Compression ring
comb	Combustion
comp	Compression
crank	Crank pin bearing
cyl	Cylinder
eng	Engine
g	Center of gravity
i	Inertia (in kinetostatics)
ine	Inertia
L	Load dependent (in bearings)
main	Main pin bearing
max	Maximum
mean	Mean
min	Minimum
n	Normal acceleration
needpump	Need in pumps
oil	Oil ring
outeng	Output in engines
P	Whatever point at the center line of the connecting rod
pis	Piston
pol	Polytropic
pump	Pump
r	Radial
r	Rolling
ring	Piston ring
skirt	Piston skirt
stroke	Stroke
t	Tangential
unc	Uncompressed
V	Oil viscosity dependent (in bearings)
w	Windage
wheel	Cardan wheel
0	Initial value (in angles and angular velocities)
0	Frame
1	Crank
2	Connecting rod
3	Piston
3in	Into the piston (in the summed forces)
3out	Out from the piston (in the summed forces)
Σ	Total (summed result)

1. Introduction

1.1 Background of this study

Rotating speeds and accelerations of the modern machines are usually high. Before **Rudolf Diesel**'s (1858 - 1913) time (**Figure 1.1**) machines rotated slowly and mass inertia did not break structures. Is there any chance to reduce high accelerations and inertial forces? We can assume that in some cases it is possible. Which are the things that cause extra accelerations and unnecessary inertial forces? Of course they are high angular and tangential accelerations, radial velocities, radial accelerations, big masses and unbalanced running. Sir **Isaac Newton** stated in his second law of motion: "Mutationem motus proportionalem esse vi motrici impressae & fieri secundum lineam rectam qua vis illa imprimitur." [***Newton 1686***]. That is: "A change in motion is proportional to the motive force impressed and takes place along the straight line in which that force is impressed." [***Newton 1999***].
Masses can be reduced by choosing lighter materials. Motion becomes smoother by balancing or by changing construction. Angular and tangential accelerations are often difficult to reduce. Angular velocities and normal accelerations are impossible to eliminate in rotating machines. So, we must focus on radial velocities, radial accelerations and coriolis accelerations. We know also that the coriolis acceleration depends on the radial and angular velocity. Nothing can be done against the angular velocity, but we must try to eliminate the radial velocity and the radial acceleration. If we find a way, is it worthwhile?
What happens, if the conventional slider-crank machine is replaced with the cardan gear machine (hypocycloid machine)?

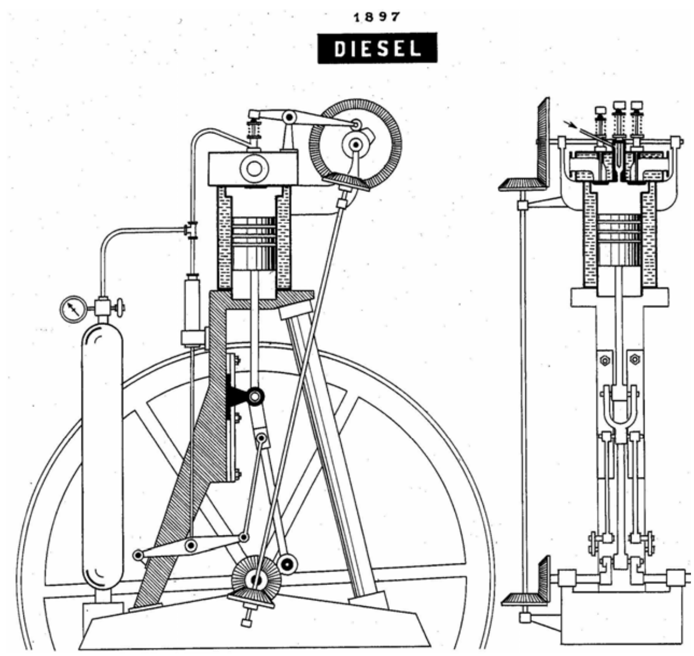

Figure 1.1. Rudolf Diesel's compression-ignition engine [*Kolin 1972*].

The slider-crank mechanism is the basic structure in the most combustion engines and air compressors. Its operating principle is well-known and reliable. The manufacturing processes have been developed workable and millions of slider-crank machines are produced all over the world every year. However the predicted fuel crisis, air pollution and the new visions of the future demand us to research new areas. The old cardan gear mechanism is one choice as the structure of the future pumps and engines. Dynamics of the slider-crank machine is well studied, but the cardan gear dynamics is not completely clarified. Especially the comparisons between the slider-crank machines and the cardan gear machines are incomplete. Everyone who knows the cardan gear construction perceives its running very smooth. The reciprocating motion of the cardan gear piston offers also new possibilities to construct pumps and engines. Piston positions and cylinder pressures, velocities and accelerations, inertial loads, thermodynamics, compression and combustion loads, total loads and mechanical efficiencies are interesting areas. Light components, eliminated piston pins, shortened piston skirts, half-size crank lengths, unlimited lengths of the connecting rods and internal gear pairs or slides of the connecting rods are the special properties of the cardan gear machines. If the cardan gear construction means higher pressures, lower accelerations, lower velocities, lower inertial loads, smaller frictions and higher mechanical efficiencies, it is worth of studying. Before making clarifying calculations we can guess that the short connecting rod will lead to high power outputs in the slider-crank engines because of the small mass inertia. The long connecting rod may lead to the higher mass inertia and that way to the smaller mechanical efficiency. The cardan gear machines may be more efficient than the slider-crank machines, but in which circumstances? Can the cardan gear machines save energy so much that they are worthwhile to design? Where do we need long rod machines, if the cardan gear construction favors them? This study tries to answer those questions.

1.2 This study and its results

Derivation of the comprehensive and universal Newtonian dynamics (kinematics, kinetostatics and kinetics) are made for the slider-crank mechanism and the cardan gear mechanism. These applied equations are derived from the basic equations of complex mathematics, Newtonian dynamics and thermodynamics. These applied universal equations have not been published in this form before and they are made by the author.
Comparative calculations are made for the slider-crank mechanism and the cardan gear mechanism applied to the air pumps and especially to the four-stroke engines. The calculations are made with a set of Mathcad programs based on the derived theory. This kind of Mathcad programs and comparative calculations have not been published before and they are made by the author.
The main results of this study are the calculation tables, charts and surface plots that show in which circumstances the cardan gear machines can be more efficient than the conventional slider-crank machines. This kind of results have not been published before and the results are drawn by the author.
Recommendations are given for the design of the new machine constructions using the cardan gear principle. The construction recommendations are also new, unpublished before and written by the author.
The final objective of the study is to find new possibilities to save fuel energy in the future. The cardan gear mechanism can be that kind of possibility.

2. State of the art

2.1 A brief history of mechanics towards the slider-crank and the cardan gear machines

Who knows, who originally invented the slider-crank mechanism and the cardan gear mechanism? Those mechanisms could have been built using the geometry of Elementa written by **Euclid of Alexandria** (325 - 265 BC) [***Commandini 1747, Heath 1956***]. Anyhow a special application of the hypocycloid mechanisms, the cardan gear mechanism, can be named according to the Italian mathematician **Girolamo Cardano** (1501 - 1576).
It is generally known that Girolamo Cardano and his father's famous colleague **Leonardo da Vinci** (1452 - 1519) studied that kind of mechanics in the 15th and 16th century [***Cardano 1570, MacCurdy 1945, Giuntini 2006***].
The English professor Sir **Isaac Newton** (1643 - 1727) stated his Three Laws of Motion in 1686 and after that we could calculate the basic kinetics [***Newton 1687***].
The Swiss mathematician **Leonhard Euler** (1707 - 1783) developed and published the basic theories and formulas of mathematics that we need to calculate machine dynamics [For example: ***Euler 1748***].
The French mathematician **Jean Le Rond d'Alembert** (1717 - 1783) developed his well known principle for mass inertia in 1758 [***D'Alembert 1968***].
The British steam engine manufacturer **Matthew Murray** (1765 - 1826) patented the hypocycloidal (cardan gear) steam engine in 1802 and the engine was manufactured for water pumping in 1805 (**Figure 2.1.1**) [***NAMES 2006***].
The French scientist Gaspard-Gustave de Coriolis (1792 - 1843) presented the earlier unknown coriolis acceleration and coriolis force in the treatise: ***Sur les Équations du Mouvement Relatif des Systèmes de Corps*** in 1835 [***O'Connor & Robertson 2006***].
Since then we have had the complete mathematical basis to calculate exact Newtonian dynamics of mechanisms and machines.
The German mechanical engineer and professor Franz Reuleaux (1829 - 1905) is treated as the originator of mechanism design. He presented the basis of the slider-crank and cardan gear mechanisms in 1875 (**Figure 2.1.2**) [***Reuleaux 1875***].
After that the slider-crank mechanism and its basic kinematics have been presented in the most books of the mechanism design. The cardan gear mechanism or its modifications have been presented by the German scientist **Ludwig Ernst Hans Burmester** (1840 - 1927) (**Figure 2.1.3**) [***Burmester 1888***], the Russian professor **Ivan Ivanovich Artobolevsky** (1905 - 1977) (**Figure 2.1.4**) [***Artobolevsky 1977***] and the German scientist **Rudolf Beyer** [***Beyer 1931***].
The German inventor **Nicolaus August Otto** (1832 - 1891) built the first slider-crank based four-stroke internal combustion engine in May 1876 [***Faires 1970***].
The German engineers **Gottlieb Daimler** (1834 - 1900) and **Wilhelm Maybach** (1846 - 1929) improved Otto's engine and patented their version of the four-stroke engine in 1885 [***Faires 1970***].
The English Sir **Charles Algernon Parsons** (1854 - 1931) developed a double cross-slider engine, Parsons epicyclic engine, originally called Parsons high-speed engine, and presented it in ***Engineering*** (journal) on the 1st of May 1885 [***Self 2005***].

Figure 2.1.1. Murray's hypocycloidal steam engine [*Clarke 2006*].

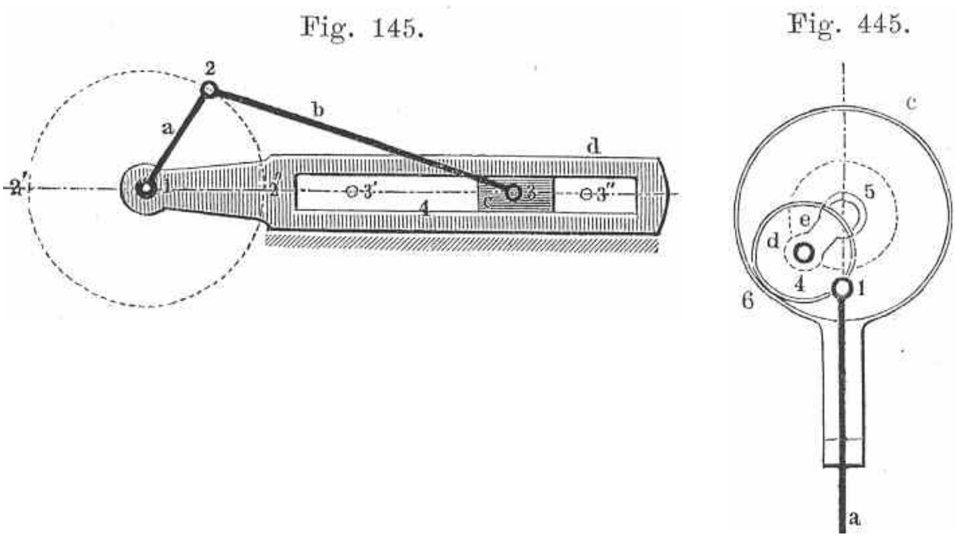

Figure 2.1.2. Reuleaux's slider-crank and cardan gear mechanisms [*Reuleaux 1875*].

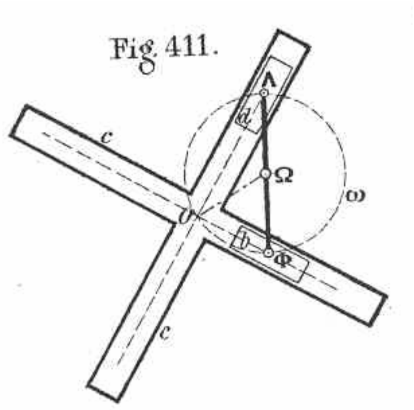

Figure 2.1.3. Burmester's elliptic trammel [*Burmester 1888*].

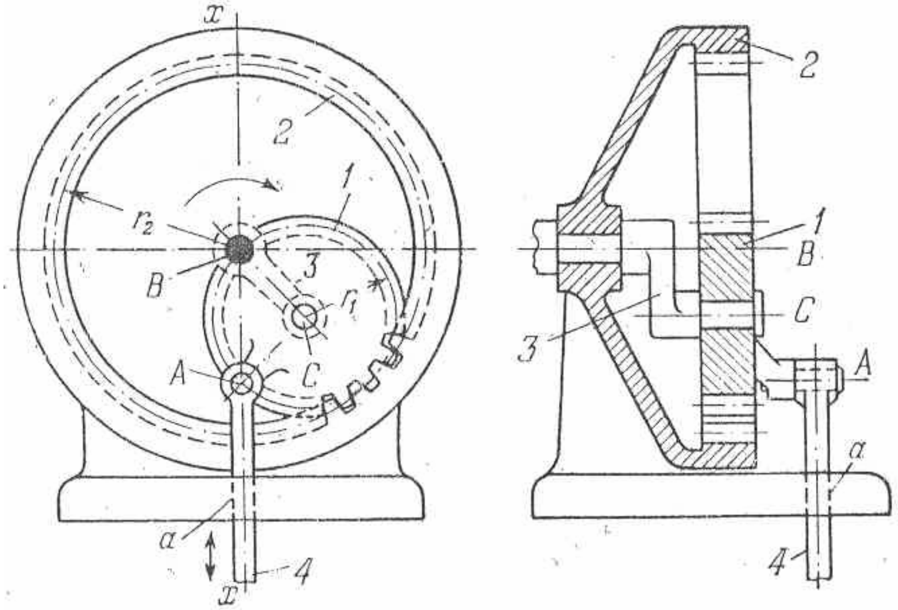

Figure 2.1.4. Artobolevsky's cardan gear mechanism [*Artobolevsky 1977*].

2.2 Cardan gear machines versus slider-crank machines

The slider-crank mechanism is the basic structure of the conventional combustion engines and pneumatic compressors.
The cardan gear mechanism has been used very rarely in any kind of machines.
It is based on the two cardan gears, an internal ring gear and a half-size planet gear. The diameter ratio between the ring gear and the planet gear is 2:1. During running each point of the planet gear reference diameter (pitch diameter) describes a straight line. The crank bearing (big end bearing) of the connecting rod can be centered on any point of the planet gear reference diameter and then the connecting rod reciprocates.
The closest cognate mechanisms of the cardan gear mechanism are the cross-slider elliptic trammel (**Figure 2.1.3**) and its modifications. Those cross-slider mechanisms are a part of the scotch-yoke mechanism family.
Kinematics, kinetostatics and kinetics of the cardan gear mechanism and the slider-crank mechanism differ a little bit from each other, but the both mechanisms can be analysed applying the basic theories of mechanism design [For example: ***Mabie & Reinholtz 1987, Erdman & Sandor 1997, Norton 1999, Weisstein 2006***].
When the slider-crank mechanism, the cardan gear mechanism or their cognate mechanisms have been used in engines or compressors, air pressures, volumes, temperatures, etc. can be calculated from the basic thermodynamics [For example: ***Faires 1970, Taylor 1985, Weisstein 2006***].
Some experimental engines and other prototypes have been built using the cardan gear mechanism and its modifications [For example: ***Smith, Churchill & Craven 1987, Badami & Andriano 1998, Rice & Egge 1998, Spitznogle & Shannon 2003***].
The cardan gear engine is one type of the straight-line engines and it has been studied because of its smoother running and to save fuel energy.
Other types of the straight-line engines are for example the above-mentioned historical Parsons epicyclic engine, Revetec's 1800SV (a controlled combustion engine manufactured by Revetec Ltd. in Australia) [***Sawyer 2003***], **Nigel Clark**'s (et al.) linear engine [***Clark et al. 1998***] in USA and almost forgotten **Matti Sampo**'s combination of the hydraulic pump and the linear engine in Finland.
Clark et al. mention also several patents of the linear engines in their essay.
When we are studying mechanism rotation, the cardan gear mechanism is a part of the hypocycloidal mechanisms. There are also epicycloidal rotary mechanisms.
Albert Shih has studied different kind of epicycloidal and hypocycloidal mechanisms that can be used as the main construction of the internal combustion engines [***Shih 1993***]. The pistons of Shih's engines have been fixed to the connecting bars and the pistons rotate between the inner and outer cylinder walls. The connecting bars drive the planetary gears that drive the flywheel. Those machines are quite complicated.

Peter Ewing has presented a very effective orbital engine, invented and patented by Australian **Ralph Sarich** in 1970's (**Figure 2.2.1**) [***Ewing 1982***]. The orbital engine is a very compact Wankel type radial engine. The size of the orbital engine is about 1/3 of the equivalent slider-crank engine. That means reduction in weight and fuel consumption. Test engines have been constructed and the basic properties have been measured. The results have been compared with the properties of the conventional slider-crank engines. The reduced size, weight, fuel consumption and emissions have been the main benefits of the well designed radial engine.

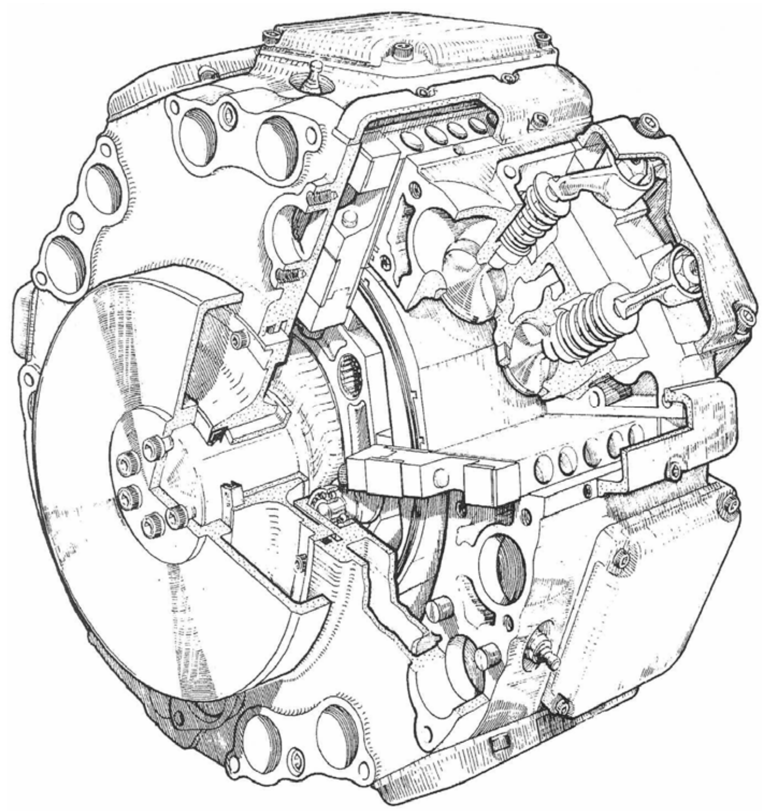

Figure 2.2.1. Ewing's and Sarich's orbital engine [*Ewing 1982*].

Straight-line mechanisms and many other rotating-reciprocating mechanisms have been applied commonly to the engine constructions but very rarely to the pump constructions. However some applications exist.
J. Peter Sadler and **D. E. Nelle** have studied an epicyclic rotary pump mechanism that is based on the Wankel type rotary piston [***Sadler & Nelle 1979***]. Trigonometric equations for the kinematics and kinetics of the pump construction have been presented and the pump has been constructed for the further studies.
Charles Wojcik has studied kinematics of an epicyclic gear pump that is based on the relative motion of the planet gears [***Wojcik 1979***]. Trigonometric equations have been presented for the geometry and kinematics of the pump construction and flow rates have been calculated.

Kenjiro Ishida has studied the fundamental principles of the cardan gear mechanism by naming it as the rotation-reciprocation mechanism [***Ishida 1974, report 1***]. Ishida has presented the theoretical equations of the inertial forces and the equivalent moment of inertia of the crankshaft. The fundamentals of the linear reciprocating motion and the perfect balancing have been the main subjects of the first study. The cardan gear mechanism and the conventional slider-crank mechanism have also been compared. Examples of the comparison curves of the displacements, velocities and accelerations of the sliders of the two mechanisms have been presented (**Figure 2.2.2**). Modifications of the eccentric geared, external geared and internal geared straight-line systems with eccentric gears and discs have been designed. Ishida declares that the internal geared system (cardan gear system) is a highly practical one among the other studied systems.

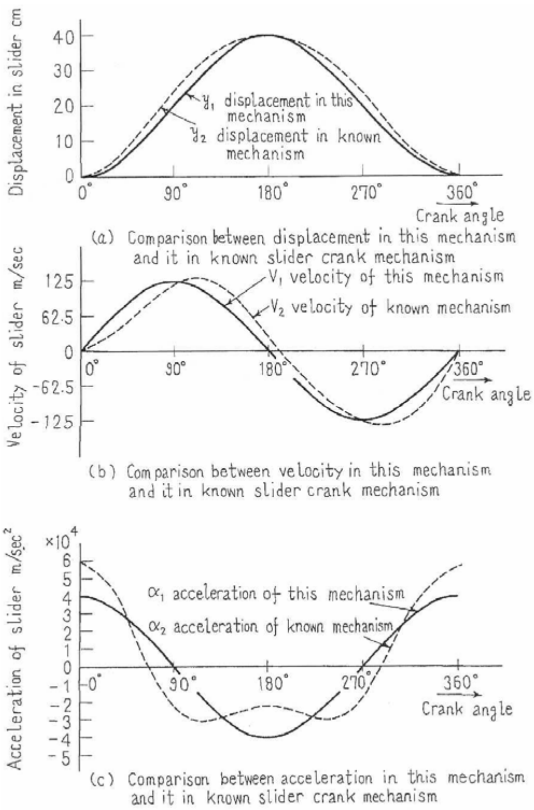

Figure 2.2.2. Ishida's comparison curves for the present mechanisms [*Ishida 1974, report 1*].

Kenjiro Ishida has continued his study with **Takashi Matsuda**, **Shigeyoshi Nagata** and **Yasuo Oshitani** [***Ishida et al. 1974, report 2***]. An epicycloidal eccentric testing device has been constructed and measured in this second study. The presented epicycloidal construction is more complicated than the hypocycloidal cardan gear construction or the conventional slider-crank construction. The epicycloidal testing device has the same properties as the cardan gear engine: linear reciprocating motion of the connecting rod, no side forces of the slider (piston), low maximum slider speed and unlimited rod length. The developers have neglected all frictions and clearances in their analysis. A part of the basic kinematics and the balancing equations have been presented. The vibrations of the testing device have been measured and the device has been perfectly balanced.
Kenjiro Ishida, Takashi Matsuda, **Shuzaburo Shinmura** and Yasuo Oshitani have continued the study and compared the hypocycloidal internal geared device (the cardan gear device) and the epicycloidal eccentric geared device [***Ishida et al. 1974, report 3***]. The developers state again that the hypocycloidal (cardan gear) construction is more practical and simpler than the epicycloidal construction. The rotating and reciprocating weights have been reduced and also some other improvements have been made in these new constructions. The joint forces and the crankshaft torque produced by the piston pressure force have been theoretically analysed for the both constructions. The derivation of the equations has been started in complex vector mode, but the final forms have been presented in trigonometric mode. The law of cosines has been used in many equations (**Figure 2.2.3**). That method requires the use of $\pm$ sign and the crank angle has to be divided in parts 0...π and π...2π.

Output / Item	Eccentric gear shaft	Reduction gear shaft
F_3	F_P	F_P
F_B	$F_3 l \sin\theta / R_2 \cos\alpha$	$F_3 l \sin\theta / R_2 \cos\alpha$
F_2	$\sqrt{F_3^2 + F_B^2 - 2F_3F_B\sin(\pm\alpha)}$	$\sqrt{F_3^2 + F_B^2 - 2F_3F_B\sin(\pm\alpha)}$
$\sin\eta$	$F_B\cos\alpha / F_2$	$F_B\cos\alpha / F_2$
F_D	$F_2 l \sin(\theta-\eta) / R_1\cos\alpha$	$F_2 l \sin(\theta-\eta) / R_1\cos\alpha$
F_C	F_D	$F_B\{l\cos(\theta\mp\alpha)+R_2\cos\alpha\}/R_1\cos\alpha$
$\sin\zeta$	$-1\ ,\ \zeta=-\pi/2$	$\{F_C\cos(\pm\alpha+\delta)-F_D\cos(\pm\alpha-\delta)\}/F_5$
F_5	$2F_C\cos(\pm\alpha-\delta)$	$\sqrt{F_C^2+F_D^2-2F_CF_D\cos 2\delta}$
F_1	$\sqrt{F_2^2+F_D^2-2F_2F_D\sin(\pm\alpha-\delta+\eta)}$	$\sqrt{F_2^2+F_D^2-2F_2F_D\sin(\pm\alpha-\delta+\eta)}$
$\sin\varepsilon$	$\{F_2\sin\eta-F_D\cos(\pm\alpha-\delta)\}/F_1$	$\{F_2\sin\eta-F_D\cos(\pm\alpha-\delta)\}/F_1$
F_4	$\sqrt{F_B^2+F_C^2+2F_BF_C\cos\delta}$	$\sqrt{F_B^2+F_C^2-2F_BF_C\cos(\pm2\alpha+\delta)}$
$\sin\varphi$	$\{F_B\cos\alpha+F_C\cos(\pm\alpha-\delta)\}/F_4$	$\{F_B\cos\alpha-F_C\cos(\pm\alpha+\delta)\}/F_4$
M	$2F_3 l \sin\theta$	$2F_3 l \sin\theta\cdot R_3/R_1$

Figure 2.2.3. Joint force equations of Ishida et al.
[*Ishida et al. 1974, report 3*].

Equations of the inertial joint forces and crankshaft torque have been taken from the first study. New testing devices have been constructed. The testing devices have been driven by an electric motor and the compression pressures have been measured. The crankshaft torque has been calculated from the pressures. The maximum pressure increases as the running speed increases. Friction losses have been estimated theoretically and then measured.

The developers state that the friction losses are almost the same in the linearly reciprocating machines and the conventional slider-crank machines in real use with heavy loads. The vibrations of the testing devices have also been measured.

Takashi Matsuda, Kenjiro Ishida, Yasuo Oshitani and **Motohiro Sato** have studied and compared the balancing of the rotation-reciprocation mechanism and the conventional slider-crank mechanism [***Ishida et al. 1974, report 4***]. The static balancing theory has been applied to the studied mechanisms. The friction losses have been approximated. Examples of the piston pressure forces and inertial loads for the different balancing types have been presented. The developers emphasize the significance to reduce the rotating weights and the reciprocating weights in order to decrease bearing loads (joint forces). The vibrations of the testing devices have been measured. Inertial forces of the connecting rod of the static balanced device have been detected very high. The inertial forces and moments have been balanced in the perfectly balanced device and the vibrations have been got reduced effectively.

Kenjiro Ishida, **Shun Kanetaka**, **Yoshiaki Omori** and Takashi Matsuda have continued the study by constructing a perfectly balanced vibrationless engine [***Ishida et al. 1977***]. It has been an eccentric geared epicycloidal two-cycle gasoline engine. The theory of kinetics of the engine has been presented. The mechanical power loss, the output torque and the vibrations of the engine have been measured. The calculated mechanical efficiency has been 62...68 %. The equivalent moment of inertia of the constructed engine has been about three times bigger than the equivalent moment of inertia of the conventional slider-crank engine. Also quite high tooth forces have affected on the gears.

Kenjiro Ishida and **Takeharu Yamada** have studied the hypocycloidal cardan gear mechanism applying it to the chain saw [***Ishida & Yamada 1986***]. The aim of the study has been to reduce severe vibrations that cause vasomotoric disturbances in the hands of the forestry workers. The perfect balancing of the engine has been presented in the theory and practice. A two-stroke test engine has been constructed. The theory of kinematics and kinetics has been presented in vector mode. Examples of the bearing loads and tooth forces have been presented. Vibrations of the front and rear handle have been measured from the cardan gear two-stroke chain saw and from the conventional two-stroke chain saw. The results have been presented. The vibration amplitudes and accelerations of the cardan gear chain saw have been smaller than the vibration amplitudes and accelerations of the slider-crank chain saw. Also the noises of the both chain saws have been measured and the results have been presented. The performance and fuel consumption have been measured with the running speed 3000...9000 r/min. The output torque and the brake power of the cardan gear chain saw have been smaller than the output torque and the brake power of the slider-crank chain saw. The fuel consumption has been vice versa. The developers state that the output power can be improved by raising the primary compression ratio.

Alfred Stiller and **James Smith** have patented and James Smith, **Robert Craven**, **Scott Butler**, **Robert Cutlip** and **Randolph Churchill** have studied and developed the double cross-slider based Stiller-Smith engine in 1984-1987 (**Figure 2.2.4**) [***Smith, Craven & Cutlip 1986, Craven, Smith & Butler 1987, Smith, Churchill & Craven 1987***].

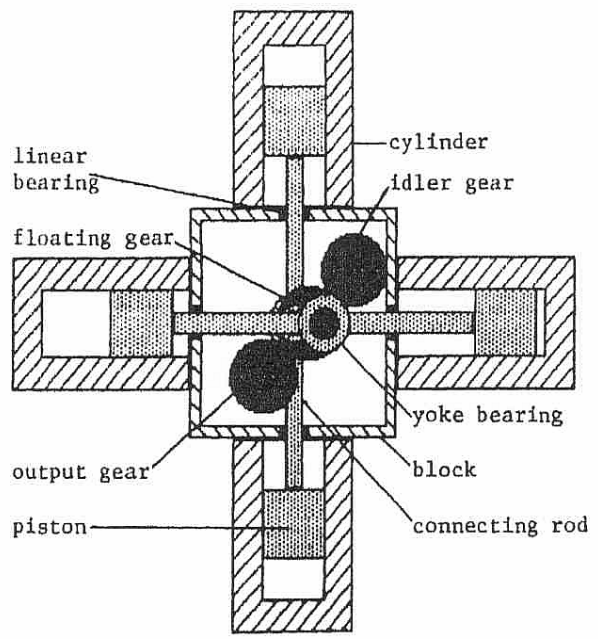

Figure 2.2.4. Stiller-Smith engine [*Craven, Smith & Butler 1987*].

The developers state that the connecting rod of the ordinary slider-crank mechanism vibrates remarkably. One possibility to reduce those vibrations and get a smoother motion is the double cross-slider Stiller-Smith engine. The developers have built a prototype of the engine and calculated its dynamics. The elliptical floating gears of the Stiller-Smith engine are difficult to manufacture and the developers have written an extra analysis of those gears. They have also balanced the engine. The ignition pressure and the combustion pressure are higher in the Stiller-Smith engine than in the slider-crank engine. The higher combustion pressure causes higher temperature and leads to the more efficient burning. The contact pressure on the cylinder walls is low because of the linear movement and linear bearings of the rods. Therefore it is possible to use brittle heat-resistant and wear-resistant materials on the sliding surfaces. The components of the cross-slider system are unique and they cannot be bought from the spare part service. The built prototype has been a two-stroke engine.

James Smith, Robert Craven and the new members, **Aubra McKisic** and **John Smith** have compared the properties of the Stiller-Smith engine and the slider-crank engine in 1990 [***Smith et al. 1990***]. The Stiller-Smith engine has less moving parts than the slider-crank engine. The journal bearings of the compared slider-crank engine were more severely loaded than those of the Stiller-Smith engine. On the other hand the linear bearings of the Stiller-Smith engine were more heavily loaded than the slider-crank piston skirts. Smith et al. mention also several patents of the scotch-yoke mechanism and its kinematic inversions applied to the internal combustion engines. One of them is the Bourke type engine, developed by **Russell Bourke** in the 1930s. The main mechanism of the Bourke type engine is the original scotch-yoke.
Smith et al. have compared an eight cylinder slider-crank diesel engine and an eight cylinder Stiller-Smith diesel engine, both with equal stroke, equal bore and equal displacement. The developers claim that any kind of Stiller-Smith engine is easily balanced and some 16 cylinder Stiller-Smith engines do not need counterweights at all. The slider-crank engine contains 42 % more bearing surfaces than the Stiller-Smith engine. The Stiller-Smith pistons have theoretically no lateral forces. In the slider-crank engine the lateral forces cause friction on the piston skirts in addition to the piston rings. The Stiller-Smith engine can have one to five output shafts. The developers have compared the bearing forces with effects of friction and with effects of the engine speed. The maximum loads of the journal bearings are bigger in the slider-crank engine than in the Stiller-Smith engine, but the maximum loads of the reciprocating bearings affect vice versa.
Shoichi Furuhama, **Masaaki Takiguchi** and **Dan Richardson** have found out that the cylinder friction of the slider-crank diesel engine is very significant [***Furuhama & Takiguchi 1979, Richardson 2000***]. Smith et al. assume that the cylinder friction is very low in the Stiller-Smith engine. The engine speed affects more to the bearing loads of the Stiller-Smith engine than to those of the slider-crank engine, but the Stiller-Smith engine produces less friction losses than the slider-crank engine.
Norman Beachley and **Martha Lenz** have presented a history and several modifications of the hypocycloid engine [***Beachley & Lenz 1988***]. For example the following facts of the hypocycloid (cardan gear) engine become clear in the report: The basic hypocycloid motion has been known at least in the middle ages. The hypocycloid construction works also without gears, but then the side loads of the pistons (or the connecting rods) become quite high. The principle of the hypocycloidal mechanism has been reinvented and patented by several inventors during the past decades. The constructions designed by **Richard Joseph Ifield** after 1930's look very best. Also the famous professor **Ferdinand Freudenstein** has studied the hypocycloidal cardanic motion. The hypocycloid engine can be perfectly balanced with any number of cylinders. The piston pin can be eliminated because of the straight-line motion. The straight-line motion eliminates also the side forces of the piston. The pistons and the rods can be manufactured very short and very light. If the skirt friction can be eliminated from the short pistons, even 6 % reduction in the fuel consumption is possible. The piston side friction increases dramatically with the running speed in the slider-crank engine because of the inertial forces of the connecting rod. Therefore the maximum output power of the hypocycloid engine may increase at a higher speed compared with the slider-crank engine. The hypocycloid engine may run uncooled as the adiabatic engine (in fact polytropic engine) without seizure. For example opposed piston engines, 90° V-engines and four-cylinder cross engines are easy to design using the hypocycloid mechanism.

The straight-line motion allows also double-acting pistons, combustion chambers on the both sides of the piston. In the different kind of engines the crank bearing can be very large ("big bearing engine") or regular ("built-up shaft engine"). If the hypocycloid engine is balanced, the gear tooth loads are independent of mass and speed being only a function of the combustion forces and friction forces. As a weakness the same gear tooth carries the maximum load in every cycle.
Martha Lenz has made a computer program in FORTRAN to calculate gear loads and bearing loads for different kinds of hypocycloid engines. Several engine types have been simulated. The authors have presented bearing load curves for the 1-cylinder 1 gear set four-stroke engine and peak load tables for the all simulated engine types. The authors claim that the countershaft is a necessary member in all "built-up shaft engines". The countershaft connects the both ends of the crankshaft and transmits torque forward to the driven machine. The crankshaft of the "big bearing engine" is strong enough to transmit torque through one end. The 1-cylinder "built-up shaft engine" has not been presented. The main weakness of the hypocycloid engine is the high tooth loads between the internal ring gear and the planet gear especially in diesel engines. The authors have tried to search the optimal gear pair to their constructions in order to reduce gear loads. A lot of patents dealing with the hypocycloid engines have also been listed in the report
David Ruch, **Frank Fronczak** and Norman Beachley have designed a modified hypocycloid engine and presented it in the beginning of 1990s (**Figure 2.2.5**) [***Ruch, Fronczak & Beachley 1991***]. The designed engine seems to be an improved cardan gear engine. The designers have named their engine as the sinusoidal engine because of the sinusoidal straight-line motion of the piston. The sinusoidal engine can be perfectly balanced and the piston friction and the piston slap are small. The designers state that the single cylinder slider-crank engine can not be perfectly balanced.

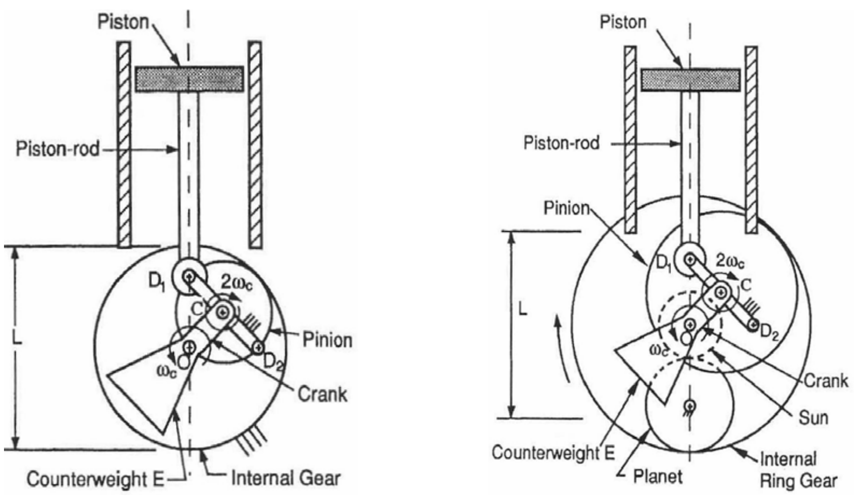

Figure 2.2.5. The ordinary hypocycloid (cardan gear) engine (left) and the modified hypocycloid engine (right) of Beachley et al. [*Ruch, Fronczak & Beachley 1991*].

However **Joseph Harkness** has presented satisfying balancer systems to prevent vibrations in the single cylinder engines [***Harkness 1968***].
Ruch et al. assume that the low vibration levels can reduce emissions and the uniform piston/cylinder clearance can reduce oil consumption of the sinusoidal engine. The piston of the sinusoidal engine stays longer in the combustion zone than the piston of the slider-crank engine. That means higher pressures, higher temperatures and possibly more efficient burning. Friction of the piston assembly can be approximately 40...50 % of the total friction in the slider-crank engine but significantly less in the sinusoidal engine. The piston rings cause 70...80 % and the piston skirt causes 20...30 % of the total piston friction in the slider-crank engine. The piston pin is required in the slider-crank engine but it can be eliminated in the sinusoidal engine. Piston slap can also be eliminated in the straight-line sinusoidal engine. The combustion chamber of the sinusoidal engine can be isolated from the crankcase and the upper and lower end of the engine can have separate lubrication systems. Then the lubrication oil contamination reduces. The developers have speculated a possibility to use gas lubrication or ceramic materials with no lubrication in the upper end of the engine. The developers have presented the cardan gear engine, named the basic hypocycloid engine, and its characteristics including balancing principles. Friction losses of the basic hypocycloid gear mesh have been very low. The connecting rod of the hypocycloid engine has no bending load. The size of the basic hypocycloid engine can be kept compact. The tooth loads of the basic hypocycloid gear mesh are very high especially in the supercharged engines. Therefore Ruch et al. have presented the above-mentioned modified hypocycloid engine. In the modified hypocycloid engine the internal ring gear rotates and it is driven by an extra planet gear. So the tooth loads and the crankshaft loads reduce significantly. The developers have presented also the equations for the primary forces and torques of the both engine types.
The developers have also built a prototype of the modified hypocycloid engine, a single cylinder, four-stroke, air-cooled, overhead cam, spark ignition engine. The prototype has been meant to be a testing machine for the further research. The prototype construction is very complicated. The developers have presented some patented design solutions for the assembly. The solutions look also quite complicated.
Marco Badami and **Matteo Andriano** have studied the cardan gear mechanism as the basic structure of a double acting compressor and a perfectly balanced two-stroke engine [***Badami & Andriano 1998***]. They have named the constructions as hypocycloid machines. The pistons of the machines have perfectly sinusoidal motion and therefore the second order inertial forces are completely zero. The machines can be perfectly balanced with any number of cylinders without additional countershafts. Badami and Andriano refer to the studies of Ruch et al. The piston spends more time in the combustion zone in the hypocycloid engine than in the slider-crank engine and that can lead to higher peak pressure and higher temperature. The straight-line motion of the connecting rod allows a remarkable reduction of the friction between the piston and the cylinder increasing mechanical efficiency. The piston rings can be simplified and then the hydrocarbon emissions can be reduced. The piston skirts can be almost eliminated in a compressor or in a four-stroke engine construction. On the other hand the geared hypocycloid machine is noisy, difficult to design and construct and highly stressed because of the short crank. The lower portion of the cylinder of the hypocycloid machine can be used as a second working chamber.

That feature requires an extra crosshead in the slider-crank engine and the cylinder friction exists high in that construction.
Applications of the two working chambers are a double acting reciprocating compressor, a two-stroke engine with the scavenging pump separated from the crankcase and a four-stroke engine with a built-in supercharger. Badami and Andriano have constructed and tested the above mentioned compressor and the two-stroke engine. The machines have been balanced. The bearing forces, the gear tooth loads and the crankshaft torque have been calculated. The construction of the compressor has been very light. The maximum operating speed has been 3000 r/min, the maximum pressure 9 bar and the displacement 170 cm^3.
The maximum loads have existed during the low angular velocity and high pressure. The planet pin load, the tangential gear tooth load, the crank pin load, the mass flow, the volumetric efficiency and the mechanical efficiency using different angular velocities and different compression ratios have been calculated from the test results. The volumetric efficiency of the single acting compressor has been 50...70 % and the double acting compressor 40...60 %. The mechanical efficiency of the single acting compressor has been approximately 80 % and the double acting compressor approximately 90 %. The frictional power and the inertial forces have been very low. The maximum operating speed of the constructed two-stroke engine has been 6000 r/min, the maximum cylinder pressure 70 bar, the displacement 121 cm^3 and the compression ratio 6.6. The designers claim that because of the scavenging pump separated from the crankcase it is possible to significantly reduce oil quantity in the fuel. The engine has been balanced completely. The weights of the piston, rod, crank pin and bearings have been reduced a lot compared with the slider-crank engine. The engine power, the brake mean effective pressure (bmep) and the specific fuel consumption have been measured using different angular velocities.
Bill Clemmons, **Jere Stahl** and **William Clemmens** have collected empirical knowledge of the car engines since 1960s and they have presented some facts of the rod lengths [***Clemmons & Stahl 2006, Clemmens 2006***]. First they have defined the short stroke as Rod/Stroke = 1.6 ... 1.8 and the long stroke as Rod/Stroke = 1.81 ... 2.00. The short rod is slower at the bottom dead center (BDC) range and faster at the top dead center (TDC) range. The long rod behaves vice versa. The piston of the long rod spends more time at the top. The short rod achieves the maximum torque position (90° angle between rod and crank) sooner than the long rod. The piston of the short rod is then a little bit higher than the piston of the long rod, relative to time. During the power stroke the long rod stresses the crank pin less at the crank angles 20...75 ° after TDC than the short rod. The piston of the long rod stays higher at the crank angles 90° before TDC ... 90° after TDC and thus the cylinder pressure can be higher. The short rod must be manufactured stronger and it requires also the stronger piston pin and the stronger crank pin than the long rod. The short rod causes bigger side loads to the piston than the long rod. The changing of the rod length affects also to the air flow through the engine. When tuning the engines optimally the shapes of the intake and the exhaust ports, the shapes of the cams, the time points of the valve openings and the time points of the ignition must be adjusted according to the rod length.

Charles Fayette Taylor has presented theories and measuring results of the mechanical frictions in the different kind of engines (**Figure 2.2.6**) [***Taylor 1985***].
The original cardan gear mechanism includes two gears, the little planet gear and the big internal ring gear.
A lot of studies have been made dealing with friction of the gear mesh [For example: ***Buckingham 1949, Martin 1978***].
Neil Anderson and **Stuart Loewenthal** have presented an analytical theory of the power loss of spur gears [***Anderson & Loewenthal 1981 and 1982***]
Ettore Pennestrì, **Pier Valentini** and **Giacomo Mantriota** have studied and presented extensively the theories of the mechanical efficiency of the epicyclic gear trains [***Pennestrì & Valentini 2003, Mantriota & Pennestrì 2003***].
In addition several studies by several researchers have been written in the dynamics of the slider-crank mechanisms.
For example **Wen-Jun Zhang** and **Q. Li** have studied the maximum velocities as the function of the crank angles in the slider-crank mechanisms [***Zhang & Li 2006***].

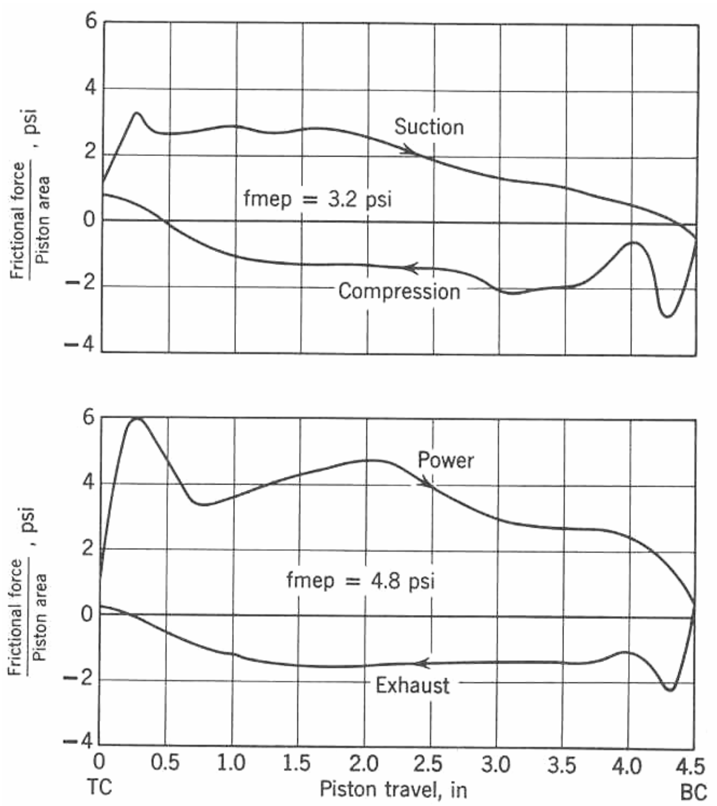

Figure 2.2.6. Piston friction diagrams of the slider-crank research engine, piston speed 4,6 m/s, oil temperature 82 °C, bmep = 0,6 MPa [*Taylor 1985*].

Some patents of the hypocycloid machines have been mentioned previously. Other interesting patents during the past decades are:

Edward Burke, 12 March 1889, U.S. patent no. 399,492
The motion principle of the hypocycloid machine (**Figure 2.2.7**).

John W. Pitts, 18 March 1913, U.S. patent no. 1,056,746
A cross-slider application of the hypocycloid machine.

John W. Pitts, 17 March 1914, U.S. patent no. 1,090,647
An internal combustion engine based on the hypocycloid mechanism.

Walter G. Collins, 30 March 1926, U.S. patent no. 1,579,083
An opposed cylinder hypocycloid machine.

Edwin E. Foster, 26 November 1940, U.S. patent no. 2,223,100
A radial engine based on the hypocycloid mechanism.

Harry A. Huebotter, 3 February 1942, U.S. patent no. 2,271,766
A hypocycloid engine including counterweights.

Myron E. Cherry, 12 February 1974, U.S. patent no. 3,791,227
A hypocycloid engine including special counterweights.

Nathaniel B. Kell, 27 June 1978, U.S. patent no. 4,096,763
A hypocycloidal reduction gearing.

Franz-Joseph, Roland and Helga Huf, 9 December 1980, U.S. patent no. 4,237,741
A special construction of the hypocycloid machine without gears.

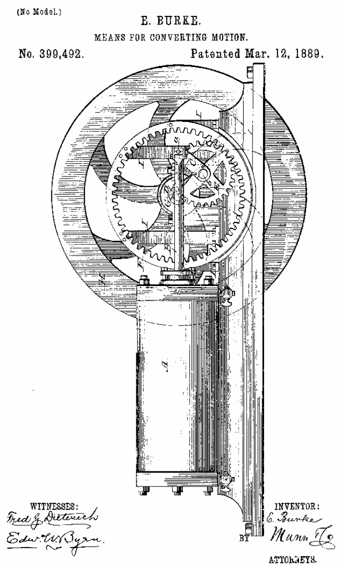

Figure 2.2.7. Burke's hypocycloid machine, U.S. patent no. 399,492.

2.3 Summary of the state of the art

The slider-crank mechanism and the cardan gear mechanism have been known at least in the 15th century, maybe much earlier.
The standard structure of the conventional combustion engines and pneumatic compressors is the slider-crank mechanism.
The cardan gear mechanism and its modifications are very rarely used.
The principle of the hypocycloidal mechanism (cardan gear mechanism) has been reinvented and patented by several inventors during the past decades.
The cardan gear engine runs smoother than the slider-crank engine.
Friction, balancing and vibrations of the slider-crank engine and the cardan gear engine have been widely studied.
The friction losses of the two machine types have been detected quite equal.
Piston friction is 40...50 % of the total friction in the slider-crank engine, but significantly less in the sinusoidal engine.
The piston rings cause 70...80 % and the piston skirt causes 20...30 % of the total piston friction in the slider-crank engine.
Kinematics of the two mechanisms has been studied, but not completely.
Ishida et al. have used the law of cosines and that kind of mathematics to solve the equations of the kinematics and kinetics of the studied mechanisms. The law of cosines do not give universal solutions without use of $\pm$ sign.
The cardan gear engine has been detected a very practical alternative to the conventional slider-crank engine.
Swinging of the slider-crank connecting rod causes high inertial joint forces.
Side forces of the slider-crank piston cause high friction loss.
Weights of the connecting rod and the piston of the cardan gear engine can be reduced a lot because of the very small side forces of the piston. Then the inertial loads reduce remarkably.
A two-stroke cardan gear chain saw has been built and tested.
The cardan gear chain saw has produced smaller output torque and output power than the conventional slider-crank chain saw, but the fuel consumption has been vice versa.
Tooth forces of the cardan gear machines have been detected high.
The hypocycloid construction works also without gears, but then the side forces of the pistons or the linear bearings of the connecting rod become quite high.
The hypocycloid engine can be perfectly balanced with any number of cylinders.
The piston pin can be eliminated because of the straight-line reciprocating motion.
Opposed piston engines are easy to design using the hypocycloid mechanism.
The straight-line motion allows double-acting pistons, where the combustion chambers can be located on the both sides of the piston.
The low vibration levels can reduce emissions and the uniform piston/cylinder clearance can reduce oil consumption of the hypocycloid engine.
The piston of the hypocycloid engine stays longer in the combustion zone than the piston of the slider-crank engine. That means higher pressures, higher temperatures and possibly more efficient burning.
In the slider-crank engines the long rod stresses the crank pin less at the crank angles 20...75 ° after TDC during the power stroke than the short rod.
The long rod allows the piston stay higher in the cylinder chamber at the crank angles 90° before TDC ... 90° after TDC and then the cylinder pressure can be higher.

3. Aim of the present study

Modern mechanical machines rotate often very fast. High speeds and high accelerations cause high inertial forces, high inertial torques and useless energy consumption. In some cases we can reduce accelerations and inertial effects. So we can design more effective and more economical machines. The main purpose of this study is to clarify one part of that area comparing the cardan gear mechanism (hypocycloid mechanism) and the conventional slider-crank mechanism, applying them to air pumps (compressors) and combustion engines **(Figure 3.1)**.

The main objectives of this study are to find out:

1. Can the old cardan gear mechanism be more efficient or more economical than the conventional slider-crank mechanism, applied to air pumps and four-stroke engines?

2. Can the inertial effects be smaller in the cardan gear machine than in the slider-crank machine?

3. Can it be worthwhile to change the conventional slider-crank construction to the cardan gear construction in the future pumps and engines?

The conventional slider-crank engine has been studied quite completely in the past decades, but what about the cardan gear mechanism from Girolamo Cardano's and Leonardo da Vinci's times? Are there any areas unknown?

The compared machines can be completely balanced and the moving components can have different weights, different frictions, different clearances and different vibrations. Those effects can compensate each other so much that the basic differences can not be distinguished. So the purposeful balancing, gravitation, clearances and vibrations are neglected in this study.

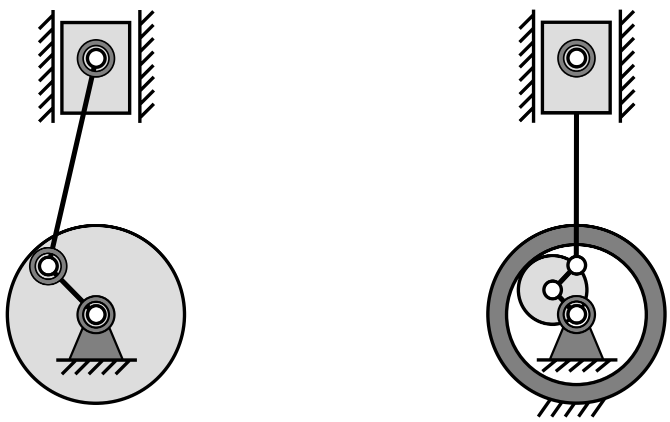

Figure 3.1. Slider-crank machine versus cardan gear machine.

4. Kinematics

The slider-crank mechanism, the cardan gear mechanism and their cognate mechanisms are typical plane mechanisms.
Therefore the Newtonian dynamics of this study has been presented in the vector mode on the complex plane (**Figure 4.1**) [***Mabie & Reinholtz 1987, Erdman & Sandor 1997, Norton 1999, Weisstein 2006***]. The necessary statics and thermodynamics have been added to the equations when the mechanisms have been applied to the pump and engine constructions.

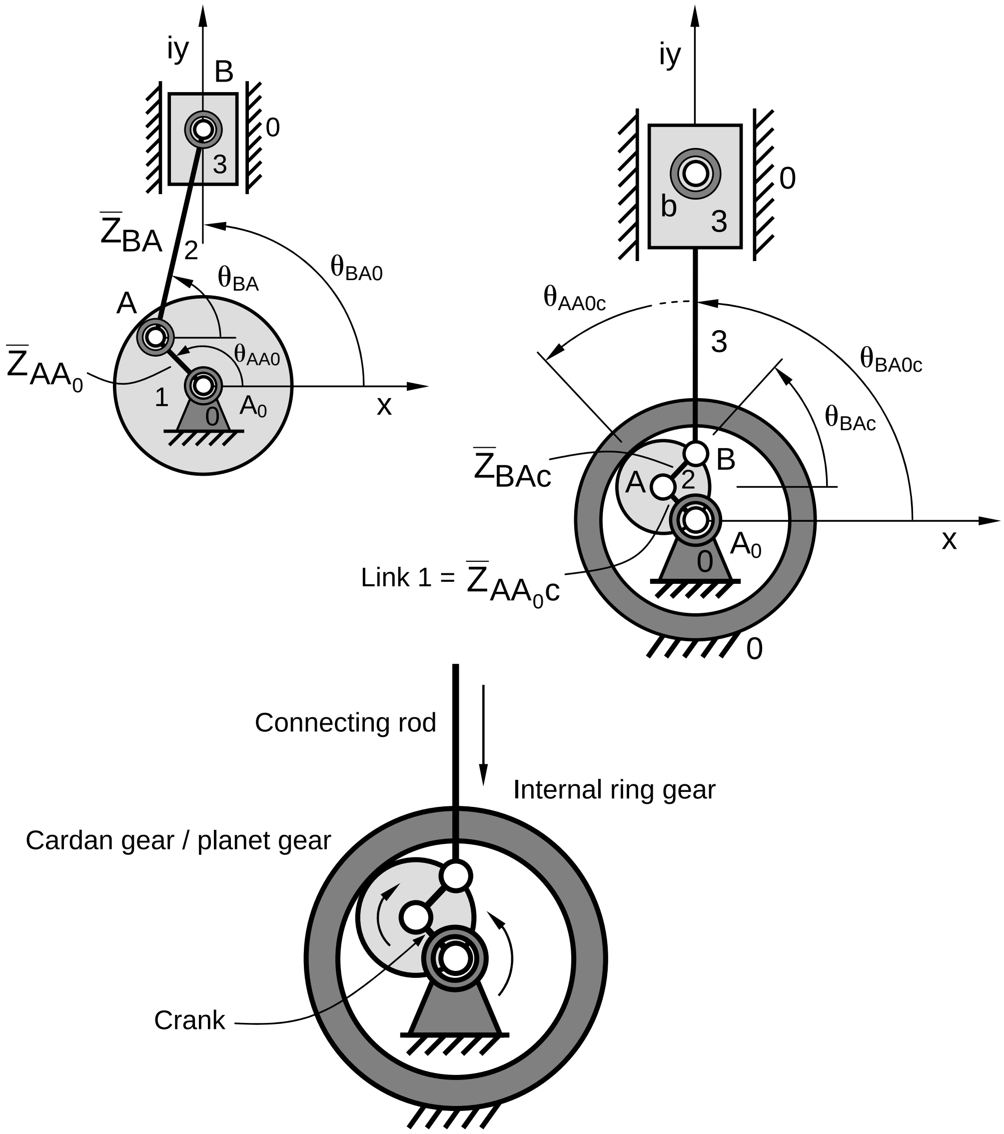

Figure 4.1. Basic symbols of the presented kinematics in the slider-crank mechanism (above left) and in the cardan gear mechanism (right and below).

4.1 Presentations of kinematics

Kinematics of the pin joints and other useful points have been presented and calculated as follows (**Equations 4.1.1 ... 4.1.3**):

Position vectors

$$\overline{Z} = Z \cdot e^{i \cdot \theta} \tag{4.1.1}$$

where Z = length
θ = angle (argument)

Velocity vectors

$$\overline{v} = \frac{d\overline{Z}}{dt} = v_r \cdot e^{i \cdot \theta} + Z \cdot i \cdot \omega \cdot e^{i \cdot \theta} \tag{4.1.2}$$

where ω = angular velocity (absolute value)
v_r = radial velocity (absolute value)

The first term is the radial velocity and the second term is the tangential velocity.

Acceleration vectors

$$\begin{aligned}\overline{a} &= \frac{d\overline{v}}{dt} = \frac{d^2\overline{Z}}{dt^2} \\ &= a_r \cdot e^{i \cdot \theta} + 2 \cdot v_r \cdot \omega \cdot i \cdot e^{i \cdot \theta} + Z \cdot \alpha \cdot i \cdot e^{i \cdot \theta} - Z \cdot \omega^2 \cdot e^{i \cdot \theta}\end{aligned} \tag{4.1.3}$$

where a_r = radial acceleration (absolute value)
α = angular acceleration (absolute value)

The first term is the radial acceleration, the second term is the coriolis acceleration, the third term is the tangential acceleration and the fourth term is the normal acceleration.

Angles, angular velocities and angular accelerations

The studied mechanisms have been treated as plane mechanisms and the angles θ, the angular velocities ω and the angular accelerations α have been treated mathematically as scalars.
In this study the slider-crank machines and the cardan gear machines have been compared during one running cycle, 4π rad. The studied cycles have different properties, different initial values. The cycles start from the crank angle $\theta_{AA0} = \pi/2$ rad (= 90 °) and finish to the crank angle $\theta_{AA0} = 9\pi/2$ rad (= 810 °).

4.2 Comparison of kinematics

The cylinder locates on the iy-axis and the angular acceleration α_A has been assumed constant. The variables have been marked as follows:
The first capital subscript means the point under discussion regarding the second capital subscript as the origin. Zero as the third subscript means the basic initial value.
The slider-crank mechanism and its motion principle are well-known. The cardan gear mechanism appears in the most figures of this study and its operating principle has been presented in the **Appendix 4.2.1**.
The kinematic equations of the studied mechanisms used in the calculations have been presented in the **Appendix 4.2.2**. The final equations of the most significant variables have been presented also in this chapter (**Figures 4.2.1 ... 4.2.2**) (**Equations 4.2.1 ... 4.2.12**).

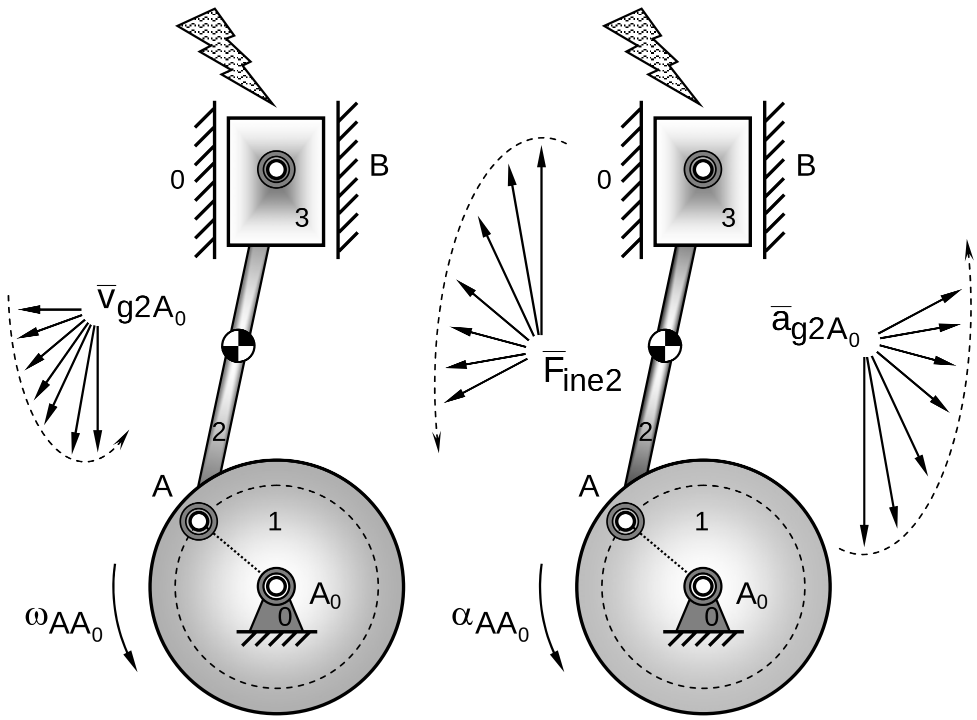

Figure 4.2.1. Kinematical behavior of the slider-crank connecting rod.

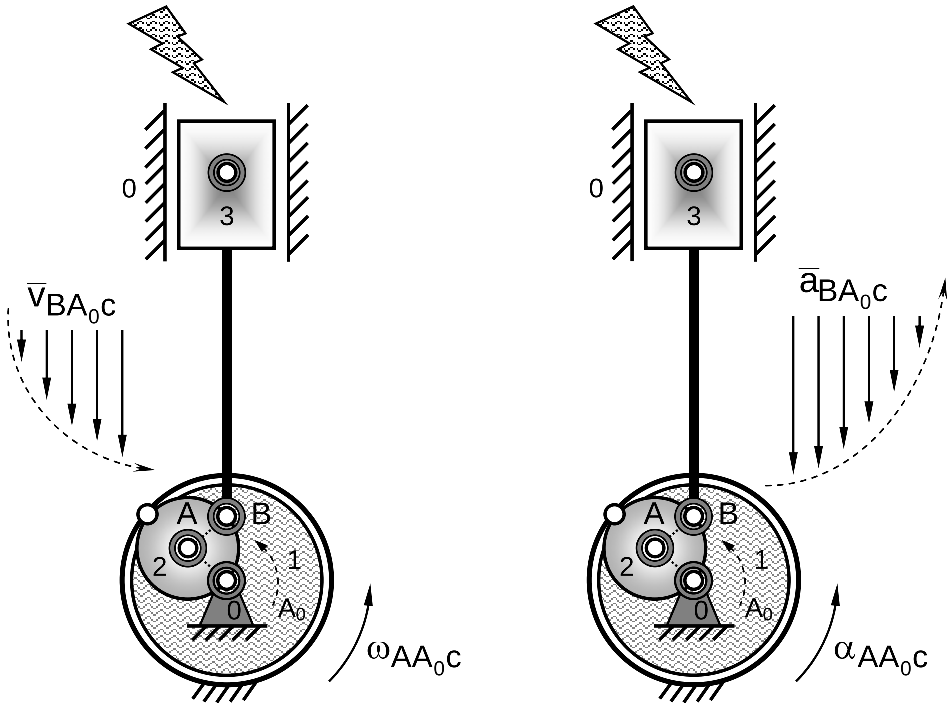

Figure 4.2.2. Kinematical behavior of the cardan gear connecting rod.

The main kinematics of the slider-crank mechanism versus the cardan gear mechanism

Piston positions of the mechanisms

$$\bar{Z}_{BA_0} = Z_{AA_0} \cdot e^{i \cdot \theta_{AA0}} + Z_{BA} \cdot e^{i \cdot \theta_{BA}} = Z_{BA_0} \cdot e^{i \cdot 90^\circ} \tag{4.2.1}$$

$$\begin{aligned} \bar{Z}_{bA_0c} &= 2 \cdot Z_{AA_0c} \cdot \sin(\theta_{AA_0c}) \cdot e^{i \cdot 90^\circ} + Z_{bBc} \cdot e^{i \cdot 90^\circ} \\ &= Z_{bA_0c} \cdot e^{i \cdot 90^\circ} \end{aligned} \tag{4.2.2}$$

Piston velocities of the mechanisms

$$\begin{aligned} \bar{v}_{BA_0} &= Z_{AA_0} \cdot i \cdot \omega_{AA_0} \cdot e^{i \cdot \theta_{AA0}} + Z_{BA} \cdot i \cdot \omega_{BA} \cdot e^{i \cdot \theta_{BA}} \\ &= \pm v_{BA0} \cdot e^{i \cdot 90^\circ} \end{aligned} \tag{4.2.3}$$

$$\begin{aligned} \bar{v}_{BA_0c} &= 2 \cdot Z_{AA_0c} \cdot \omega_{AA_0c} \cdot \cos(\theta_{AA_0c}) \cdot e^{i \cdot 90^\circ} \\ &= \pm v_{BA_0c} \cdot e^{i \cdot 90^\circ} = \bar{v}_{rBA_0c} \end{aligned} \tag{4.2.4}$$

Connecting rod velocities of the mechanisms

See the **Figures 4.2.1. and 4.2.2**.

$$\begin{aligned} \bar{v}_{PA_0} &= Z_{AA_0} \cdot i \cdot \omega_{AA_0} \cdot e^{i \cdot \theta_{AA0}} + Z_{PA} \cdot i \cdot \omega_{BA} \cdot e^{i \cdot \theta_{BA}} \\ &= v_{PA_0} \cdot e^{i \cdot \chi_{PA0}} = \bar{v}_{g2A_0} \end{aligned} \tag{4.2.5}$$

$$\bar{v}_{PA_0c} = \bar{v}_{BA_0c} \tag{4.2.6}$$

In the cardan gear mechanism the connecting rod velocity is equal to the piston velocity.

Connecting rod angular velocity of the slider-crank mechanism

$$\omega_{PA_0} = \frac{v_{tPA_0}}{Z_{PA_0}} = \frac{\bar{v}_{PA_0} - \bar{v}_{rPA_0}}{Z_{PA_0} \cdot e^{i \cdot (\theta_{PA0} + 90^\circ)}} \tag{4.2.7}$$

Piston accelerations of the mechanisms

$$\bar{a}_{BA_0} = Z_{AA_0} \cdot (i \cdot \alpha_{AA_0} - \omega_{AA_0}{}^2) \cdot e^{i \cdot \theta_{AA0}} + \\ + Z_{BA} \cdot (i \cdot \alpha_{BA} - \omega_{BA}{}^2) \cdot e^{i \cdot \theta_{BA}} \\ = \pm a_{BA_0} \cdot e^{i \cdot 90^\circ} \tag{4.2.8}$$

$$\bar{a}_{BA_0c} = 2 \cdot Z_{AA_0c} \cdot \\ \cdot \left(\alpha_{AA_0c} \cdot \cos(\theta_{AA_0c}) - \omega_{AA_0c}{}^2 \cdot \sin(\theta_{AA_0c})\right) \cdot e^{i \cdot 90^\circ} \\ = \pm a_{BA_0c} \cdot e^{i \cdot 90^\circ} = \bar{a}_{rBA_0c} \tag{4.2.9}$$

Connecting rod accelerations of the mechanisms

See the **Figures 4.2.1 and 4.2.2**.

$$\bar{a}_{PA_0} = Z_{AA_0} \cdot (i \cdot \alpha_{AA_0} - \omega_{AA_0}{}^2) \cdot e^{i \cdot \theta_{AA0}} + \\ + Z_{PA} \cdot (i \cdot \alpha_{BA} - \omega_{BA}{}^2) \cdot e^{i \cdot \theta_{BA}} \\ = a_{PA_0} \cdot e^{i \cdot \psi_{PA0}} = \bar{a}_{g2A_0} \tag{4.2.10}$$

$$\bar{a}_{PA_0c} = \bar{a}_{BA_0c} \tag{4.2.11}$$

In the cardan gear mechanism the connecting rod acceleration is equal to the piston acceleration.

Connecting rod angular acceleration of the slider-crank mechanism

$$\alpha_{PA_0} = \frac{a_{tPA_0}}{Z_{PA_0}} = \frac{\bar{a}_{PA_0} - \bar{a}_{rPA_0} - \bar{a}_{cPA_0} - \bar{a}_{nPA_0}}{Z_{PA_0} \cdot e^{i \cdot (\theta_{PA0} + 90^\circ)}} \tag{4.2.12}$$

5. Kinetostatics

Statics of the mechanisms including kinetostatics have been presented and calculated using the conventional theories [***Beer & Johnston 1997, Hibbeler 2004***].

5.1 Inertial loads

Inertial forces and inertial torques have been presented and calculated as follows (**Equations 5.1.1 ... 5.1.2**):

Inertial force

$$\overline{F}_{ine} = -m \cdot \overline{a} \tag{5.1.1}$$

where m = mass
$\overline{a}$ = acceleration

Inertial torque

$$T_{ine} = -J \cdot \alpha \tag{5.1.2}$$

where J = mass moment of inertia
α = angular acceleration

5.2 Comparison of kinetostatics

The kinetostatic equations of the studied mechanisms used in the calculations have been presented in the **Appendix 5.2.1**. The final equations of the most significant variables have been presented also in this chapter (**Figures 5.2.1 ... 5.2.6**) (**Equations 5.2.1 ... 5.2.12**).

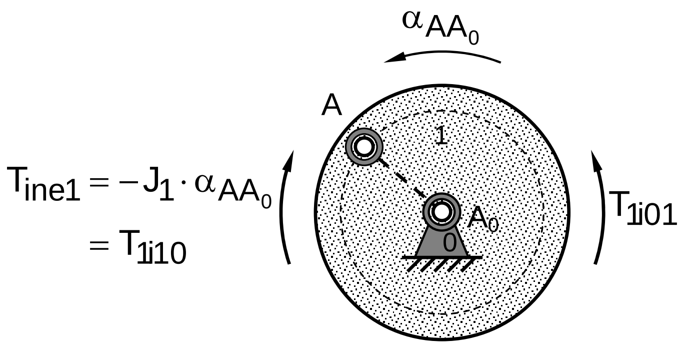

Figure 5.2.1. Kinetostatics of the slider-crank crankshaft.

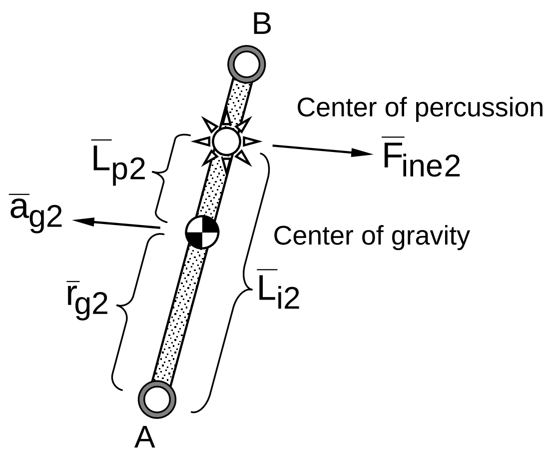

Figure 5.2.2. Center of percussion of the slider-crank connecting rod.

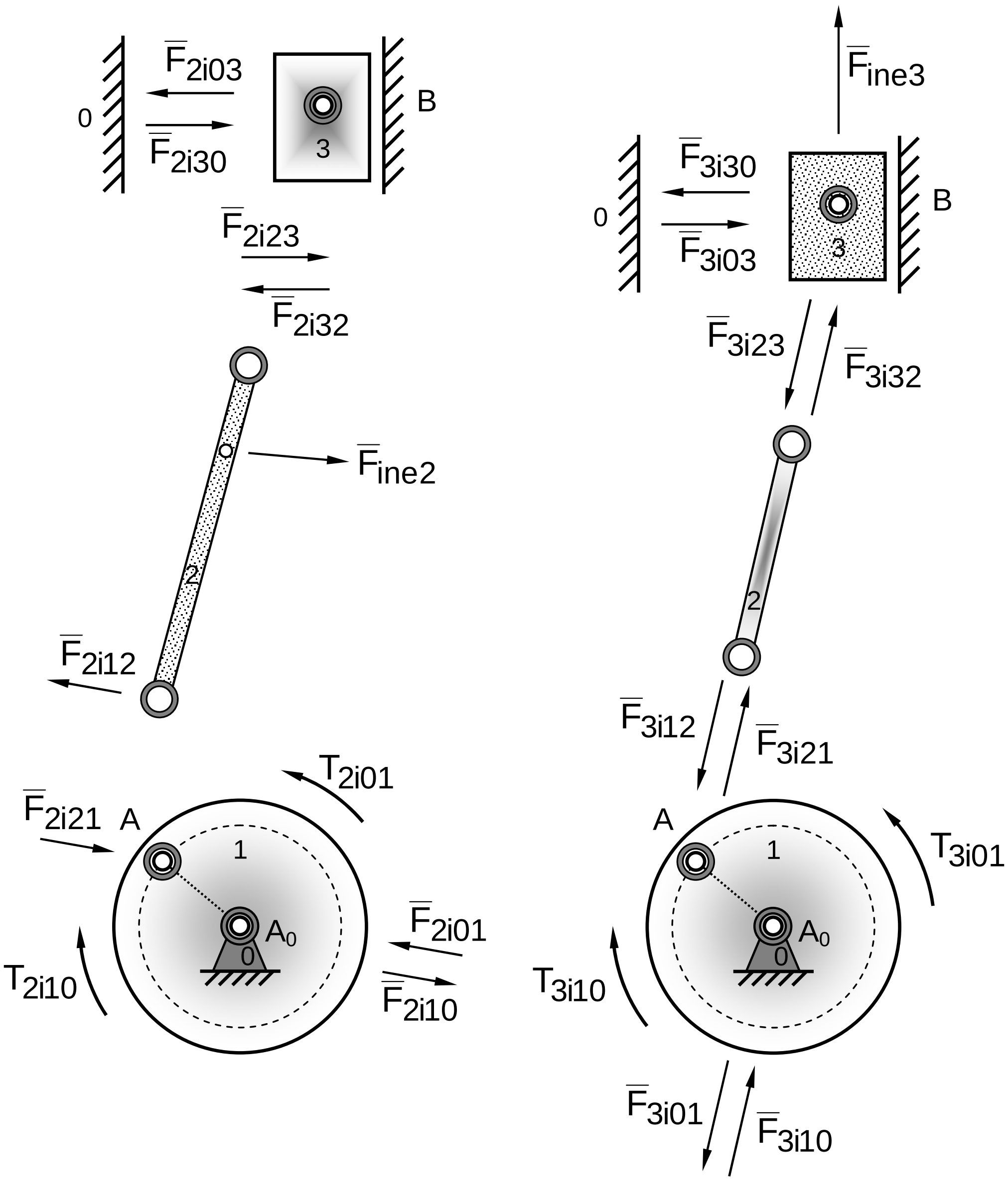

Figure 5.2.3. Kinetostatics of the slider-crank connecting rod and piston.

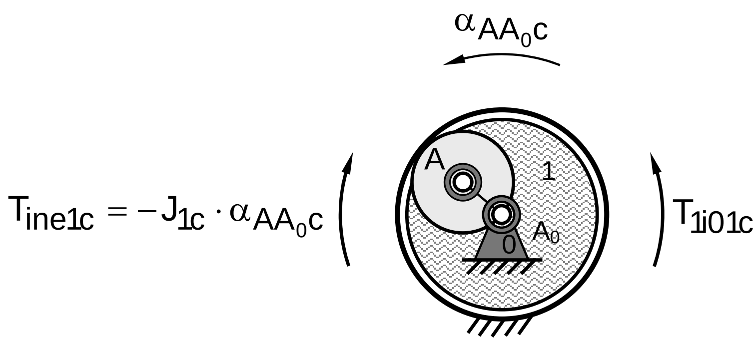

Figure 5.2.4. Kinetostatics of the cardan gear crankshaft.

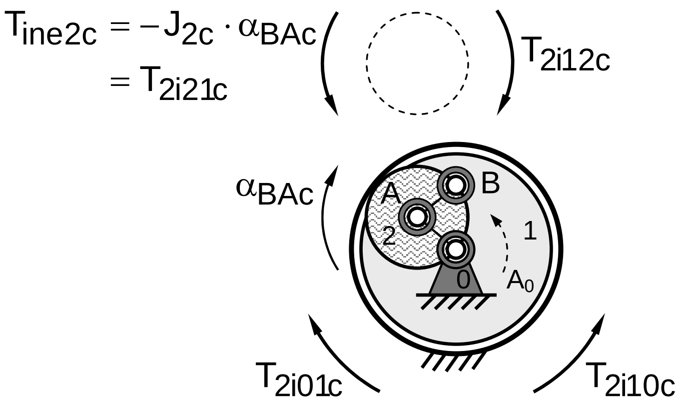

Figure 5.2.5. Kinetostatics of the cardan wheel.

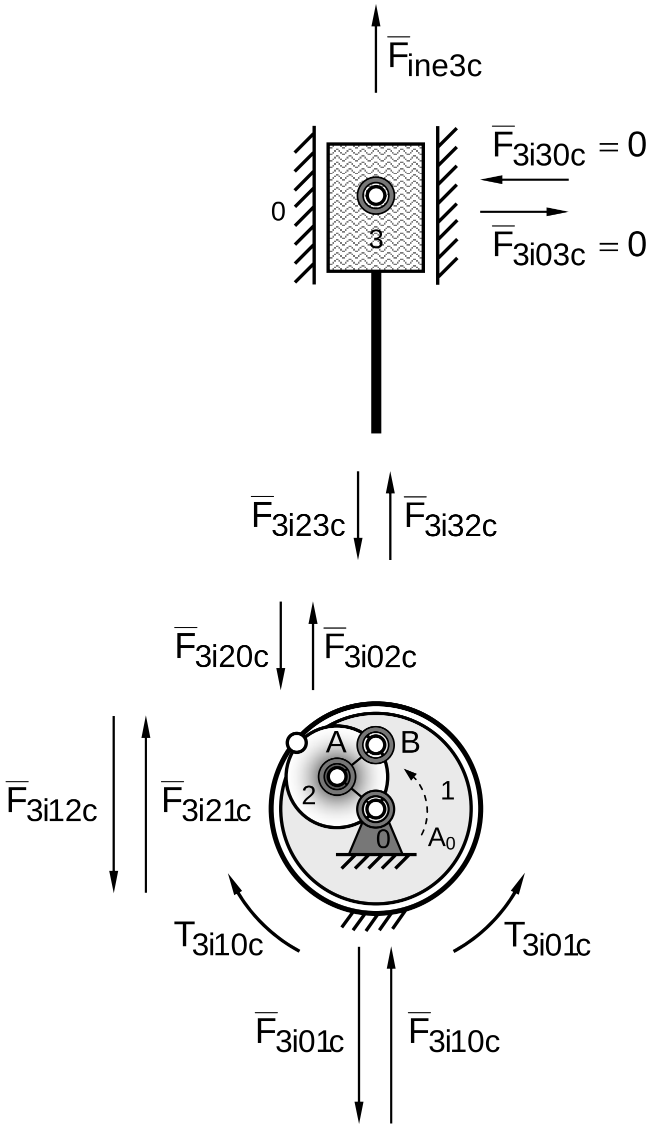

Figure 5.2.6. Kinetostatics of the cardan gear piston.

The main kinetostatics of the slider-crank mechanism versus the cardan gear mechanism

Piston pin inertial joint forces of the mechanisms

$$\overline{F}_{\Sigma i3in} = \overline{F}_{\Sigma i03} + \overline{F}_{\Sigma i23} \quad (5.2.1)$$

$$\overline{F}_{\Sigma i3inc} = \overline{F}_{\Sigma i23c} \quad (5.2.2)$$

Crank pin inertial joint forces of the mechanisms

$$\overline{F}_{\Sigma i12} = \overline{F}_{2i12} + \overline{F}_{3i12} \quad (5.2.3)$$

$$\overline{F}_{\Sigma i12c} = \overline{F}_{3i12c} \quad (5.2.4)$$

Main pin inertial joint forces of the mechanisms

$$\overline{F}_{\Sigma i01} = \overline{F}_{2i01} + \overline{F}_{3i01} = \overline{F}_{\Sigma i12} \quad (5.2.5)$$

$$\overline{F}_{\Sigma i01c} = \overline{F}_{3i01c} = \overline{F}_{\Sigma i12c} \quad (5.2.6)$$

Inertial torques of the crankshafts of the mechanisms

$$T_{\Sigma i10} = T_{1i10} + T_{2i10} + T_{3i10} \quad (5.2.7)$$

$$T_{\Sigma i10c} = T_{1i10c} + T_{2i10c} + T_{3i10c} \quad (5.2.8)$$

Inertial works per one cycle (= 4π rad) of the mechanisms

$$\Sigma W_{ine} = \int_{\pi/2}^{9\pi/2} T_{\Sigma i10} \cdot d\theta_{AA_0} \quad (5.2.9)$$

$$\Sigma W_{inec} = \int_{\pi/2}^{9\pi/2} T_{\Sigma i10c} \cdot d\theta_{AA_0c} \quad (5.2.10)$$

Inertial powers of the crankshafts of the mechanisms

$$P_{ine} = T_{\Sigma i10} \cdot \omega_{AA_0} \quad (5.2.11)$$

$$P_{inec} = T_{\Sigma i10c} \cdot \omega_{AA_0c} \quad (5.2.12)$$

6. Kinetics

In this study gravitation, clearances, vibrations and the purposeful balancing have been neglected in order to bring out the real differences between the slider-crank and the cardan gear machines.
The crank length of the cardan gear machine is half of the crank length of the slider-crank machine (**Equation 6.1**).

$$Z_{AA_0} = 2 \cdot Z_{AA_0 c} \tag{6.1}$$

6.1 Thermodynamics

Thermodynamics of the pumps and engines have been presented and calculated using the conventional theories [***Faires 1970, Taylor 1985, Weisstein 2006***].
Compression ratios of the pumps and gasoline engines are typically 6 ... 15.
Diesel engines have higher compression ratios, generally 14 ... 24.
The equations of thermodynamics used in the calculations have been presented in the **Appendix 6.1.1**.

6.2 Comparison of kinetics

The kinetic equations of the studied machines used in the calculations have been presented in the **Appendix 6.2.1**. The final equations of the most significant variables have been presented also in this chapter (**Figures 6.2.1 ... 6.2.2**) (**Equations 6.2.1 ... 6.2.16**).

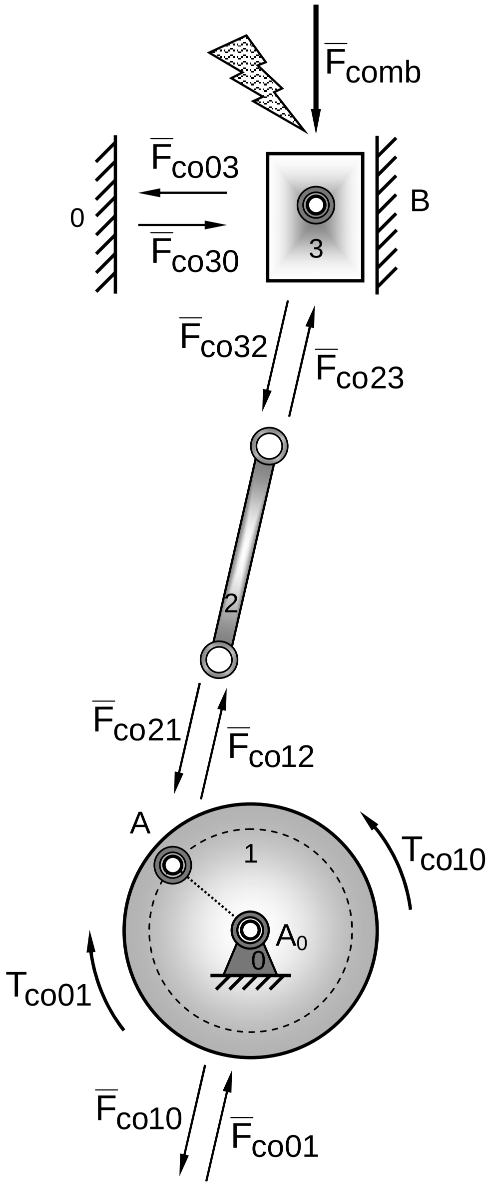

Figure 6.2.1. Kinetics of the slider-crank engine combustion.

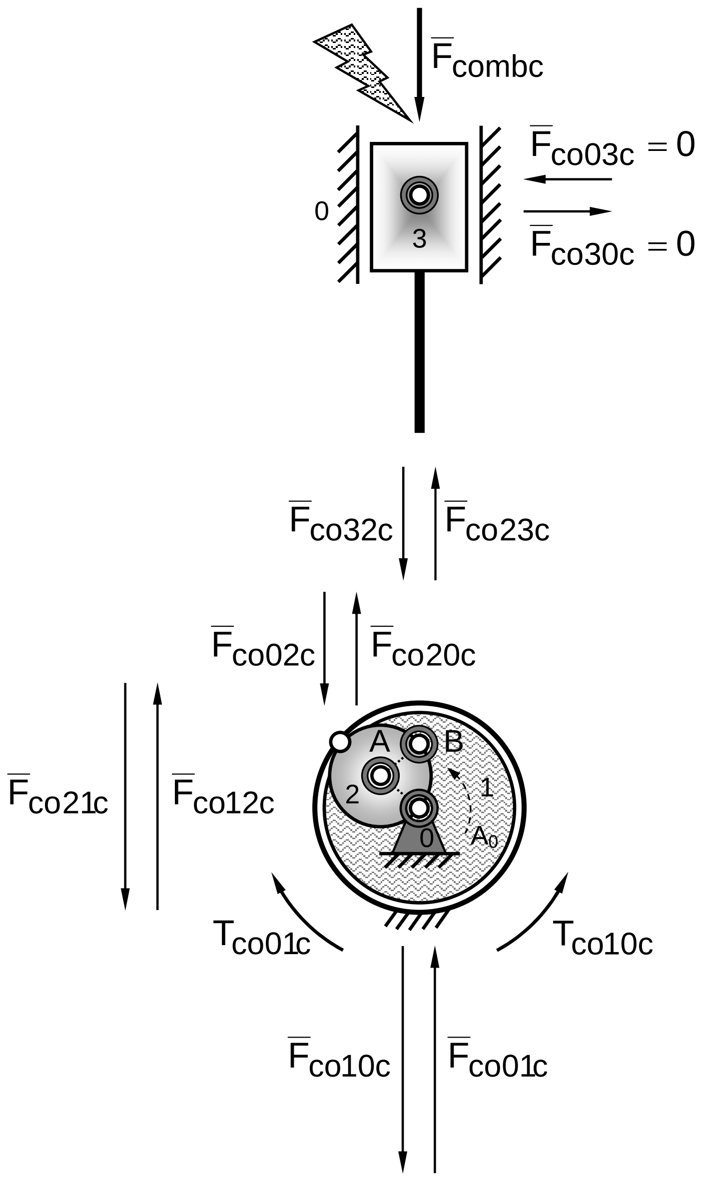

Figure 6.2.2. Kinetics of the cardan gear engine combustion.

Compression in pumps and combustion in engines act equal when the forces in the **Figures 6.2.1 and 6.2.2** are discussed. The subscript "co" means both compression and combustion, although the pressure force has been illustrated as combustion. In the following theory the subscript "co" has been replaced with "comp" and "comb" respectively.

The main kinetics of the slider-crank machines versus the cardan gear machines

Polytropic compression pressures of the machines

In this study the different strokes for the pumps and the four-stroke engines in the studied cycles are:

Pumps

Intake strokes	π/2 ... 3π/2 rad	90 ... 270 °
	5π/2 ... 7π/2 rad	450 ... 630 °
Compression strokes	3π/2 ... 5π/2 rad	270 ... 450 °
	7π/2 ... 9π/2 rad	630 ... 810 °

The valves of the pumps have been assumed to be closed during the compression strokes (zero air flow) in order to find the highest loads.

Four-stroke engines

Intake stroke	π/2 ... 3π/2 rad	90 ... 270 °
Compression stroke	3π/2 ... 5π/2 rad	270 ... 450 °
Power stroke	5π/2 ... 7π/2 rad	450 ... 630 °
Exhaust stroke	7π/2 ... 9π/2 rad	630 ... 810 °

The machines have been assumed well designed and the overfilling during the intake strokes has been approximated 107 %.

Compression strokes of the pumps

Compression strokes and power strokes of the four-stroke engines as the initial values for the calculation of the combustion pressures

$$p_{pol107}\left(\theta_{AA_0}\right) = \frac{p_{atm}\cdot\left(1.07\cdot V_{unc}\right)^{\gamma_{pol}}}{V_{cyl}{}^{\gamma_{pol}}} \tag{6.2.1}$$

$$p_{polc107}\left(\theta_{AA_0c}\right) = \frac{p_{atm}\cdot\left(1.07\cdot V_{unc}\right)^{\gamma_{pol}}}{V_{cylc}{}^{\gamma_{pol}}} \tag{6.2.2}$$

In the preceding equations:

p_{atm} = atmospheric pressure
V_{unc} = maximum uncompressed volume
V_{cyl} = cylinder volume during running in the slider-crank machine
V_{cylc} = cylinder volume during running in the cardan gear machine

Compression torques of the crankshafts of the pumps

$$T_{comp} = F_{BAcomp} \cdot Z_{AA_0} \cdot \sin(\theta_{BA} + \pi - \theta_{AA_0}) \tag{6.2.3}$$

$$T_{compc} = 2 \cdot F_{BAcompc} \cdot Z_{AA_0c} \cdot \sin(-90^\circ - \theta_{AA_0c}) \tag{6.2.4}$$

Compression works per one cycle (= 4π rad) of the pumps

$$\Sigma W_{comp} = \int_{\pi/2}^{9\pi/2} T_{comp} \cdot d\theta_{AA_0} \tag{6.2.5}$$

$$\Sigma W_{compc} = \int_{\pi/2}^{9\pi/2} T_{compc} \cdot d\theta_{AA_0c} \tag{6.2.6}$$

Compression powers of the pumps

$$P_{comp} = T_{comp} \cdot \omega_{AA_0} \tag{6.2.7}$$

$$P_{compc} = T_{compc} \cdot \omega_{AA_0c} \tag{6.2.8}$$

Combustion pressures of the four-stroke engines

$$p_{comb}(\theta_{AA_0}) = \frac{p_{comb\,max}}{p_{pol\,max}} \cdot p_{pol}(\theta_{AA_0} - 8...10^\circ) \tag{6.2.9}$$

$$p_{combc}(\theta_{AA_0c}) = \frac{p_{combc\,max}}{p_{polc\,max}} \cdot p_{polc}(\theta_{AA_0c} - 8...10^\circ) \tag{6.2.10}$$

In the preceding equations:

p_{pol} = polytropic compression pressure in the slider-crank engine
p_{polc} = polytropic compression pressure in the cardan gear engine
p_{polmax} = maximum polytropic compression pressure in the slider-crank engine
$p_{polcmax}$ = maximum polytropic compression pressure in the cardan gear engine
$p_{combmax}$ = maximum combustion pressure in the slider-crank engine
$p_{combcmax}$ = maximum combustion pressure in the cardan gear engine

Combustion torques of the crankshafts of the four-stroke engines

$$T_{comb} = F_{BAcomb} \cdot Z_{AA_0} \cdot \sin(\theta_{BA} + \pi - \theta_{AA_0}) \qquad (6.2.11)$$

$$T_{combc} = 2 \cdot F_{BAcombc} \cdot Z_{AA_0c} \cdot \sin(-90^\circ - \theta_{AA_0c}) \qquad (6.2.12)$$

Combustion works per one cycle (= 4π rad) of the four-stroke engines

$$\Sigma W_{comb} = \int_{\pi/2}^{9\pi/2} T_{comb} \cdot d\theta_{AA_0} \qquad (6.2.13)$$

$$\Sigma W_{combc} = \int_{\pi/2}^{9\pi/2} T_{combc} \cdot d\theta_{AA_0c} \qquad (6.2.14)$$

Combustion powers of the crankshafts of the four-stroke engines

$$P_{comb} = T_{comb} \cdot \omega_{AA_0} \qquad (6.2.15)$$

$$P_{combc} = T_{combc} \cdot \omega_{AA_0c} \qquad (6.2.16)$$

7. Comparison of the summed lossless Newtonian dynamics

The equations of the studied machines used in the calculations of the lossless Newtonian dynamics have been presented in the **Appendix 7.1**. The final equations of the most significant variables have been presented also in this chapter (**Equations 7.1 ... 7.24**).

The summed Newtonian dynamics of the lossless slider-crank machines versus the lossless cardan gear machines

Lossless piston pin joint forces of the pumps and the four-stroke engines

$$\overline{F}_{\Sigma pump3in} = \overline{F}_{\Sigma comp3in} + \overline{F}_{\Sigma i3in} \tag{7.1}$$

$$\overline{F}_{\Sigma pump3inc} = \overline{F}_{\Sigma pump23c} = \overline{F}_{comp23c} + \overline{F}_{\Sigma i23c} \tag{7.2}$$

$$\overline{F}_{\Sigma eng3in} = \overline{F}_{\Sigma comb3in} + \overline{F}_{\Sigma i3in} \tag{7.3}$$

$$\overline{F}_{\Sigma eng3inc} = \overline{F}_{\Sigma eng23c} = \overline{F}_{comb23c} + \overline{F}_{\Sigma i23c} \tag{7.4}$$

Lossless crank pin joint forces of the pumps and the four-stroke engines

$$\overline{F}_{\Sigma pump12} = \overline{F}_{comp12} + \overline{F}_{\Sigma i12} \tag{7.5}$$

$$\overline{F}_{\Sigma pump12c} = \overline{F}_{comp12c} + \overline{F}_{\Sigma i12c} \tag{7.6}$$

$$\overline{F}_{\Sigma eng12} = \overline{F}_{comb12} + \overline{F}_{\Sigma i12} \tag{7.7}$$

$$\overline{F}_{\Sigma eng12c} = \overline{F}_{comb12c} + \overline{F}_{\Sigma i12c} \tag{7.8}$$

Lossless main pin joint forces of the pumps and the four-stroke engines

$$\overline{F}_{\Sigma pump01} = \overline{F}_{comp01} + \overline{F}_{\Sigma i01} \tag{7.9}$$

$$\overline{F}_{\Sigma pump01c} = \overline{F}_{comp01c} + \overline{F}_{\Sigma i01c} \tag{7.10}$$

$$\overline{F}_{\Sigma eng01} = \overline{F}_{comb01} + \overline{F}_{\Sigma i01} \tag{7.11}$$

$$\overline{F}_{\Sigma eng01c} = \overline{F}_{comb01c} + \overline{F}_{\Sigma i01c} \tag{7.12}$$

Lossless crankshaft torques of the pumps and the four-stroke engines

$$T_{\Sigma pump10} = T_{comp10} + T_{\Sigma i10} \tag{7.13}$$

$$T_{\Sigma pump10c} = T_{comp10c} + T_{\Sigma i10c} \tag{7.14}$$

$$T_{\Sigma eng10} = T_{comb10} + T_{\Sigma i10} \tag{7.15}$$

$$T_{\Sigma eng10c} = T_{comb10c} + T_{\Sigma i10c} \tag{7.16}$$

Lossless works per one cycle (= 4π rad) of the pumps and the four-stroke engines

$$\Sigma W_{pump} = \int_{\pi/2}^{9\pi/2} T_{\Sigma pump10} \cdot d\theta_{AA_0} \tag{7.17}$$

$$\Sigma W_{pumpc} = \int_{\pi/2}^{9\pi/2} T_{\Sigma pump10c} \cdot d\theta_{AA_0c} \tag{7.18}$$

$$\Sigma W_{eng} = \int_{\pi/2}^{9\pi/2} T_{\Sigma eng10} \cdot d\theta_{AA_0} \tag{7.19}$$

$$\Sigma W_{engc} = \int_{\pi/2}^{9\pi/2} T_{\Sigma eng10c} \cdot d\theta_{AA_0c} \tag{7.20}$$

Lossless crankshaft powers of the pumps and the four-stroke engines

$$P_{pump} = T_{\Sigma pump10} \cdot \omega_{AA_0} \tag{7.21}$$

$$P_{pumpc} = T_{\Sigma pump10c} \cdot \omega_{AA_0c} \tag{7.22}$$

$$P_{eng} = T_{\Sigma eng10} \cdot \omega_{AA_0} \tag{7.23}$$

$$P_{engc} = T_{\Sigma eng10c} \cdot \omega_{AA_0c} \tag{7.24}$$

8. Dynamic tooth loads of the cardan gear mesh

To avoid the dynamic tooth loads the cardan gear mesh can be replaced with the linear bearings (**Figure 8.1**). In this study the dynamic tooth loads have been calculated applying the original Buckingham's method in US units [***Buckingham 1949***] (**Equation 8.1**). The cardan gear pair has been calculated as straight-tooth spur gears. The other suitable gear type would be herringbone gears. Helical gears are not suitable because of their axial loads. The equations used in the calculations have been presented in the **Appendix 8.1**.

Dynamic loads of the gear teeth

$$F_{dync} = F_{twheelc} + \sqrt{f_{ac} \cdot (2 \cdot f_{2c} - f_{ac})} \quad [lb] \qquad (8.1)$$

where $F_{twheelc}$ = tangential load of the gear mesh
f_{ac} = acceleration load of the gear teeth
f_{2c} = force required to deform gear teeth amount of the error (backlash)

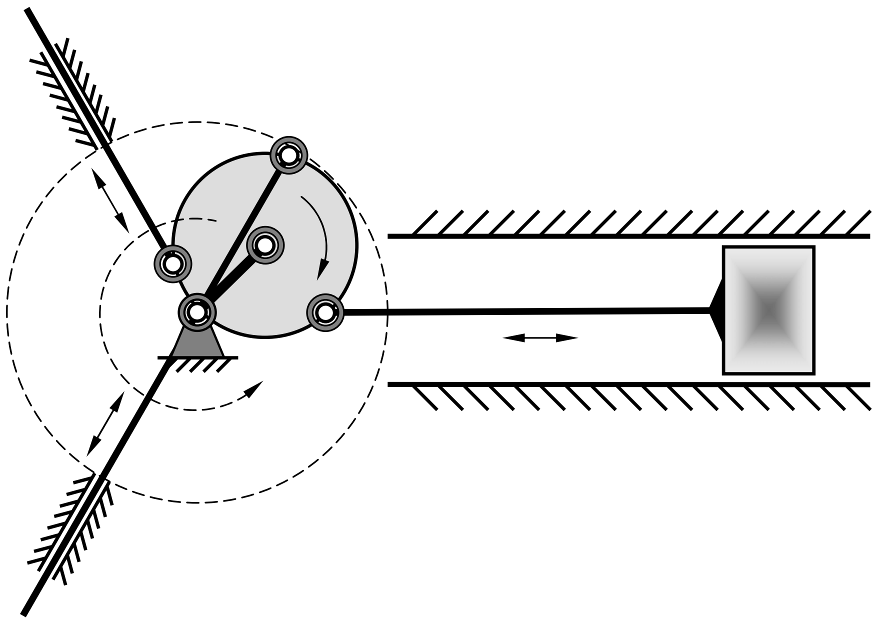

Figure 8.1. Cardan gear mechanism without gears.

9. Comparison of the operational torques, powers and mechanical efficiencies

When we want to save energy, the mechanical efficiency indicates, which machine is the most economical. In this study the mechanical efficiencies have been calculated applying Anderson's & Loewenthal's method connected with Pennestrì's, Mantriota's and Valentini's studies [***Anderson & Loewenthal 1981 and 1982, Pennestrì & Valentini 2003, Mantriota & Pennestrì 2003***].
The equations used in the calculations have been presented in the **Appendix 9.1**.
The final equations of the most significant variables have been presented also in this chapter (**Equations 9.1 ... 9.16**).

Total power losses of the slider-crank and the cardan gear machines

Total power losses of the pumps

$$P_{\mu pump} = P_{\mu pis} + \Sigma P_{\mu b} \tag{9.1}$$

$$P_{\mu pumpc} = P_{\mu pisc} + \Sigma P_{\mu bc} + P_{\mu wheelc} \tag{9.2}$$

Total power losses of the four-stroke engines

$$P_{\mu eng} = P_{\mu pis} + \Sigma P_{\mu b} \tag{9.3}$$

$$P_{\mu engc} = P_{\mu pisc} + \Sigma P_{\mu bc} + P_{\mu wheelc} \tag{9.4}$$

In the preceding equations:

$P_{\mu pis}$ = power loss of the slider-crank piston
$P_{\mu pisc}$ = power loss of the cardan gear piston
$\Sigma P_{\mu b}$ = sum of the power losses of the piston pin, crank pin and main pin bearings of the slider-crank machine
$\Sigma P_{\mu bc}$ = sum of the power losses of the piston pin, crank pin and main pin bearings of the cardan gear machine
$P_{\mu wheelc}$ = total power loss of the cardan wheel

Operational powers and torques of the slider-crank and the cardan gear machines

Power needs of the pumps

$$P_{needpump} = P_{pump} + P_{\mu pump} \tag{9.5}$$

$$P_{needpumpc} = P_{pumpc} + P_{\mu pumpc} \tag{9.6}$$

Output powers of the four-stroke engines

$$P_{outeng} = P_{eng} - P_{\mu eng} \tag{9.7}$$

$$P_{outengc} = P_{engc} - P_{\mu engc} \tag{9.8}$$

Torque needs of the pumps

$$T_{needpump} = \frac{P_{needpump}}{\omega_{AA_0}} \tag{9.9}$$

$$T_{needpumpc} = \frac{P_{needpumpc}}{\omega_{AA_0 c}} \tag{9.10}$$

Output torques of the four-stroke engines

$$T_{outeng} = \frac{P_{outeng}}{\omega_{AA_0}} \tag{9.11}$$

$$T_{outengc} = \frac{P_{outengc}}{\omega_{AA_0 c}} \tag{9.12}$$

Mechanical efficiencies of the slider-crank and the cardan gear machines

Mechanical efficiencies of the pumps

$$\eta_{mpump} = \frac{\Sigma W_{comp}}{\Sigma W_{pump} + \Sigma W_{\mu pump}} \tag{9.13}$$

$$\eta_{mpumpc} = \frac{\Sigma W_{compc}}{\Sigma W_{pumpc} + \Sigma W_{\mu pumpc}} \tag{9.14}$$

Mechanical efficiencies of the engines

$$\eta_{meng} = \frac{\Sigma W_{eng} - \Sigma W_{\mu eng}}{\Sigma W_{eng}} \tag{9.15}$$

$$\eta_{mengc} = \frac{\Sigma W_{engc} - \Sigma W_{\mu engc}}{\Sigma W_{engc}} \tag{9.16}$$

In the preceding equations:

ΣW_{comp} = total compression work of the slider-crank pump
ΣW_{compc} = total compression work of the cardan gear pump
ΣW_{pump} = lossless work of the slider-crank pump
ΣW_{pumpc} = lossless work of the cardan gear pump
$\Sigma W_{\mu pump}$ = total work loss of the slider-crank pump
$\Sigma W_{\mu pumpc}$ = total work loss of the cardan gear pump
ΣW_{eng} = lossless work of the slider-crank engine
ΣW_{engc} = lossless work of the cardan gear engine
$\Sigma W_{\mu eng}$ = total work loss of the slider-crank engine
$\Sigma W_{\mu engc}$ = total work loss of the cardan gear engine

10. Calculations

A set of 8 different computer programs in Mathcad have been made by the author to calculate Newtonian dynamics of the slider-crank pumps and the four-stroke engines versus the cardan gear pumps and the four-stroke engines.

The calculation areas are:

Kinematics of the studied mechanisms
Kinetostatics of the studied mechanisms
Kinetics of the studied machines, including the necessary thermodynamics
Summed lossless Newtonian dynamics of the studied machines
Dynamic tooth loads of the cardan gear mesh
Mechanical efficiencies of the studied machines

The required initial values for the calculation processes are:

Angular acceleration of the crankshaft
Initial angular velocity of the crankshaft
Initial crank angle
Final crank angle
Crank length
Connecting rod lengths
Material density of the moving components
Main dimensions of the crankshafts
Main dimensions of the connecting rods
Piston diameter
Atmospheric pressure
Compression ratio
Polytropic exponent
Filling factor (volumetric efficiency)
Piston head height
Maximum combustion pressure
Backlash acting at the pitch line of the cardan gear pair
Modulus of elasticity of the materials of the cardan gear pair
Pressure angle of the cardan gear pair
Numbers of teeth of the cardan gear pair
Piston ring heights
Contact pressures of the piston rings
Friction coefficient of the piston rings
Friction coefficient of the piston skirt
Pitch diameters of the rolling bearings of the pin joints
Static load ratings of the pin bearings
Bearing lubrication factor
Lubrication oil kinematic viscosity at the running temperature
Module of the cardan gear pair
Lubrication oil density

The angular acceleration of the machines varies from 2π rad/s^2 (very old pumps and engines) to 200π rad/s^2 (new racing engines).
The initial angular velocity of the studied machines can be 0...400π rad/s (0...12000 r/min).
The initial crank angle is $\pi/2$ rad (= 90 °), when the zero position is at the x-axis.
The final crank angle is $9\pi/2$ rad (= 810 °), corresponding the whole cycle of the four-stroke engine.
The crank length of the slider-crank mechanism is 20...100 mm for the normal sized machines. The crank length of the cardan gear machine is half of the crank length of the slider-crank machine.
The connecting rod length is "1.35...2 · stroke (= 2.7...4 · crank length)" in the normal sized slider-crank machines. In this study also an extremely short and overlong rod lengths "1.165 · stroke (= 2.33 · crank length)" and "2.5 · stroke (= 5 · crank length)" have been included in the calculations.
The moving components of the pumps and engines, except the pistons, are generally made of steel. The material density of steel is approximately 7850 kg/m^3.
The connecting rod of the cardan gear machine can be very thin and made of titanium alloy. The material density of titanium is approximately 4820 kg/m^3.
The maximum diameter of the crankshaft flywheel is approximately "2 · crank length + 10...60 mm" in the normal sized slider-crank machines.
The mass of the crankshaft can be estimated using volume "π · (crank length)^2 · 2 · crank length" in the normal sized slider-crank machines.
The cross section of the connecting rod can be approximated as "length/10 · length/5 ... length/8 · length/4" in the normal sized slider-crank machines.
The piston diameter is "1...1.8 · stroke (= 2...3.6 · crank length)" in the normal sized slider-crank machines. When the piston diameter is smaller, the slider-crank machine is unable to run constructively (**Figure 12.1**).
The standard atmospheric pressure is $1.01325 \cdot 10^5$ Pa.
Compression ratios are 6...15 in pumps and gasoline engines and 14...24 in diesel engines [***Faires 1970, Taylor 1985***].
Working pumps and heat engines are thermodynamically polytropic systems near adiabatic system. The polytropic exponent for the working machines is 1.3...1.4.
The continuous air flow in the rotating machines can overfill the cylinder during the intake stroke. The filling factor of the best machines is 1...1.1.
The maximum combustion pressure is 7...17 MPa in the normal engines [***Faires 1970, Taylor 1985***].
For the cardan gear drives the average backlash is 0.1 ... 0.2 mm.
The suitable material for the cardan wheel and the internal ring gear is carburizing steel. The modulus of elasticity of the normal steel is approximately 210 000 N/mm^2.
The pressure angle of the normal gears is 20 °.
The suitable number of teeth for the cardan wheel is 20 ... 25 and for the ring gear respectively 40 ... 50.
The heights of the piston rings of the normal sized machines are approximately 2 mm for the compression rings and 4 mm for the oil rings [***Andersson et al. 2002***].
The contact pressures of the compression rings are approximately 0.19 N/mm^2 and the oil rings approximately 1 N/mm^2 [***Andersson et al. 2002***].
The friction coefficient of the piston rings is approximately 0.07 and the piston skirt approximately 0.09 [***Andersson et al. 2002***].

The pitch diameters of the rolling bearings of the normal sized machines are approximately 15 ... 70 mm.
The static load ratings of the rolling bearings of the normal sized machines are approximately 15 000 ... 150 000 N [***INA / FAG 2007***].
The lubrication factor for the normal lubrication is f_0 = 1... 2.5 [***INA / FAG 2007***].
The kinematic viscosity of the lubrication oil in the running temperature is $\lesssim$ 5 mm^2/s (cSt).
The module of the teeth of the cardan gear pair for the normal sized machines is 2 ... 4 mm.
Density of the lubrication oil is 860 ... 930 kg/m^3.

The computer programs (Mathcad programs) of this study calculate and compare the following variables of the presented machines:

Kinematics

Positions

Points of time for the calculations
Global crank angles
Global positions of the crank pins
Global angles of the connecting rods
Local and global positions of the piston pins
Local and global positions of the center of gravity or any other point at the center line of the connecting rods

Velocities

Global angular velocities of the cranks
Global velocities of the crank pins
Local and global angular velocities of the connecting rods
Local and global velocities of the piston pins
Global radial velocities of the piston pins
Global tangential velocities of the piston pins
Total global velocities of the center of gravity or any other point at the center line of the connecting rods
Global radial and tangential velocities of the center of gravity or any other point at the center line of the connecting rods

Accelerations

Global accelerations of the crank pins
Local and global angular accelerations of the connecting rods
Local and global accelerations of the piston pins
Global radial, coriolis, tangential and normal accelerations of the piston pins
Total global accelerations of the center of gravity or any other point at the center line of the connecting rods
Global radial, coriolis, tangential and normal accelerations of the center of gravity or any other point at the center line of the connecting rods

Kinetostatics

Estimated volumes of the crankshafts
Masses of the crankshafts
Mass moments of inertia of the crankshafts
Inertial torques and countertorques of the crankshafts caused by the crankshafts themselves
Volume of the cardan wheel
Mass of the cardan wheel
Mass moment of inertia of the cardan wheel
Inertial torque and countertorque of the crankshaft caused by the cardan wheel
Estimated volumes of the connecting rods
Masses of the connecting rods
Mass moments of inertia of the connecting rods
Inertial forces of the connecting rods
Local positions of the center of percussion of the connecting rods
Inertial joint forces and counterforces (piston pins, crank pins and main pins) caused by the connecting rods
Inertial torques of the crankshafts caused by the connecting rods
Total masses of the pistons with the pins
Inertial forces of the pistons with the pins
Inertial joint forces and counterforces (piston pins, crank pins and main pins) caused by the pistons with the pins
Inertial torques of the crankshafts caused by the pistons with the pins
Summed piston pin inertial joint forces and counterforces
Total inertial joint forces and counterforces of the piston pins, crank pins and main pins
Total inertial torques and countertorques of the crankshafts
Inertial works of the crankshafts
Inertial powers of the crankshafts

Kinetics including thermodynamics

Stroke
Piston area
Displacement, stroke volume
Compressed volume
Theoretical maximum compression pressure
Uncompressed volume
Maximum polytropic compression pressures
Minimum height of the cylinder chamber
Deck height
Cylinder volumes during running
Polytropic compression pressures during running
Compression forces during running
Connecting rod forces caused by the compression
Compression joint forces and counterforces of the piston pins, crank pins and main pins
Summed piston pin compression joint forces and counterforces
Crankshaft torques caused by the compression
Mean compression torques of the crankshafts
Compression works of the crankshafts
Compression powers of the crankshafts
Combustion pressures during running
Combustion forces during running
Connecting rod forces caused by the combustion
Combustion joint forces and counterforces of the piston pins, crank pins and main pins
Summed piston pin combustion joint forces and counterforces
Crankshaft torques caused by the combustion
Mean combustion torques of the crankshafts
Combustion works of the crankshafts
Combustion powers of the crankshafts

Summed lossless Newtonian dynamics

Total joint forces of the piston pins, crank pins and main pins
Total torques of the crankshafts
Mean total torques of the crankshafts
Total works of the crankshafts
Total powers of the crankshafts

Dynamic tooth loads of the cardan gear mesh

Pitch line velocity of the gears
Tangential loads of the cardan wheel gear mesh
Tooth deformation of the gears
Dynamic loads of the gear teeth

Mechanical efficiencies including friction losses

Friction forces of the piston rings
Friction forces of the piston skirts
Total friction forces of the pistons
Power losses of the pistons
Rotational speeds of the pin bearings
Load dependent torque losses of the pin bearings
Oil viscosity dependent torque losses of the pin bearings
Total torque losses of the pin bearings
Power losses of the pin bearings
Average normal load of the cardan wheel gear mesh
Friction coefficient of the cardan wheel gear mesh
Average sliding power loss of the cardan wheel gear mesh
Central EHD oil film thickness
Average rolling power loss of the cardan wheel gear mesh
Windage loss of the cardan wheel
Total power loss of the cardan wheel
Total power losses of the pumps
Total power losses of the four-stroke engines
Total work losses of the pumps
Total work losses of the four-stroke engines
Power needs of the pumps
Output powers of the four-stroke engines
Torque needs of the pumps
Output torques of the four-stroke engines
Mechanical efficiencies of the pumps
Mechanical efficiencies of the four-stroke engines

11. Results

The main results of this study are the comparison data (results of the Mathcad calculations, carried out by the author) and information of the cardan gear machine versus the slider-crank machine. The calculated data show the differences between the two machines in Newtonian dynamics and tell which mechanism is better in which area.
The most informative data are presented in this chapter and in the appendixes.

The piston position determines the cylinder volume, the compression pressure and the combustion pressure. The higher is the pressure the higher is the crankshaft torque.
High velocities mean high linear momentums and high angular velocities mean high angular momentums.
High accelerations lead to high inertial forces and high angular accelerations lead to high inertial torques.
High inertial forces of the links cause high inertial joint forces and high crankshaft torque.
Continuous and high inertial torques consume energy and waste power.

The initial values that actually affect to the comparison results and that have been mainly varied in the calculation programs are:

Angular acceleration of the crankshaft	0...200π rad/s^2
Initial angular velocity of the crankshaft	3π...200π rad/s (= 90...6000 r/min)
Crank length (= ZAA0 in the programs)	0.027...0.06 m
Connecting rod lengths (= ZBA in the programs)	0.08...0.24 m
Masses (main dimensions) of the connecting rods	"steel and titanium"
Piston diameter	1...3.4 · crank length
Maximum combustion pressure	12...14 MPa

Curves of the **Figures 11.1.2, 11.1.3, 11.1.5, 11.1.6, 11.2.1, 11.2.2, 11.2.3 and 11.4.3** present absolute values (magnitudes) of the functions. The originally negative half-waves of the curves have been converted to positive mirror-images regarding the "x-axis". That way the differences between the two machines can be better observed.

The main results of this study have been presented in the **Chapters 11.1 ... 11.8** and in the **Appendixes 11.1.1 ... 11.7.1**.
A lot of verifying and defining calculations have also been made by the author outside these results.

11.1 Results of kinematics

The connecting rod lengths used in the calculations of kinematics are "2.33, 3 and 4 · ZAA0".
"2.33 · ZAA0" is an extremely short rod and "4 · ZAA0" is a long rod.
The percentage differences have been calculated regarding the values of the slider-crank mechanism.

Piston positions

The piston of the cardan gear mechanism locates higher between the TDC and the BDC than the piston of the equal slider-crank mechanism.
The maximum piston position difference is 3...11 %, depending on the rod length.
The shorter is the rod, the higher is the cardan gear piston position compared to the piston position of the equal slider-crank mechanism.
(**Figure 11.1.1, Appendix 11.1.1**)

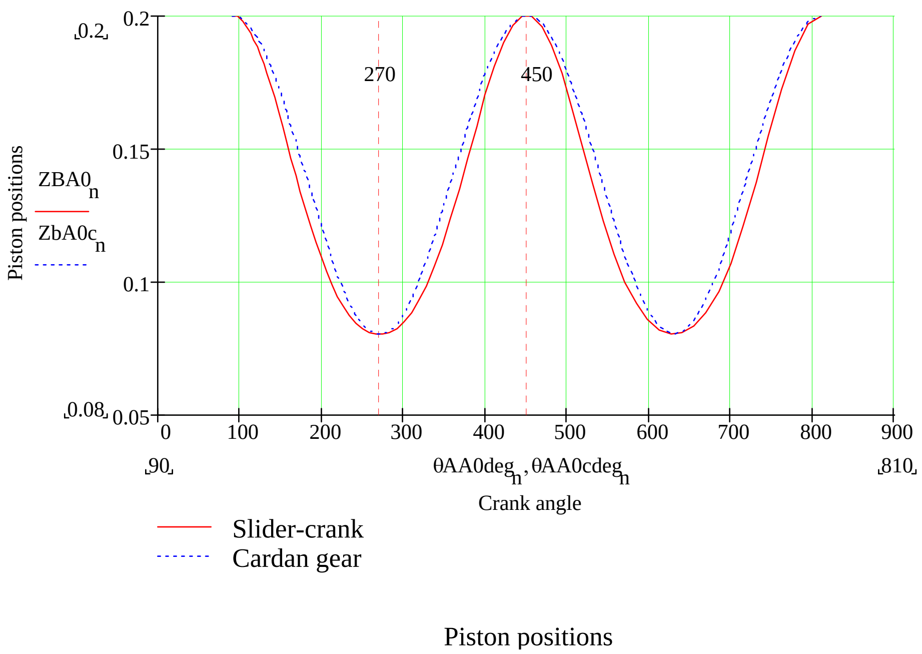

Figure 11.1.1. Piston positions, ZBA = 2.33·ZAA0, ZAA0 = 0.06 m, ZBA = 0.14 m.

Piston velocities

The maximum piston velocity is 3...8 % lower in the cardan gear mechanism than in the slider-crank mechanism, depending on the rod length. The shorter is the rod, the lower is the cardan gear piston velocity compared to the piston velocity of the equal slider-crank mechanism.
(**Figure 11.1.2, Appendix 11.1.1**)

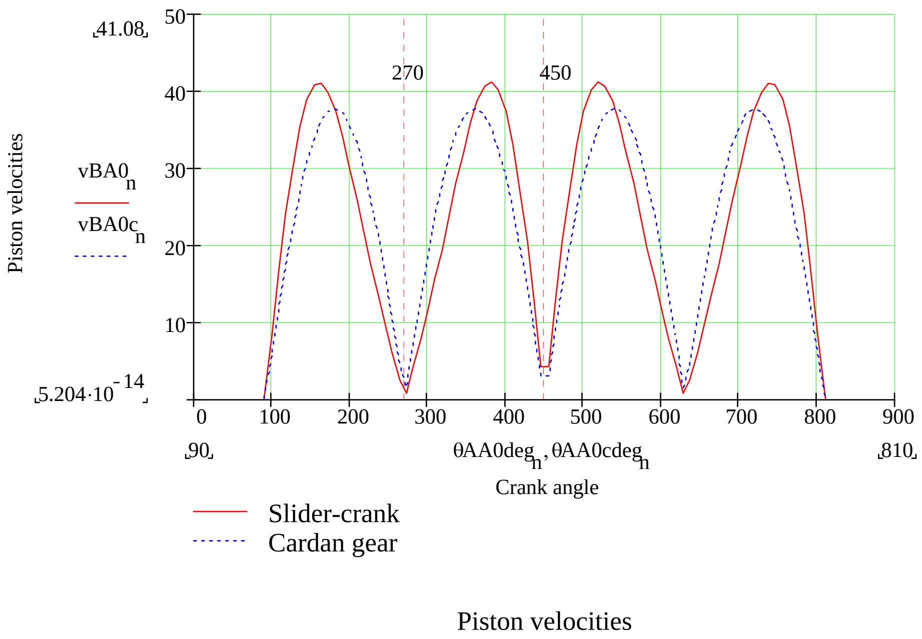

Figure 11.1.2. Piston velocities, ZBA = 2.33·ZAA0, ZAA0 = 0.06 m, ZBA = 0.14 m, αAA0 = 0, ωAA00 = 200π rad/s.

Piston accelerations

The maximum piston acceleration is 20...30 % lower in the cardan gear mechanism than in the slider-crank mechanism, depending on the rod length. The shorter is the rod, the lower is the cardan gear piston acceleration compared to the piston acceleration of the equal slider-crank mechanism.
(**Figure 11.1.3, Appendix 11.1.1**)

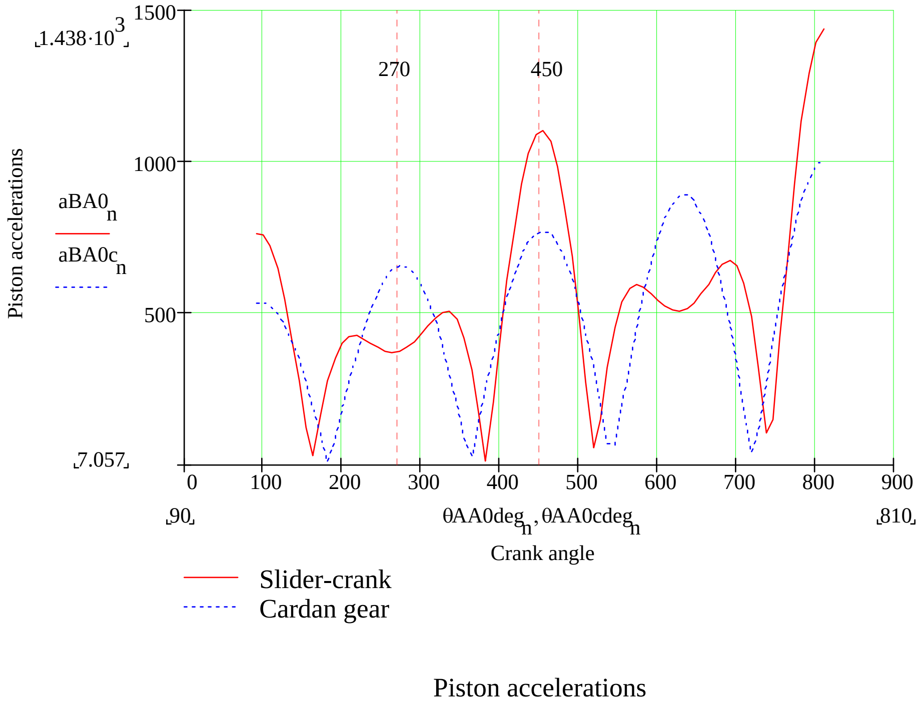

Figure 11.1.3. Piston accelerations, ZBA = 2.33·ZAA0, ZAA0 = 0.06 m, ZBA = 0.14 m, αAA0 = 100π rad/s^2, ωAA00 = 30π rad/s.

Connecting rod angular velocities and angular accelerations

The cardan gear rod does not rotate. Only the slider-crank rod has angular velocity and angular acceleration. (**Figure 11.1.4**)

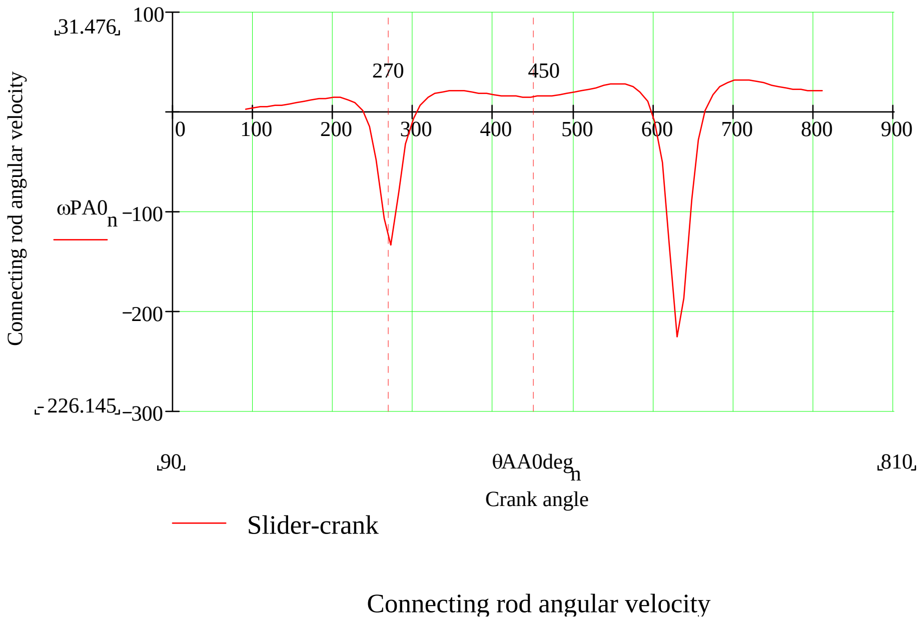

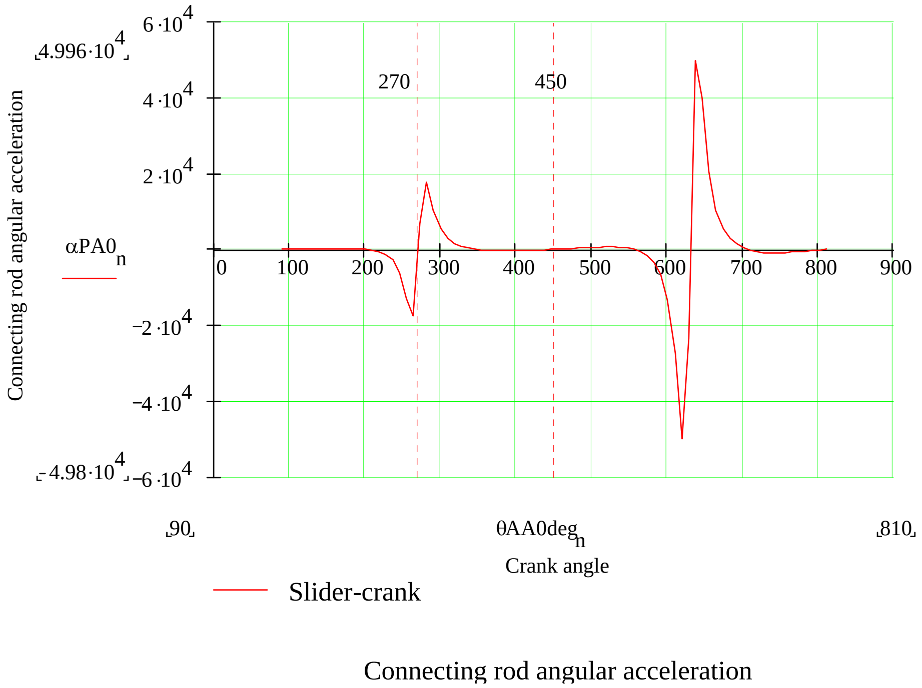

Figure 11.1.4. Connecting rod angular velocity and angular acceleration, slider-crank mechanism, ZBA = 2.33·ZAA0, ZAA0 = 0.06 m, ZBA = 0.14 m, αAA0 = 100π rad/s^2, ωAA00 = 3π rad/s.

Connecting rod velocities

The maximum rod velocity is 1...3 % lower in the cardan gear mechanism than in the slider-crank mechanism, depending on the rod length. The shorter is the rod, the lower is its velocity in the cardan gear mechanism.
(**Figure 11.1.5, Appendix 11.1.1**)

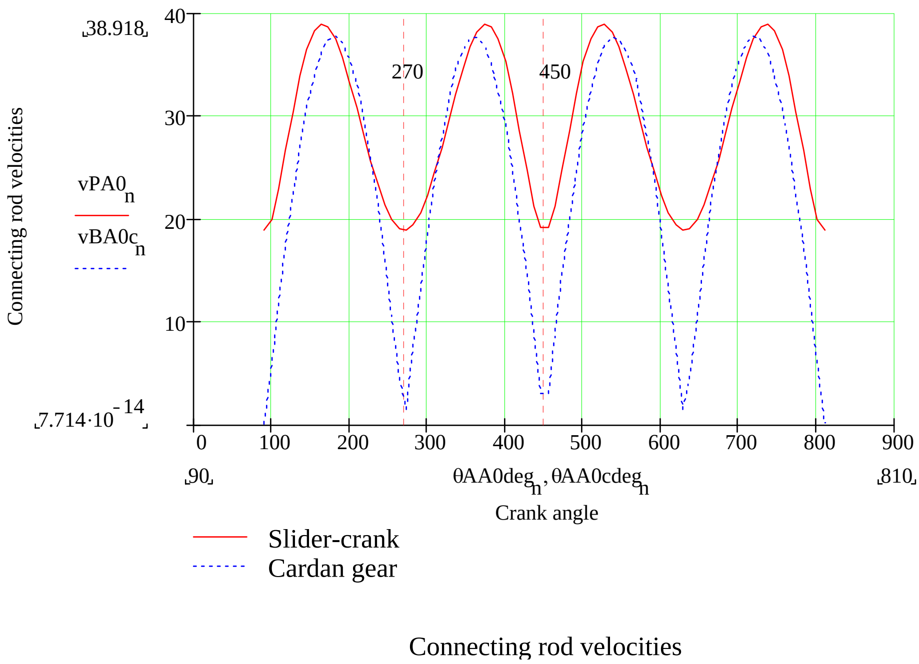

Figure 11.1.5. Connecting rod velocities, ZBA = 2.33·ZAA0, ZAA0 = 0.06 m, ZBA = 0.14 m, αAA0 = 0, ωAA00 = 200π rad/s.

Connecting rod accelerations

The maximum rod acceleration is 11...18 % lower in the cardan gear mechanism than in the slider-crank mechanism, depending on the rod length. The shorter is the rod, the lower is its acceleration in the cardan gear mechanism.
(**Figure 11.1.6, Appendix 11.1.1**)

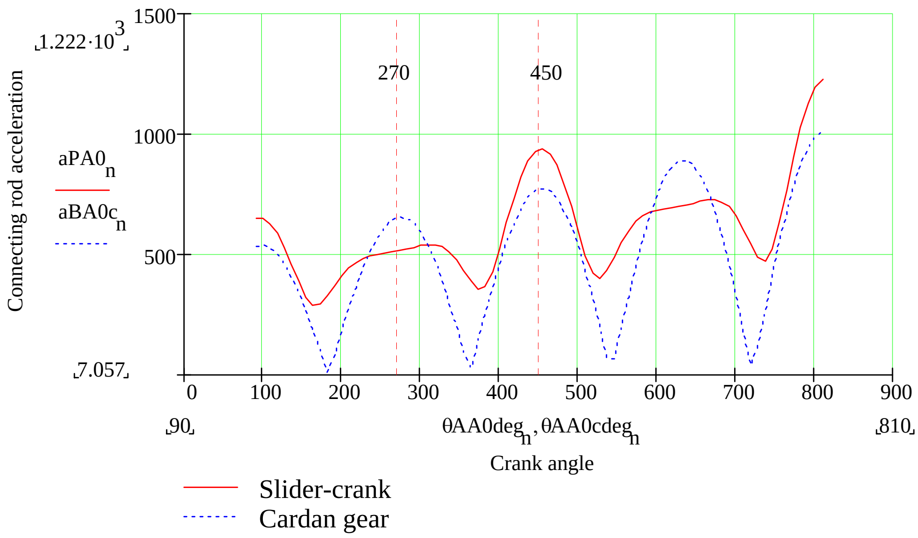

Connecting rod accelerations

Figure 11.1.6. Connecting rod accelerations, ZBA = 2.33·ZAA0, ZAA0 = 0.06 m, ZBA = 0.14 m, αAA0 = 100π rad/s^2, ωAA00 = 30π rad/s.

11.2 Results of kinetostatics

In this study the two mechanisms have been treated as equal as possible. The masses of the components have been estimated so that the pistons are made of aluminum, the crankshafts of steel, the cardan wheel of steel and the connecting rods of steel or titanium. The rotating masses of the bearings have been included in the above-mentioned main components.
The pure pistons and the crankshaft assemblies of the two machines have been treated equal. The cardan gear piston assembly includes the pin and the rod. Also the mass of the cardan gear crankshaft assembly includes the mass of the cardan wheel.

Piston pin inertial joint forces

The conventional piston pin of the cardan gear mechanism can be eliminated because of the straight-line motion and the piston assembly includes also the rod. The two constructions differ from each other at that part and the piston pin inertial joint forces are not comparable.
(**Figure 11.2.1, Appendixes 11.4.1 and 11.6.1**)

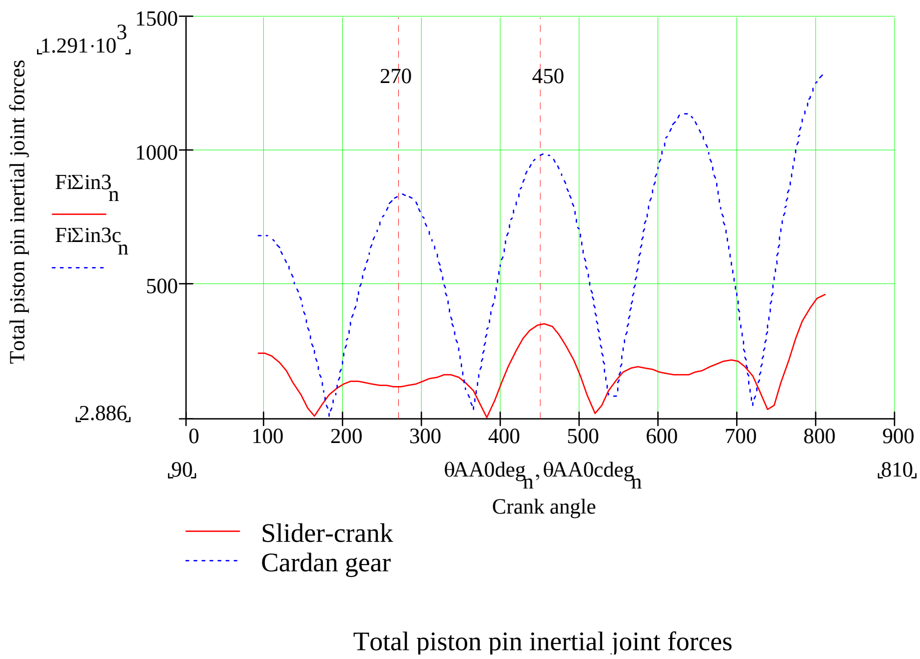

Figure 11.2.1. Piston pin inertial joint forces, ZBA = 2.33·ZAA0, ZAA0 = 0.06 m, ZBA = 0.14 m, αAA0 = 100π rad/s^2, ωAA00 = 30π rad/s.

Crank pin inertial joint forces

When the masses of the moving components are equal, the crank pin inertial joint force maximums are over 50 % bigger in the cardan gear machines than in the slider-crank machines. The main reason to that is the half-size crank length of the cardan gear mechanism. If the light titanium rod is used in the cardan gear machine, the crank pin inertial joint force maximums are approximately equal.
(**Figure 11.2.2, Appendix 11.2.1**)

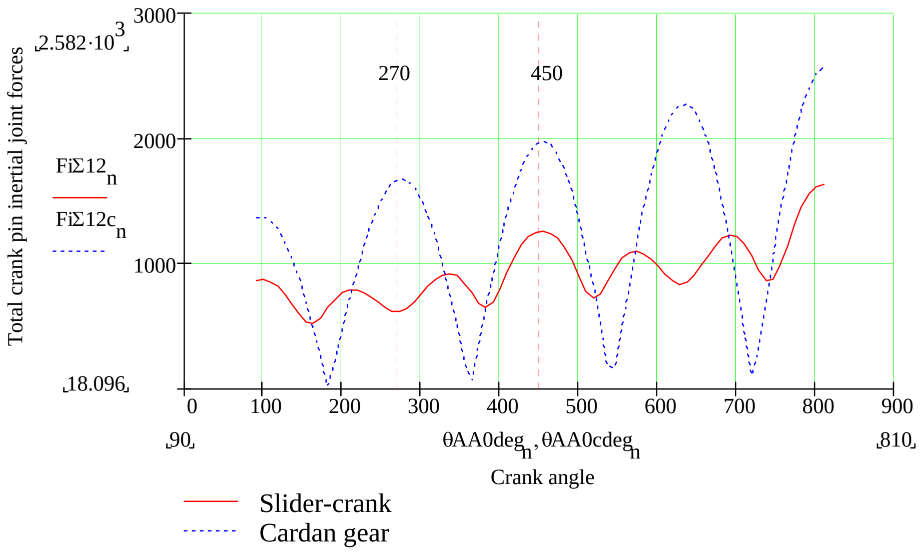

Total crank pin inertial joint forces

Figure 11.2.2. Crank pin inertial joint forces, ZBA = 2.33·ZAA0, ZAA0 = 0.06 m, ZBA = 0.14 m, αAA0 = 100π rad/s², ωAA00 = 30π rad/s.

Main pin inertial joint forces

The main pin inertial joint forces are calculatorily equal with the crank pin inertial joint forces in the present constructions, because the purposeful balancing, clearances and vibrations are neglected.
(**Figure 11.2.3, Appendix 11.2.1**)

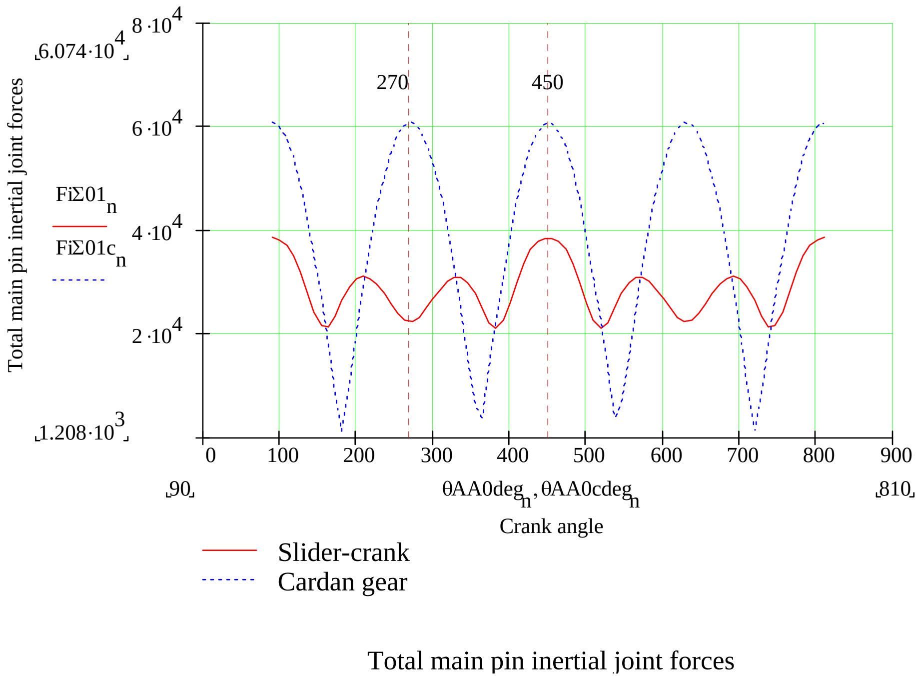

Figure 11.2.3. Main pin inertial joint forces, ZBA = 2.33·ZAA0, ZAA0 = 0.06 m, ZBA = 0.14 m, αAA0 = 0, ωAA00 = 200π rad/s.

The angular acceleration and the angular velocity are different in the examples of the **Figures 11.2.2 and 11.2.3**. So the curves are also different, although the crank pin inertial joint forces and the main pin inertial joint forces are calculatorily equal between the two constructions.

Inertial torques of the crankshafts

When the masses of the moving components are equal, the inertial torque maximum is over 50 % bigger in the cardan gear crankshaft than in the slider-crank crankshaft. The difference results from the clearly different constructions. If the light titanium rod is used in the cardan gear machine, the inertial torque maximums are approximately equal.
The mean inertial torque is 10...30 % smaller in the cardan gear machine than in the slider-crank machine, depending on the rod length and the displacement (= piston mass). The longer is the rod and the bigger is the displacement, the better is the cardan gear machine.
(**Figure 11.2.4, Appendixes 11.2.1 and 11.2.2**)

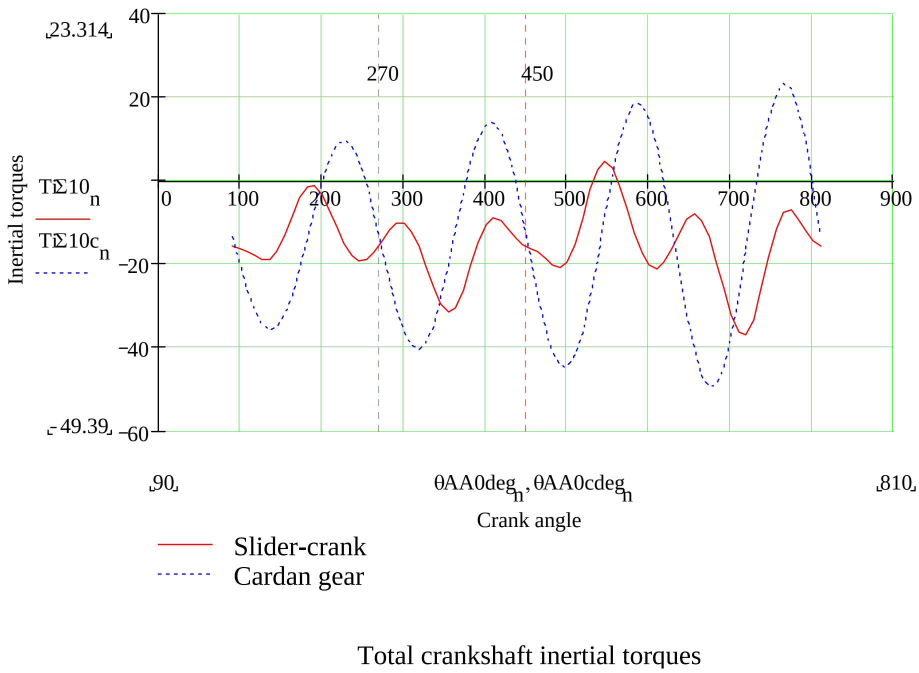

Figure 11.2.4. Crankshaft inertial torques, ZBA = 2.33·ZAA0, ZAA0 = 0.06 m, ZBA = 0.14 m, αAA0 = 100π rad/s², ωAA00 = 30π rad/s.

Inertial works

The inertial works act identically with the mean inertial torques.
(**Appendix 11.2.2**)

Inertial powers

The mean inertial power consumption is 12...40 % smaller in the cardan gear machine than in the slider-crank machine, depending on the rod length and the displacement. That difference is very significant. The longer is the rod and the bigger is the displacement (piston mass), the better is the cardan gear machine. The mass of the rod (steel or titanium) affects the results very little, because the effects of the mass inertia of the different components compensate each other.
(**Figure 11.2.5, Appendix 11.2.2**)

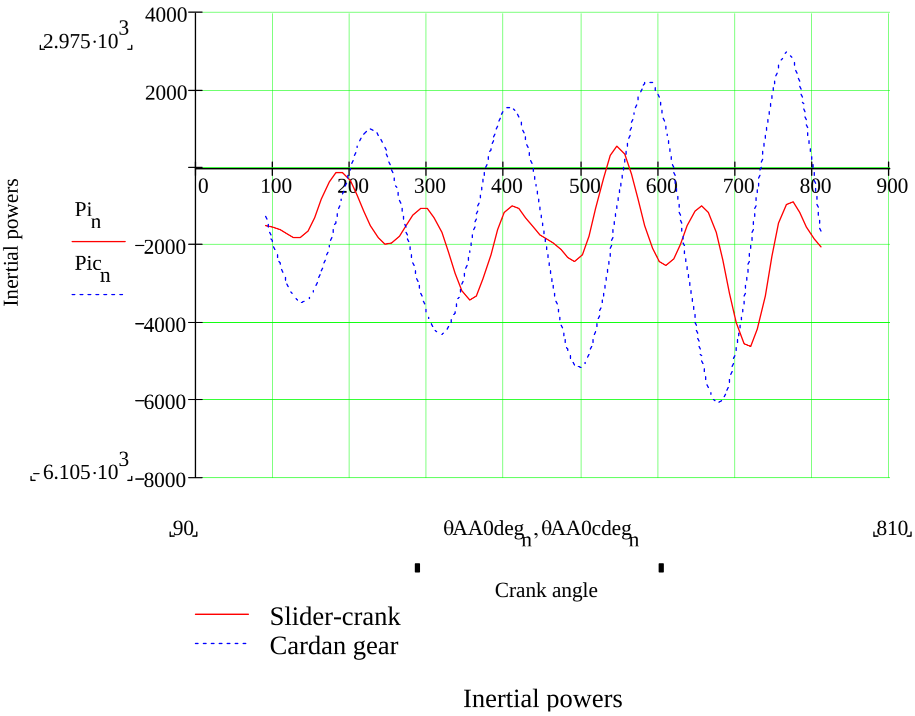

Figure 11.2.5. Inertial powers, ZBA = 2.33·ZAA0, ZAA0 = 0.06 m, ZBA = 0.14 m, αAA0 = 100π rad/s^2, ωAA00 = 30π rad/s.

11.3 Results of kinetics including thermodynamics

The standard atmospheric pressure (= 1 atm) used in calculations is
p_{atm} = 1.01325 · 10^5 Pa.

Compression pressures

The maximum compression pressures at the TDC of the two machines are equal. The compression pressures of the cardan gear machines are 0...10 % bigger between the TDC and the BDC than the compression pressures of the slider-crank machines, when the valves are closed.
(**Figure 11.3.1, Appendix 11.3.1**)

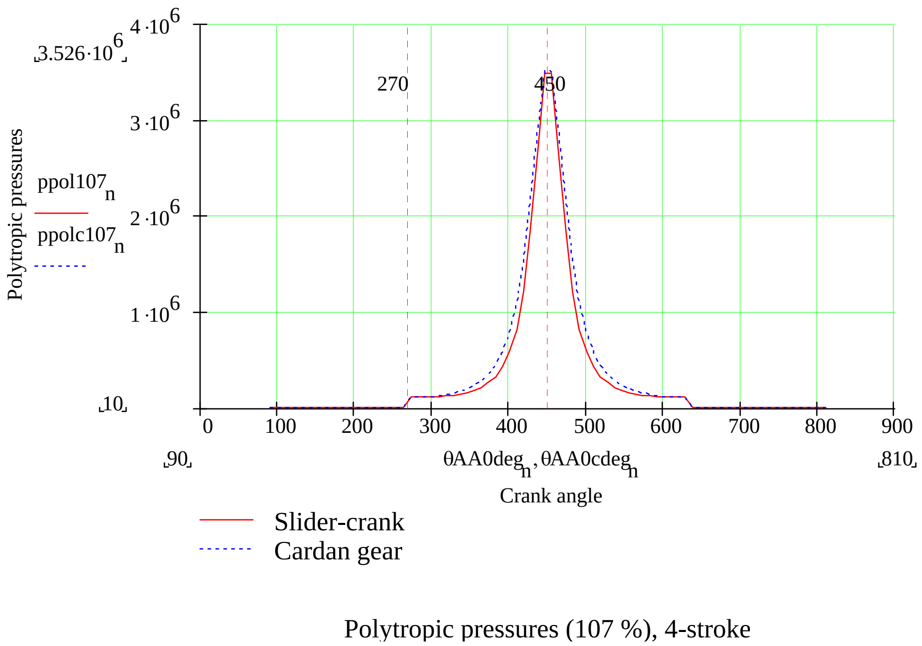

Figure 11.3.1. Compression pressures, four-stroke engine without combustion, cylinder filling 107 %, compression ratio 12:1, polytropic exponent 1.4, ZBA = 2.33·ZAA0, ZAA0 = 0.06 m, ZBA = 0.14 m, displacement 1357 cm^3.

Compression torques of the crankshafts

The maximum compression torque is 10...16 % smaller in the cardan gear machine (Piston diameter = 2·ZAA0) than in the slider-crank machine, depending on the rod length. The shorter is the rod, the lower is the compression torque of the cardan gear machine compared to the compression torque of the equal slider-crank machine. That means power savings (smaller motor size) in pump constructions.
The mean compression torques of the cardan gear machine and the slider-crank machine are equal.
(**Figure 11.3.2, Appendix 11.3.1**)

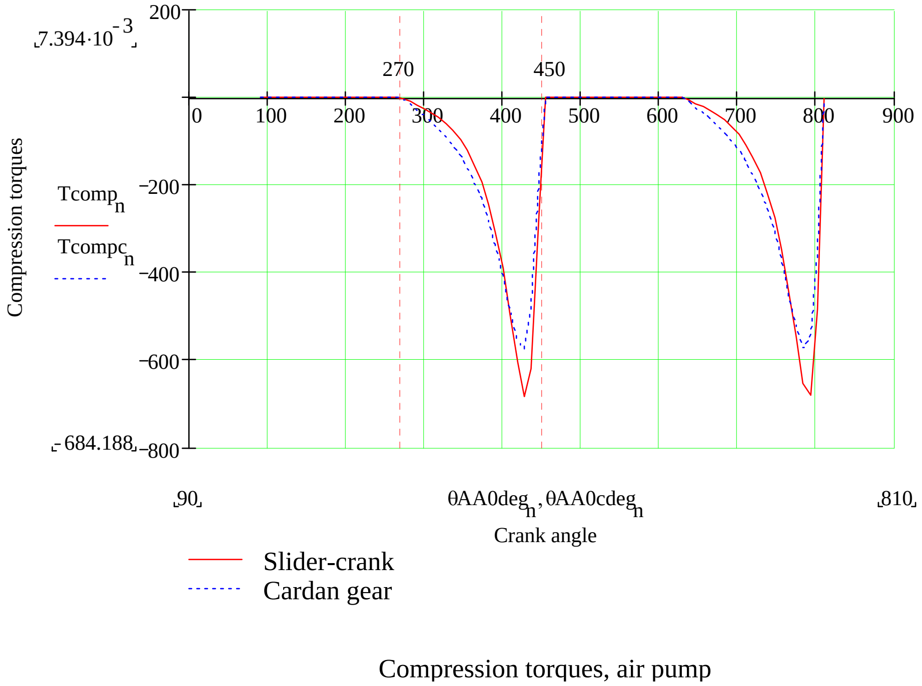

Figure 11.3.2. Compression torques, air pump, cylinder filling 107 %, compression ratio 12:1, maximum pressures, zero flow rate, polytropic exponent 1.4, piston diameter 2·ZAA0, ZBA = 2.33·ZAA0, ZAA0 = 0.06 m, ZBA = 0.14 m, displacement 1357 cm^3.

Compression works

The compression works act identically with the mean compression torques and are equal between the two machines.
(**Appendix 11.3.1**)

Compression powers

The mean compression powers of the compared machines are calculatorily equal.
(**Figure 11.3.3, Appendix 11.3.1**)

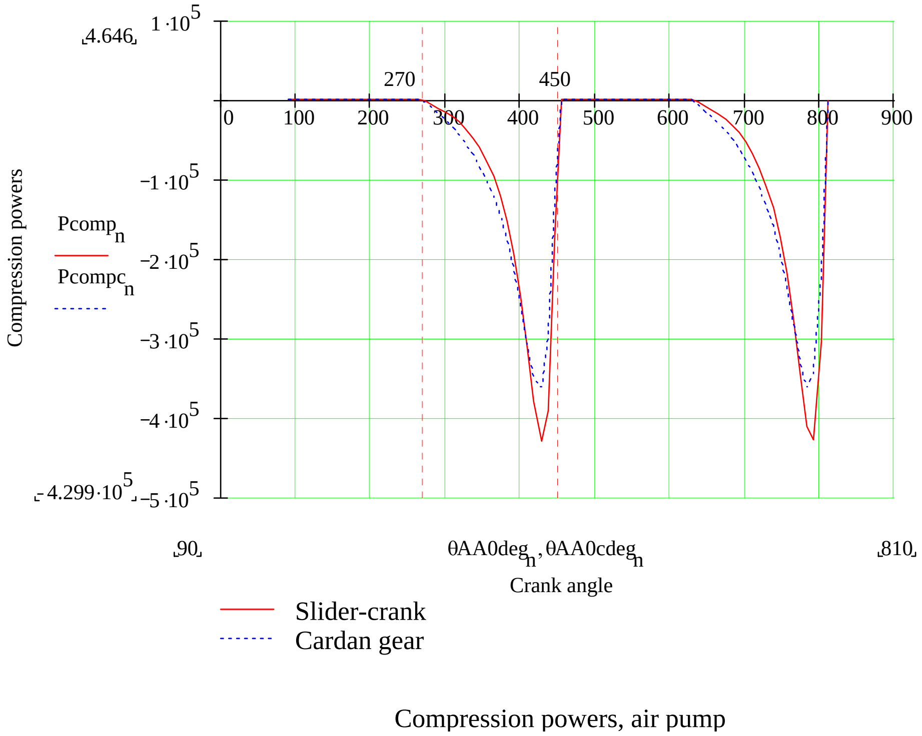

Figure 11.3.3. Compression powers, air pump, cylinder filling 107 %, compression ratio 12:1, maximum pressures, zero flow rate, polytropic exponent 1.4, piston diameter 2·ZAA0, ZBA = 2.33·ZAA0, ZAA0 = 0.06 m, ZBA = 0.14 m, displacement 1357 cm^3, αAA0 = 0, ωAA00 = 200π rad/s.

Combustion pressures

The maximum combustion pressures at the TDC of the engines are equal.
The combustion pressure is 0...10 % bigger during the power stroke, after the TDC, in the cardan gear engine than in the slider-crank engine. The shorter is the rod, the higher is the combustion pressure of the cardan gear machine compared to the combustion pressure of the equal slider-crank machine.
(**Figure 11.3.4, Appendix 11.3.2**)

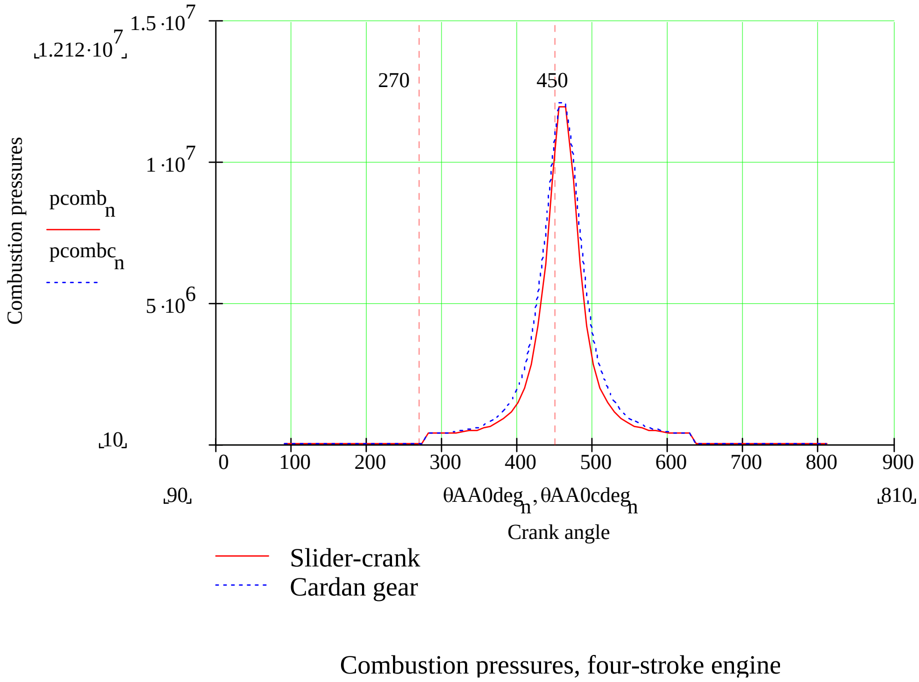

Figure 11.3.4. Combustion pressures, four-stroke engine, cylinder filling 107 %, compression ratio 12:1, maximum combustion pressure 12 MPa, gasoline combustion, ZBA = 2.33·ZAA0, ZAA0 = 0.06 m, ZBA = 0.14 m, displacement 1357 cm^3.

Combustion torques of the crankshafts

The maximum combustion torque is 13...22 % smaller in the cardan gear engine (Piston diameter = 2·ZAA0) than in the slider-crank engine, depending on the rod length.
The mean combustion torque is 8...15 % smaller in the cardan gear engine than in the slider-crank engine. The main reason is the half-size crank length of the cardan gear mechanism. The shorter is the rod, the lower is the combustion torque of the cardan gear machine compared to the combustion torque of the equal slider-crank machine.
(**Figure 11.3.5, Appendix 11.3.2**)

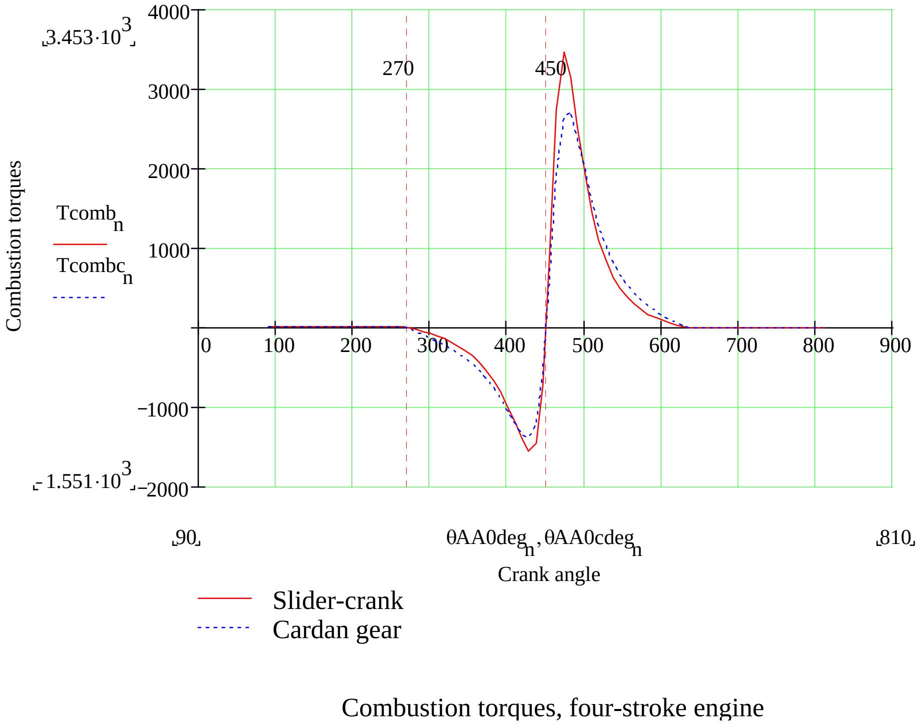

Figure 11.3.5. Combustion torques, four-stroke engine, cylinder filling 107 %, compression ratio 12:1, maximum combustion pressure 12 MPa, gasoline combustion, piston diameter 2·ZAA0, ZBA = 2.33·ZAA0, ZAA0 = 0.06 m, ZBA = 0.14 m, displacement 1357 cm^3.

Combustion works

The combustion works act identically with the mean combustion torques.
(Appendix 11.3.2)

Combustion powers

The mean combustion powers act quite identically with the mean combustion torques and also with the combustion works.
(**Figure 11.3.6, Appendix 11.3.2**)

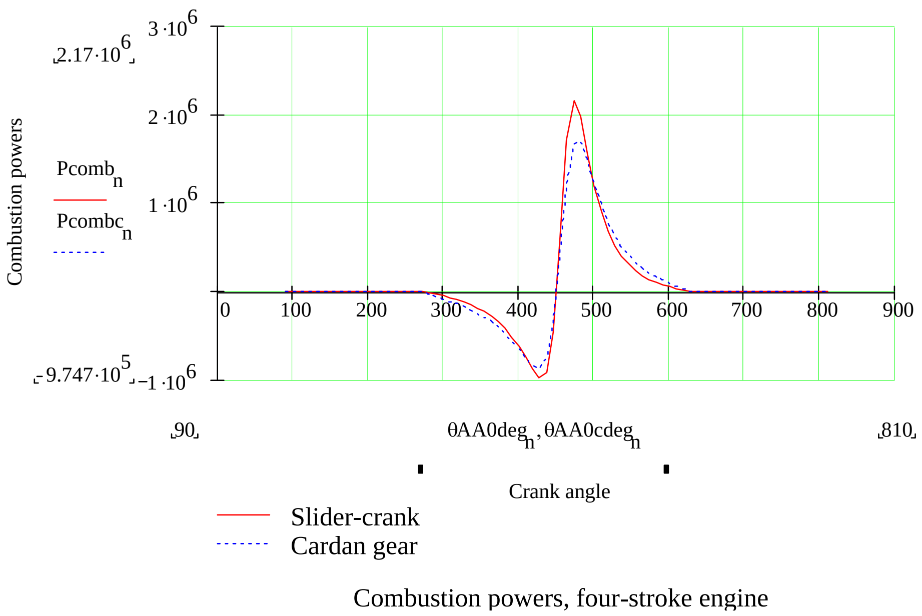

Figure 11.3.6. Combustion powers, four-stroke engine, cylinder filling 107 %, compression ratio 12:1, maximum combustion pressure 12 MPa, gasoline combustion, piston diameter 2·ZAA0, ZBA = 2.33·ZAA0, ZAA0 = 0.06 m, ZBA = 0.14 m, displacement 1357 cm^3, αAA0 = 0, ωAA00 = 200π rad/s.

11.4 Results of the summed lossless Newtonian dynamics

Lossless piston pin total joint forces

The conventional piston pin of the cardan gear mechanism can be eliminated because of the straight-line motion and the piston assembly includes also the rod. The two constructions differ from each other at that part and the piston pin total joint forces are not comparable.
(**Figure 11.4.1, Appendix 11.4.1**)

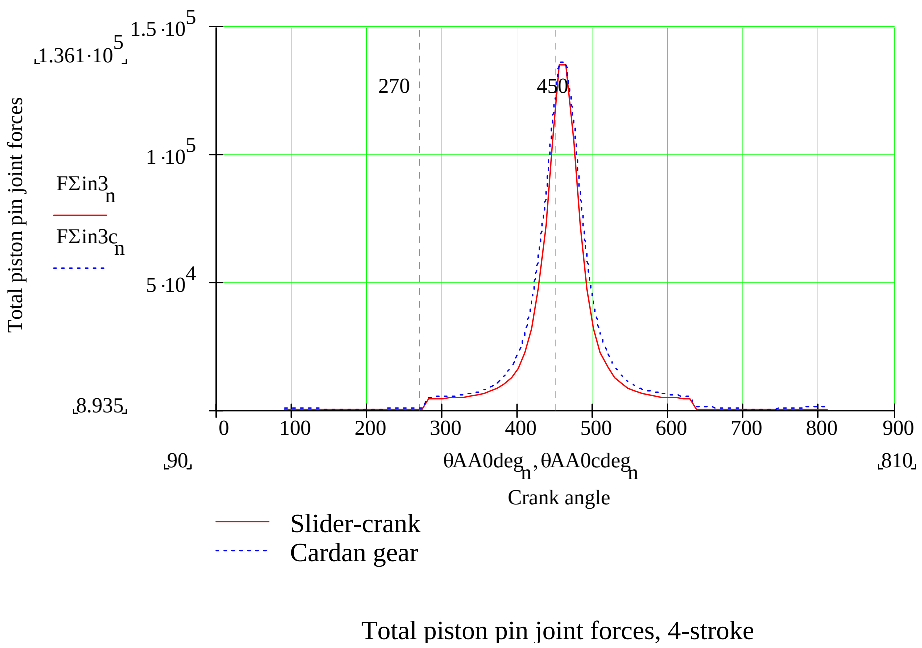

Figure 11.4.1. Piston pin total joint forces, four-stroke engine, cylinder filling 107 %, compression ratio 12:1, maximum combustion pressure 12 MPa, gasoline combustion, piston diameter 2·ZAA0, ZBA = 2.33·ZAA0, ZAA0 = 0.06 m, ZBA = 0.14 m, displacement 1357 cm^3, αAA0 = 100π rad/s^2, ωAA00 = 30π rad/s.

Lossless crank pin total joint forces

The crank pin total joint force maximums are at least 100 % bigger in the cardan gear machines than in the slider-crank machines. The main reason is the half-size crank length of the cardan gear mechanism.
(**Figure 11.4.2, Appendix 11.4.1**)

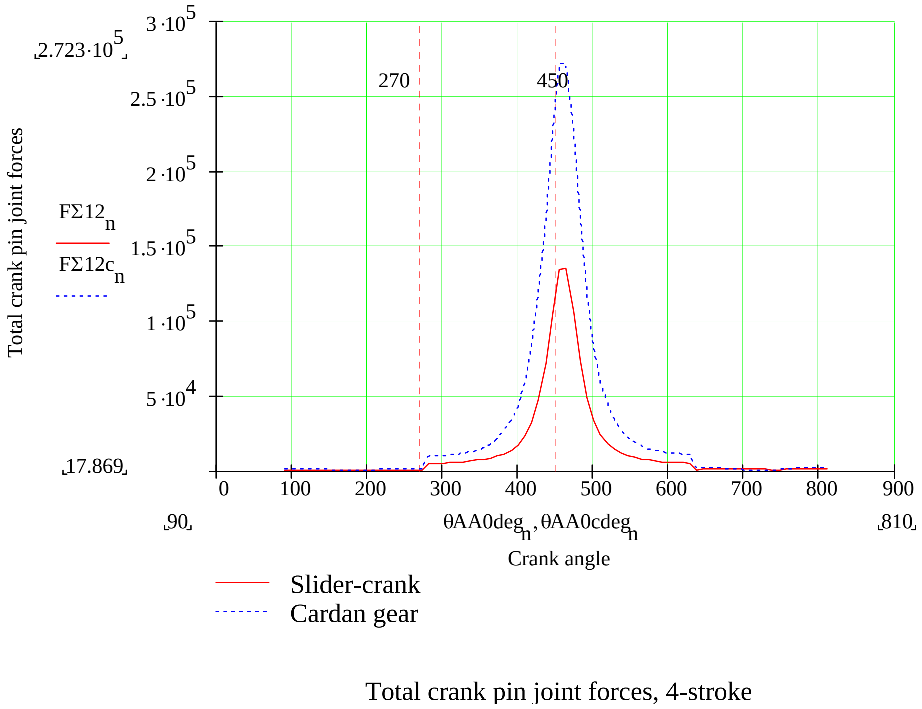

Figure 11.4.2. Crank pin total joint forces, four-stroke engine, cylinder filling 107 %, compression ratio 12:1, maximum combustion pressure 12 MPa, gasoline combustion, piston diameter 2·ZAA0, ZBA = 2.33·ZAA0, ZAA0 = 0.06 m, ZBA = 0.14 m, displacement 1357 cm^3, αAA0 = 100π rad/s^2, ωAA00 = 30π rad/s.

Lossless main pin total joint forces

The main pin total joint forces are calculatorily equal with the crank pin total joint forces in the present constructions, when the purposeful balancing, gravitation, frictions, clearances and vibrations have been neglected.
(**Figure 11.4.3, Appendix 11.4.1**)

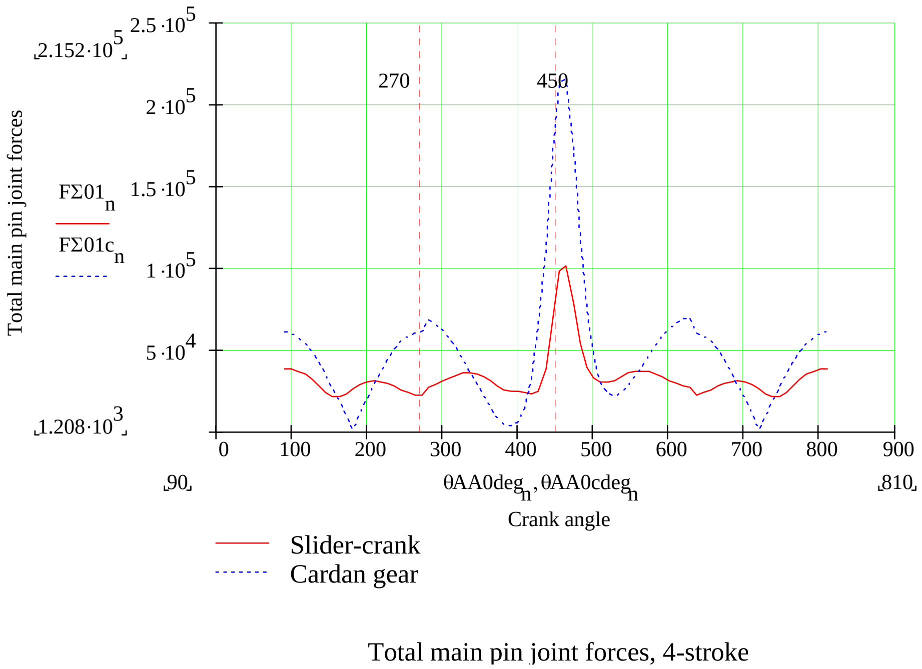

Figure 11.4.3. Main pin total joint forces, four-stroke engine, cylinder filling 107 %, compression ratio 12:1, maximum combustion pressure 12 MPa, gasoline combustion, piston diameter 2·ZAA0, ZBA = 2.33·ZAA0, ZAA0 = 0.06 m, ZBA = 0.14 m, displacement 1357 cm^3, αAA0 = 0, ωAA00 = 200π rad/s.

The angular acceleration and the angular velocity are different in the examples of the **Figures 11.4.2 and 11.4.3**. So the curves are also different, although the crank pin total joint forces and the main pin total joint forces are calculatorily equal between the two constructions.

Lossless total torques of the crankshafts

In pumps and engines the total torque maximums of the cardan gear crankshafts are 11...25 % smaller at low angular velocities than the total torque maximums of the slider-crank crankshafts. At the angular velocity range 100π...140π rad/s (= 3000...4200 r/min) the total torque maximums vary a lot, but the maximums of the cardan gear crankshaft can be seen 30 % smaller than the maximums of the slider-crank crankshaft. At these and higher angular velocities the inertial torques either compensate or increase the compression torques quite variably.
In the air pumps the mean total torque of the cardan gear crankshaft is 1...8 % smaller than the mean total torque of the slider-crank crankshaft, depending on the rod length and the displacement.
In the four-stroke engines the mean total torque difference between the cardan gear crankshaft and the slider-crank crankshaft is -14 ... +6 %, depending on the rod length and the displacement. The longer is the rod and the bigger is the displacement, the better is the cardan gear pump or the cardan gear engine.
(**Figure 11.4.4, Appendixes 11.4.1 and 11.4.2**)

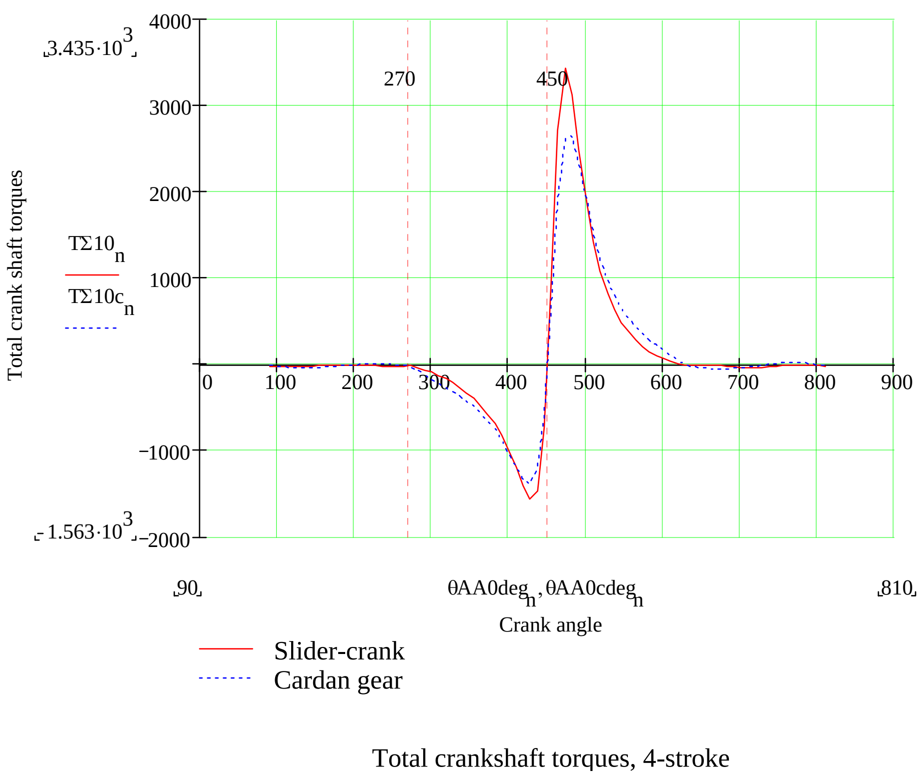

Figure 11.4.4. Lossless total torques, four-stroke engine, cylinder filling 107 %, compression ratio 12:1, maximum combustion pressure 12 MPa, gasoline combustion, piston diameter 2·ZAA0, ZBA = 2.33·ZAA0, ZAA0 = 0.06 m, ZBA = 0.14 m, displacement 1357 cm^3, αAA0 = 100π rad/s^2, ωAA00 = 30π rad/s.

Lossless total works

The total work act identically with the mean total torque.
The smaller work of the cardan gear air pump means energy savings.
(Appendix 11.4.2)

Lossless total powers

The mean total power consumption is 1...10 % smaller in the cardan gear air pump than in the slider-crank air pump, depending on the rod length and the displacement. The difference of the mean total power output between the cardan gear four-stroke engine and the slider-crank four-stroke engine is -14 ... +12 %, depending on the rod length and the displacement. The longer is the rod and the bigger is the displacement, the better is the cardan gear pump or the cardan gear engine.
(**Figure 11.4.5, Appendix 11.4.2**)

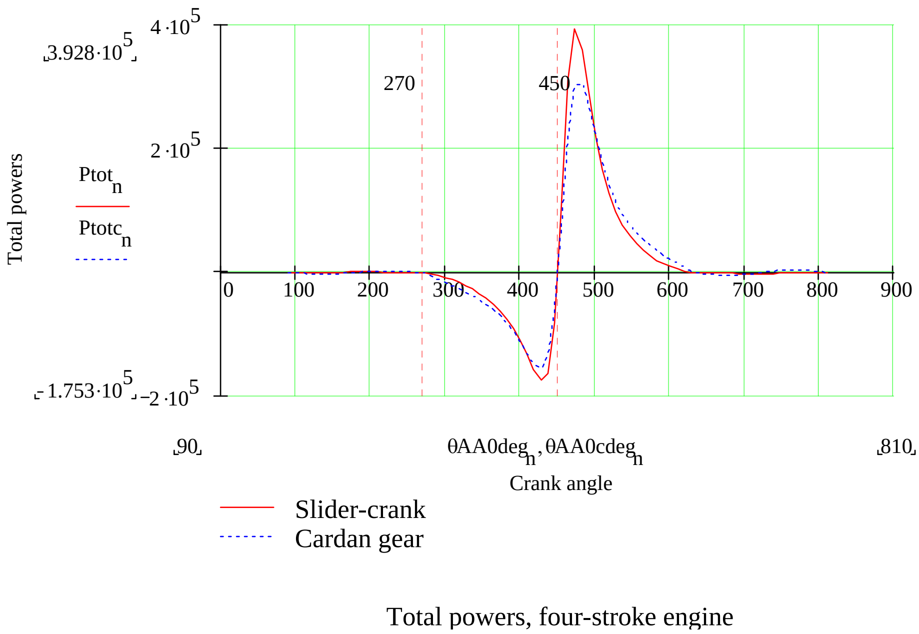

Figure 11.4.5. Lossless total powers, four-stroke engine, cylinder filling 107 %, compression ratio 12:1, maximum combustion pressure 12 MPa, gasoline combustion, piston diameter 2·ZAA0, ZBA = 2.33·ZAA0, ZAA0 = 0.06 m, ZBA = 0.14 m, displacement 1357 cm^3, αAA0 = 100π rad/s^2, ωAA00 = 30π rad/s.

11.5 Results of the dynamic tooth loads of the cardan gear mesh

If the cardan gear machines are constructed in the original way with gears, we may assume that the dynamic loads of the gear mesh are very high. The calculated results do not completely support that thought. In the air pumps the calculated dynamic tooth loads are 25...160 % bigger and in the four-stroke engines ≲ 40 % bigger than the steady piston pin joint forces.
(**Figures 11.4.1 and 11.5.1, Appendixes 11.4.1 and 11.6.1**)

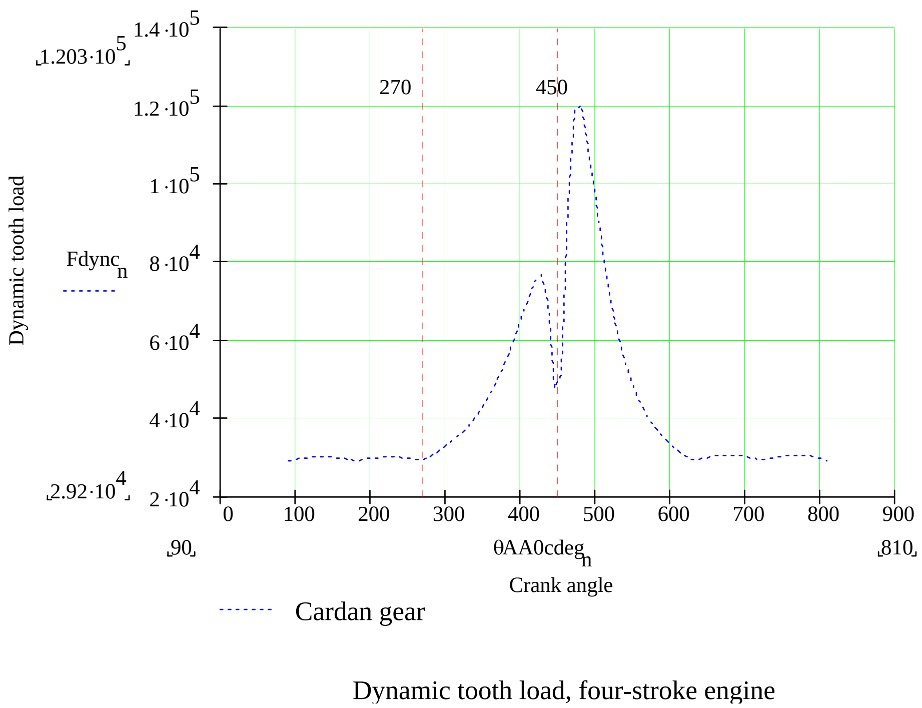

Figure 11.5.1. Dynamic tooth load of the cardan wheel gear mesh, four-stroke engine, cylinder filling 107 %, compression ratio 12:1, maximum combustion pressure 12 MPa, gasoline combustion, piston diameter 2·ZAA0, ZBA = 2.33·ZAA0, ZAA0 = 0.06 m, ZBA = 0.14 m, displacement 1357 cm^3, αAA0 = 100π rad/s^2, ωAA00 = 30π rad/s.

11.6 Results of the operational torques, powers and mechanical efficiencies

Total power losses

The mean power losses are generally 0...75 % smaller in the cardan gear machines than in the slider-crank machines. Only at the very low angular velocities the mean power losses of the cardan gear machines are 0...35 % bigger than the mean power losses of the slider-crank machines. The longer is the rod and the bigger is the displacement, the better is the cardan gear pump or the cardan gear engine. (**Figure 11.6.1, Appendix 11.6.1**)

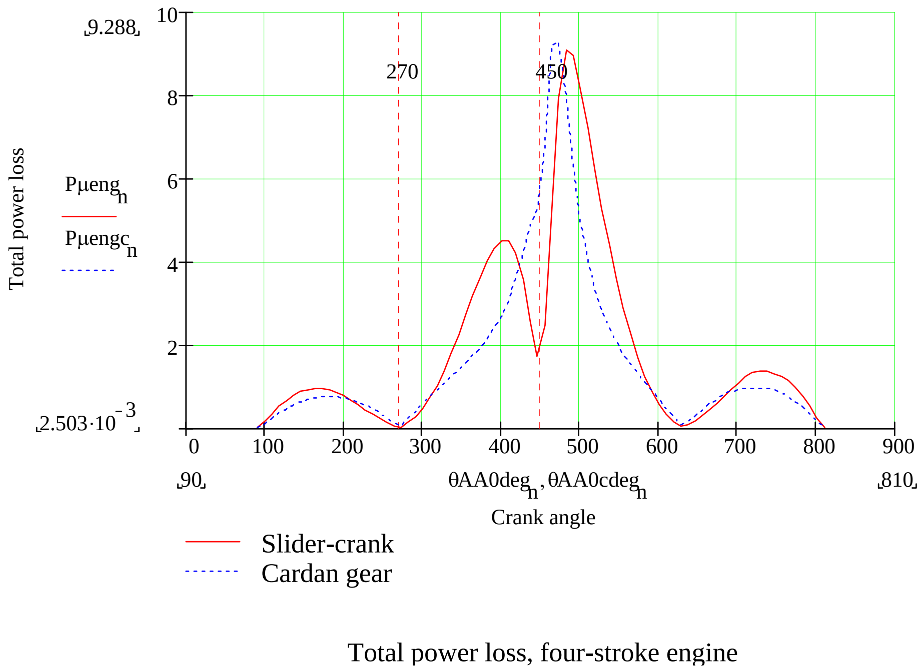

Figure 11.6.1. Total power loss, four-stroke engine, cylinder filling 107 %, compression ratio 12:1, maximum combustion pressure 12 MPa, gasoline combustion, piston diameter 2·ZAA0, ZBA = 2.33·ZAA0, ZAA0 = 0.06 m, ZBA = 0.14 m, displacement 1357 cm^3, αAA0 = 100π rad/s^2, ωAA00 = 30π rad/s.

Operational torques

The operational mean torque need is generally 0...30 % smaller in the cardan gear air pumps than in the slider-crank air pumps.
The higher are the angular velocities and the angular accelerations, the bigger are the output torques of the cardan gear four-stroke engines compared to the slider-crank four-stroke engines. At the low angular velocities the mean output torques are 0...15 % smaller in the cardan gear engines than in the slider-crank engines. At the high angular velocities and angular accelerations the mean output torques of the cardan gear engines are 0...30...50... even hundreds of percent bigger.
(**Figures 11.6.2, 11.6.4, 11.6.7, 11.6.10, 11.6.13 and 11.6.16, Appendix 11.6.1**)

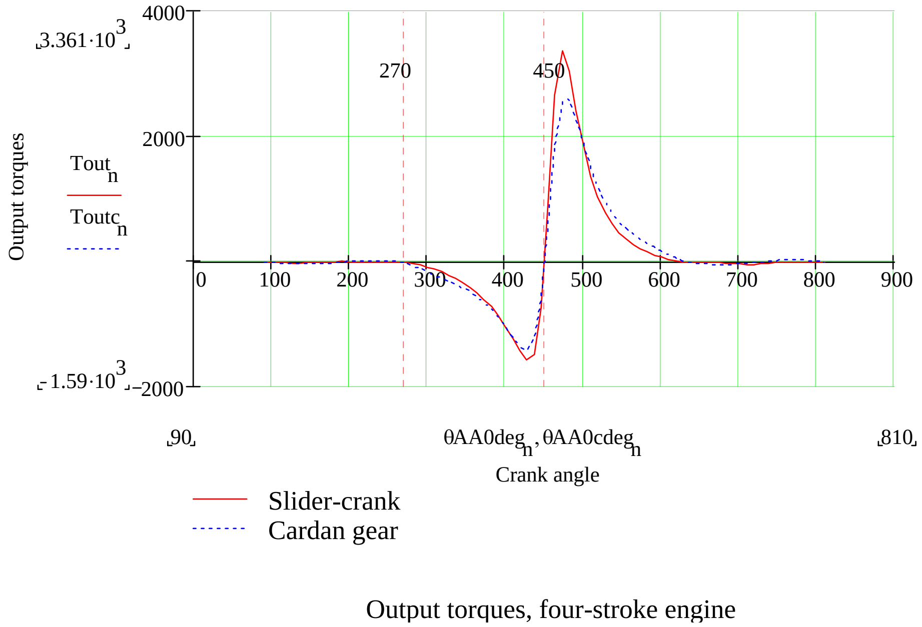

Figure 11.6.2. Output torques, four-stroke engine, cylinder filling 107 %, compression ratio 12:1, maximum combustion pressure 12 MPa, gasoline combustion, piston diameter 2·ZAA0, ZBA = 2.33·ZAA0, ZAA0 = 0.06 m, ZBA = 0.14 m, displacement 1357 cm^3, αAA0 = 100π rad/s^2, ωAA00 = 30π rad/s.

Operational powers

The operational powers act quite identically with the operational torques.
The operational mean power need is 0...30 % smaller in the cardan gear air pumps than in the slider-crank air pumps.
At the low angular velocities the mean output power is 0...15 % smaller in the cardan gear engines than in the slider-crank engines. At the high angular velocities and angular accelerations the mean output power of the cardan gear engine is even hundreds of percent bigger.
(**Figures 11.6.3, 11.6.5, 11.6.8, 11.6.11, 11.6.14 and 11.6.17, Appendix 11.6.1**)

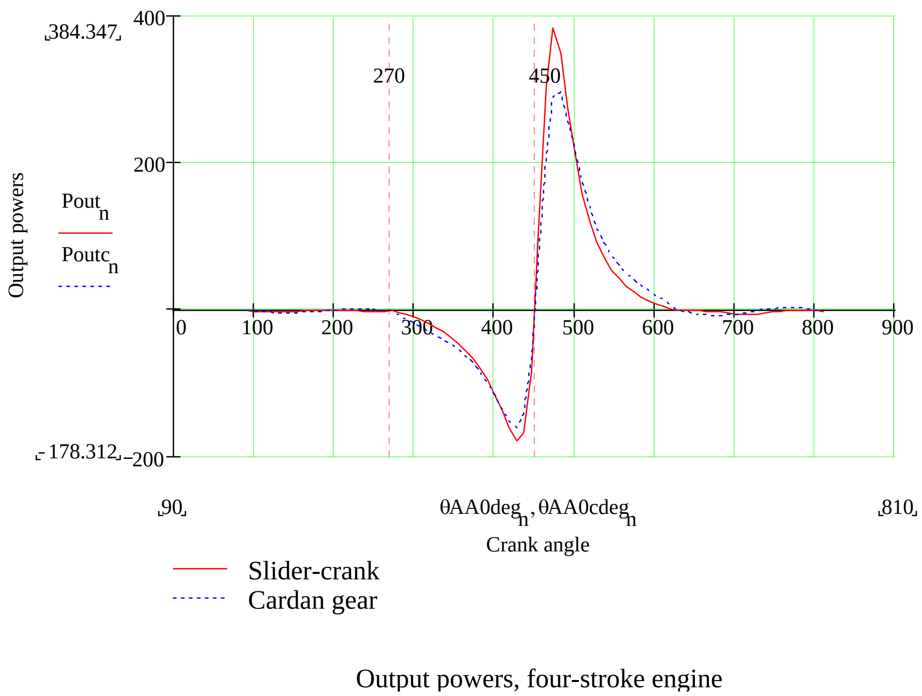

Figure 11.6.3. Output powers, four-stroke engine, cylinder filling 107 %, compression ratio 12:1, maximum combustion pressure 12 MPa, gasoline combustion, piston diameter 2·ZAA0, ZBA = 2.33·ZAA0, ZAA0 = 0.06 m, ZBA = 0.14 m, displacement 1357 cm^3, αAA0 = 100π rad/s^2, ωAA00 = 30π rad/s.

Mechanical efficiencies

The mechanical efficiencies of the cardan gear machines are generally 0...30...50... even hundreds of percent bigger than the mechanical efficiencies of the slider-crank machines. Only at the very low angular velocities the mechanical efficiencies of the cardan gear machines are 0...8 % smaller than the mechanical efficiencies of the slider-crank machines. The longer is the rod and the bigger is the displacement, the better is the cardan gear pump or the cardan gear engine.
(**Figures 11.6.6, 11.6.9, 11.6.12, 11.6.15 and 11.6.18, Appendix 11.6.1**)

Design charts that include examples of the operational torques, powers and mechanical efficiencies of the studied air pumps and four-stroke engines have been presented in the **Figures 11.6.4 ... 11.6.18**.

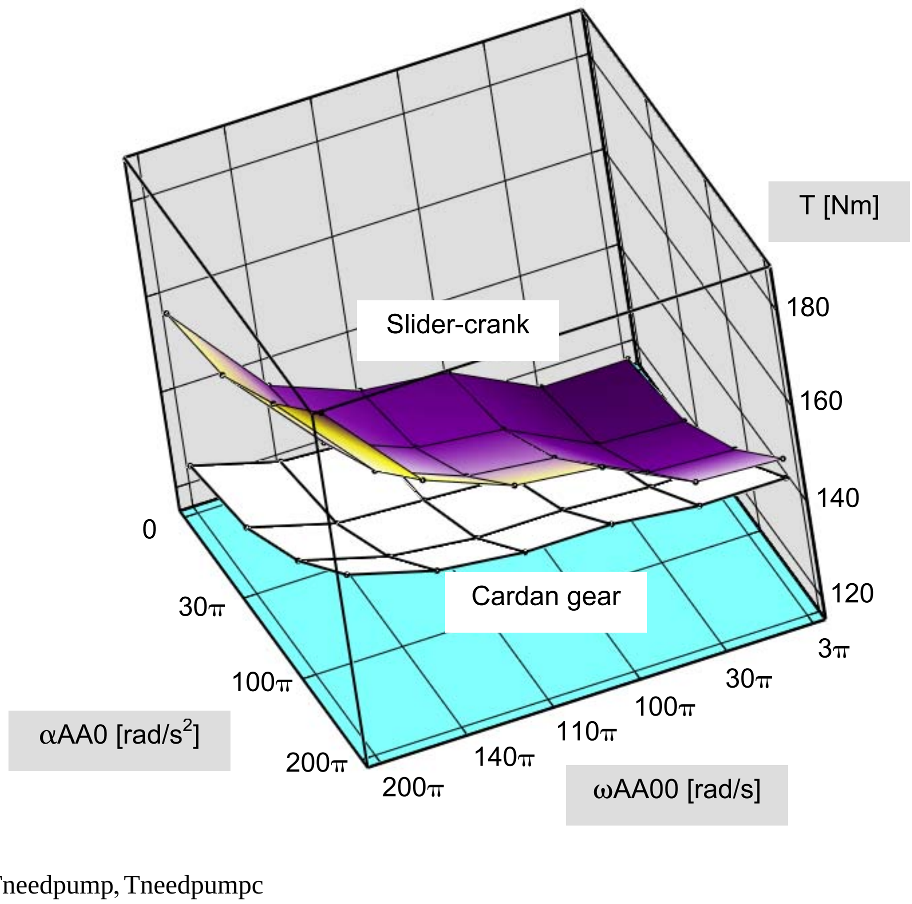

Figure 11.6.4. Torque needs, air pump, cylinder filling 107 %, compression ratio 12:1, maximum pressures, zero flow rate, polytropic exponent 1.4, piston diameter 2·ZAA0, ZBA = 2.33·ZAA0, ZAA0 = 0.06 m, ZBA = 0.14 m, displacement 1357 cm^3.

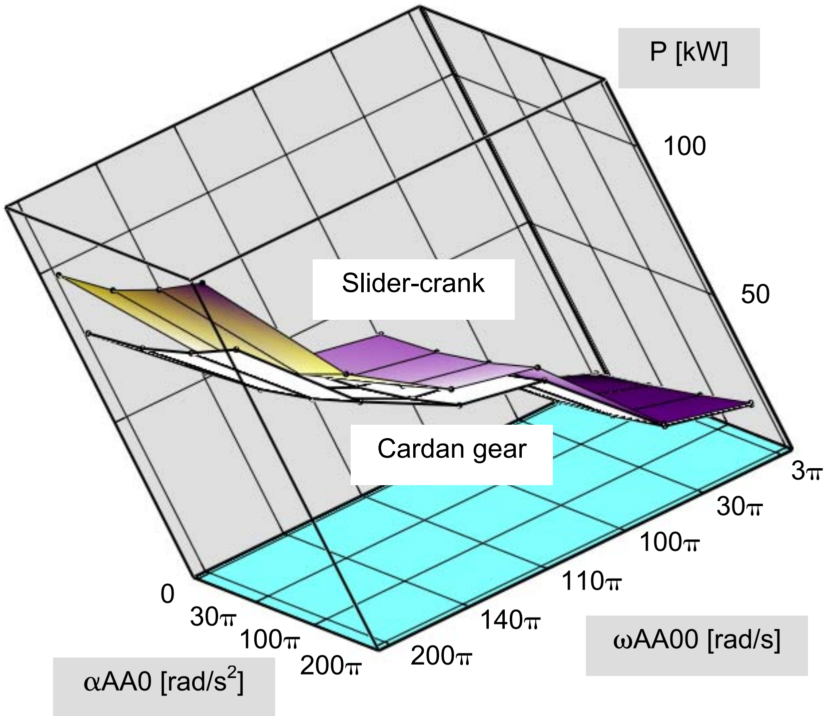

Pneedpump, Pneedpumpc

Figure 11.6.5. Power needs, air pump, cylinder filling 107 %, compression ratio 12:1, maximum pressures, zero flow rate, polytropic exponent 1.4, piston diameter 2·ZAA0, ZBA = 2.33·ZAA0, ZAA0 = 0.06 m, ZBA = 0.14 m, displacement 1357 cm^3.

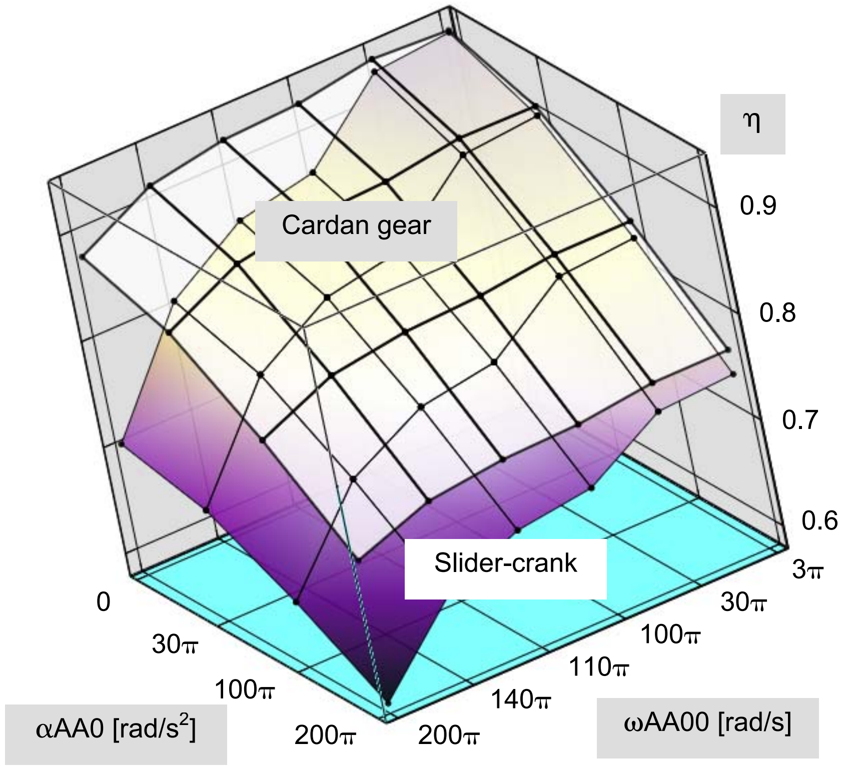

ηmpump, ηmpumpc

Figure 11.6.6. Mechanical efficiencies, air pump, cylinder filling 107 %, compression ratio 12:1, maximum pressures, zero flow rate, polytropic exponent 1.4, piston diameter 2·ZAA0, ZBA = 2.33·ZAA0, ZAA0 = 0.06 m, ZBA = 0.14 m, displacement 1357 cm^3.

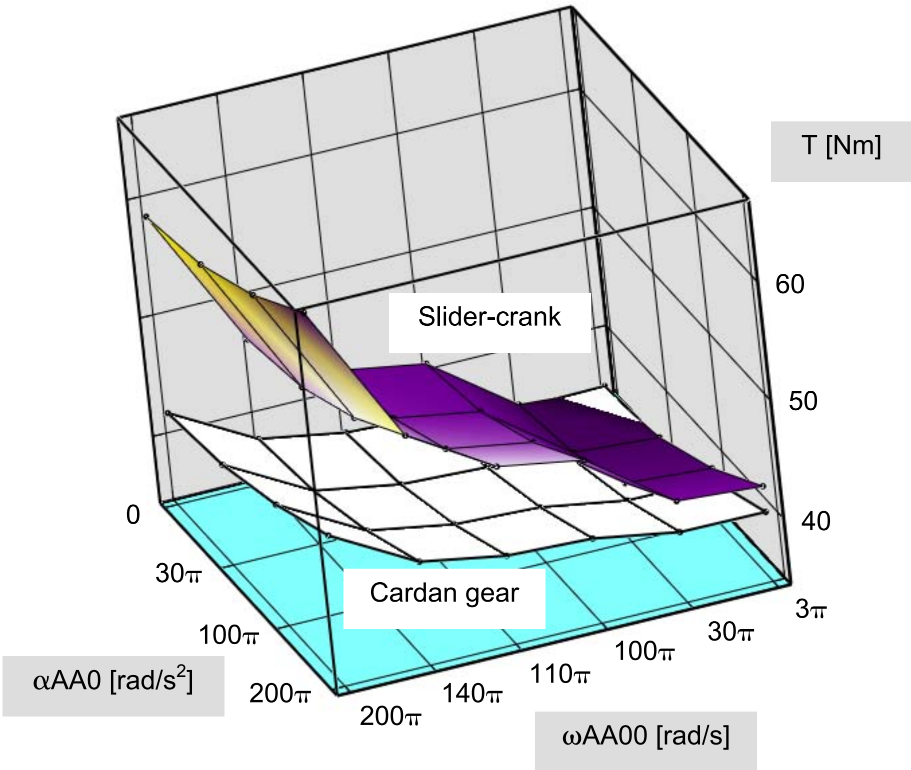

Tneedpump, Tneedpumpc

Figure 11.6.7. Torque needs, air pump, cylinder filling 107 %, compression ratio 12:1, maximum pressures, zero flow rate, polytropic exponent 1.4, piston diameter 2·ZAA0, ZBA = 4·ZAA0, ZAA0 = 0.04 m, ZBA = 0.16 m, displacement 402 cm^3.

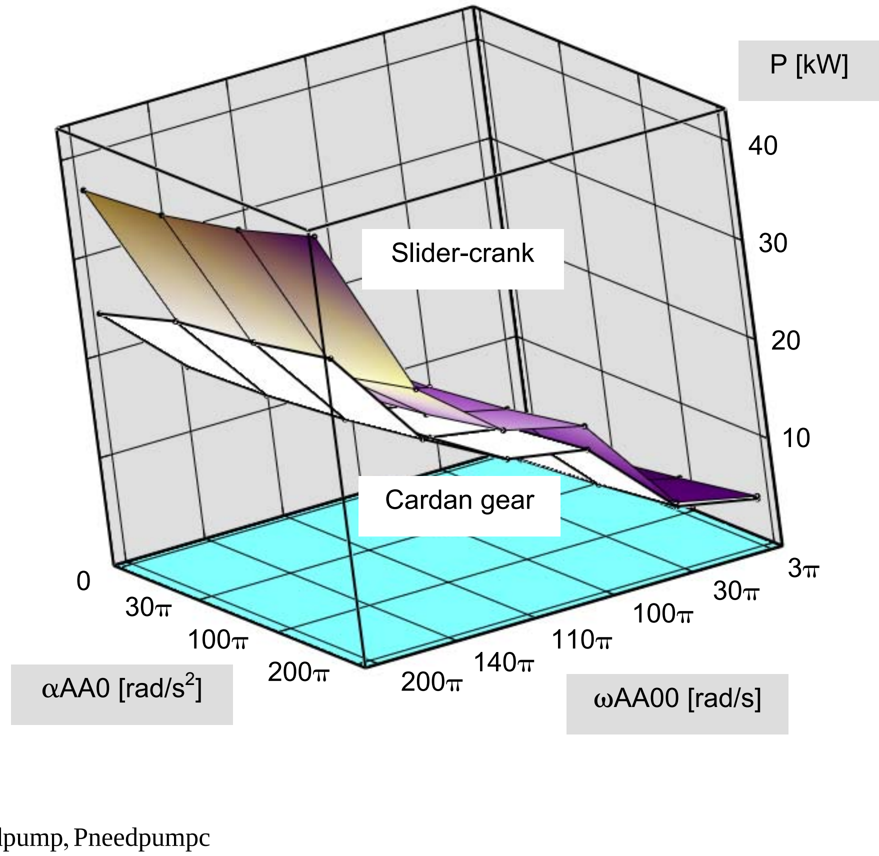

Figure 11.6.8. Power needs, air pump, cylinder filling 107 %, compression ratio 12:1, maximum pressures, zero flow rate, polytropic exponent 1.4, piston diameter 2·ZAA0, ZBA = 4·ZAA0, ZAA0 = 0.04 m, ZBA = 0.16 m, displacement 402 cm^3.

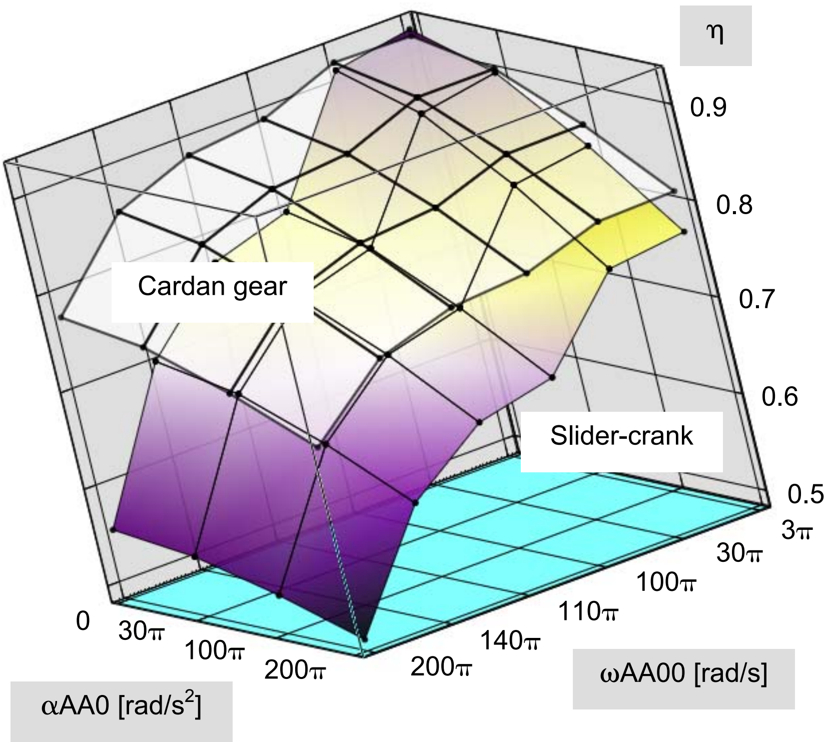

ηmpump, ηmpumpc

Figure 11.6.9. Mechanical efficiencies, air pump, cylinder filling 107 %, compression ratio 12:1, maximum pressures, zero flow rate, polytropic exponent 1.4, piston diameter 2·ZAA0, ZBA = 4·ZAA0, ZAA0 = 0.04 m, ZBA = 0.16 m, displacement 402 cm^3.

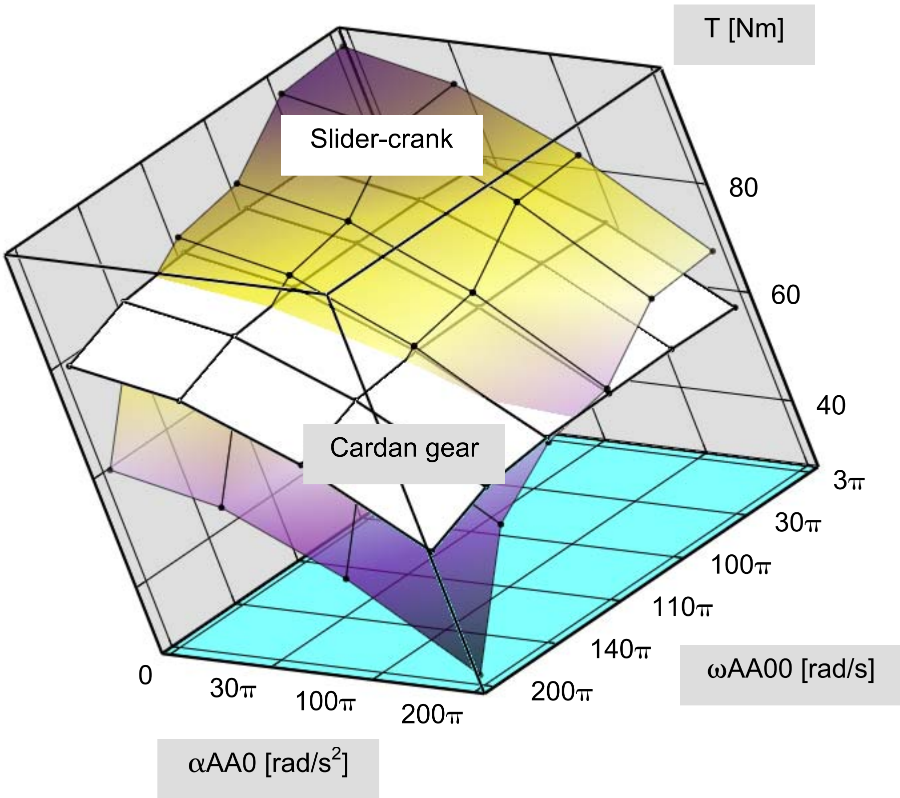

Touteng, Toutengc

Figure 11.6.10. Output torques, four-stroke engine, cylinder filling 107 %, compression ratio 12:1, maximum combustion pressure 12 MPa, gasoline combustion, polytropic exponent 1.4, piston diameter 2·ZAA0, ZBA = 2.33·ZAA0, ZAA0 = 0.06 m, ZBA = 0.14 m, displacement 1357 cm^3.

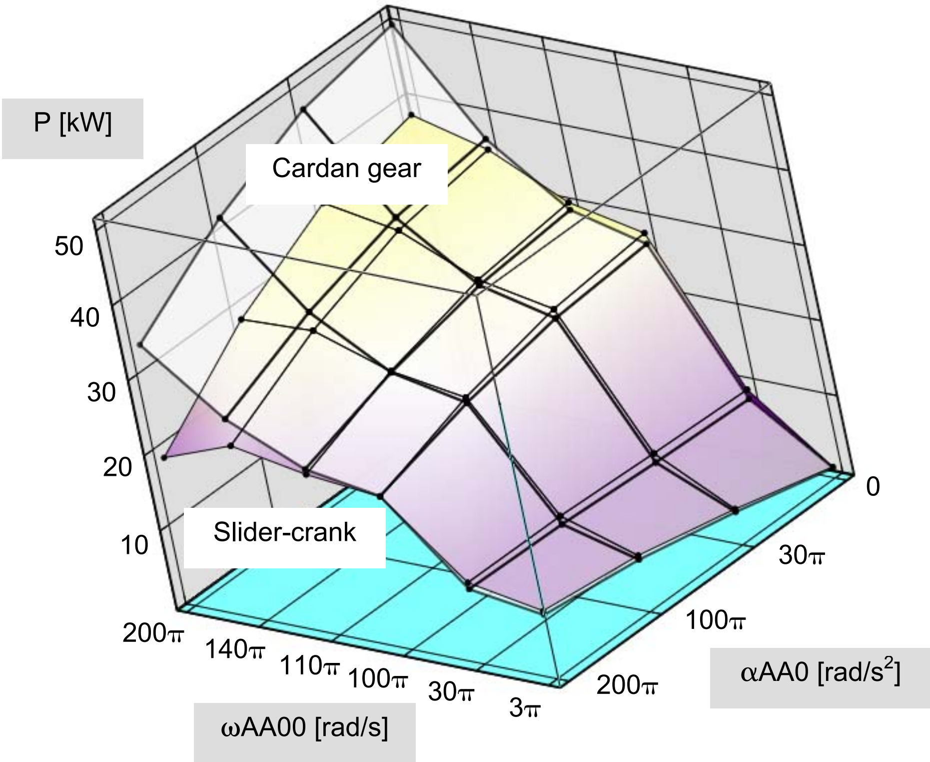

Pouteng, Poutengc

Figure 11.6.11. Output powers, four-stroke engine, cylinder filling 107 %, compression ratio 12:1, maximum combustion pressure 12 MPa, gasoline combustion, polytropic exponent 1.4, piston diameter 2·ZAA0, ZBA = 2.33·ZAA0, ZAA0 = 0.06 m, ZBA = 0.14 m, displacement 1357 cm^3.

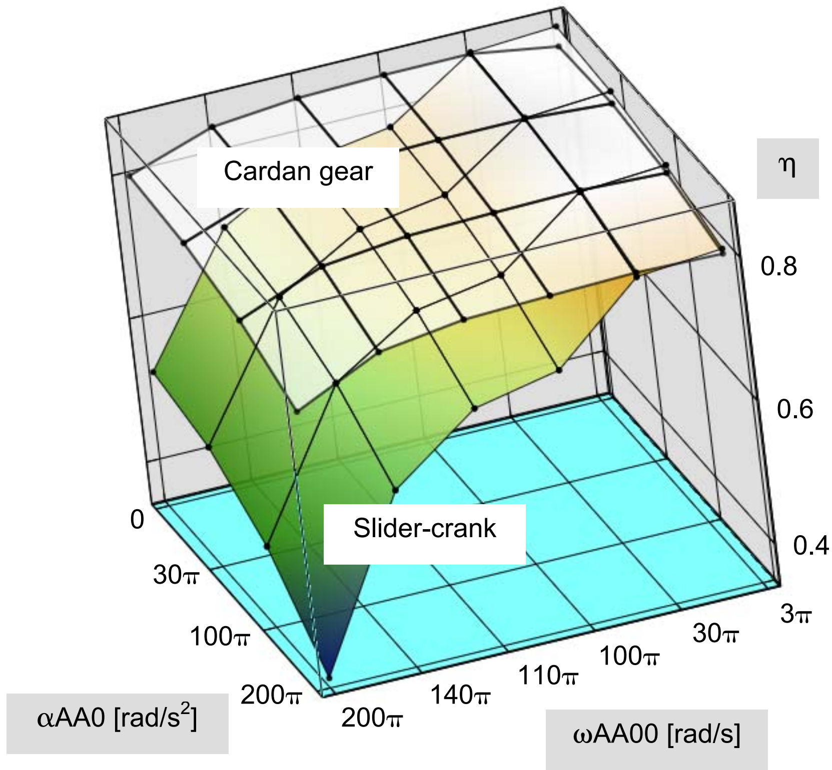

ηmeng, ηmengc

Figure 11.6.12. Mechanical efficiencies, four-stroke engine, cylinder filling 107 %, compression ratio 12:1, maximum combustion pressure 12 MPa, gasoline combustion, polytropic exponent 1.4, piston diameter 2·ZAA0, ZBA = 2.33·ZAA0, ZAA0 = 0.06 m, ZBA = 0.14 m, displacement 1357 cm^3.

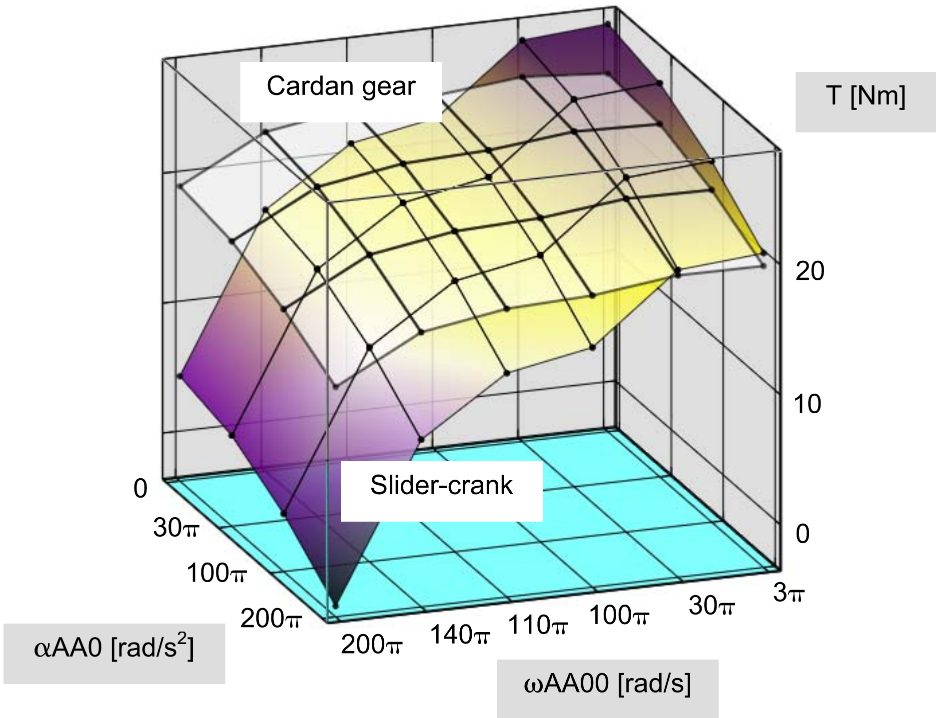

Touteng, Toutengc

Figure 11.6.13. Output torques, four-stroke engine, cylinder filling 107 %, compression ratio 12:1, maximum combustion pressure 12 MPa, gasoline combustion, polytropic exponent 1.4, piston diameter 2·ZAA0, ZBA = 4·ZAA0, ZAA0 = 0.04 m, ZBA = 0.16 m, displacement 402 cm^3.

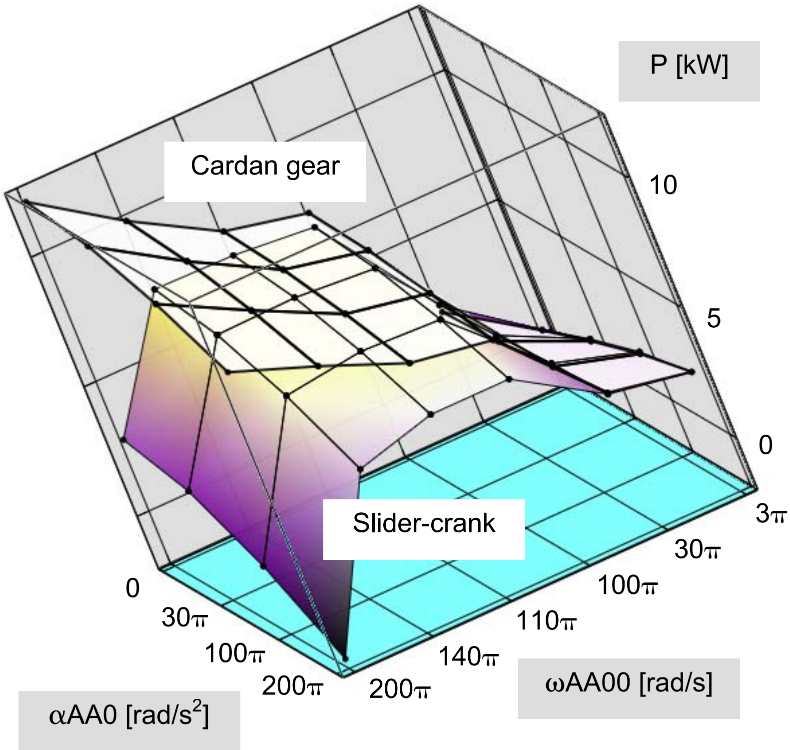

Pouteng, Poutengc

Figure 11.6.14. Output powers, four-stroke engine, cylinder filling 107 %, compression ratio 12:1, maximum combustion pressure 12 MPa, gasoline combustion, polytropic exponent 1.4, piston diameter 2·ZAA0, ZBA = 4·ZAA0, ZAA0 = 0.04 m, ZBA = 0.16 m, displacement 402 cm^3.

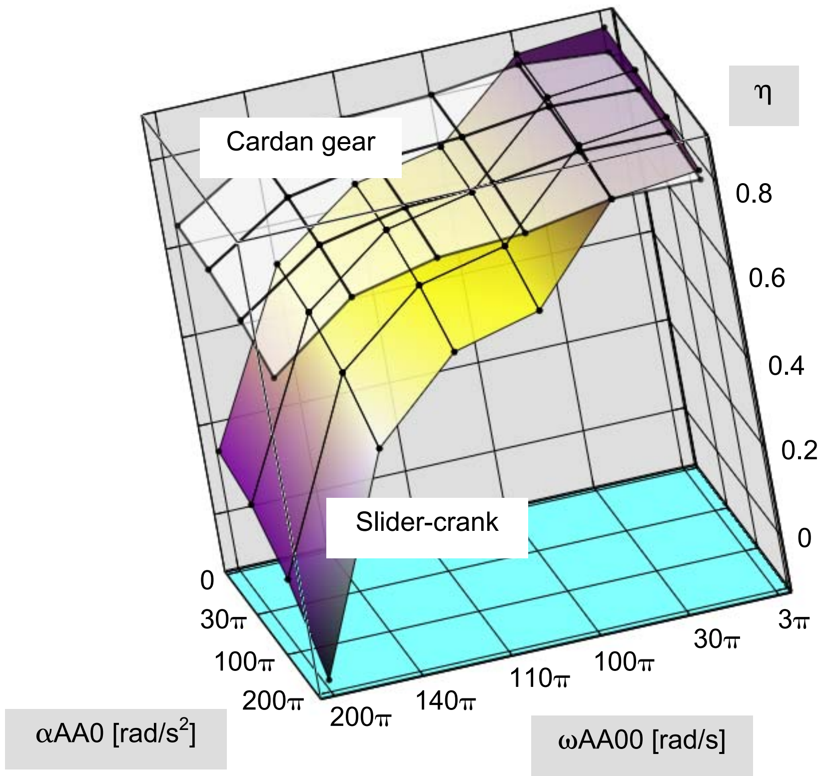

ηmeng, ηmengc

Figure 11.6.15. Mechanical efficiencies, four-stroke engine, cylinder filling 107 %, compression ratio 12:1, maximum combustion pressure 12 MPa, gasoline combustion, polytropic exponent 1.4, piston diameter 2·ZAA0, ZBA = 4·ZAA0, ZAA0 = 0.04 m, ZBA = 0.16 m, displacement 402 cm^3.

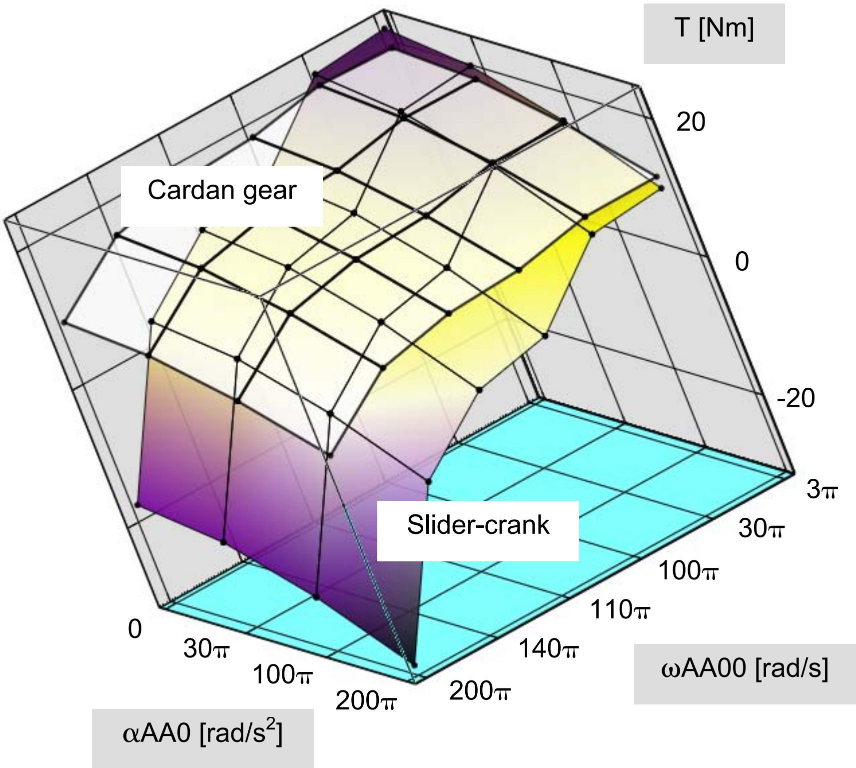

Touteng, Toutengc

Figure 11.6.16. Output torques, four-stroke engine, cylinder filling 107 %, compression ratio 12:1, maximum combustion pressure 12 MPa, gasoline combustion, polytropic exponent 1.4, piston diameter 1.5·ZAA0, ZBA = 5·ZAA0, ZAA0 = 0.046 m, ZBA = 0.229 m, displacement 339 cm^3.

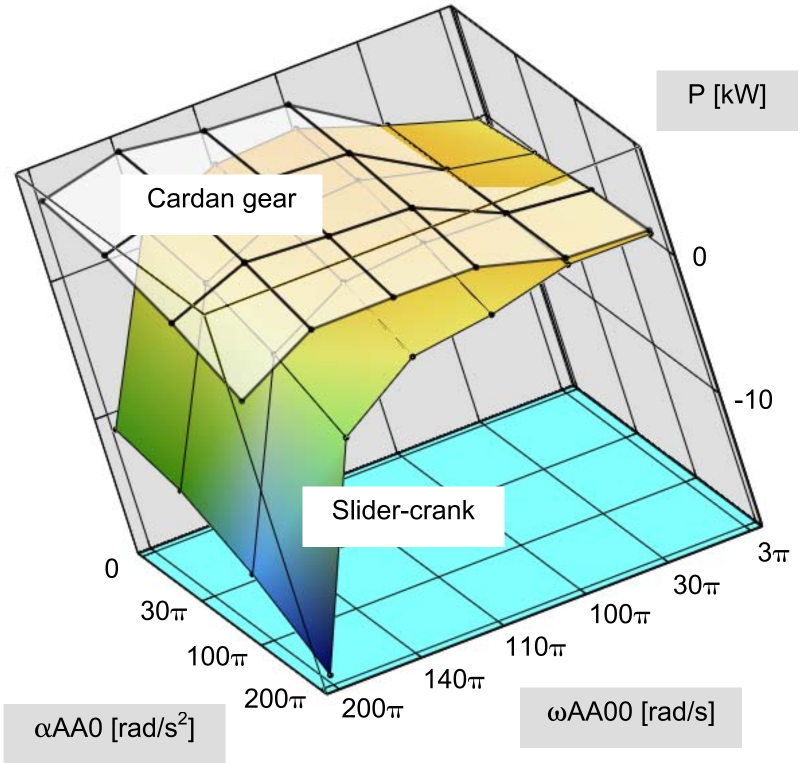

Pouteng, Poutengc

Figure 11.6.17. Output powers, four-stroke engine, cylinder filling 107 %, compression ratio 12:1, maximum combustion pressure 12 MPa, gasoline combustion, polytropic exponent 1.4, piston diameter 1.5·ZAA0, ZBA = 5·ZAA0, ZAA0 = 0.046 m, ZBA = 0.229 m, displacement 339 cm^3.

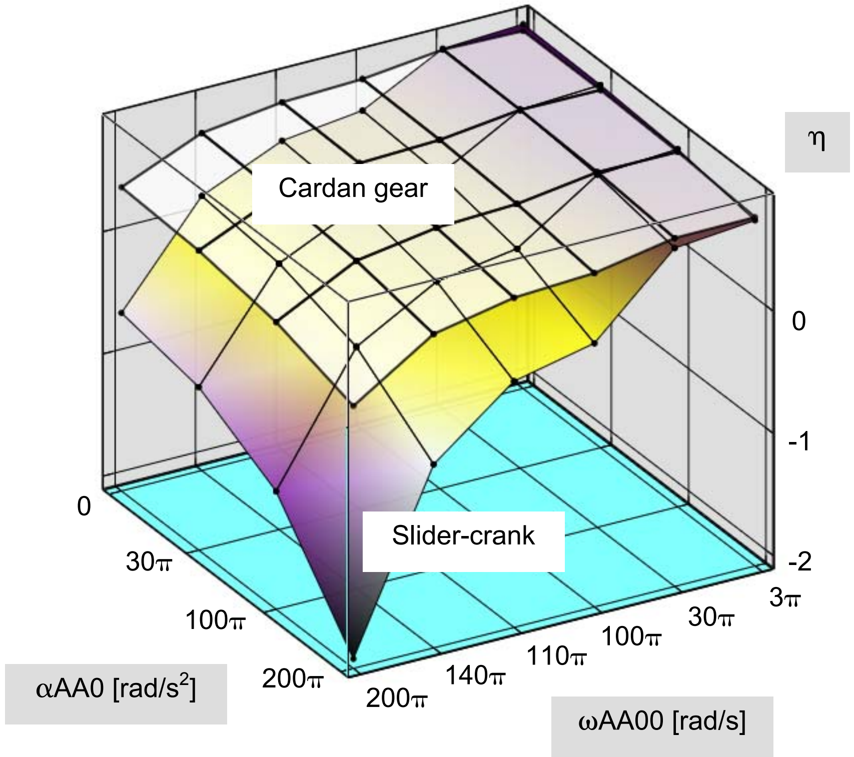

ηmeng, ηmengc

Figure 11.6.18. Mechanical efficiencies, four-stroke engine, cylinder filling 107 %, compression ratio 12:1, maximum combustion pressure 12 MPa, gasoline combustion, polytropic exponent 1.4, piston diameter 1.5·ZAA0, ZBA = 5·ZAA0, ZAA0 = 0.046 m, ZBA = 0.229 m, displacement 339 cm^3.

11.7 Results of the special applications

The preceding results show that the cardan gear machines can be more efficient than the slider-crank machines when the power losses (friction losses) are included in the calculations (**Figures 11.6.4 ... 11.6.18, Appendix 11.6.1**). As the lossless machines the both types fight evenly in normal constructions. The kinematic properties of the cardan gear machines are always better than those of the slider-crank machines (**Chapter 11.1**).

The cardan gear construction is at its best, if we want to build an engine with an overlong connecting rod and a thin piston, running at high angular velocity and intermittently high angular acceleration. It can be a suitable airplane engine, a modern motorcycle engine or a modern car engine especially as a radial or a half-radial construction.

The rod length $\lesssim$ "5 · crank length", the piston diameter ≈ "1.5 · crank length", the angular velocity $\lesssim 100\pi$ rad/s ($\lesssim$ 3000 r/min) with the varying angular acceleration is a very effective combination.

The masses of the moving components (pistons, rods, crankshafts, etc.) can not be very big when the angular velocity and the angular acceleration are high. That means the cylinder capacity below 500 cm^3.

The mean inertial torque and the inertial work consumption per one cycle of that kind of lossless cardan gear machine are $\lesssim$ 28 % smaller than those of the lossless slider-crank machine.

The mean inertial power consumption of the cardan gear machine is then $\lesssim$ 37 % smaller.

The mean total torque and the total work consumption per one cycle of that kind of lossless cardan gear air pump are $\lesssim$ 8 % smaller.

The mean total power consumption of that kind of lossless cardan gear air pump is $\lesssim$ 11 % smaller.

The mean total torque output and the total work output per one cycle of that kind of lossless cardan gear engine are $\lesssim$ 11 % bigger.

The mean total power output of that kind of lossless cardan gear engine is $\lesssim$ 111 % bigger.

When the friction losses are included in the preceding results, the cardan gear machine is superior.

The frictional power loss of that kind of cardan gear engine is $\lesssim$ 60 % smaller than the power loss of the equal slider-crank engine.

The mechanical efficiency of that kind of cardan gear engine is $\lesssim$ 200 % better.
(**Figures 11.6.16 ... 11.6.18, Appendixes 11.6.1 and 11.7.1**)

11.8 Applied results

The calculation results of this study have been presented for the normal sized machines, for example motor cycle engines. Very big sized machines have also been studied outside the presented results, but nothing extraordinary has been found.
The basic construction of the slider-crank machine is always the same, but the cardan gear machine can be manufactured conventionally with gears or as the slide construction without gears (**Figures 4.1 and 8.1**).
If the cardan gear machine is constructed with gears, the modules of gears (for SI specifications), the number of teeth of the gears and the cardan wheel diameters can be chosen preliminarily according to the **Table 11.8.1**.
In this study the cardan gear dynamics has been calculated for the gear construction. In the slide construction the gear mesh can be replaced with the linear bearings. Then the sliding pair components may increase the mass inertia, but correspondingly the mass of the cardan wheel can be reduced. The lightened cardan wheel can be constructed as a steel plate. The suitable face width of the conventional cardan wheel is $b_{wheelc} \approx d_{1c}/3$ (**Table 11.8.1**).

Table 11.8.1. Preliminary parameters for the cardan gear design.

Nominal power P [kW]	Module m_c [mm]	Number of teeth		Pitch diameters $d = m \cdot z$	
		Cardan wheel z_1	Ring gear $z_2 = 2 \cdot z_1$	Cardan wheel d_{1c} [mm]	Ring gear d_{2c} [mm]
1 ... 10	2	19 ... 25	38 ... 50	38 ... 50	76 ... 100
10 ... 25	3	19 ... 25	38 ... 50	57 ... 75	114 ... 150
25 ... 40	4	19 ... 25	38 ... 50	76 ... 100	152 ... 200
Face width b_{wheelc} [mm]				10 ... 35	10 ... 35

When the cardan gear construction can be used, when it is worthwhile to use and when it is at its best?
First there are some design constraints for the pumps and engines and then there are some suitable design parameters. The next numerical values are valid for the normal sized machines (air compressors, car engines, motor cycle engines, etc.).

Design constraints:

Minimum length of the connecting rod	≈ 2.3 · crank length
Maximum length of the connecting rod	≈ 5 · crank length
Compression ratio	
(air pumps, gasoline combustion engines)	10 ... 14
Maximum combustion pressure	7 ...17 MPa
Gear ratio of the cardan gear pair	2

Design parameters (normal sized pumps and engines):

Crank length	20 ... 100 mm
Length of the connecting rod	60 ... 500 mm
Piston diameter	1 ... 3.4 · crank length
	20 ... 150 mm
Face width of the cardan wheel	10 ... 35 mm
Pressure angle of the cardan gear pair	20 °

The conventional piston pin of the cardan gear construction can be eliminated because of the straight-line motion. Then the piston skirts can be shortened and the connecting rod can be thinned.
When the connecting rod has to be lengthened from "2.3 · crank length" towards "5 · crank length", the cardan gear machines become more and more efficient compared with the equal slider-crank machines.
The magnitude of the compression ratio (10...14) affects very little to the efficiencies of the machines.
The smaller is the piston diameter (piston area) the more efficient is the cardan gear machine, because the pressure stays then high longer time (larger angle of the crankshaft, longer motion of the piston).
The lower are the maximum combustion pressures, the lower are the mechanical efficiencies and the more efficient are the cardan gear engines compared to the slider-crank engines.
The smaller are the machines, the higher can be the angular velocities and the angular accelerations. The kinetostatic calculations show that the inertial loads are always smaller in the cardan gear machines than in the equal slider-crank machines. The same angular velocities and angular accelerations allow us to construct bigger cardan gear machines than slider-crank machines.

The maximum sizes (displacements) of the slider-crank machines and the cardan gear machines in the normal use have been estimated in the **Table 11.8.2**.

Table 11.8.2. Approximations for the maximum displacements of the normal sized pumps and engines.

Crank length = 20...60 mm Piston diameter = 1...2 · crank length Angular acceleration = 0...200π rad/s^2 Angular velocity = 0...200π rad/s	Maximum displacement / one cylinder [cm^3]	
Rod length	Slider-crank machines	Cardan gear machines
2.33 · crank length ≈ 60...140 mm	1500	2000
3 · crank length ≈ 75...150 mm	600	800
4 · crank length ≈ 100...160 mm	100	400
5 · crank length ≈ 125...225 mm	50	300

The strength of the moving components must be checked separately, if the displacement is over 1000 cm^3. Although the construction is workable, the inertial loads can be too high in the big machines.

12. Discussion

The cardan gear mechanism, a special application of the hypocycloid mechanisms, is practical and a real competing alternative to the slider-crank mechanism in the conventional air pumps and four-stroke combustion engines. The equivalent epicycloidal mechanisms are more complicated and impractical. That has been stated also in Ishida's reports [***Ishida 1974, report 1, Ishida et al. 1974, reports 2...3, Ishida et al. 1975, report 4***]. The advantages of the cardan gear mechanism have been brought out in this study.

General properties

The clear advantages of the cardan gear mechanism are:

Any length of the connecting rod is possible.
The connecting rod can be very thin and light.
The piston skirt of the cardan gear machine does not wear because of the straight-line motion.
The conventional piston pin can be eliminated.
The piston can be very short and the piston skirt can be eliminated if the piston pin is eliminated.
Friction between the cardan gear piston and the cylinder wall is low, because there are theoretically no side forces.
Because of the low friction the fuel consumption can be reduced.

The undoubted advantages of the conventional slider-crank mechanism are:

The construction of the slider-crank mechanism is well-known and reliable.
No gears are needed in the crank-case.
The manufacturing processes are workable and the vehicle industry produces millions of slider-crank machines all over the world as a nonstop flow.
Maybe thousands of different kinds of slider-crank pumps and engines have been tested in real use since Nicolaus Otto's and Rudolf Diesel's times.

When the previous advantages of the slider-crank mechanism are observed, it is clear that the cardan gear construction does not totally replace the slider-crank mechanism for a long time. However the predicted fuel crisis, air pollution and the new winds of change demand us to find out new possibilities. One choice is the cardan gear mechanism and its applications. In this study the Newtonian dynamics has been clarified for the both machine types. Most parts of the Newtonian dynamics of the slider-crank mechanism and the engine thermodynamics have been presented in the books and journal articles, but the Newtonian dynamics of the cardan gear mechanism has not been completely presented before this study.

Kinematics

The kinematics of the cardan gear mechanism is superior to the slider-crank mechanism.
The straight-line motion of the cardan gear rod makes it possible to construct very high "open-heart" machines with the long, thin and light connecting rods. The piston and the crankcase can have separate lubrication systems and that means smaller amounts of contaminated oil. Ruch et al. have had the same idea [***Ruch, Fronczak & Beachley 1991***].
The cardan gear piston stays higher in the cylinder during the power stroke than the slider-crank piston. So the cardan gear cylinder pressure and the rod force are also higher.
The maximum velocity and the maximum acceleration of the cardan gear piston are clearly lower than those of the slider-crank piston. Then the linear momentum and the inertial force of the cardan gear piston are smaller.
The maximum velocity and the maximum acceleration of the connecting rod are also lower in the cardan gear mechanism than in the slider-crank mechanism. Then the linear momentum and the inertial force of the cardan gear rod are smaller.
Cardan gear rod does not rotate. In the slider-crank mechanism the rotating rod has angular velocity, angular acceleration, angular momentum and inertial torque.
The cardan gear motion is very smooth, because the accelerations and velocities of the components are sinusoidal.
Ishida's studies and the presented comparison curves [***Ishida 1974, report 1, Ishida et al. 1974, report 2***] agree with the kinematic results of this study.

Kinetostatics

The cardan gear piston assembly can be constructed clearly lighter than the slider-crank piston assembly because of the straight-line motion. The cardan gear piston can include the rod and the "piston pin" can be situated in the lower end of the rod. So the piston pin inertial joint forces of the two machines can not be compared directly. The piston pin inertial joint forces are therefore clearly bigger in the cardan gear machine than in the slider-crank machine.
The half-size crank length of the cardan gear machine causes over 50 % bigger crank pin inertial joint force maximums compared to the equal slider-crank machine. The lightweight titanium rod in the cardan gear machine can eliminate that difference.
In this study the main pin inertial joint forces have been set equal with the crank pin inertial joint forces, because the purposeful balancing, clearances and vibrations are neglected.
The mean inertial torque of the cardan gear crankshaft is clearly smaller than that of the slider-crank machine.
The inertial work acts identically with the inertial torque.
The inertial power consumption is significantly smaller in the cardan gear machine than in the slider-crank machine.
The rod material, in this study steel or titanium, affects very little to the torques, works and powers, because the inertial effects of the different components compensate each other very effectively.
The cardan gear motion is sinusoidal and very smooth.

Kinetics

The compression and the combustion pressures of the cardan gear machine are bigger before and after the top dead center than those of the slider-crank machine, when the valves are closed. The bigger pressure means the bigger piston force. The bigger combustion pressure may improve the combustion process and reduce air pollution. The high combustion pressure means also hot burning gases and that may reduce fuel consumption.
Ruch et al. have had the same thought [***Ruch, Fronczak & Beachley 1991***].
The maximum compression torque is smaller in the cardan gear machine than in the slider-crank machine. That means savings in motor sizes in the pump constructions. The mean compression torques, the compression works per one cycle and the mean compression power are equal in the both machines.
Because of the half-size crank length the combustion torque, the combustion work per one cycle and the combustion power of the cardan gear engine are clearly smaller than those of the slider-crank engine in the normal constructions.

Summed lossless Newtonian dynamics in normal constructions

When the kinematic, kinetostatic and kinetic properties are summed for the lossless machines, the competition tightens.
Because of the half-size crank length the total crank pin and the main pin total joint force maximums of the cardan gear machine are at least 100 % bigger than those of the slider-crank machine. Therefore the crankshafts of the cardan gear machines must be stronger and more rigid than those of the slider-crank machines. Bigger component size does not automatically mean heavier and more massive structures, because the components can always be lightened with hollows and tubes.
The total torque maximum of the lossless cardan gear crankshaft is clearly smaller than the total torque maximum of the lossless slider-crank crankshaft.
In pump constructions the mean total torque, the total work per one cycle and the mean total power are smaller in the cardan gear machine than in the slider-crank machine. That means energy savings.
In the four-stroke engines the mean total torque, the total work per one cycle and the mean total power of the cardan gear machine are equal or a little smaller than those of the slider-crank machine in the lossless constructions.
Ishida and Yamada have measured the total power output (brake power) of the cardan gear two-stroke chain saw and found it be a little lower than that of the conventional chain saw [***Ishida & Yamada 1986***]. That result is in agreement with this study. Beachley and Lenz have concluded that the maximum output power of the hypocycloid engine may increase at high speeds compared with the slider-crank engine because of the very low piston side friction [***Beachley & Lenz 1988***].

Dynamic tooth loads

If the cardan gear machines are constructed conventionally with the two gears, there are also tooth loads. Dynamic tooth loads depend highly on the gear clearances and they are often very high in the ordinary gear trains. In this study the backlash acting at the pitch line of the cardan gear pair has been approximated as 0.005 inch (= 0.127 mm). That clearance is quite tight and it must be tight for pump and engine constructions. So the dynamic tooth loads are not very high compared to the steady bearing forces (calculated pin joint forces). The calculated differences between the dynamic tooth loads and the piston pin joint forces (the tooth loads are bigger) are approximately 25...160 % in pumps and 0 ... 40 % in engines. The gear mesh can be noisy and the teeth can wear or break. Therefore the cardan gear machines could be constructed without gears using linear bearings (**Figure 8.1**). Especially the multi-cylinder machines may run very smoothly with sliding guides (**Figure 12.3**).

Operational torques, powers and mechanical efficiencies

In this study no accessories have been included into the constructions. Only the friction loads have been calculated as the power losses. So the numerical values of the calculated mechanical efficiencies are high (**Figures 11.6.6, 11.6.9, 11.6.12, 11.6.15 and 11.6.18, Appendix 11.6.1**). The cardan gear machines are generally more efficient than the slider-crank machines. The calculated difference is even hundreds of percent. The main reasons to that are the higher pressures of the cardan gear machines and the bigger inertial loads of the slider-crank machines. Only at the very low angular velocities the slider-crank machines are more efficient than the cardan gear machines. The better mechanical efficiency of the cardan gear machines means that the same work can be done with less energy. Although the slider-crank engine produces higher maximum torque and higher maximum power, the mean total torque and the mean total power are quite close to the values of the cardan gear engine even in the lossless case. When the friction losses are included in the calculations, the cardan gear engine is clearly better (**Figures 11.6.4, 11.6.5, 11.6.7, 11.6.8, 11.6.10, 11.6.11, 11.6.13, 11.6.14, 11.6.16 and 11.6.17, Appendix 11.6.1**). So the cardan gear machine can be seen a real competitor to the slider-crank machine.

Special applications

When we design pumps and engines, we always want to save space and produce as much power as possible.
The cardan gear machines are clearly more efficient than the slider-crank machines when the friction losses are included in the calculations. The kinematic properties of the cardan gear machines are also better than those of the slider-crank machines.
The cardan gear mechanism is even superior, when we want to build a pump or an engine with an overlong connecting rod (≈ 2.5 · stroke length) and thin piston (≈ 0.75 · stroke length), running at high angular velocity and intermittently high angular acceleration.
The inertial torque, the inertial work per one cycle (= 4π rad) and the inertial power consumption of that kind of cardan gear machine are clearly smaller than those of the slider-crank machine.
The mean total torque, the total work consumption per one cycle and the mean total power consumption of that kind of cardan gear air pump are also clearly smaller than those of the slider-crank air pump.
The mean total torque output, the total work output per one cycle and the mean total power output of that kind of cardan gear four-stroke engine are much bigger than those of the equal slider-crank four-stroke engine.
The slider-crank machines have also constructive restrictions.
If the rod length is over "2.5 · stroke length", the piston diameter must be over "1 · stroke length" in the slider-crank constructions (**Figure 12.1**).
If the piston diameter of the multi-cylinder radial machines is over "0.75 · stroke length", the slider-crank construction can not be built, because there is not enough space for the cylinder fastenings (**Figure 12.2**).
So the long rod cardan gear construction is superior and the equal slider-crank construction can not even be built.
The cardan gear machine can be worthwhile to manufacture also as the radial construction without gears. The running of that kind of machine may be very smooth.
For example Craven, Smith et al. have developed a double cross-slider based Stiller-Smith engine, in which the vibrations have been got reduced using the radial structure [***Smith, Craven & Cutlip 1986, Craven, Smith & Butler 1987, Smith, Churchill & Craven 1987***].
Several old airplane engines are also radial engines. They are very powerful and their construction is compact.

Conclusions of the achieved results

Equations of the Newtonian dynamics have been derived for the slider-crank machines and the cardan gear machines and the running modes of the both machine types have been clarified. The calculation results of this study show that the cardan gear machine is a real alternative to the slider-crank machine, if we want to save energy in the future. The testing devices and prototypes have not been built or measured in this study and so the calculation results have not been verified in reality. However the results of this study are in agreement with the previous studies, presented in the **Chapter 2: State of the art**.

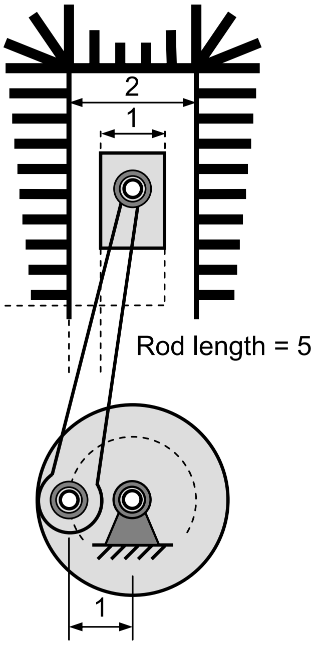

Figure 12.1. Constructive restriction of the slider-crank machine.

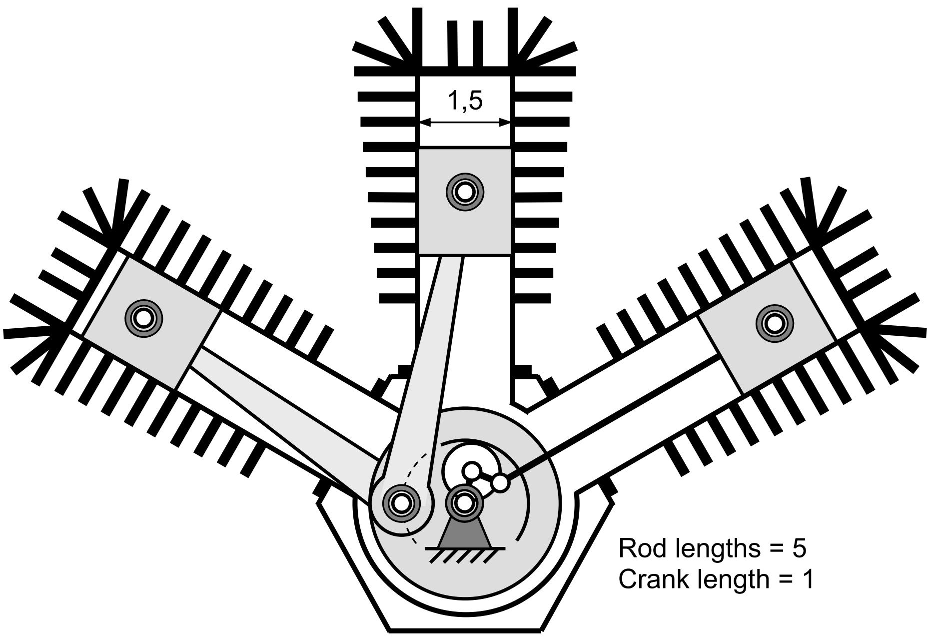

**Figure 12.2. Constructive restriction of the half-radial machine.
Cardan gear mechanism versus slider-crank mechanism.**

Sources of error

The purposeful balancing, gravitation, clearances and vibrations have been neglected in this study. So the calculated results can not be applied straight to the real machines. The purpose of this study has been to find out relative differences of the simplified and equal models. Only the percentages of the relative differences are meant to be directly comparable with the real machines.
The mathematical models of the two machines can not be absolutely equal, because the constructions are different. For example the piston pin joint forces can not be compared, when the conventional piston pin of the cardan gear construction has been eliminated.
Testing devices have not been constructed. Unexpected effects are always possible and they can not be estimated without real tests.
The geometries, the masses and the centers of gravities of the moving components can not be approximated accurately. So the inertial properties can not be calculated accurately.
Angular accelerations and angular velocities of the real machines are not constant. The measured dynamics of the real machines would be very complicated compared with the theoretical calculations. However the main behavior of the machines can be calculated and the results can be compared reliably enough using constant angular accelerations and constant angular velocities.
Dynamic tooth loads of the cardan gear machines can not be calculated accurately because the mass and the polar moment of inertia of the cardan wheel and the suitable backlash acting at the pitch line of the gears can not be approximated accurately.
The friction forces of the piston rings can be different in the slider-crank and the cardan gear machines, but in this study they have been approximated equal.
There are many kinds of bearing types and sizes to be chosen into the pin joints and therefore the bearing frictions can not be approximated accurately.
The real lubrication mode and the oil viscosity can not be predicted accurately.

Suggestions for the further research

Equal prototypes of the cardan gear machines and the slider-crank machines should be constructed and tested. Dynamics of the prototypes and the real machines should be measured and compared. Ishida et al., Ruch et al. and Smith et al. have constructed some testing devices, but they are not enough. Rod lengths and piston diameters should be varied to optimize the best construction for the cardan gear machine. Although the long-rod cardan gear engine seems to be the best, does the higher combustion pressure offer extra power also in the short rod construction?
The combustion process of the cardan gear engine should be studied. Does the higher pressure really improve combustion and reduce exhaust emissions? Does the separate lubrication system reduce oil contamination?
The radial engine constructions should be studied.
The most interesting constructions are the cardan gear engines without gears (**Figures 8.1 and 12.3**). The gear mesh can be replaced with the linear bearings. How smooth is the running of the six-cylinder cardan gear radial engine?
Can the half-radial engine (**Figure 12.2**) be a new super engine in motorcycles?
Optimizing the balancing, minimizing the vibrations, adjusting the clearances, minimizing friction and minimizing the masses are the advanced areas to study.

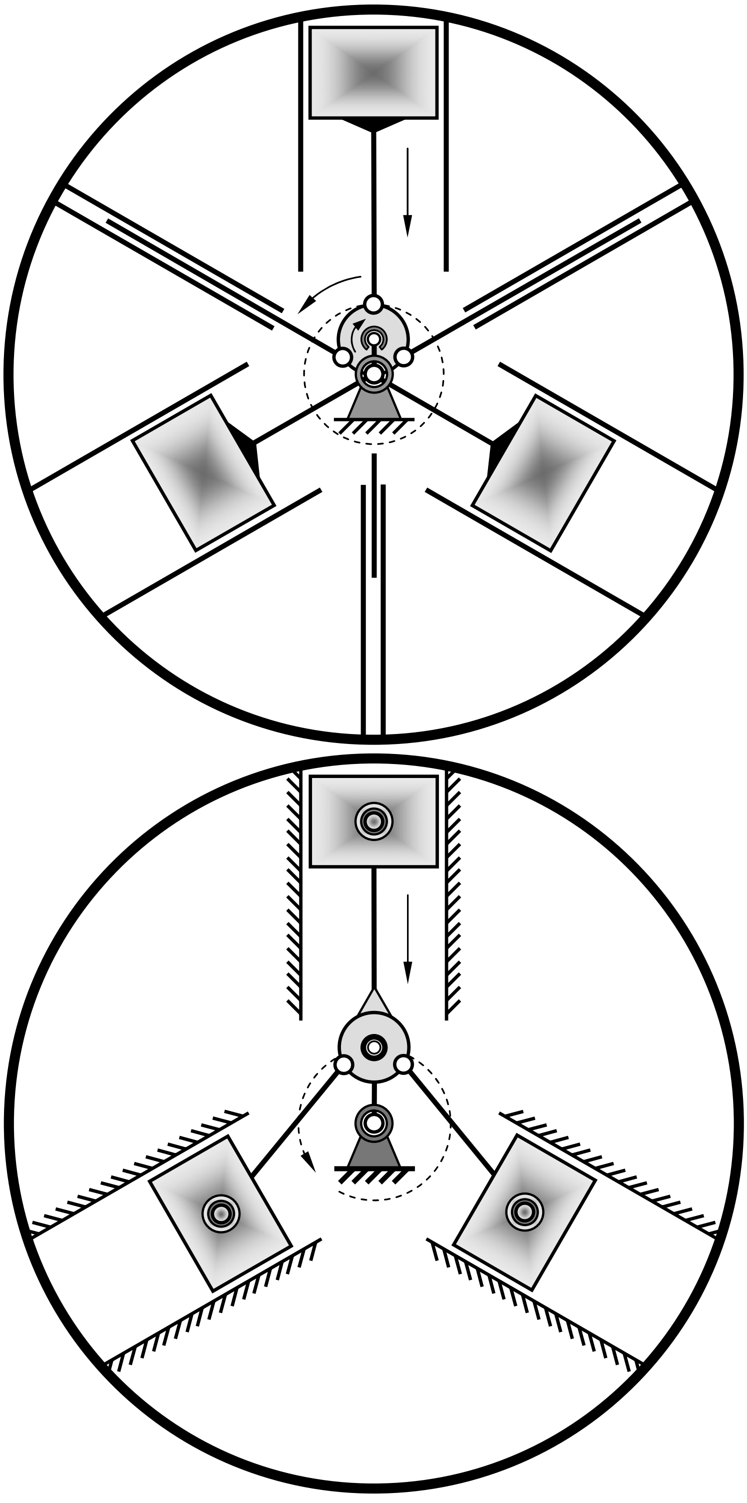

Figure 12.3. Cardan gear radial engine without gears (above) versus slider-crank radial engine (below).

13. Conclusions

The main purpose of this study has been to compare the cardan gear mechanism with the slider-crank mechanism in air pumps and four-stroke engines. Can the cardan gear mechanism be better than the slider-crank mechanism and in which circumstances?
Comprehensive and universal Newtonian dynamics of the slider-crank machines and the cardan gear machines have been derived for the comparative calculations.
The mechanisms have been compared by calculating the Newtonian dynamics using 8 different Mathcad programs. Calculations have been made for the air pumps and the four-stroke engines in kinematics, kinetostatics, kinetics and their total effects.
This kind of derivation of the theory, Mathcad programs (not presented in the text), calculations, calculation results (tables, curves and surface plots) and recommendations presented in this study have novelty value. They have not been published before, but made and written by the author first time in this study.
The calculated results, unpublished before, made and written by the author, show and confirm the following facts for the normal sized machines:
The kinematic properties of the cardan gear mechanism are excellent.
Its motion is smooth and the maximum accelerations and the maximum velocities are lower than in the slider-crank mechanism. The connecting rod of the cardan gear mechanism does not rotate and the cardan gear piston stays higher in the cylinder between the bottom dead center and the top dead center than the slider-crank piston.
The reduced mass inertia of the cardan gear machine saves energy.
The mean inertial torques, the inertial works per one cycle (= 4π rad) and the mean inertial powers are 10...30 % smaller in the cardan gear machines than in the slider-crank machines.
When the lossless crankshaft torques are compared, the cardan gear pump is more efficient, but the cardan gear engine is weaker than the equal slider-crank machines.
The compression pressures, the combustion pressures and the resulting piston forces are 0...10 % bigger in the cardan gear machines than in the slider-crank machines. Because of the half-size crank length the maximum compression torque need of the cardan gear pump is 10...16 % smaller. The mean compression torques, the compression works per one cycle and the mean compression power needs of the slider-crank pump and the cardan gear pump are equal.
The maximum combustion torques are 13...22 % smaller in the cardan gear engines than in the slider-crank engines. The mean combustion torques, the combustion works per one cycle and the mean combustion powers are also 8...15 % smaller in the cardan gear engines.
The cardan gear mechanism and the slider-crank mechanism fight equally in the summed lossless Newtonian dynamics as normal constructions.
The ***lossless machines*** work as follows:
The total joint forces are at least 100 % bigger in the cardan gear machines than in the slider-crank machines, because of the half-size crank length of the cardan gear construction. At the low angular velocities ($\lesssim$ 50 rad/s, $\lesssim$ 500 r/min) the total torque maximums are 11...25 % smaller in the cardan gear machines than in the slider-crank machines. At the higher angular velocities the difference is bigger. The mean torque need and the total work (energy need) per one cycle are 1...8 % smaller in the cardan gear air pump than in the slider-crank air pump.

The mean torque output and the total work per one cycle are at their best $\lesssim$ 6 % bigger in the cardan gear engines than in the slider-crank engines.
The mean power consumption is 1...10 % smaller in the cardan gear air pump than in the slider-crank air pump. The mean power output is at its best $\lesssim$12 % bigger in the cardan gear four-stroke engine than in the slider-crank four-stroke engine.
The preceding results are valid in the ***lossless one-cylinder constructions*** using the rod length "2.33...4 · crank length" and the piston diameter ≈ "2 · crank length".
When the cardan gear machines are constructed in the original way with gears, the dynamic loads of the gear mesh are one of the most critical parts of the design. The calculated results do not confirm the general thought that the dynamic loads are always high. When the tooth clearances are kept tight, the dynamic tooth loads are only 1.5 ... 2.5 times higher than the steady joint forces of the (piston) pin at the lower end of the connecting rod at the opposite side of the cardan wheel.
When we ***include the friction losses*** into the calculations, the cardan gear machines become almost superior to the slider-crank machines.
The mean power losses are 0...75 % smaller in the cardan gear machines than in the slider-crank machines. Only at very low angular velocities the power losses of the cardan gear machines are bigger than the power losses of the slider-crank machines.
The mechanical efficiencies are 0...30...50... even hundreds of percent bigger in the cardan gear machines than in the slider-crank machines. Only at very low angular velocities the mechanical efficiencies of the cardan gear machines are smaller than the mechanical efficiencies of the slider-crank machines.
The cardan gear construction is at its best with an overlong rod (≈ 5·crank length), thin piston ($\lesssim$ 1.5·crank length), high angular velocity and intermittently high angular acceleration.
The mean inertial torque and the inertial work consumption per one cycle of that kind of cardan gear machine are almost 30 % smaller than those of the equal slider-crank machine even in the lossless construction. The inertial power consumption is almost 40 % smaller. The total torque, the total work consumption per one cycle and the total power consumption of this cardan gear air pump are almost 10 % smaller. The total torque output and the total work output per one cycle of this cardan gear four-stroke engine are about 10 % bigger. The total power output is almost 20 % bigger.
When the friction losses are included in the previous results, the cardan gear construction is even better.
According to the calculation results of this study the cardan gear construction is worthwhile to utilize in pumps and four-stroke engines. The smooth running connected with the good mechanical efficiency of the cardan gear machine can be one step towards better energy savings in the future.
Preliminary guidelines, unpublished before, written by the author, have also been presented in this study as designing instructions of the cardan gear machines.
It is worthwhile to build and study different kind of prototypes of the cardan gear machines. Engine manufacturers should build some prototypes of the cardan gear machines, especially constructions without gears. They can be for example three-cylinder half-radial engines ("W-engines") for the motorcycles, six-cylinder radial engines for the airplanes or six-cylinder double half-radial engines ("double W-engines") for the sport cars.
Also the mathematical models are needed. Especially the cardan gear engines with overlong connecting rods and thin pistons can offer progressive solutions for the future.

References

Literary documents

Anderson, N. E. & Loewenthal, S. H., 1981.
Effect of Geometry and Operating Conditions on Spur Gear System Power Loss. Journal of Mechanical Design, Transactions of the ASME, January 1981, Vol. 103. pp. 151-159.

Anderson, N. E. & Loewenthal, S. H., 1982.
Design of Spur Gears for Improved Efficiency. Journal of Mechanical Design, Transactions of the ASME, October 1982, Vol. 104. pp. 767-774.

Andersson, P., Tamminen J. & Sandström C. - E., 2002.
Piston ring tribology. A literature survey. VTT Research Notes 2178. Espoo. 105 p.

Artobolevsky, I. I., 1977.
Mechanisms in Modern Engineering Design. Volume III, Gear Mechanisms. Translated from the Russian by Nicholas Weinstein. Mir Publishers, Moskow. pp. 34, 240.

Badami, M. & Andriano, M., 1998.
Design, Construction and Testing of Hypocycloid Machines. Advanced Powerplant Concepts 1998, SAE International Congress and Exposition, Detroit, Michigan, February 23-26, 1998, SAE. pp. 39-48.

Beachley, N. H. & Lenz, M. A., 1988.
A Critical Evaluation of the Geared Hypocycloid Mechanism for Internal Combustion Engine Application. International Congress and Exposition, Detroit, Michigan, February 29 - March 4, 1988, SAE Technical Paper Series. 12 p.

Benedict, G. H. & Kelley, B. W., 1961.
Instantaneous Coefficients of Gear Tooth Friction. ASLE Transactions, Vol. 4, No. 1, April 1961. pp. 59-70.

Beer, F. P. & Johnston, E. R., 1997.
Vector Mechanics for Engineers: Statics and Dynamics. Sixth Edition, McGraw-Hill, New York. 1280 p.

Beyer, R., 1931.
Technishe Kinematik: Zwanglaufmechanik Nebst Bewegungsgeometrie und Dynamik der Getriebe in Theorie und Praxis. Verlag von Johann Ambrosius Barth, Leipzig. pp. 195-196.

Buckingham, E., 1949.
Analytical Mechanics of Gears. First edition. McGraw-Hill Book Company, Inc., New York. pp. 395-454.

Burmester, L., 1888.
Lehrbuch der Kinematik. Erster Band: Die Ebene Bewegung, mit einem Atlas von 57 Lithographirten Tafeln. Verlag von Arthur Felix, Leipzig. 941 p.

Burmester, L., 1888.
Atlas zu Lehrbuch der Kinematik. Erster Band: Die Ebene Bewegung. Verlag von Arthur Felix, Leipzig. Taf. XXVIII.

Cardano, G., 1570.
Hieronymi Cardani; Opus Novum de Proportionibus Numerorum. Cum Caes. Maiest. Gratia & Priuilegio, Basileae. 271 p.

Clark, N. N. et al., 1998.
Modeling and Development of a Linear Engine. Paper No. 98-ICE-95, ICE-Vol.30-2, 1998 Spring Technical Conference, ASME 1998. pp. 49-57.

Commandini, F., 1747.
Euclidis Elementorum Libri Priores Sex, Item Undecimus & Duodecimus. Ex Versione Latina Frederici Commandini. Quibus Accedunt. Trigonometriae Planae & Sphaericae Elementa. Item Tractatus de Natura & Arithmetica Logarithmorum. In usum Juventutis Academicae. Editio Quinta, Auctior & Emendatior. Oxoniae, E Theatro Sheldoniano, MDCCXLVII. Impenfis Ric. Clements Bibliop. Oxon. Proftat apud J. & J. Knapton, S. Birt, & J. & J. Rivington, Bibliop. London. 306 numbered p.

Craven, R., Smith, J. E. & Butler S., 1987.
The Stiller-Smith Engine: Floating Gear Analysis. SAE International Congress and Exposition, Detroit, Michigan, February 23-27, 1987, SAE Technical Paper Series. 8 p.

D'Alembert, J., 1968.
Traité de Dynamique. A Reprint of the Second Edition, Paris 1758, With a new Introduction and Bibliography by Thomas L. Hankins, The Sources of Science, No. 72. Johnson Reprint Corporation, New York. 272 p.

Erdman, A. G. & Sandor, G. N., 1997.
Mechanism Design: Analysis and Synthesis. Vol. 1, Third Edition, Prentice-Hall Inc., Upper Saddle River, New Jersey. 645 p.

Euler, L., 1748.
Introductio in Analysin Infinitorum. Tomus Primus. Apud Marcum-Michaelem Bousquet & Socios., Lausannae. p. 104.

Ewing, P., 1982.
The Orbital Engine. The International Congress & Exposition, Detroit, Michigan, February 22-26, 1982, SAE Technical Paper Series. 20 p.

Faires, V. M., 1970.
Thermodynamics. Fifth Edition. The Macmillan Company, Collier-Macmillan Ltd., London. 542 p.

Furuhama, S. & Takiguchi, M., 1979.
Measurement of Piston Frictional Force in Actual Operating Diesel Engine. Off-Highway Vehicle Meeting and Exposition, MECCA, Milwaukee, September 10-13. SAE Technical Paper Series. 19 p.

Harkness, J. R., 1968.
Methods of Balancing Single Cylinder Engines. SAE National Combined Farm Construction and Industrial Machinery, Powerplant, and Transportation Meetings, Milwaukee, Wisconsin, September 9-12, 1968, SAE Technical Paper Series. 9 p.

Heath, T. L. Sir, 1956.
The Thirteen Books of Euclid's Elements. Translated from the text of Heiberg, with Introduction and Commentary, Second Edition, Revised with additions, Volume I: Introduction and Books I, II. Dover Publications, Inc., New York. 432 p.

Heath, T. L. Sir, 1956.
The Thirteen Books of Euclid's Elements. Translated from the text of Heiberg, with Introduction and Commentary, Second Edition, Revised with additions, Volume II: Books III - IX. Dover Publications, Inc., New York. 436 p.

Heath, T. L. Sir, 1956.
The Thirteen Books of Euclid's Elements. Translated from the text of Heiberg, with Introduction and Commentary, Second Edition, Revised with additions, Volume III: Books X - XIII and Appendix. Dover Publications, Inc., New York. 546 p.

Hibbeler, R. C., 2004.
Engineering Mechanics, Statics and Dynamics. Tenth Edition. Pearson Prentice Hall, Pearson Education, Inc., Upper Saddle River, New Jersey. 688 p.

Ishida, K., 1974.
Fundamental Researches on a Perfectly Balanced Rotation-Reciprocation Mechanism (Report 1, Basic Theories of This Mechanism and Basic Constitutions). Bulletin of the JSME, Vol. 17, No. 103, January 1974. pp. 132-140.

Ishida, K. et al., 1974.
Fundamental Researches on a Perfectly Balanced Rotation-Reciprocation Mechanism (Report 2, Vibration on an Eccentric Geared Device of a Crankshaft Planetary Motion System and a Dynamic Balancing Machine).
Bulletin of the JSME, Vol. 17, No. 103, January 1974. pp. 141-148.

Ishida, K. et al., 1974.
Fundamental Researches on a Perfectly Balanced Rotation-Reciprocation Mechanism (Report 3, Structural Analysis on Vibrationless Geared Devices of a Crankshaft Rotary Motion System, and their Vibration and Friction Loss).
Bulletin of the JSME, Vol. 17, No. 108, June 1974. pp. 818-827.

Ishida, K. et al., 1975.
Fundamental Researches on a Perfectly Balanced Rotation-Reciprocation Mechanism (Report 4, Static Balanced Theory of Rotation-Reciprocation Mechanism, and Comparison between Perfectly Balanced Rotation-Reciprocation Device and Known Piston-Crank Devices).
Bulletin of the JSME, Vol. 18, No. 116, February 1975. pp. 185-192.

Ishida, K. et al., 1977.
A Vibrationless Reciprocating Engine (Trial Manufacture and Experiments of a Small Two-cycle Vibrationless Reciprocating Engine).
Bulletin of the JSME, Vol. 20, No. 142, April 1977. pp. 466-474.

Ishida, K. & Yamada, T., 1986.
Research on a Two-Stroke Cycle Single Cylinder Vibrationless Reciprocating Engine Chain Saw Utilizing an Internal Gearing System (1st Report, Analysis of This Engine and Numerical Computation). Bulletin of the JSME, Vol. 29, No. 257, November 1986. pp. 3846-3853.

Ishida, K. & Yamada, T., 1986.
Research on a Two-Stroke Cycle Single Cylinder Vibrationless Reciprocating Engine Chain Saw Utilizing an Internal Gearing System (2nd Report, Trial Manufacture and Experiments). Bulletin of the JSME, Vol. 29, No. 257, November 1986.
pp. 3854-3860.

Kolin, I., 1972.
The evolution of the heat engine. Longman Group Limited, London. 105 p.

Mabie, H. H. & Reinholtz, C. F., 1987.
Mechanisms and Dynamics of Machinery. Fourth Edition, John Wiley & Sons, New York. 644 p.

MacCurdy, E., 1945.
The Notebooks of Leonardo da Vinci. Jonathan Cape Ltd., London. pp. 521-624.

Mantriota, G. & Pennestri, E., 2003.
Theoretical and Experimental Efficiency Analysis of Multi-Degrees-of-Freedom Epicyclic Gear Trains. Multibody System Dynamics, Vol. 9, Issue 4, May 2003.
pp. 389-407.

Martin, K. F., 1978.
A review of Friction Predictions in Gear Teeth. Wear, An International Journal on the Science and Technology of Friction, Lubrication and Wear, Vol. 49, Issue 2, August 1978. pp. 201-238.

Newton, I. Sir, 1687.
Philosophiae Naturalis Principia Mathematica. Imprimatur S. Pepys, Reg. Soc. Praeses, Julii 5. 1686., Londini, Jussu Societatis Regiae ac Typis Josephi Streater. Proftat apud plures Bibliopolas. Anno MDCLXXXVII. 510 p.

Norton, R. L., 1999.
Design of Machinery: An introduction to the Synthesis and Analysis of Mechanisms and Machines. Second Edition, WBC / McGraw-Hill, Singapore. 809 p.

Pennestrì, E. & Valentini, P. P., 2003.
A Review of Formulas for the Mechanical Efficiency Analysis of Two Degrees-of-Freedom Epicyclic Gear Trains. Journal of Mechanical Design, Transactions of the ASME, September 2003, Vol. 125. pp. 602-608.

Reuleaux, F., 1875.
Theoretische Kinematik. Grundzuge einer Theorie des Maschinenwesens, mit einem Atlas. Druck und Verlag von Friedrich Vieweg und Sohn, Braunschweig.
pp. 180, 585.

Richardson, D. E., 2000.
Review of Power Cylinder Friction for Diesel Engines. Journal of Engineering for Gas Turbines and Power, October 2000, Volume 122, Issue 4. pp. 506-519.

Ruch, D. M., Fronczak, F. J. & Beachley N. H., 1991.
Design of a Modified Hypocycloid Engine. International Off-Highway & Powerplant Congress and Exposition, Milwaukee, Wisconsin, September 9-12, 1991, SAE Technical Paper Series. pp. 73-90.

Sadler, J. P. & Nelle, D. E., 1979.
Design Analysis of an Epicyclic Rotary Pump Mechanism.
ASME Journal of Mechanical design, Vol. 101, January 1979. pp. 99-107.

Senft, J. R., 1990.
A General Formula for the Work Output of Reciprocating Heat Engines. Proceedings of the 25th Intersociety Energy Conversion Engineering Conference, Volume 2, American Institute of Chemical Engineers, New York 1990. pp. 179-184.

Shih, A. J., 1993.
Kinematics of the Cycloidal Internal Combustion Engine Mechanism. Journal of Mechanical Design, Transactions of the ASME, December 1993, Vol. 115.
pp. 953-959.

Shih, A. J., 1993.
Analysis and Comparison of Epicycloidal and Hypocycloidal Internal Combustion Engine Mechanisms. Journal of Mechanical Design, Transactions of the ASME, December 1993, Vol. 115. pp. 960-966.

Smith, J. E., Craven, R. P. & Cutlip R. G., 1986.
The Stiller-Smith Mechanism: A Kinematic Analysis. SAE International Congress and Exposition, Detroit, Michigan, February 24-28, 1986, SAE Technical Paper Series.
8 p.

Smith, J. E., Churchill, R. & Craven, R., 1987.
The History of the Stiller-Smith Mechanism / Engine. 87-ICE-44, Sixth ASME Wind Energy Symposium, Tenth Annual Energy-Sources Technology Conference and Exhibition, Dallas, Texas, February 15-18, 1987, ASME. 6 p.

Smith, J. E. et al., 1990.
A Compression Ignition Engine Comparison Between a Slider-Crank and a Cross-Slider based Engine. SAE International Congress and Exposition, Detroit, Michigan, February 26 - March 2, 1990, SAE Technical Paper Series. 12 p.

Taylor, C. F., 1985.
The Internal Combustion Engine in Theory and Practice. Volume 1: Thermodynamics, Fluid Flow, Performance, Second Edition, Revised. The M.I.T. Press, Massachusetts Institute of Technology, Cambridge, Massachusetts. 574 p.

Taylor, C. F., 1985.
The Internal Combustion Engine in Theory and Practice. Volume 2: Combustion, Fuels, Materials, Design, Revised Edition. The M.I.T. Press, Massachusetts Institute of Technology, Cambridge, Massachusetts. 783 p.

Wojcik, C. K., 1979.
Kinematics of an Epicyclic Gear Pump. ASME Journal of Mechanical design, Vol. 101, July 1979. pp. 449-454.

Zhang, W. J. & Li, Q., 2006.
A Closed-Form Solution to the Crank Position Corresponding to the Maximum Velocity of the Slider in a Centric Slider-Crank Mechanism. Journal of Mechanical Design, Transactions of the ASME, May 2006, Vol. 128. pp. 654-656.

Electronic documents

Clarke, A., 2006.
Polly Model Engineering Limited [www-document]. [Cited 18 Dec. 2006].
Available: http://www.pollymodelengineering.co.uk/sections/stationary-engines/anthony-mount-models/murrays-Hypocycloidal-Engine.asp

Clemmens, W. B., 2006.
Connecting Rod Length Influence on Power [www-document]. Stahl Headers Article. [Cited 29. Aug. 2006].
Available: http://www.stahlheaders.com/Lit_Rod%20Length.htm

Clemmons, B. & Stahl, J., 2006.
Rod Length Relationships [www-document]. Stahl Headers Article.
[Cited 29. Aug. 2006].
Available: http://www.stahlheaders.com/Lit_Rod%20Length.htm

Giuntini, L., 2006.
Leonet, Touristic Towns / Comuni, Il Museo Leonardiano Di Vinci [www-document]. [Cited 29 Aug. 2006].
Available: http://www.leonet.it/comuni/vincimus/invinmus.html

INA / FAG, 2007.
INA- / FAG-bearing catalogue, product information [www-document]. [Cited 2 Apr. 2007]
Available: http://www.fag.com/content.fag.de/en/index.jsp

NAMES, 2006.
Hypocycloidal Steam Pumping Engine [www-document]. North American Model Engineering Society. [Cited 17 Dec. 2006].
Available: http://neme-s.org/NAMES_2005/NAMES_30.htm

O'Connor, J. J. & Robertson, E. F., 2006.
The MacTutor History of Mathematics archive [www-document]. University of St Andrews, Scotland. Updated Oct. 2001 [Cited 29 Aug. 2006].
Available: http://www-history.mcs.st-andrews.ac.uk/history/index.html

Rice, R. & Egge, R., 1998.
Straight Arrow, A newly designed Flame Licker [www-document]. The Little Engine Pages. Updated 10 Aug. 1998 [Cited 29 Aug. 2006].
Available: http://www.geocities.com/~rrice2/my_engines/starrow/str_arro.html

Sawyer, C. A., 2003.
Cams Replace Crank in new Engine Design [www-document]. Automotive Design and Production, May 2003 [Cited 3 Sep. 2006].
Available: http://www.autofieldguide.com/articles/050302.html

Self, D., 2005.
The Parsons Epicyclic Engine [www-document]. The Museum of RetroTechnology. Updated 25 Aug. 2006 [Cited 29 Aug. 2006].
Available: http://www.dself.dsl.pipex.com/MUSEUM/POWER/parsep/parsep.htm

Spitznogle, L. & Shannon, S., 2003.
Unleashing the Power Moving Wheelchairs More Efficiently [www-document]. West Virginia University Alumni Magazine, Spring 2003, Volume 26, Number One [Cited 29 Aug. 2006]
Available: http://www.ia.wvu.edu/Catalogs/AlumniMag/wvualumnimag/issues/spring2003/htmlfiles/wheelchair.html

Weisstein, E. W., 2006.
Eric Weisstein's Treasure Troves of Science [www-document]. [Cited 29 Aug. 2006].
Available: http://www.treasure-troves.com/

Appendix 4.2.1

Cardan gear operating principle

The cardan gear mechanism is a special application of the hypocycloid mechanisms. The operating principle has been presented in the **Figure A4.2.1.1**.

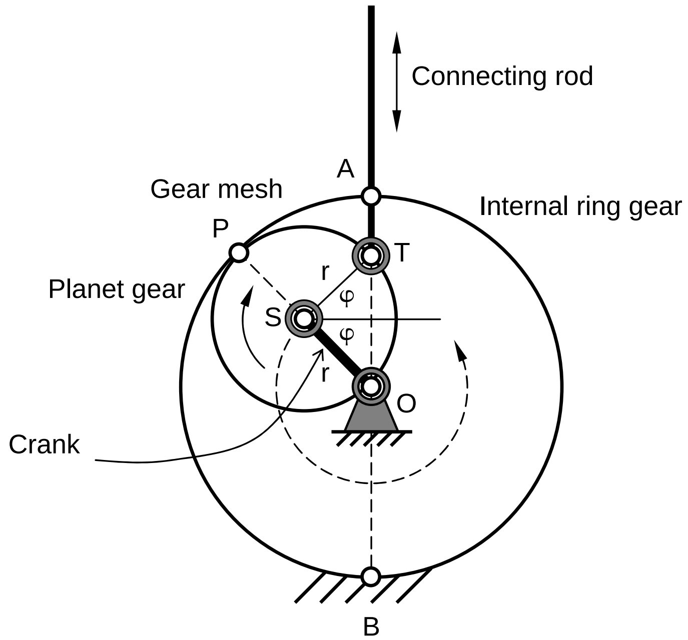

Figure A4.2.1.1. Operating principle of the cardan gear mechanism.

The frame consists of the internal ring gear APB and the coaxial revolute joint O (main bearings) of the crankshaft. Inside the ring gear rotates the planet gear (cardan wheel) OTP, the pitch circle of which is exactly half of the pitch circle of the ring gear. The planet gear has been connected to the crank OS with the revolute joint (crank bearings) S. The length of the crank is exactly the same as the radius r of the planet gear pitch circle. The connecting rod TA has been connected to the planet gear with the revolute joint (bearing) T exactly at the pitch circle. The mechanism has to be assembled so, that at the top dead center the connecting rod and the crank are at the same vertical line. The revolute joint T and the gear mesh point P are then one on the other at the point A. When the mechanism is started to run, the planet gear rolls inside the ring gear driving the crank. The connecting rod drives the planet gear. The revolute joint T reciprocates through the center O between the points A and B that are situated at the pitch circle of the ring gear. The magnitudes of the angles φ stay equal all the time. The line segment AB is exact. The planet gear and the crankshaft rotate in the opposite directions with the same angular velocity. So the angular velocity of the crank bearing S is two times higher than the angular velocity of the crankshaft or the planet gear. The pump or engine piston can be connected to the upper end of the connecting rod. The crank of the equal slider-crank mechanism corresponds the line segment OP, two times longer than the crank OS of the cardan gear mechanism.

Appendix 4.2.2

Kinematics of the slider-crank mechanism versus the cardan gear mechanism

(**Equations A4.2.2.1 ... A4.2.2.74**)

Kinematics of the slider-crank mechanism

Positions

$$\theta_{AA_0} = \theta_{AA_0 0} + \omega_{AA_0 0} \cdot t + \frac{1}{2} \cdot \alpha_{AA_0} \cdot t^2 \qquad \text{(A4.2.2.1)}$$

$$\overline{Z}_{AA_0} = Z_{AA_0} \cdot e^{i \cdot \theta_{AA_0}} \qquad \text{(A4.2.2.2)}$$

$$\theta_{BA} = \arccos\left(-\frac{Z_{AA_0} \cdot \cos(\theta_{AA_0})}{Z_{BA}} \right) \qquad \text{(A4.2.2.3)}$$

$$\overline{Z}_{BA} = Z_{BA} \cdot e^{i \cdot \theta_{BA}} \qquad \text{(A4.2.2.4)}$$

$$\overline{Z}_{BA_0} = \overline{Z}_{AA_0} + \overline{Z}_{BA} = Z_{BA_0} \cdot e^{i \cdot \theta_{BA_0}} = Z_{BA_0} \cdot e^{i \cdot 90^\circ} \qquad \text{(A4.2.2.5)}$$

$$\theta_{BA_0} = \arg(\overline{Z}_{BA_0}) = 90^\circ \qquad \text{(A4.2.2.6)}$$

Whatever point P at the center line of the connecting rod

$$\theta_{PA} = \theta_{BA} \qquad \text{(A4.2.2.7)}$$

$$\overline{Z}_{PA} = Z_{PA} \cdot e^{i \cdot \theta_{BA}} \qquad \text{(A4.2.2.8)}$$

$$\overline{Z}_{PA_0} = \overline{Z}_{AA_0} + \overline{Z}_{PA} = Z_{PA_0} \cdot e^{i \cdot \theta_{PA_0}} \qquad \text{(A4.2.2.9)}$$

$$\theta_{PA_0} = \arg(\overline{Z}_{PA_0}) \qquad \text{(A4.2.2.10)}$$

Velocities

$$\overline{v}_{AA_0} = Z_{AA_0} \cdot i \cdot \omega_{AA_0} \cdot e^{i \cdot \theta_{AA_0}} \qquad \text{(A4.2.2.11)}$$

$$\omega_{BA} = -\frac{Z_{AA_0} \cdot \omega_{AA_0} \cdot \sin(\theta_{AA_0})}{Z_{BA} \cdot \sin(\theta_{BA})} \qquad \text{(A4.2.2.12)}$$

$$\overline{v}_{BA} = Z_{BA} \cdot i \cdot \omega_{BA} \cdot e^{i \cdot \theta_{BA}} \qquad \text{(A4.2.2.13)}$$

$$\begin{aligned} \overline{v}_{BA_0} &= \overline{v}_{AA_0} + \overline{v}_{BA} = v_{BA_0} \cdot e^{i \cdot \chi_{BA_0}} = \overline{v}_{rBA_0} + \overline{v}_{tBA_0} \\ &= v_{rBA_0} \cdot e^{i \cdot \theta_{BA_0}} + Z_{BA_0} \cdot i \cdot \omega_{BA_0} \cdot e^{i \cdot \theta_{BA_0}} \end{aligned} \qquad \text{(A4.2.2.14)}$$

where $\omega_{BA_0} = 0$ and $\overline{v}_{tBA_0} = 0$

$$\chi_{BA_0} = \arg(\overline{v}_{BA_0}) = 90^\circ \text{ or } -90^\circ \qquad \text{(A4.2.2.15)}$$

$$v_{rBA_0} = \left|\overline{v}_{BA_0}\right| \cdot \cos(\chi_{BA_0} - \theta_{BA_0}) \qquad \text{(A4.2.2.16)}$$

$$\overline{v}_{rBA_0} = v_{rBA_0} \cdot e^{i \cdot \theta_{BA_0}} \qquad \text{(A4.2.2.17)}$$

$$v_{tBA_0} = \left|\overline{v}_{BA_0}\right| \cdot \sin(\chi_{BA_0} - \theta_{BA_0}) = 0 \qquad \text{(A4.2.2.18)}$$

$$\overline{v}_{tBA_0} = v_{tBA_0} \cdot e^{i \cdot (\theta_{BA_0} + 90^\circ)} = 0 \qquad \text{(A4.2.2.19)}$$

$$\omega_{BA_0} = \frac{v_{tBA_0}}{Z_{BA_0}} = 0 \qquad \text{(A4.2.2.20)}$$

Whatever point P at the center line of the connecting rod

$$\omega_{PA} = \omega_{BA} \tag{A4.2.2.21}$$

$$\bar{v}_{PA} = Z_{PA} \cdot i \cdot \omega_{BA} \cdot e^{i \cdot \theta_{BA}} \tag{A4.2.2.22}$$

$$\begin{aligned} \bar{v}_{PA_0} &= \bar{v}_{AA_0} + \bar{v}_{PA} = v_{PA_0} \cdot e^{i \cdot \chi_{PA_0}} = \bar{v}_{rPA_0} + \bar{v}_{tPA_0} \\ &= v_{rPA_0} \cdot e^{i \cdot \theta_{PA_0}} + Z_{PA_0} \cdot i \cdot \omega_{PA_0} \cdot e^{i \cdot \theta_{PA_0}} \end{aligned} \tag{A4.2.2.23}$$

$$\chi_{PA_0} = \arg(\bar{v}_{PA_0}) \tag{A4.2.2.24}$$

$$v_{rPA_0} = \left|\bar{v}_{PA_0}\right| \cdot \cos(\chi_{PA_0} - \theta_{PA_0}) \tag{A4.2.2.25}$$

$$\bar{v}_{rPA_0} = v_{rPA_0} \cdot e^{i \cdot \theta_{PA_0}} \tag{A4.2.2.26}$$

$$v_{tPA_0} = \left|\bar{v}_{PA_0}\right| \cdot \sin(\chi_{PA_0} - \theta_{PA_0}) \tag{A4.2.2.27}$$

$$\bar{v}_{tPA_0} = v_{tPA_0} \cdot e^{i \cdot (\theta_{PA_0} + 90^\circ)} \tag{A4.2.2.28}$$

$$\omega_{PA_0} = \frac{v_{tPA_0}}{Z_{PA_0}} = \frac{\bar{v}_{PA_0} - \bar{v}_{rPA_0}}{Z_{PA_0} \cdot e^{i \cdot (\theta_{PA_0} + 90^\circ)}} \tag{A4.2.2.29}$$

Accelerations

$$\bar{a}_{AA_0} = Z_{AA_0} \cdot (i \cdot \alpha_{AA_0} - \omega_{AA_0}{}^2) \cdot e^{i \cdot \theta_{AA_0}} \tag{A4.2.2.30}$$

$$\alpha_{BA} = -\frac{\begin{pmatrix} Z_{AA_0} \cdot \alpha_{AA_0} \cdot \sin(\theta_{AA_0}) + \\ + Z_{AA_0} \cdot \omega_{AA_0}{}^2 \cdot \cos(\theta_{AA_0}) + \\ + Z_{BA} \cdot \omega_{BA}{}^2 \cdot \cos(\theta_{BA}) \end{pmatrix}}{Z_{BA} \cdot \sin(\theta_{BA})} \tag{A4.2.2.31}$$

$$\bar{a}_{BA} = Z_{BA} \cdot (i \cdot \alpha_{BA} - \omega_{BA}{}^2) \cdot e^{i \cdot \theta_{BA}} \tag{A4.2.2.32}$$

$$\begin{aligned} \bar{a}_{BA_0} &= \bar{a}_{AA_0} + \bar{a}_{BA} = a_{BA_0} \cdot e^{i \cdot \psi_{BA_0}} \\ &= \bar{a}_{rBA_0} + \bar{a}_{cBA_0} + \bar{a}_{tBA_0} + \bar{a}_{nBA_0} \\ &= a_{rBA_0} \cdot e^{i \cdot \theta_{BA_0}} + 2 \cdot v_{rBA_0} \cdot \omega_{BA_0} \cdot i \cdot e^{i \cdot \theta_{BA_0}} + \\ &\quad + Z_{BA_0} \cdot \alpha_{BA_0} \cdot i \cdot e^{i \cdot \theta_{BA_0}} - Z_{BA_0} \cdot \omega_{BA_0}{}^2 \cdot e^{i \cdot \theta_{BA_0}} \end{aligned} \tag{A4.2.2.33}$$

where $\omega_{BA_0} = 0$ and $\alpha_{BA_0} = 0$

$$\psi_{BA_0} = \arg(\bar{a}_{BA_0}) = 90^\circ \text{ or } -90^\circ \tag{A4.2.2.34}$$

$$a_{rBA_0} = \left|\bar{a}_{BA_0}\right| \cdot \cos(\psi_{BA_0} - \theta_{BA_0}) + Z_{BA_0} \cdot \omega_{BA_0}{}^2 \tag{A4.2.2.35}$$

$$\bar{a}_{rBA_0} = a_{rBA_0} \cdot e^{i \cdot \theta_{BA_0}} \tag{A4.2.2.36}$$

$$a_{cBA_0} = 2 \cdot v_{rBA_0} \cdot \omega_{BA_0} = 0 \tag{A4.2.2.37}$$

$$\bar{a}_{cBA_0} = a_{cBA_0} \cdot e^{i \cdot (\theta_{BA_0} + 90^\circ)} = 0 \tag{A4.2.2.38}$$

$$\begin{aligned} a_{tBA_0} &= Z_{BA_0} \cdot \alpha_{BA_0} \\ &= \left|\bar{a}_{BA_0}\right| \cdot \sin(\psi_{BA_0} - \theta_{BA_0}) - 2 \cdot v_{rBA_0} \cdot \omega_{BA_0} = 0 \end{aligned} \tag{A4.2.2.39}$$

$$\bar{a}_{tBA_0} = a_{tBA_0} \cdot e^{i \cdot (\theta_{BA_0} + 90^\circ)} = 0 \tag{A4.2.2.40}$$

$$a_{nBA_0} = -Z_{BA_0} \cdot \omega_{BA_0}{}^2 = 0 \tag{A4.2.2.41}$$

$$\bar{a}_{nBA_0} = a_{nBA_0} \cdot e^{i \cdot \theta_{BA_0}} = Z_{BA_0} \cdot \omega_{BA_0}{}^2 \cdot e^{i \cdot (\theta_{BA_0} + 180^\circ)} = 0 \tag{A4.2.2.42}$$

Whatever point P at the center line of the connecting rod

$$\alpha_{PA} = \alpha_{BA} \tag{A4.2.2.43}$$

$$\bar{a}_{PA} = Z_{PA} \cdot (i \cdot \alpha_{BA} - \omega_{BA}{}^2) \cdot e^{i \cdot \theta_{BA}} \tag{A4.2.2.44}$$

$$\begin{aligned} \bar{a}_{PA_0} &= \bar{a}_{AA_0} + \bar{a}_{PA} = a_{PA_0} \cdot e^{i \cdot \psi_{PA_0}} \\ &= \bar{a}_{rPA_0} + \bar{a}_{cPA_0} + \bar{a}_{tPA_0} + \bar{a}_{nPA_0} \\ &= a_{rPA_0} \cdot e^{i \cdot \theta_{PA_0}} + 2 \cdot v_{rPA_0} \cdot \omega_{PA_0} \cdot i \cdot e^{i \cdot \theta_{PA_0}} + \\ &\quad + Z_{PA_0} \cdot \alpha_{PA_0} \cdot i \cdot e^{i \cdot \theta_{PA_0}} - Z_{PA_0} \cdot \omega_{PA_0}{}^2 \cdot e^{i \cdot \theta_{PA_0}} \end{aligned} \tag{A4.2.2.45}$$

$$\psi_{PA_0} = \arg(\bar{a}_{PA_0}) \tag{A4.2.2.46}$$

$$a_{rPA_0} = \left|\bar{a}_{PA_0}\right| \cdot \cos(\psi_{PA_0} - \theta_{PA_0}) + Z_{PA_0} \cdot \omega_{PA_0}{}^2 \tag{A4.2.2.47}$$

$$\bar{a}_{rPA_0} = a_{rPA_0} \cdot e^{i \cdot \theta_{PA_0}} \tag{A4.2.2.48}$$

$$a_{cPA_0} = 2 \cdot v_{rPA_0} \cdot \omega_{PA_0} \tag{A4.2.2.49}$$

$$\bar{a}_{cPA_0} = a_{cPA_0} \cdot e^{i \cdot (\theta_{PA_0} + 90^\circ)} \tag{A4.2.2.50}$$

$$\begin{aligned} a_{tPA_0} &= Z_{PA_0} \cdot \alpha_{PA_0} \\ &= \left|\bar{a}_{PA_0}\right| \cdot \sin(\psi_{PA_0} - \theta_{PA_0}) - 2 \cdot v_{rPA_0} \cdot \omega_{PA_0} \end{aligned} \tag{A4.2.2.51}$$

$$\bar{a}_{tPA_0} = a_{tPA_0} \cdot e^{i \cdot (\theta_{PA_0} + 90^\circ)} \tag{A4.2.2.52}$$

$$a_{nPA_0} = -Z_{PA_0} \cdot \omega_{PA_0}{}^2 \tag{A4.2.2.53}$$

$$\bar{a}_{nPA_0} = a_{nPA_0} \cdot e^{i \cdot \theta_{PA_0}} = Z_{PA_0} \cdot \omega_{PA_0}{}^2 \cdot e^{i \cdot (\theta_{PA_0} + 180^\circ)} \tag{A4.2.2.54}$$

$$\alpha_{PA_0} = \frac{a_{tPA_0}}{Z_{PA_0}} = \frac{\bar{a}_{PA_0} - \bar{a}_{rPA_0} - \bar{a}_{cPA_0} - \bar{a}_{nPA_0}}{Z_{PA_0} \cdot e^{i \cdot (\theta_{PA_0} + 90^\circ)}} \tag{A4.2.2.55}$$

Kinematics of the cardan gear mechanism

Positions

$$\theta_{AA_0c} = \theta_{AA_0 0c} + \omega_{AA_0 0c} \cdot t + \frac{1}{2} \cdot \alpha_{AA_0c} \cdot t^2 \tag{A4.2.2.56}$$

$$\overline{Z}_{AA_0c} = Z_{AA_0c} \cdot e^{i \cdot \theta_{AA_0c}} \tag{A4.2.2.57}$$

$$\theta_{BAc} = 180^\circ - \theta_{AA_0c} \tag{A4.2.2.58}$$

$$\overline{Z}_{BAc} = Z_{BAc} \cdot e^{i \cdot \theta_{BAc}} = Z_{AA_0c} \cdot e^{i \cdot (180^\circ - \theta_{AA_0c})} \tag{A4.2.2.59}$$

$$\begin{aligned} \overline{Z}_{BA_0c} &= \overline{Z}_{AA_0c} + \overline{Z}_{BAc} = 2 \cdot Z_{AA_0c} \cdot \sin(\theta_{AA_0c}) \cdot e^{i \cdot 90^\circ} \\ &= Z_{BA_0c} \cdot e^{i \cdot \theta_{BA_0c}} \end{aligned} \tag{A4.2.2.60}$$

$$\theta_{BA_0c} = \arg(\overline{Z}_{BA_0c}) = 90^\circ \text{ or } -90^\circ \tag{A4.2.2.61}$$

$$\overline{Z}_{bBc} = Z_{bBc} \cdot e^{i \cdot 90^\circ} \tag{A4.2.2.62}$$

$$\overline{Z}_{bA_0c} = \overline{Z}_{BA_0c} + \overline{Z}_{bBc} = Z_{bA_0c} \cdot e^{i \cdot 90^\circ} \tag{A4.2.2.63}$$

Velocities

$$\omega_{AA_0c} = \omega_{AA_0 0c} + \alpha_{AA_0c} \cdot t \tag{A4.2.2.64}$$

$$\overline{v}_{AA_0c} = Z_{AA_0c} \cdot i \cdot \omega_{AA_0c} \cdot e^{i \cdot \theta_{AA_0c}} \tag{A4.2.2.65}$$

$$\omega_{BAc} = -\omega_{AA_0c} \tag{A4.2.2.66}$$

$$\begin{aligned} \overline{v}_{BAc} &= Z_{BAc} \cdot i \cdot \omega_{BAc} \cdot e^{i \cdot \theta_{BAc}} \\ &= Z_{AA_0c} \cdot i \cdot \omega_{AA_0c} \cdot e^{i \cdot (-\theta_{AA_0c})} \end{aligned} \tag{A4.2.2.67}$$

$$\begin{aligned} \overline{v}_{BA_0c} &= \overline{v}_{AA_0c} + \overline{v}_{BAc} \\ &= 2 \cdot Z_{AA_0c} \cdot \omega_{AA_0c} \cdot \cos(\theta_{AA_0c}) \cdot e^{i \cdot 90^\circ} \\ &= v_{BA_0c} \cdot e^{i \cdot \chi_{BA_0c}} = \overline{v}_{rBA_0c} \end{aligned} \tag{A4.2.2.68}$$

$$\chi_{BA_0c} = \arg(\overline{v}_{BA_0c}) = 90^\circ \text{ or } -90^\circ \tag{A4.2.2.69}$$

Accelerations

$$\bar{a}_{AA_0c} = Z_{AA_0c} \cdot (i \cdot \alpha_{AA_0c} - \omega_{AA_0c}{}^2) \cdot e^{i \cdot \theta_{AA_0c}} \qquad \text{(A4.2.2.70)}$$

$$\alpha_{BAc} = -\alpha_{AA_0c} \qquad \text{(A4.2.2.71)}$$

$$\begin{aligned} \bar{a}_{BAc} &= Z_{BAc} \cdot (i \cdot \alpha_{BAc} - \omega_{BAc}{}^2) \cdot e^{i \cdot \theta_{BAc}} \\ &= Z_{AA_0c} \cdot (-i \cdot \alpha_{AA_0c} - \omega_{AA_0c}{}^2) \cdot e^{i \cdot (180^\circ - \theta_{AA_0c})} \end{aligned} \qquad \text{(A4.2.2.72)}$$

$$\begin{aligned} &\bar{a}_{BA_0c} = \bar{a}_{AA_0c} + \bar{a}_{BAc} \\ &= 2 \cdot Z_{AA_0c} \cdot \\ &\cdot \left(\alpha_{AA_0c} \cdot \cos(\theta_{AA_0c}) - \omega_{AA_0c}{}^2 \cdot \sin(\theta_{AA_0c})\right) \cdot e^{i \cdot 90^\circ} \\ &= a_{BA_0c} \cdot e^{i \cdot \psi_{BA_0c}} = \bar{a}_{rBA_0c} \end{aligned} \qquad \text{(A4.2.2.73)}$$

$$\psi_{BA_0c} = \arg(\bar{a}_{BA_0c}) = 90^\circ \text{ or } -90^\circ \qquad \text{(A4.2.2.74)}$$

Appendix 5.2.1

Kinetostatics of the slider-crank mechanism versus the cardan gear mechanism

(**Equations A5.2.1.1 ... A5.2.1.72**)

Kinetostatics of the slider-crank mechanism

Crankshaft

$$T_{ine1} = -J_1 \cdot \alpha_{AA_0} \tag{A5.2.1.1}$$

$$T_{1i10} = T_{ine1} \tag{A5.2.1.2}$$

$$T_{1i01} = -T_{1i10} \tag{A5.2.1.3}$$

Connecting rod

$$\overline{F}_{ine2} = -m_2 \cdot \overline{a}_{g2A_0} \tag{A5.2.1.4}$$

$$\beta_{g2} = \arg(\overline{a}_{g2A_0}) \tag{A5.2.1.5}$$

$$L_{p2} = \frac{-J_2 \cdot \alpha_{BA}}{\left|\overline{F}_{ine2}\right| \cdot \sin(\beta_{g2} + \pi - \theta_{BA})} \tag{A5.2.1.6}$$

$$L_{i2} = r_{g2} + L_{p2} \tag{A5.2.1.7}$$

$$\overline{L}_{i2} = L_{i2} \cdot e^{i \cdot \theta_{BA}} \tag{A5.2.1.8}$$

$$\begin{cases} \overline{F}_{2i12} + \overline{F}_{ine2} + \overline{F}_{2i32} = 0 \\ \overline{Z}_{BA} \times \overline{F}_{2i32} + \overline{L}_{i2} \times \overline{F}_{ine2} = 0 \end{cases} \tag{A5.2.1.9}$$

$$\overline{F}_{2i32} = -\frac{L_{i2} \cdot \left|\overline{F}_{ine2}\right| \cdot \sin(\beta_{g2} + \pi - \theta_{BA})}{Z_{BA} \cdot \sin(0 - \theta_{BA})} \cdot e^{i \cdot 0} \tag{A5.2.1.10}$$

$$\overline{F}_{2i12} = -\overline{F}_{ine2} - \overline{F}_{2i32} \tag{A5.2.1.11}$$

$$\overline{F}_{2i21} = \overline{F}_{2i10} = -\overline{F}_{2i12} \tag{A5.2.1.12}$$

$$\overline{F}_{2i23} = \overline{F}_{2i30} = -\overline{F}_{2i32} \tag{A5.2.1.13}$$

$$\overline{F}_{2i01} = \overline{F}_{2i12} \tag{A5.2.1.14}$$

$$T_{2i10} = \left|\overline{F}_{2i21}\right| \cdot Z_{AA_0} \cdot \sin\left(\arg(\overline{F}_{2i21}) - \theta_{AA_0}\right) \tag{A5.2.1.15}$$

$$T_{2i01} = -T_{2i10} \tag{A5.2.1.16}$$

Piston with the pin

$$\overline{F}_{ine3} = -m_3 \cdot \overline{a}_{g3A_0} \tag{A5.2.1.17}$$

$$\overline{F}_{ine3} + \overline{F}_{3i03} + \overline{F}_{3i23} = 0 \tag{A5.2.1.18}$$

$$\begin{aligned}\overline{F}_{3i23} &= \frac{\left|\overline{F}_{ine3}\right| \cdot \sin\left(\arg(\overline{a}_{g3A_0}) + \pi\right)}{\sin(\theta_{BA})} \cdot e^{i\cdot(\theta_{BA} - \pi)} \\ &= \frac{\left|\overline{F}_{ine3}\right|}{\sin(\theta_{BA})} \cdot e^{i\cdot(\theta_{BA} - \pi)}\end{aligned} \tag{A5.2.1.19}$$

$$\overline{F}_{3i03} = \left|\overline{F}_{3i23}\right| \cdot \cos(\theta_{BA}) \cdot e^{i\cdot 0} = \frac{\left|\overline{F}_{3i23}\right|}{\tan(\theta_{BA})} \cdot e^{i\cdot 0} \tag{A5.2.1.20}$$

$$\overline{F}_{3i30} = -\overline{F}_{3i03} \tag{A5.2.1.21}$$

$$\overline{F}_{3i01} = -\overline{F}_{3i10} = \overline{F}_{3i12} = -\overline{F}_{3i21} = -\overline{F}_{3i32} = \overline{F}_{3i23} \tag{A5.2.1.22}$$

$$T_{3i10} = \left|\overline{F}_{3i21}\right| \cdot Z_{AA_0} \cdot \sin\left(\arg(\overline{F}_{3i21}) - \theta_{AA_0}\right) \tag{A5.2.1.23}$$

$$T_{3i01} = -T_{3i10} \tag{A5.2.1.24}$$

Total inertial joint forces of the slider-crank mechanism

$$\overline{F}_{\Sigma i01} = \overline{F}_{2i01} + \overline{F}_{3i01} \tag{A5.2.1.25}$$

$$\overline{F}_{\Sigma i10} = \overline{F}_{2i10} + \overline{F}_{3i10} \tag{A5.2.1.26}$$

$$\overline{F}_{\Sigma i12} = \overline{F}_{2i12} + \overline{F}_{3i12} \tag{A5.2.1.27}$$

$$\overline{F}_{\Sigma i21} = \overline{F}_{2i21} + \overline{F}_{3i21} \tag{A5.2.1.28}$$

$$\overline{F}_{\Sigma i23} = \overline{F}_{2i23} + \overline{F}_{3i23} \tag{A5.2.1.29}$$

$$\overline{F}_{\Sigma i32} = \overline{F}_{2i32} + \overline{F}_{3i32} \tag{A5.2.1.30}$$

$$\overline{F}_{\Sigma i03} = \overline{F}_{2i03} + \overline{F}_{3i03} \tag{A5.2.1.31}$$

$$\overline{F}_{\Sigma i30} = \overline{F}_{2i30} + \overline{F}_{3i30} \tag{A5.2.1.32}$$

Summed piston pin inertial joint forces of the slider-crank mechanism

$$\overline{F}_{\Sigma i3in} = \overline{F}_{\Sigma i03} + \overline{F}_{\Sigma i23} \tag{A5.2.1.33}$$

$$\overline{F}_{\Sigma i3out} = \overline{F}_{\Sigma i30} + \overline{F}_{\Sigma i32} \tag{A5.2.1.34}$$

Total inertial crankshaft torques of the slider-crank mechanism

$$T_{\Sigma i01} = T_{1i01} + T_{2i01} + T_{3i01} \tag{A5.2.1.35}$$

$$T_{\Sigma i10} = T_{1i10} + T_{2i10} + T_{3i10} \tag{A5.2.1.36}$$

Total inertial work of the slider-crank mechanism

$$\Sigma W_{ine} = \int_{\theta_{AA_0 \min}}^{\theta_{AA_0 \max}} T_{\Sigma i10} \cdot d\theta_{AA_0} \tag{A5.2.1.37}$$

Mean crankshaft inertial torque of the slider-crank mechanism

$$T_{inemean} = \frac{\Sigma W_{ine}}{\theta_{AA_0 \max} - \theta_{AA_0 \min}} \tag{A5.2.1.38}$$

Crankshaft inertial power of the slider-crank mechanism

$$P_{ine} = T_{\Sigma i10} \cdot \omega_{AA_0} \tag{A5.2.1.39}$$

Kinetostatics of the cardan gear mechanism

Crankshaft

$$T_{ine1c} = -J_{1c} \cdot \alpha_{AA_0c} \tag{A5.2.1.40}$$

$$T_{1i10c} = T_{ine1c} \tag{A5.2.1.41}$$

$$T_{1i01c} = -T_{1i10c} \tag{A5.2.1.42}$$

Cardan wheel

$$T_{ine2c} = -J_{2c} \cdot \alpha_{BAc} \tag{A5.2.1.43}$$

$$T_{2i21c} = T_{ine2c} \tag{A5.2.1.44}$$

$$T_{2i12c} = T_{2i01} = -T_{2i21c} \tag{A5.2.1.45}$$

$$T_{2i10c} = T_{2i21c} \tag{A5.2.1.46}$$

Piston with the pin and the connecting rod

$$\overline{F}_{ine3c} = -m_{3c} \cdot \overline{a}_{g3A_0c} \tag{A5.2.1.47}$$

$$\overline{F}_{3i32c} = \overline{F}_{ine3c} \tag{A5.2.1.48}$$

$$\overline{F}_{3i23c} = \overline{F}_{3i20c} = -\overline{F}_{3i02c} = -\overline{F}_{3i32c} \tag{A5.2.1.49}$$

$$\overline{F}_{3i30c} = \overline{F}_{3i03c} = 0 \tag{A5.2.1.50}$$

$$\overline{F}_{3i21c} = -\overline{F}_{3i12c} = \overline{F}_{3i10c} = -\overline{F}_{3i01c} = 2 \cdot \overline{F}_{3i32c} \tag{A5.2.1.51}$$

$$T_{3i10c} = \left|\overline{F}_{3i21c}\right| \cdot Z_{AA_0c} \cdot \sin\left(\arg(\overline{F}_{3i21c}) - \theta_{AA_0c}\right) \tag{A5.2.1.52}$$

$$T_{3i01c} = -T_{3i10c} \tag{A5.2.1.53}$$

Total inertial joint forces of the cardan gear mechanism

$$\overline{F}_{\Sigma i01c} = \overline{F}_{3i01c} \tag{A5.2.1.54}$$
$$\overline{F}_{\Sigma i10c} = \overline{F}_{3i10c} \tag{A5.2.1.55}$$
$$\overline{F}_{\Sigma i02c} = \overline{F}_{3i02c} \tag{A5.2.1.56}$$
$$\overline{F}_{\Sigma i20c} = \overline{F}_{3i20c} \tag{A5.2.1.57}$$
$$\overline{F}_{\Sigma i12c} = \overline{F}_{3i12c} \tag{A5.2.1.58}$$
$$\overline{F}_{\Sigma i21c} = \overline{F}_{3i21c} \tag{A5.2.1.59}$$
$$\overline{F}_{\Sigma i23c} = \overline{F}_{3i23c} \tag{A5.2.1.60}$$
$$\overline{F}_{\Sigma i32c} = \overline{F}_{3i32c} \tag{A5.2.1.61}$$
$$\overline{F}_{\Sigma i03c} = \overline{F}_{3i03c} = 0 \tag{A5.2.1.62}$$
$$\overline{F}_{\Sigma i30c} = \overline{F}_{3i30c} = 0 \tag{A5.2.1.63}$$

Summed piston pin inertial joint forces of the cardan gear mechanism

$$\overline{F}_{\Sigma i3inc} = \overline{F}_{\Sigma i03c} + \overline{F}_{\Sigma i23c} = \overline{F}_{\Sigma i23c} \tag{A5.2.1.64}$$
$$\overline{F}_{\Sigma i3outc} = \overline{F}_{\Sigma i30c} + \overline{F}_{\Sigma i32c} = \overline{F}_{\Sigma i32c} \tag{A5.2.1.65}$$

Total inertial crankshaft torques of the cardan gear mechanism

$$T_{\Sigma i12c} = T_{2i12c} \tag{A5.2.1.66}$$
$$T_{\Sigma i21c} = T_{2i21c} \tag{A5.2.1.67}$$
$$T_{\Sigma i01c} = T_{1i01c} + T_{2i01c} + T_{3i01c} \tag{A5.2.1.68}$$
$$T_{\Sigma i10c} = T_{1i10c} + T_{2i10c} + T_{3i10c} \tag{A5.2.1.69}$$

Total inertial work of the cardan gear mechanism

$$\Sigma W_{inec} = \int_{\theta_{AA_0 c\,min}}^{\theta_{AA_0 c\,max}} T_{\Sigma i10c} \cdot d\theta_{AA_0 c} \qquad \text{(A5.2.1.70)}$$

Mean crankshaft inertial torque of the cardan gear mechanism

$$T_{inemeanc} = \frac{\Sigma W_{inec}}{\theta_{AA_0 c\,max} - \theta_{AA_0 c\,min}} \qquad \text{(A5.2.1.71)}$$

Crankshaft inertial power of the cardan gear mechanism

$$P_{inec} = T_{\Sigma i10c} \cdot \omega_{AA_0 c} \qquad \text{(A5.2.1.72)}$$

Appendix 6.1.1

Thermodynamics of the slider-crank machines versus the cardan gear machines

[*Faires 1970, Taylor 1985*] (**Equations A6.1.1.1 ... A6.1.1.14**)

Stroke

$$Stroke = 2 \cdot Z_{AA_0} = 4 \cdot Z_{AA_0c} \qquad (A6.1.1.1)$$

Displacement (stroke volume)

$$V_{stroke} = A_{pis} \cdot Stroke \qquad (A6.1.1.2)$$

where A_{pis} = piston area

Compressed volume

$$V_{comp} = \frac{V_{stroke}}{Comp.ratio - 1} \qquad (A6.1.1.3)$$

Maximum isothermal compression pressure

The standard atmospheric pressure is $p_{atm} = 1.01325 \cdot 10^5$ Pa.

$$p_{comp\,max} = \frac{p_{atm} \cdot (V_{stroke} + V_{comp})}{V_{comp}} \qquad (A6.1.1.4)$$

Maximum uncompressed volume

$$V_{unc} = V_{stroke} + V_{comp} \qquad (A6.1.1.5)$$

Polytropic exponent

For the air pumps and engines the polytropic exponent is γ_{pol} = 1.3 ... 1.4.

Maximum polytropic compression pressure

The cylinder filling of the engines and pumps varies from 100 % to 110 %.

$$p_{polmax} = \frac{p_{atm} \cdot (C_{fill} \cdot V_{unc})^{\gamma_{pol}}}{V_{comp}{}^{\gamma_{pol}}} \quad \text{(A6.1.1.6)}$$

where C_{fill} = filling coefficient (≈ 1.0 ... 1.1)

The maximum polytropic compression pressure is typically 1.3 ... 5 MPa in pumps and gasoline engines and 4 ... 10 MPa in diesel engines.

Minimum height of the cylinder chamber (flat piston, flat deck)

$$h_{cha} = \frac{V_{comp}}{A_{piston}} \quad \text{(A6.1.1.7)}$$

Deck height

$$h_{deck} = h_{cha} + h_{pishead} + Z_{BA} + Z_{AA_0} \quad \text{(A6.1.1.8)}$$

where $h_{pishead}$ = piston head height

Theoretical cylinder volumes during running

$$V_{cyl} = (h_{deck} - (h_{pishead} + Z_{BA_0})) \cdot A_{pis} \quad \text{(A6.1.1.9)}$$

$$V_{cylc} = (h_{deck} - (h_{pishead} + Z_{bA_0c})) \cdot A_{pis} \quad \text{(A6.1.1.10)}$$

where Z_{BA0} = piston pin position of the slider-crank machine
Z_{bA0c} = piston pin position of the cardan gear machine

Polytropic compression pressures during running

Polytropic compression pressure is acting in the pumps during compression strokes. It is also needed as an initial value for the calculations of the combustion pressures of the four-stroke engines.

$$p_{pol}(\theta_{AA_0}) = \frac{p_{atm} \cdot (C_{fill} \cdot V_{unc})^{\gamma_{pol}}}{V_{cyl}{}^{\gamma_{pol}}} \quad \text{(A6.1.1.11)}$$

$$p_{polc}(\theta_{AA_0c}) = \frac{p_{atm} \cdot (C_{fill} \cdot V_{unc})^{\gamma_{pol}}}{V_{cylc}{}^{\gamma_{pol}}} \quad \text{(A6.1.1.12)}$$

Approximated combustion pressures of the four-stroke engines

In the engine cylinders the maximum combustion pressure exists, when the crankshaft angle is 8 ...10 ° after the top dead center.
The maximum combustion pressure is typically 7 ... 17 MPa depending on the engine type.
The maximum combustion temperature is near 2500 °C.
When the maximum combustion pressure and the compression pressure distribution are known, the combustion pressure distribution has been approximated in this study as follows:

$$p_{comb}(\theta_{AA_0}) = \frac{p_{combmax}}{p_{polmax}} \cdot p_{pol}(\theta_{AA_0} - 8...10^\circ) \qquad \text{(A6.1.1.13)}$$

$$p_{combc}(\theta_{AA_0c}) = \frac{p_{combcmax}}{p_{polcmax}} \cdot p_{polc}(\theta_{AA_0c} - 8...10^\circ) \qquad \text{(A6.1.1.14)}$$

In the preceding equations:

p_{pol} = polytropic compression pressure in the slider-crank engine
p_{polc} = polytropic compression pressure in the cardan gear engine
p_{polmax} = maximum polytropic compression pressure in the slider-crank engine
$p_{polcmax}$ = maximum polytropic compression pressure in the cardan gear engine
$p_{combmax}$ = maximum combustion pressure in the slider-crank engine
$p_{combcmax}$ = maximum combustion pressure in the cardan gear engine

Appendix 6.2.1

Kinetics of the slider-crank machines versus the cardan gear machines

(**Equations A6.2.1.1 ... A6.2.1.54**)

Compression forces of the pistons

$$F_{comp} = p_{pol} \cdot A_{pis} \quad \text{(A6.2.1.1)}$$

$$F_{compc} = p_{polc} \cdot A_{pis} \quad \text{(A6.2.1.2)}$$

Compression forces of the connecting rods

$$F_{BAcomp} = \frac{F_{comp}}{\sin(\theta_{BA})} \quad \text{(A6.2.1.3)}$$

$$F_{BAcompc} = F_{compc} \quad \text{(A6.2.1.4)}$$

Compression torques of the crankshafts

$$T_{comp} = F_{BAcomp} \cdot Z_{AA_0} \cdot \sin(\theta_{BA} + \pi - \theta_{AA_0}) \quad \text{(A6.2.1.5)}$$

$$T_{compc} = 2 \cdot F_{BAcompc} \cdot Z_{AA_0c} \cdot \sin(-90^\circ - \theta_{AA_0c}) \quad \text{(A6.2.1.6)}$$

Total compression works

$$\Sigma W_{comp} = \int_{\theta_{AA_0 min}}^{\theta_{AA_0 max}} T_{comp} \cdot d\theta_{AA_0} \quad \text{(A6.2.1.7)}$$

$$\Sigma W_{compc} = \int_{\theta_{AA_0c min}}^{\theta_{AA_0c max}} T_{compc} \cdot d\theta_{AA_0c} \quad \text{(A6.2.1.8)}$$

Mean compression torques of the crankshafts

$$T_{compmean} = \frac{\Sigma W_{comp}}{\theta_{AA_0 max} - \theta_{AA_0 min}} \quad \text{(A6.2.1.9)}$$

$$T_{compmeanc} = \frac{\Sigma W_{compc}}{\theta_{AA_0c max} - \theta_{AA_0c min}} \quad \text{(A6.2.1.10)}$$

Compression powers of the crankshafts

$$P_{comp} = T_{comp} \cdot \omega_{AA_0} \qquad \text{(A6.2.1.11)}$$

$$P_{compc} = T_{compc} \cdot \omega_{AA_0c} \qquad \text{(A6.2.1.12)}$$

Combustion forces of the pistons

$$F_{comb} = p_{comb} \cdot A_{pis} \qquad \text{(A6.2.1.13)}$$

$$F_{combc} = p_{combc} \cdot A_{pis} \qquad \text{(A6.2.1.14)}$$

Combustion forces of the connecting rods

$$F_{BAcomb} = \frac{F_{comb}}{\sin(\theta_{BA})} \qquad \text{(A6.2.1.15)}$$

$$F_{BAcombc} = F_{combc} \qquad \text{(A6.2.1.16)}$$

Combustion torques of the crankshafts

$$T_{comb} = F_{BAcomb} \cdot Z_{AA_0} \cdot \sin(\theta_{BA} + \pi - \theta_{AA_0}) \qquad \text{(A6.2.1.17)}$$

$$T_{combc} = 2 \cdot F_{BAcombc} \cdot Z_{AA_0c} \cdot \sin(-90^\circ - \theta_{AA_0c}) \qquad \text{(A6.2.1.18)}$$

Total combustion works

$$\Sigma W_{comb} = \int_{\theta_{AA_0\,min}}^{\theta_{AA_0\,max}} T_{comb} \cdot d\theta_{AA_0} \qquad \text{(A6.2.1.19)}$$

$$\Sigma W_{combc} = \int_{\theta_{AA_0c\,min}}^{\theta_{AA_0c\,max}} T_{combc} \cdot d\theta_{AA_0c} \qquad \text{(A6.2.1.20)}$$

Mean combustion torques of the crankshafts

$$T_{combmean} = \frac{\Sigma W_{comb}}{\theta_{AA_0\,max} - \theta_{AA_0\,min}} \qquad \text{(A6.2.1.21)}$$

$$T_{combmeanc} = \frac{\Sigma W_{combc}}{\theta_{AA_0c\,max} - \theta_{AA_0c\,min}} \qquad \text{(A6.2.1.22)}$$

Combustion powers of the crankshafts

$$P_{comb} = T_{comb} \cdot \omega_{AA_0} \tag{A6.2.1.23}$$

$$P_{combc} = T_{combc} \cdot \omega_{AA_0c} \tag{A6.2.1.24}$$

Compression joint forces and torques of the slider-crank machines

Compression joint forces of the slider-crank machines

$$\overline{F}_{comp23} = \frac{F_{comp}}{\sin(\theta_{BA})} \cdot e^{i \cdot \theta_{BA}} \tag{A6.2.1.25}$$

$$\overline{F}_{comp03} = -\frac{F_{comp}}{\tan(\theta_{BA})} \cdot e^{i \cdot 0^\circ} \tag{A6.2.1.26}$$

$$\overline{F}_{comp30} = -\overline{F}_{comp03} \tag{A6.2.1.27}$$

$$\begin{aligned} \overline{F}_{comp01} &= -\overline{F}_{comp10} = \overline{F}_{comp12} = -\overline{F}_{comp21} \\ &= -\overline{F}_{comp32} = \overline{F}_{comp23} \end{aligned} \tag{A6.2.1.28}$$

Summed piston pin compression joint forces of the slider-crank machines

$$\overline{F}_{\Sigma comp3in} = \overline{F}_{comp03} + \overline{F}_{comp23} \tag{A6.2.1.29}$$

$$\overline{F}_{\Sigma comp\,3out} = \overline{F}_{comp\,30} + \overline{F}_{comp\,32} \tag{A6.2.1.30}$$

Crankshaft compression torques of the slider-crank machines

$$T_{comp01} = -\left|\overline{F}_{comp21}\right| \cdot Z_{AA_0} \cdot \sin(\arg(\overline{F}_{comp21}) - \theta_{AA_0}) \tag{A6.2.1.31}$$

$$T_{comp10} = -T_{comp01} \tag{A6.2.1.32}$$

Compression joint forces and torques of the cardan gear machines

Compression joint forces of the cardan gear machines

$$\overline{F}_{comp23c} = F_{compc} \cdot e^{i \cdot 90^\circ} \quad \text{(A6.2.1.33)}$$

$$\overline{F}_{comp03c} = 0 \quad \text{(A6.2.1.34)}$$

$$\overline{F}_{comp30c} = -\overline{F}_{comp03c} = 0 \quad \text{(A6.2.1.35)}$$

$$\overline{F}_{comp02c} = -\overline{F}_{comp20c} = -\overline{F}_{comp32c} = \overline{F}_{comp23c} \quad \text{(A6.2.1.36)}$$

$$\begin{aligned}\overline{F}_{comp01c} &= -\overline{F}_{comp10c} = \overline{F}_{comp12c} = -\overline{F}_{comp21c} \\ &= 2 \cdot \overline{F}_{comp23c}\end{aligned} \quad \text{(A6.2.1.37)}$$

Compression torques of the cardan gear machines

$$\begin{aligned}T_{comp01c} &= -\left|\overline{F}_{comp21c}\right| \cdot Z_{AA_0c} \cdot \\ &\cdot \sin(\arg(\overline{F}_{comp21c}) - \theta_{AA_0c})\end{aligned} \quad \text{(A6.2.1.38)}$$

$$T_{comp10c} = -T_{comp01c} \quad \text{(A6.2.1.39)}$$

Combustion joint forces and torques of the slider-crank engines

Combustion joint forces of the slider-crank engines

$$\overline{F}_{comb23} = \frac{F_{comb}}{\sin(\theta_{BA})} \cdot e^{i \cdot \theta_{BA}} \quad \text{(A6.2.1.40)}$$

$$\overline{F}_{comb03} = -\frac{F_{comb}}{\tan(\theta_{BA})} \cdot e^{i \cdot 0^\circ} \quad \text{(A6.2.1.41)}$$

$$\overline{F}_{comb30} = -\overline{F}_{comb03} \quad \text{(A6.2.1.42)}$$

$$\begin{aligned}\overline{F}_{comb01} &= -\overline{F}_{comb10} = \overline{F}_{comb12} = -\overline{F}_{comb21} \\ &= -\overline{F}_{comb32} = \overline{F}_{comb23}\end{aligned} \quad \text{(A6.2.1.43)}$$

Summed piston pin combustion joint forces of the slider-crank engines

$$\overline{F}_{\Sigma comb3in} = \overline{F}_{comb03} + \overline{F}_{comb23} \quad \text{(A6.2.1.44)}$$

$$\overline{F}_{\Sigma comb3out} = \overline{F}_{comb30} + \overline{F}_{comb32} \quad \text{(A6.2.1.45)}$$

Combustion torques of the slider-crank engines

$$T_{comb01} = -\left|\overline{F}_{comb21}\right| \cdot Z_{AA_0} \cdot \sin(\arg(\overline{F}_{comb21}) - \theta_{AA_0}) \quad \text{(A6.2.1.46)}$$

$$T_{comb10} = -T_{comb01} \quad \text{(A6.2.1.47)}$$

Combustion joint forces and torques of the cardan gear engines

Combustion joint forces of the cardan gear engines

$$\overline{F}_{comb23c} = F_{combc} \cdot e^{i \cdot 90^\circ} \quad \text{(A6.2.1.48)}$$

$$\overline{F}_{comb03c} = 0 \quad \text{(A6.2.1.49)}$$

$$\overline{F}_{comb30c} = -\overline{F}_{comb03c} = 0 \quad \text{(A6.2.1.50)}$$

$$\overline{F}_{comb02c} = -\overline{F}_{comb20c} = -\overline{F}_{comb32c} = \overline{F}_{comb23c} \quad \text{(A6.2.1.51)}$$

$$\begin{aligned} \overline{F}_{comb01c} &= -\overline{F}_{comb10c} = \overline{F}_{comb12c} = -\overline{F}_{comb21c} \\ &= 2 \cdot \overline{F}_{comb23c} \end{aligned} \quad \text{(A6.2.1.52)}$$

Combustion torques of the cardan gear engines

$$\begin{aligned} T_{comb01c} = &-\left|\overline{F}_{comb21c}\right| \cdot Z_{AA_0c} \cdot \\ &\cdot \sin(\arg(\overline{F}_{comb21c}) - \theta_{AA_0c}) \end{aligned} \quad \text{(A6.2.1.53)}$$

$$T_{comb10c} = -T_{comb01c} \quad \text{(A6.2.1.54)}$$

Appendix 7.1

Summed lossless Newtonian dynamics of the slider-crank machines versus the cardan gear machines

(**Equations A7.1.1 ... A7.1.60**)

Lossless joint forces and torques of the slider-crank pump

Lossless joint forces of the slider-crank pump

$$\overline{F}_{\Sigma pump01} = \overline{F}_{comp01} + \overline{F}_{\Sigma i01} \qquad (A7.1.1)$$
$$\overline{F}_{\Sigma pump10} = \overline{F}_{comp10} + \overline{F}_{\Sigma i10} \qquad (A7.1.2)$$
$$\overline{F}_{\Sigma pump12} = \overline{F}_{comp12} + \overline{F}_{\Sigma i12} \qquad (A7.1.3)$$
$$\overline{F}_{\Sigma pump21} = \overline{F}_{comp21} + \overline{F}_{\Sigma i21} \qquad (A7.1.4)$$
$$\overline{F}_{\Sigma pump23} = \overline{F}_{comp23} + \overline{F}_{\Sigma i23} \qquad (A7.1.5)$$
$$\overline{F}_{\Sigma pump32} = \overline{F}_{comp32} + \overline{F}_{\Sigma i32} \qquad (A7.1.6)$$
$$\overline{F}_{\Sigma pump03} = \overline{F}_{comp03} + \overline{F}_{\Sigma i03} \qquad (A7.1.7)$$
$$\overline{F}_{\Sigma pump30} = \overline{F}_{comp30} + \overline{F}_{\Sigma i30} \qquad (A7.1.8)$$

Lossless piston pin joint forces of the slider-crank pump

$$\overline{F}_{\Sigma pump3in} = \overline{F}_{\Sigma comp3in} + \overline{F}_{\Sigma i3in} \qquad (A7.1.9)$$
$$\overline{F}_{\Sigma pump3out} = \overline{F}_{\Sigma comp3out} + \overline{F}_{\Sigma i3out} \qquad (A7.1.10)$$

Lossless crankshaft torques of the slider-crank pump

$$T_{\Sigma pump01} = T_{comp01} + T_{\Sigma i01} \qquad (A7.1.11)$$
$$T_{\Sigma pump10} = T_{comp10} + T_{\Sigma i10} \qquad (A7.1.12)$$

Lossless joint forces and torques of the cardan gear pump

Lossless joint forces of the cardan gear pump

$$\overline{F}_{\Sigma pump01c} = \overline{F}_{comp01c} + \overline{F}_{\Sigma i01c} \quad (A7.1.13)$$
$$\overline{F}_{\Sigma pump10c} = \overline{F}_{comp10c} + \overline{F}_{\Sigma i10c} \quad (A7.1.14)$$
$$\overline{F}_{\Sigma pump02c} = \overline{F}_{comp02c} + \overline{F}_{\Sigma i02c} \quad (A7.1.15)$$
$$\overline{F}_{\Sigma pump20c} = \overline{F}_{comp20c} + \overline{F}_{\Sigma i20c} \quad (A7.1.16)$$
$$\overline{F}_{\Sigma pump12c} = \overline{F}_{comp12c} + \overline{F}_{\Sigma i12c} \quad (A7.1.17)$$
$$\overline{F}_{\Sigma pump21c} = \overline{F}_{comp21c} + \overline{F}_{\Sigma i21c} \quad (A7.1.18)$$
$$\overline{F}_{\Sigma pump23c} = \overline{F}_{comp23c} + \overline{F}_{\Sigma i23c} \quad (A7.1.19)$$
$$\overline{F}_{\Sigma pump32c} = \overline{F}_{comp32c} + \overline{F}_{\Sigma i32c} \quad (A7.1.20)$$
$$\overline{F}_{\Sigma pump03c} = \overline{F}_{comp03c} + \overline{F}_{\Sigma i03c} \quad (A7.1.21)$$
$$\overline{F}_{\Sigma pump30c} = \overline{F}_{comp30c} + \overline{F}_{\Sigma i30c} \quad (A7.1.22)$$

Lossless crankshaft torques of the cardan gear pump

$$T_{\Sigma pump01c} = T_{comp01c} + T_{\Sigma i01c} \quad (A7.1.23)$$
$$T_{\Sigma pump10c} = T_{comp10c} + T_{\Sigma i10c} \quad (A7.1.24)$$

Lossless joint forces and torques of the slider-crank combustion engine

Lossless joint forces of the slider-crank combustion engine

$$\overline{F}_{\Sigma eng01} = \overline{F}_{comb01} + \overline{F}_{\Sigma i01} \quad (A7.1.25)$$
$$\overline{F}_{\Sigma eng10} = \overline{F}_{comb10} + \overline{F}_{\Sigma i10} \quad (A7.1.26)$$
$$\overline{F}_{\Sigma eng12} = \overline{F}_{comb12} + \overline{F}_{\Sigma i12} \quad (A7.1.27)$$
$$\overline{F}_{\Sigma eng21} = \overline{F}_{comb21} + \overline{F}_{\Sigma i21} \quad (A7.1.28)$$
$$\overline{F}_{\Sigma eng23} = \overline{F}_{comb23} + \overline{F}_{\Sigma i23} \quad (A7.1.29)$$
$$\overline{F}_{\Sigma eng32} = \overline{F}_{comb32} + \overline{F}_{\Sigma i32} \quad (A7.1.30)$$
$$\overline{F}_{\Sigma eng03} = \overline{F}_{comb03} + \overline{F}_{\Sigma i03} \quad (A7.1.31)$$
$$\overline{F}_{\Sigma eng30} = \overline{F}_{comb30} + \overline{F}_{\Sigma i30} \quad (A7.1.32)$$

Lossless piston pin joint forces of the slider-crank combustion engine

$$\overline{F}_{\Sigma eng3in} = \overline{F}_{\Sigma comb3in} + \overline{F}_{\Sigma i3in} \tag{A7.1.33}$$

$$\overline{F}_{\Sigma eng3out} = \overline{F}_{\Sigma comb3out} + \overline{F}_{\Sigma i3out} \tag{A7.1.34}$$

Lossless crankshaft torques of the slider-crank combustion engine

$$T_{\Sigma eng01} = T_{comb01} + T_{\Sigma i01} \tag{A7.1.35}$$

$$T_{\Sigma eng10} = T_{comb10} + T_{\Sigma i10} \tag{A7.1.36}$$

Lossless joint forces and torques of the cardan gear combustion engine

Lossless joint forces of the cardan gear combustion engine

$$\overline{F}_{\Sigma eng01c} = \overline{F}_{comb01c} + \overline{F}_{\Sigma i01c} \tag{A7.1.37}$$

$$\overline{F}_{\Sigma eng10c} = \overline{F}_{comb10c} + \overline{F}_{\Sigma i10c} \tag{A7.1.38}$$

$$\overline{F}_{\Sigma eng02c} = \overline{F}_{comb02c} + \overline{F}_{\Sigma i02c} \tag{A7.1.39}$$

$$\overline{F}_{\Sigma eng20c} = \overline{F}_{comb20c} + \overline{F}_{\Sigma i20c} \tag{A7.1.40}$$

$$\overline{F}_{\Sigma eng12c} = \overline{F}_{comb12c} + \overline{F}_{\Sigma i12c} \tag{A7.1.41}$$

$$\overline{F}_{\Sigma eng21c} = \overline{F}_{comb21c} + \overline{F}_{\Sigma i21c} \tag{A7.1.42}$$

$$\overline{F}_{\Sigma eng23c} = \overline{F}_{comb23c} + \overline{F}_{\Sigma i23c} \tag{A7.1.43}$$

$$\overline{F}_{\Sigma eng32c} = \overline{F}_{comb32c} + \overline{F}_{\Sigma i32c} \tag{A7.1.44}$$

$$\overline{F}_{\Sigma eng03c} = \overline{F}_{comb03c} + \overline{F}_{\Sigma i03c} \tag{A7.1.45}$$

$$\overline{F}_{\Sigma eng30c} = \overline{F}_{comb30c} + \overline{F}_{\Sigma i30c} \tag{A7.1.46}$$

Lossless crankshaft torques of the cardan gear combustion engine

$$T_{\Sigma eng01c} = T_{comb01c} + T_{\Sigma i01c} \tag{A7.1.47}$$

$$T_{\Sigma eng10c} = T_{comb10c} + T_{\Sigma i10c} \tag{A7.1.48}$$

Lossless works, torques and powers of the machines

Lossless works of the pumps

$$\Sigma W_{pump} = \int_{\theta_{AA_0\,min}}^{\theta_{AA_0\,max}} T_{\Sigma pump10} \cdot d\theta_{AA_0} \tag{A7.1.49}$$

$$\Sigma W_{pumpc} = \int_{\theta_{AA_0c\,min}}^{\theta_{AA_0c\,max}} T_{\Sigma pump10c} \cdot d\theta_{AA_0c} \tag{A7.1.50}$$

Lossless mean crankshaft torques of the pumps

$$T_{pumpmean} = \frac{\Sigma W_{pump}}{\theta_{AA_0\,max} - \theta_{AA_0\,min}} \tag{A7.1.51}$$

$$T_{pumpmeanc} = \frac{\Sigma W_{pumpc}}{\theta_{AA_0c\,max} - \theta_{AA_0c\,min}} \tag{A7.1.52}$$

Lossless crankshaft powers of the pumps

$$P_{pump} = T_{\Sigma pump10} \cdot \omega_{AA_0} \tag{A7.1.53}$$

$$P_{pumpc} = T_{\Sigma pump10c} \cdot \omega_{AA_0c} \tag{A7.1.54}$$

Lossless works of the combustion engines

$$\Sigma W_{eng} = \int_{\theta_{AA_0\,min}}^{\theta_{AA_0\,max}} T_{\Sigma eng10} \cdot d\theta_{AA_0} \tag{A7.1.55}$$

$$\Sigma W_{engc} = \int_{\theta_{AA_0c\,min}}^{\theta_{AA_0c\,max}} T_{\Sigma eng10c} \cdot d\theta_{AA_0c} \tag{A7.1.56}$$

Lossless mean crankshaft torques of the combustion engines

$$T_{engmean} = \frac{\Sigma W_{eng}}{\theta_{AA_0 max} - \theta_{AA_0 min}} \tag{A7.1.57}$$

$$T_{engmeanc} = \frac{\Sigma W_{engc}}{\theta_{AA_0 c max} - \theta_{AA_0 c min}} \tag{A7.1.58}$$

Lossless crankshaft powers of the combustion engines

$$P_{eng} = T_{\Sigma eng10} \cdot \omega_{AA_0} \tag{A7.1.59}$$

$$P_{engc} = T_{\Sigma eng10c} \cdot \omega_{AA_0 c} \tag{A7.1.60}$$

Appendix 8.1

Dynamic tooth loads of the cardan gear machines

[*Buckingham 1949*] (**Equations A8.1.1 ... A8.1.14**)

The cardan wheel has been named as gear 1 and the ring gear as gear 2.
The cardan gear pair has been treated as straight-tooth spur gears.

Radii of the pitch circles of the gears

$$r_{1c} = Z_{AA_0c} \quad [in] \tag{A8.1.1}$$

$$r_{2c} = Z_{AA_0} \quad [in] \tag{A8.1.2}$$

Auxiliary coefficient H (for the pressure angle α = 20 °)

$$H = 0.00120 \cdot \left(\frac{1}{r_{1c}} - \frac{1}{r_{2c}} \right) \tag{A8.1.3}$$

Pitch diameter of the cardan wheel

$$d_{1c} = 2 \cdot r_{1c} = Z_{AA_0} \quad [in] \tag{A8.1.4}$$

Polar moment of inertia of the cardan wheel

$$I_{p1c} = \frac{\pi \cdot d_{1c}^{\;4}}{32} \quad \left[in^4\right] \tag{A8.1.5}$$

Reduced mass of the cardan wheel

$$m_{1redc} = \frac{I_{p1c}}{r_{1c}^{\;2}} \quad \left[in^2\right] \tag{A8.1.6}$$

Pitch line velocity of the gears

$$v_c = 2 \cdot v_{AA_0c} \quad [ft/min] \tag{A8.1.7}$$

Force required to accelerate the cardan wheel mass as a rigid body

$$f_{1c} = H \cdot m_{1redc} \cdot v_c^{\;2} \quad [lb] \tag{A8.1.8}$$

Backlash (gear clearance) at the pitch line of the gears

For the normal sized cardan gear drives the backlash is $e_c \approx 0.005$ in ≈ 0.127 mm.

Modulus of elasticity of the gear materials

The suitable material for the cardan wheel and the internal ring gear is carburizing steel. The modulus of elasticity is $E \approx 210000$ N/mm^2 ≈ $30 \cdot 10^6$ psi.

Face width of the cardan wheel

$$b_{wheelc} \approx \frac{d_{1c}}{3} \quad [in] \qquad \text{(A8.1.9)}$$

Tangential load of the gear mesh

$$F_{twheelc} = \left| \left| \overline{F}_{\Sigma 02c} \right| \cdot \cos\left[\arg(\overline{F}_{\Sigma 02c}) - \left(\theta_{AA_0c} - \frac{\pi}{2} \right) \right] \right| \quad [lb] \qquad \text{(A8.1.10)}$$

Tooth deformation of the gears (pressure angle α = 20 °)

$$def_c = 9.00 \cdot \frac{F_{twheelc}}{b_{wheelc}} \cdot \left(\frac{1}{E_1} + \frac{1}{E_2} \right) \quad [in] \qquad \text{(A8.1.11)}$$

Force required to deform gear teeth amount of the error (backlash)

$$f_{2c} = F_{twheelc} \cdot \left(\frac{e_c}{def_c} + 1 \right) \quad [lb] \qquad \text{(A8.1.12)}$$

Acceleration load of the gear teeth

$$f_{ac} = \frac{f_{1c} \cdot f_{2c}}{f_{1c} + f_{2c}} \quad [lb] \qquad \text{(A8.1.13)}$$

Dynamic load of the gear teeth

$$F_{dync} = F_{twheelc} + \sqrt{f_{ac} \cdot (2 \cdot f_{2c} - f_{ac})} \quad [lb] \qquad \text{(A8.1.14)}$$

The preceding theory has been presented and applied as original in US units.

Appendix 9.1

Mechanical efficiencies of the slider-crank machines versus the cardan gear machines

[*Anderson & Loewenthal 1981 and 1982, Pennestrì & Valentini 2003, Mantriota & Pennestrì 2003*] (**Equations A9.1.1 ... A9.1.75**)

Power losses of the pistons

Piston diameter

For the conventional pumps and engines the piston diameter is:

$$d_{pis} \approx 0.5...1.7 \cdot stroke \qquad \text{(A9.1.1)}$$

Piston ring heights

For the normal sized pumps and engines the piston ring heights are:

Compression rings: $h_{co} \approx 2$ mm
Oil rings: $h_{oil} \approx 4$ mm

Contact area of the piston rings

$$A_{ring} = \pi \cdot d_{pis} \cdot h_{ring} \qquad \text{(A9.1.2)}$$

Contact pressures of the piston rings

The contact pressures of the piston rings are [*Andersson et al. 2002*]:

Compression rings: $p_{co} \approx 0.19$ N/mm^2
Oil rings: $p_{oil} \approx 1$ N/mm^2

Contact force of the piston rings

Pumps and four-stroke engines, 2 compression rings + 1 oil ring

$$F_{cont} = 2 \cdot p_{co} \cdot A_{coring} + 1 \cdot p_{oil} \cdot A_{oilring} \quad [N] \qquad \text{(A9.1.3)}$$

Friction coefficient of the piston rings

The friction coefficient of the piston rings is $\mu_{ring} \approx 0.07$ [*Andersson et al. 2002*].

Friction force of the piston rings

$$\overline{F}_{\mu ring} = \mu_{ring} \cdot F_{cont} \cdot e^{i \cdot [\arg(\overline{v}_{BA0}) + \pi]} \quad [N] \tag{A9.1.4}$$

Friction coefficient of the piston skirt

The friction coefficient of the piston skirt is $\mu_{skirt} \approx 0.09$ [***Andersson et al. 2002***].

Friction force of the piston skirt

Piston skirt friction exists only in the slider-crank machines.

$$\overline{F}_{\mu skirt} = \mu_{skirt} \cdot \left|F_{\Sigma 03}\right| \cdot e^{i \cdot [\arg(\overline{v}_{BA0}) + \pi]} \quad [N] \tag{A9.1.5}$$

Total friction forces of the pistons

$$\overline{F}_{\mu pis} = \overline{F}_{\mu ring} + \overline{F}_{\mu skirt} \quad [N] \tag{A9.1.6}$$

$$\overline{F}_{\mu pisc} = \overline{F}_{\mu ring} \quad [N] \tag{A9.1.7}$$

Power losses of the pistons

$$P_{\mu pis} = \left|\overline{F}_{\mu pis}\right| \cdot v_{BA_0} \quad [W] \tag{A9.1.8}$$

$$P_{\mu pisc} = \left|\overline{F}_{\mu pisc}\right| \cdot v_{BA_0 c} \quad [W] \tag{A9.1.9}$$

Power losses of the pin joints / bearings

Pin bearings

The piston pin bearings are most commonly needle bearings and sometimes journal bearings, one bearing per piston. In the cardan gear construction the piston pin bearing is situated in the lower end (big end) of the connecting rod.
The crank pin bearings are most commonly cylindrical roller bearings and sometimes journal bearings. Slider-crank machines have one bearing per crank pin, but the cardan gear machines need two crank pin bearings side by side to hold the cardan wheel steady.
The main pin bearings are commonly deep groove ball bearings or cylindrical roller bearings and sometimes journal bearings.
In this study all pin bearings of the machines are considered as rolling bearings.

Pitch diameters of the pin bearings

In this study the pitch diameters of the pin bearings have been approximated as follows:

Piston pin bearings

$$d_{bmpis} \approx \frac{d_{pis}}{4} \quad [m] \tag{A9.1.10}$$

Crank pin bearings and main pin bearings

$$d_{bmcrank} \approx d_{bmmain} \approx 1.5 \cdot d_{bmpis} \quad [m] \tag{A9.1.11}$$

Static load ratings of the pin bearings

Coincidentally the static load ratings for the pin bearings are [***INA / FAG 2007***]:

Piston pin bearings

$$C_{0bpis} \approx d_{bmpis}[mm] \cdot 10^3 \quad [N] \tag{A9.1.12}$$

Crank pin bearings and main pin bearings

$$C_{0bcrank} \approx C_{0bmain} \approx 2 \cdot C_{0bpis} \quad [N] \tag{A9.1.13}$$

Rotating speeds of the pin bearings

Piston pin bearings

$$n_{bpis} = \frac{|\omega_{BA}|}{2 \cdot \pi} \cdot 60 \quad [rpm] \tag{A9.1.14}$$

$$n_{bpisc} = \frac{|\omega_{BAc}|}{2 \cdot \pi} \cdot 60 \quad [rpm] \tag{A9.1.15}$$

Crank pin bearings

$$n_{bcrank} = \frac{|\omega_{AA_0} - \omega_{BA}|}{2 \cdot \pi} \cdot 60 \quad [rpm] \tag{A9.1.16}$$

$$n_{bcrankc} = \frac{|\omega_{AA_0c} - \omega_{BAc}|}{2 \cdot \pi} \cdot 60 \quad [rpm] \tag{A9.1.17}$$

Main pin bearings

$$n_{bmain} = \frac{\left|\omega_{AA_0}\right|}{2 \cdot \pi} \cdot 60 \quad [rpm] \tag{A9.1.18}$$

$$n_{bmainc} = \frac{\left|\omega_{AA_0c}\right|}{2 \cdot \pi} \cdot 60 \quad [rpm] \tag{A9.1.19}$$

Static equivalent bearing loads (for one bearing)

Piston pin bearings

$$F_{stbpis} = \left|\overline{F}_{\Sigma in3}\right| \quad [N] \tag{A9.1.20}$$

$$F_{stbpisc} = \left|\overline{F}_{\Sigma in3c}\right| \quad [N] \tag{A9.1.21}$$

Crank pin bearings

$$F_{stbcrank} = \left|\overline{F}_{\Sigma 12}\right| \quad [N] \tag{A9.1.22}$$

$$F_{stbcrankc} = \left|\frac{\overline{F}_{\Sigma 12c}}{2}\right| \quad [N] \quad \text{(Two bearings in the cardan wheel)} \tag{A9.1.23}$$

Main pin bearings

$$F_{stbmain} = \left|\frac{\overline{F}_{\Sigma 01}}{2}\right| \quad [N] \tag{A9.1.24}$$

$$F_{stbmainc} = \left|\frac{\overline{F}_{\Sigma 01c}}{2}\right| \quad [N] \tag{A9.1.25}$$

Load dependent torque losses of the pin bearings

$$T_{\mu Lb} = 0.009 \cdot F_{stb}^{\ 1.55} \cdot C_{0b}^{\ -0.55} \cdot d_{bm} \quad [Nm] \tag{A9.1.26}$$

$$T_{\mu Lbc} = 0.009 \cdot F_{stbc}^{\ 1.55} \cdot C_{0b}^{\ -0.55} \cdot d_{bm} \quad [Nm] \tag{A9.1.27}$$

Bearing lubrication factor

For the normal lubrication modes from the mixed lubrication to the EHD (elastohydrodynamic) lubrication the lubrication factor is f_0 = 1... 2.5.
For the calculations of this study the lubrication factor has been approximated as f_0 = 2.

Lubrication oil kinematic viscosity at the running temperature

In the conventional pumps and engines the lubrication oil kinematic viscosity at the running temperature is $\upsilon_{oil} \lesssim 5$ mm^2/s (cSt).

Oil viscosity dependent torque losses of the pin bearings

For the conditions: $(\upsilon_{oil} \cdot n_b), (\upsilon_{oil} \cdot n_{bc}) > 2000$

$$T_{\mu Vb} = 9.79 \cdot 10^{-2} \cdot f_0 \cdot (\upsilon_{oil} \cdot n_b)^{2/3} \cdot d_{bm}^{\ 3} \quad [Nm] \qquad (A9.1.28)$$

$$T_{\mu Vbc} = 9.79 \cdot 10^{-2} \cdot f_0 \cdot (\upsilon_{oil} \cdot n_{bc})^{2/3} \cdot d_{bm}^{\ 3} \quad [Nm] \qquad (A9.1.29)$$

For the conditions: $(\upsilon_{oil} \cdot n_b), (\upsilon_{oil} \cdot n_{bc}) \le 2000$

$$T_{\mu Vb} = 24.1 \cdot f_0 \cdot d_{bm}^{\ 3} \quad [Nm] \qquad (A9.1.30)$$

$$T_{\mu Vbc} = 24.1 \cdot f_0 \cdot d_{bm}^{\ 3} \quad [Nm] \qquad (A9.1.31)$$

Total torque losses of the pin bearings

$$T_{\mu b} = T_{\mu Lb} + T_{\mu Vb} \quad [Nm] \qquad (A9.1.32)$$

$$T_{\mu bc} = T_{\mu Lbc} + T_{\mu Vbc} \quad [Nm] \qquad (A9.1.33)$$

Power losses of the pin bearings

$$P_{\mu b} = T_{\mu b} \cdot |\omega_{BA}| \quad [W] \qquad (A9.1.34)$$

$$P_{\mu bc} = T_{\mu bc} \cdot |\omega_{BAc}| \quad [W] \qquad (A9.1.35)$$

Power loss of the cardan wheel in the cardan gear machines

The cardan wheel has been named as gear 1 and the ring gear as gear 2. The cardan gear pair has been calculated as straight-tooth spur gears.

Pressure angle

The pressure angle of the involute gears is normally α = 20 °.

Numbers of the gear teeth in the cardan gear machines

The gear ratio of the cardan gear construction is i = 2.
The suitable numbers of the gear teeth are:

Cardan wheel: $z_1 = 20$
Ring gear: $z_2 = 40$

Gear ratio

$$i = \frac{z_2}{z_1} \tag{A9.1.36}$$

Gear module

For SI-specifications

$$m_c = \frac{Z_{AA_0}\,(m)}{z_1} \quad [m] \tag{A9.1.37}$$

Pitch diameters

$$d_{1c} = m_c \cdot z_1 \quad [m] \tag{A9.1.38}$$
$$d_{2c} = m_c \cdot z_2 \quad [m] \tag{A9.1.39}$$

Length of path of contact of the cardan wheel gear mesh

$$\begin{aligned} L_{tc} = {} & \frac{\sqrt{(d_{1c} + 2 \cdot m_c)^2 - (d_{1c} \cdot \cos(\alpha))^2}}{2} - \\ & - \frac{\sqrt{(d_{2c} - 2 \cdot m_c)^2 - (d_{2c} \cdot \cos(\alpha))^2}}{2} + \\ & + \frac{d_{2c} - d_{1c}}{2} \cdot \sin(\alpha) \quad [m] \end{aligned} \tag{A9.1.40}$$

Rotational speed of the cardan wheel

$$n_{wheelc} = \frac{|\omega_{BAc}|}{2 \cdot \pi} \cdot 60 \quad [rpm] \tag{A9.1.41}$$

Average sliding velocity of the cardan wheel gear mesh

$$v_{swheelc} = 0.0262 \cdot n_{wheelc} \cdot \left(\frac{1+i}{i} \right) \cdot L_{tc} \quad [m/s] \tag{A9.1.42}$$

Average rolling velocity of the cardan wheel gear mesh

$$v_{rwheelc} =$$
$$0.1047 \cdot n_{wheelc} \cdot \left[d_{1c} \cdot \sin(\alpha) - \frac{L_{tc}}{4} \cdot \left(\frac{i-1}{i} \right) \right] \quad [m/s] \tag{A9.1.43}$$

Tangential load of the cardan wheel gear mesh

$$F_{twheelc} = \left| \left| \overline{F}_{\Sigma 02c} \right| \cdot \cos\left[\arg(\overline{F}_{\Sigma 02c}) - \left(\theta_{AA_0c} - \frac{\pi}{2} \right) \right] \right| \quad [N] \tag{A9.1.44}$$

Average normal load of the cardan wheel gear mesh

The transverse contact ratio of the internal gear pair is normally $\varepsilon_\alpha \approx 1.8$ and therefore the normal load is divided on average to two teeth in the mesh.

$$F_{nwheelc} = \frac{F_{twheelc}}{2 \cdot \cos(\alpha)} \quad [N] \tag{A9.1.45}$$

Face width of the cardan wheel

$$b_{wheelc} \approx \frac{d_{1c}}{3} \quad [m] \tag{A9.1.46}$$

Lubrication oil density

Lubrication oil density is approximately $\rho_{oil} \approx 900$ kg/m^3.

Lubrication oil dynamic (absolute) viscosity

$$\eta_{oil} = \upsilon_{oil}(mm^2/s) \cdot 10^{-6} \cdot \rho_{oil}(kg/m^3) \quad [Pas] \tag{A9.1.47}$$

Friction coefficient of the cardan wheel gear mesh

There are a lot of equations to calculate friction coefficients of the gear mesh [***Martin 1978***]. In this study the friction coefficients of the gear mesh have been calculated using the equation presented by Benedict and Kelley [***Benedict & Kelley 1961, Martin 1978, Anderson & Loewenthal 1982***].

$$\mu_{wheelc} = 0.0127 \cdot \log\left(\frac{29.66 \cdot F_{nwheelc}}{b_{wheelc} \cdot \eta_{oil} \cdot v_{swheelc} \cdot v_{rwheelc}^{2}}\right) \qquad \text{(A9.1.48)}$$

Average sliding power loss of the cardan wheel gear mesh

$$P_{\mu swheelc} = 2 \cdot 10^{-3} \cdot v_{swheelc} \cdot \mu_{wheelc} \cdot F_{nwheelc} \quad [kW] \qquad \text{(A9.1.49)}$$

Equivalent contact radius of the internal gear pair

$$R_{eqc} = \frac{\left(d_{1c} \cdot \sin(\alpha) + \frac{L_{tc}}{2}\right) \cdot \left(d_{2c} \cdot \sin(\alpha) - \frac{L_{tc}}{2}\right)}{2 \cdot \left(d_{2c} \cdot \sin(\alpha) + \frac{L_{tc}}{2}\right)} \quad [m] \qquad \text{(A9.1.50)}$$

Central EHD oil film thickness

$$h_{fwheelc} = 2.051 \cdot 10^{-7} \cdot (v_{rwheelc} \cdot \eta_{oil})^{0.67} \cdot F_{nwheelc}^{-0.067} \cdot R_{eqc}^{0.464} \quad [m] \qquad \text{(A9.1.51)}$$

Contact ratio

$$CR_{c} = \frac{39.37 \cdot L_{tc} \cdot \left(\frac{25.4}{m_{c}\ (mm)}\right)}{\pi \cdot \cos(\alpha)} \qquad \text{(A9.1.52)}$$

Average rolling power loss of the cardan wheel gear mesh

$$P_{\mu rwheelc} = 9 \cdot 10^{4} \cdot v_{rwheelc} \cdot h_{fwheelc} \cdot b_{wheelc} \cdot CR_{c} \quad [kW] \qquad \text{(A9.1.53)}$$

Windage loss of the cardan wheel

The ring gear does not rotate and only the cardan wheel can have windage loss.

$$P_{\mu wwheelc} = 2.82 \cdot 10^{-7} \cdot \left(1 + \frac{2.3 \cdot b_{wheelc}}{d_{1c}}\right) \cdot n_{wheelc}^{2.8} \cdot \left(\frac{d_{1c}}{2}\right)^{4.6} \cdot (0.028 \cdot \eta_{oil} + 0.019)^{0.2} \quad [kW] \tag{A9.1.54}$$

Total power loss of the cardan wheel

$$P_{\mu wheelc} = P_{\mu swheelc} + P_{\mu rwheelc} + P_{\mu wwheelc} \quad [kW] \tag{A9.1.55}$$

Total power losses of the slider-crank and the cardan gear machines

Total power losses of the pumps

$$P_{\mu pump} = P_{\mu pis} + \Sigma P_{\mu b} \tag{A9.1.56}$$

$$P_{\mu pumpc} = P_{\mu pisc} + \Sigma P_{\mu bc} + P_{\mu wheelc} \tag{A9.1.57}$$

Total power losses of the four-stroke engines

$$P_{\mu eng} = P_{\mu pis} + \Sigma P_{\mu b} \tag{A9.1.58}$$

$$P_{\mu engc} = P_{\mu pisc} + \Sigma P_{\mu bc} + P_{\mu wheelc} \tag{A9.1.59}$$

In the preceding equations:

$\Sigma P_{\mu b}$ = sum of the power losses of the piston pin, crank pin and main pin bearings of the slider-crank machine (pump or engine)
$\Sigma P_{\mu bc}$ = sum of the power losses of the piston pin, crank pin and main pin bearings of the cardan gear machine (pump or engine)

Operational powers and torques of the slider-crank and the cardan gear machines

Power needs of the pumps

$$P_{needpump} = P_{pump} + P_{\mu pump} \tag{A9.1.60}$$

$$P_{needpumpc} = P_{pumpc} + P_{\mu pumpc} \tag{A9.1.61}$$

Output powers of the four-stroke engines

$$P_{outeng} = P_{eng} - P_{\mu eng} \tag{A9.1.62}$$

$$P_{outengc} = P_{engc} - P_{\mu engc} \tag{A9.1.63}$$

Torque needs of the pumps

$$T_{needpump} = \frac{P_{needpump}}{\omega_{AA_0}} \tag{A9.1.64}$$

$$T_{needpumpc} = \frac{P_{needpumpc}}{\omega_{AA_0c}} \tag{A9.1.65}$$

Output torques of the four-stroke engines

$$T_{outeng} = \frac{P_{outeng}}{\omega_{AA_0}} \tag{A9.1.66}$$

$$T_{outengc} = \frac{P_{outengc}}{\omega_{AA_0c}} \tag{A9.1.67}$$

Total work losses of the slider-crank and the cardan gear machines

Total work losses of the pumps

$$\Sigma W_{\mu pump} = \int_{t_{(\pi/2)}}^{t_{(9\pi/2)}} P_{\mu pump} \cdot dt \tag{A9.1.68}$$

$$\Sigma W_{\mu pumpc} = \int_{t_{(\pi/2)}}^{t_{(9\pi/2)}} P_{\mu pumpc} \cdot dt \tag{A9.1.69}$$

Total work losses of the four-stroke engines

$$\Sigma W_{\mu eng} = \int_{t_{(\pi/2)}}^{t_{(9\pi/2)}} P_{\mu eng} \cdot dt \tag{A9.1.70}$$

$$\Sigma W_{\mu engc} = \int_{t_{(\pi/2)}}^{t_{(9\pi/2)}} P_{\mu engc} \cdot dt \tag{A9.1.71}$$

In the preceding equations:

$t_{(\pi/2)}$ = time point of the beginning of the calculated cycle
$t_{(9\pi/2)}$ = time point of the end of the calculated cycle

Mechanical efficiencies of the slider-crank and the cardan gear machines

Mechanical efficiencies of the pumps

$$\eta_{mpump} = \frac{\Sigma W_{comp}}{\Sigma W_{pump} + \Sigma W_{\mu pump}} \tag{A9.1.72}$$

$$\eta_{mpumpc} = \frac{\Sigma W_{compc}}{\Sigma W_{pumpc} + \Sigma W_{\mu pumpc}} \tag{A9.1.73}$$

Mechanical efficiencies of the engines

$$\eta_{meng} = \frac{\Sigma W_{eng} - \Sigma W_{\mu eng}}{\Sigma W_{eng}} \tag{A9.1.74}$$

$$\eta_{mengc} = \frac{\Sigma W_{engc} - \Sigma W_{\mu engc}}{\Sigma W_{engc}} \tag{A9.1.75}$$

Appendix 11.1.1

Comparison of the kinematic properties: Positions, velocities and accelerations Pumps and four-stroke engines

Variables			
Rod length relative to crank length (Generally ZBA > 2.5·ZAA0)	ZBA = 2.33·ZAA0 ZAA0 = 0.06 m, ZBA = 0.14 m Displacement 1357 cm^3	ZBA = 3·ZAA0 ZAA0 = 0.05 m, ZBA = 0.15 m Displacement 785 cm^3	ZBA = 4·ZAA0 ZAA0 = 0.04 m, ZBA = 0.16 m Displacement 402 cm^3
Maximum piston position difference ΔZBA0 [mm] and [%/S]	+14 mm +11 %	+9 mm +6 %	+5 mm +3 %
The following variables depend only on the link length ratio. [%/S] = Percentage difference between the two mechanisms regarding the values of the slider-crank mechanism.			
Piston maximum velocity difference ΔvBA0 [%/S]	-8 %	-5 %	-3 %
Piston maximum acceleration difference ΔaBA0 [%/S]	-30 %	-25 %	-20 %
Connecting rod maximum velocity difference ΔvPA0 [%/S]	-3 %	-2 %	-1 %
Connecting rod maximum acceleration difference ΔaPA0 [%/S]	-18 %	-14 %	-11 %

Appendix 11.2.1

Comparison of the kinetostatic properties: Inertial joint forces and crankshaft torques Pumps and four-stroke engines

Variables		ZBA = 2.33·ZAA0, ZAA0 = 0.06 m, ZBA = 0.14 m, steel links, equal masses Displacement 1357 cm³								
Angular acceleration αAA0 [rad/s²]		0			100π			200π		
Initial angular velocity ωAA00 [rad/s]		3π	200π	Δ % /S	3π	200π	Δ % /S	3π	200π	Δ % /S
Total crank pin inertial joint force	S	9	38510	+58	780	39280	+58	1551	40050	+58
maximums [N]	C	14	60740		1228	61960		2443	63170	
Total main pin inertial joint force	S	9	38510	+58	780	39280	+58	1551	40050	+58
maximums [N]	C	14	60740		1228	61960		2443	63170	
Total crankshaft inertial torque	S	0.125	556	+64	25	575	+18...63	49	596	+18...62
maximums [Nm]	C	0.205	911		29	938	Inexact	58	967	Inexact

Variables		ZBA = 2.33·ZAA0, ZAA0 = 0.06 m, ZBA = 0.14 m, "titanium" rod in the cardan gear, otherwise steel links Displacement 1357 cm³								
Angular acceleration αAA0 [rad/s²]		0			100π			200π		
Initial angular velocity ωAA00 [rad/s]		3π	200π	Δ % /S	3π	200π	Δ % /S	3π	200π	Δ % /S
Total crank pin inertial joint force	S	8.7	38510	-1.4	780	39280	-1.4 ...	1551	40050	-1.4...
maximums [N]	C	8.5	37960		768	38720	-1.5	1527	39480	-1.5
Total main pin inertial joint force	S	8.7	38510	-1.4	780	39280	-1.4 ...	1551	40050	-1.4...
maximums [N]	C	8.5	37960		768	38720	-1.5	1527	39480	-1.5
Total crankshaft inertial torque	S	0.125	556	+2.5	25	575	-6...+3	49	596	-6...+3
maximums [Nm]	C	0.128	569		23	592	Inexact	46	615	Inexact

S = slider crank   C = cardan gear

Variables		ZBA = 3·ZAA0, ZAA0 = 0.05 m, ZBA = 0.15 m, steel links, equal masses Displacement 785 cm³								
Angular acceleration αAA0 [rad/s²]		0			100π			200π		
Initial angular velocity ωAA00 [rad/s]		3π	200π	Δ % /S	3π	200π	Δ % /S	3π	200π	Δ % /S
Total crank pin inertial joint force	S	8	36870	+65	747	37600	+65...66	1485	38340	+65...66
maximums [N]	C	14	61010		1234	62230		2454	63450	
Total main pin inertial joint force	S	8	36870	+65	747	37600	+65...66	1485	38340	+65...66
maximums [N]	C	14	61010		1234	62230		2454	63450	
Total crankshaft inertial torque	S	0.082	366	+108	14	380	+41...106	27	393	+41...103
maximums [Nm]	C	0.172	763		19	780	Inexact	38	799	Inexact

Variables		ZBA = 3·ZAA0, ZAA0 = 0.05 m, ZBA = 0.15 m, "titanium" rod in the cardan gear, otherwise steel links Displacement 785 cm³								
Angular acceleration αAA0 [rad/s²]		0			100π			200π		
Initial angular velocity ωAA00 [rad/s]		3π	200π	Δ % /S	3π	200π	Δ % /S	3π	200π	Δ % /S
Total crank pin inertial joint force	S	8	36870	+3	747	37600	+3	1485	38340	+3
maximums [N]	C	9	38130		771	38900		1534	39660	
Total main pin inertial joint force	S	8	36870	+3	747	37600	+3	1485	38340	+3
maximums [N]	C	9	38130		771	38900		1534	39660	
Total crankshaft inertial torque	S	0.082	366	+30	14	380	+5...29	27	393	+5...28
maximums [Nm]	C	0.107	477		14	490	Inexact	29	504	Inexact

S = slider crank C = cardan gear

Variables		ZBA = 4·ZAA0, ZAA0 = 0.04 m, ZBA = 0.16 m, steel links, equal masses Displacement 402 cm³								
Angular acceleration αAA0 [rad/s²]		0			100π			200π		
Initial angular velocity ωAA00 [rad/s]		3π	200π	Δ % /S	3π	200π	Δ % /S	3π	200π	Δ % /S
Total crank pin inertial joint force	S	8	34120	+70...71	684	34720	+71...72	1361	35390	+71...72
maximums [N]	C	13	58180		1177	59340		2340	60510	
Total main pin inertial joint force	S	8	34120	+70...71	684	34720	+71...72	1361	35390	+71...72
maximums [N]	C	13	58180		1177	59340		2340	60510	
Total crankshaft inertial torque	S	0.051	225	+158	7	232	+72...155	14	239	+72...153
maximums [Nm]	C	0.131	582		12	593	Inexact	25	605	Inexact

Variables		ZBA = 4·ZAA0, ZAA0 = 0.04 m, ZBA = 0.16 m, "titanium" rod in the cardan gear, otherwise steel links Displacement 402 cm³								
Angular acceleration αAA0 [rad/s²]		0			100π			200π		
Initial angular velocity ωAA00 [rad/s]		3π	200π	Δ % /S	3π	200π	Δ % /S	3π	200π	Δ % /S
Total crank pin inertial joint force	S	7.7	34120	+7	684	34720	+7	1361	35390	+7
maximums [N]	C	8.2	36360		735	37090		1463	37820	
Total main pin inertial joint force	S	7.7	34120	+7	684	34720	+7	1361	35390	+7
maximums [N]	C	8.2	36360		735	37090		1463	37820	
Total crankshaft inertial torque	S	0.051	225	+62	7	232	+20...60	14	239	+20...59
maximums [Nm]	C	0.082	364		9	372	Inexact	17	380	Inexact

S = slider crank C = cardan gear

Appendix 11.2.2

Comparison of the kinetostatic properties: Inertial torques, works and powers Pumps and four-stroke engines

Variables		ZBA = 2.33·ZAA0, ZAA0 = 0.06 m, ZBA = 0.14 m, steel links, equal masses Displacement 1357 cm³							
Angular acceleration αAA0 [rad/s²]		100π				200π			
Initial angular velocity ωAA00 [rad/s]		3π	30π	200π	Δ % /S	3π	30π	200π	Δ % /S
Inertial work consumption / cycle [J]	S	189	189	189	-10	378	378	378	-10
	C	170	170	170		340	340	340	
Mean inertial torque [Nm]	S	15.03	15.03	15.03	-10	30.05	30.05	30.05	-10
	C	13.51	13.51	13.51		27.03	27.03	27.03	
Mean inertial power consumption [kW]	S	0.908	1.705	9.547	-13	2.547	3.878	19.19	-13
	C	0.790	1.484	8.309		2.216	3.375	16.70	

Variables		ZBA = 2.33·ZAA0, ZAA0 = 0.06 m, ZBA = 0.14 m, "titanium" rod in the cardan gear, otherwise steel links Displacement 1357 cm³							
Angular acceleration αAA0 [rad/s²]		100π				200π			
Angular velocity ωAA00 [rad/s]		3π	30π	200π	Δ % /S	3π	30π	200π	Δ % /S
Inertial work consumption / cycle [J]	S	189	189	189	-10	378	378	378	-10
	C	170	170	170		340	340	340	
Mean inertial torque [Nm]	S	15.03	15.03	15.03	-10	30.05	30.05	30.05	-10
	C	13.51	13.51	13.51		27.02	27.02	27.02	
Mean inertial power consumption [kW]	S	0.908	1.705	9.547	-12	2.547	3.878	19.19	-12
	C	0.798	1.499	8.392		2.239	3.409	16.87	

S = slider crank C = cardan gear

Variables		ZBA = 3·ZAA0, ZAA0 = 0.05 m, ZBA = 0.15 m, steel links, equal masses Displacement 785 cm³							
Angular acceleration αAA0 [rad/s²]		100π				200π			
Initial angular velocity ωAA00 [rad/s]		3π	30π	200π	Δ % /S	3π	30π	200π	Δ % /S
Inertial work consumption / cycle [J]	S	93.37	93.35	93.34	-17	187	187	187	-17
	C	77.71	77.71	77.71		155	155	155	
Mean inertial torque [Nm]	S	7.430	7.428	7.428	-17	14.86	14.86	14.86	-17
	C	6.184	6.184	6.184		12.37	12.37	12.37	
Mean inertial power consumption [kW]	S	0.451	0.847	4.743	-22	1.265	1.927	9.533	-22
	C	0.353	0.664	3.717		0.991	1.510	7.471	

Variables		ZBA = 3·ZAA0, ZAA0 = 0.05 m, ZBA = 0.15 m, "titanium" rod in the cardan gear, otherwise steel links Displacement 785 cm³							
Angular acceleration αAA0 [rad/s²]		100π				200π			
Angular velocity ωAA00 [rad/s]		3π	30π	200π	Δ % /S	3π	30π	200π	Δ % /S
Inertial work consumption / cycle [J]	S	93.37	93.35	93.34	-17	187	187	187	-17
	C	77.69	77.69	77.69		155	155	155	
Mean inertial torque [Nm]	S	7.430	7.428	7.428	-17	14.86	14.86	14.86	-17
	C	6.182	6.182	6.182		12.37	12.37	12.37	
Mean inertial power consumption [kW]	S	0.451	0.847	4.743	-20	1.265	1.927	9.533	-20
	C	0.360	0.676	3.787		1.010	1.538	7.610	

S = slider crank C = cardan gear

Variables		ZBA = 4·ZAA0, ZAA0 = 0.04 m, ZBA = 0.16 m, steel links, equal masses Displacement 402 cm³							
Angular acceleration αAA0 [rad/s²]		100π				200π			
Initial angular velocity ωAA00 [rad/s]		3π	30π	200π	Δ % /S	3π	30π	200π	Δ % /S
Inertial work consumption / cycle [J]	S	42.37	42.36	42.35	-28	84.71	84.75	84.70	-28
	C	30.50	30.50	30.50		61.01	61.01	61.01	
Mean inertial torque [Nm]	S	3.371	3.371	3.370	-28	6.741	6.744	6.740	-28
	C	2.427	2.427	2.427		4.855	4.855	4.855	
Mean inertial power consumption [kW]	S	0.206	0.388	2.172	-36	0.579	0.882	4.366	-36
	C	0.132	0.248	1.390		0.370	0.564	2.793	

Variables		ZBA = 4·ZAA0, ZAA0 = 0.04 m, ZBA = 0.16 m, "titanium" rod in the cardan gear, otherwise steel links Displacement 402 cm³							
Angular acceleration αAA0 [rad/s²]		100π				200π			
Angular velocity ωAA00 [rad/s]		3π	30π	200π	Δ % /S	3π	30π	200π	Δ % /S
Inertial work consumption / cycle [J]	S	42.37	42.36	42.35	-28	84.71	84.75	84.70	-28
	C	30.49	30.49	30.49		60.97	60.97	60.97	
Mean inertial torque [Nm]	S	3.371	3.371	3.370	-28	6.741	6.744	6.740	-28
	C	2.426	2.426	2.426		4.852	4.852	4.852	
Mean inertial power consumption [kW]	S	0.206	0.388	2.172	-34	0.579	0.882	4.366	-34
	C	0.137	0.258	1.442		0.385	0.586	2.899	

S = slider crank   C = cardan gear

Appendix 11.3.1

Comparison of the kinetic properties: Compression, torques, works and powers Pumps (and four-stroke engines)

Variables		Compression ratio 12 :1, standard atmospheric pressure $1.01325 \cdot 10^5$ Pa, polytropic exponent γ = 1.4, cylinder filling 107 %, AIR PUMP					
Rod length relative to crank length (Generally ZBA > 2.5·ZAA0)		ZBA = 2.33·ZAA0 ZAA0 = 0.06 m, ZBA = 0.14 m Displacement 1357 cm³		ZBA = 3·ZAA0 ZAA0 = 0.05 m, ZBA = 0.15 m Displacement 785 cm³		ZBA = 4·ZAA0 ZAA0 = 0.04 m, ZBA = 0.16 m Displacement 402 cm³	
Maximum isothermal compression pressure [MPa]		1.216		1.216		1.216	
Maximum polytropic compression pressure [MPa]		3.612		3.612		3.612	
Maximum polytropic compression pressure difference "C - S" [MPa]		0.3384		0.2719		0.2102	
Maximum compression torque [Nm]			Δ % /S		Δ % /S		Δ % /S
Piston diameter = 2·ZAA0	S	684	-16	384	-13	191	-10
	C	576		333		171	
Mean compression torque [Nm]							
Piston diameter = 2·ZAA0	S	111	0	64.47	0	33.01	0
	C	111		64.51		33.03	
Compression work / cycle [J]							
Cycle = 4π rad	S	1382	0	810	0	415	0
2 compression strokes / cycle	C	1383		811		415	
Mean compression power [kW]							
Constant angular velocity	S	69.11	0	40.00	0	20.48	0
200π rad/s	C	69.17		40.03		20.49	

S = slider-crank C = cardan gear

Appendix 11.3.2

Comparison of the kinetic properties: Combustion, torques, works and powers Four-stroke engines

Variables		Compression ratio 12 :1, standard atmospheric pressure $1.01325 \cdot 10^5$ Pa, polytropic exponent $\gamma = 1.4$, cylinder filling 107 %, gasoline combustion, FOUR-STROKE ENGINE					
Rod length relative to crank length (Generally ZBA > 2.5·ZAA0)		ZBA = 2.33·ZAA0 ZAA0 = 0.06 m, ZBA = 0.14 m Displacement 1357 cm³		ZBA = 3·ZAA0 ZAA0 = 0.05 m, ZBA = 0.15 m Displacement 785 cm³		ZBA = 4·ZAA0 ZAA0 = 0.04 m, ZBA = 0.16 m Displacement 402 cm³	
Maximum combustion pressure [MPa]		12		12		12	
Maximum combustion pressure difference "C - S" [MPa]		1.142		0.9103		0.6985	
Maximum combustion torque [Nm]			Δ % /S		Δ % /S		Δ % /S
Piston diameter = 2·ZAA0	S	3453	-22	1897	-18	925	-14
	C	2701		1560		797	
Mean combustion torque [Nm]							
Piston diameter = 2·ZAA0	S	116	-13	64.95	-10	32.26	-8
	C	101		58.23		29.75	
Combustion work / cycle [J]							
Cycle = 4π rad, 4 strokes	S	1461	-13	816	-10	405	-8
	C	1267		732		374	
Mean combustion power [kW]							
Constant angular velocity 200π rad/s	S	72.16	-13	40.30	-10	20.02	-8
	C	62.57		36.13		18.46	

S = slider-crank   C = cardan gear

Appendix 11.4.1

Comparison of the summed lossless Newtonian dynamics:
Total joint forces and crankshaft torques
Pumps and four-stroke engines

Variables		ZBA = 2.33·ZAA0, ZAA0 = 0.06 m, ZBA = 0.14 m, steel links, equal masses, compression ratio 12 :1, standard atmospheric pressure 1.01325·10^5 Pa, polytropic exponent γ = 1.4, cylinder filling 107 %, piston diameter = 2·ZAA0, displacement 1357 cm³, AIR PUMP								
Angular acceleration αAA0 [rad/s²]		0			0			0		
Initial angular velocity ωAA00 [rad/s]		3π	30π	Δ % /S	100π	110π	Δ % /S	140π	200π	Δ % /S
Total piston pin joint force	S	40840	40600	0,	38140	37570	-13,	35530	31000	-27,
maximums [N] DISPARATE	C	40840	40160	-1	33250	31660	-16	25970	31610	+5
Total crank pin joint force	S	40840	39980	+100,	31220	29200	+113,	21980	38510	+136,
maximums [N]	C	81680	80330	+101	66510	63320	+117	51930	63210	+64
Total main pin joint force	S	40840	39980	+100,	31220	29200	+113,	21980	38510	+136,
maximums [N]	C	81680	80330	+101	66510	63320	+117	51930	63210	+64
Total crankshaft torque	S	684	682	-16,	662	658	-38,	644	682	-20,
maximums [Nm]	C	576	561	-18	413	381	-42	515	977	+43
Angular acceleration αAA0 [rad/s²]		30π			100π			200π		
Initial angular velocity ωAA00 [rad/s]		3π	30π	Δ % /S	100π	110π	Δ % /S	140π	200π	Δ % /S
Total piston pin joint force	S	40780	40540	-0.3,	37920	37350	-14,	35100	29570	-29,
maximums [N] DISPARATE	C	40660	39980	-1	32650	31050	-17	24750	32340	+9
Total crank pin joint force	S	40610	39750	+100,	30450	28430	+114,	20440	39200	+142,
maximums [N]	C	81320	79960	+101	65290	62100	+118	49500	64680	+65
Total main pin joint force	S	40610	39750	+100,	30450	28430	+114,	20440	39200	+142,
maximums [N]	C	81320	79960	+101	65290	62100	+118	49500	64680	+65
Total crankshaft torque	S	688	686	-16,	676	672	-38,	671	731	-15,
maximums [Nm]	C	578	563	-18	421	387	-42	568	1030	+41

S = slider-crank   C = cardan gear

Variables		ZBA = 2.33·ZAA0, ZAA0 = 0.06 m, ZBA = 0.14 m, "titanium" rod in the cardan gear, otherwise steel links, compression ratio 12 :1, standard atmospheric pressure $1.01325 \cdot 10^5$ Pa, polytropic exponent γ = 1.4, cylinder filling 107 %, piston diameter = 2·ZAA0, displacement 1357 cm³, AIR PUMP								
Angular acceleration αAA0 [rad/s²]		0			0			0		
Initial angular velocity ωAA00 [rad/s]		3π	30π	Δ % /S	100π	110π	Δ % /S	140π	200π	Δ % /S
Total piston pin joint force	S	40840	40600	0,	38140	37570	-5,	35530	31000	-11,
maximums [N] DISPARATE	C	40840	40420	-0.5	36100	35110	-7	31550	21870	-27
Total crank pin joint force	S	40840	39980	+100,	31220	29200	+131,	21980	38510	+14,
maximums [N]	C	81690	80840	+102	72200	70210	+140	63090	43730	+187
Total main pin joint force	S	40840	39980	+100,	31220	29200	+131,	21980	38510	+14,
maximums [N]	C	81690	80840	+102	72200	70210	+140	63090	43730	+187
Total crankshaft torque	S	684	682	-16,	662	658	-28,	644	682	-41,
maximums [Nm]	C	576	567	-17	474	453	-31	379	637	-7
Angular acceleration αAA0 [rad/s²]		30π			100π			200π		
Initial angular velocity ωAA00 [rad/s]		3π	30π	Δ % /S	100π	110π	Δ % /S	140π	200π	Δ % /S
Total piston pin joint force	S	40780	40540	-0.1,	37920	37350	-6,	35100	29570	-12,
maximums [N] DISPARATE	C	40730	40310	-0.6	35720	34730	-7	30790	21110	-29
Total crank pin joint force	S	40610	39750	+101,	30450	28430	+135,	20440	39200	+201,
maximums [N]	C	81460	80610	+103	71440	69450	+144	61570	42210	+8
Total main pin joint force	S	40610	39750	+101,	30450	28430	+135,	20440	39200	+201,
maximums [N]	C	81460	80610	+103	71440	69450	+144	61570	42210	+8
Total crankshaft torque	S	688	686	-16,	676	672	-28,	671	731	-41,
maximums [Nm]	C	579	570	-17	484	463	-31	396	677	-7

S = slider-crank C = cardan gear

Variables		ZBA = 3·ZAA0, ZAA0 = 0.05 m, ZBA = 0.15 m, steel links, equal masses, compression ratio 12 :1, standard atmospheric pressure 1.01325·10^5 Pa, polytropic exponent γ = 1.4, cylinder filling 107 %, piston diameter = 2·ZAA0, displacement 785 cm³, AIR PUMP								
Angular acceleration αAA0 [rad/s²]		0			0			200π		
Initial angular velocity ωAA00 [rad/s]		3π	30π	Δ % /S	100π	110π	Δ % /S	140π	200π	Δ % /S
Total piston pin joint force	S	28360	28140	0,	25820	25290	-20,	22980	17790	-28,
maximums [N] DISPARATE	C	28360	27680	-2	20740	19140	-24	16650	32090	+80
Total crank pin joint force	S	28360	27540	+100,	19150	17220	+117,	18810	37620	+77,
maximums [N]	C	56720	55360	+101	41480	38280	+122	33290	64190	+71
Total main pin joint force	S	28360	27540	+100,	19150	17220	+117,	18810	37620	+77,
maximums [N]	C	56720	55360	+101	41480	38280	+122	33290	64190	+71
Total crankshaft torque	S	384	384	-13,	389	391	-41,	415	460	+8,
maximums [Nm]	C	333	321	-16	230	270	-31	447	836	+82

Variables		ZBA = 3·ZAA0, ZAA0 = 0.05 m, ZBA = 0.15 m, "titanium" rod in the cardan gear, otherwise steel links, compression ratio 12 :1, standard atmospheric pressure 1.01325·10^5 Pa, polytropic exponent γ = 1.4, cylinder filling 107 %, piston diameter = 2·ZAA0, displacement 785 cm³, AIR PUMP								
Angular acceleration αAA0 [rad/s²]		0			0			200π		
Initial angular velocity ωAA00 [rad/s]		3π	30π	Δ % /S	100π	110π	Δ % /S	140π	200π	Δ % /S
Total piston pin joint force	S	28360	28140	0,	25820	25290	-9,	22980	17790	-21,
maximums [N] DISPARATE	C	28360	27940	-0.7	23600	22600	-11	18260	20390	+15
Total crank pin joint force	S	28360	27540	+100,	19150	17220	+146,	18810	37620	+94,
maximums [N]	C	56720	55870	+103	47200	45200	+163	36520	40780	+8
Total main pin joint force	S	28360	27540	+100,	19150	17220	+146,	18810	37620	+94,
maximums [N]	C	56720	55870	+103	47200	45200	+163	36520	40780	+8
Total crankshaft torque	S	384	384	-13,	389	391	-36,	415	460	-28,
maximums [Nm]	C	333	326	-15	248	230	-41	300	540	+18

S = slider-crank C = cardan gear

Variables		ZBA = 4·ZAA0, ZAA0 = 0.04 m, ZBA = 0.16 m, steel links, equal masses, compression ratio 12 :1, standard atmospheric pressure 1.01325·10^5 Pa, polytropic exponent γ = 1.4, cylinder filling 107 %, piston diameter = 2·ZAA0, displacement 402 cm³, AIR PUMP								
Angular acceleration αAA0 [rad/s²]		0			0			200π		
Initial angular velocity ωAA00 [rad/s]		3π	30π	Δ % /S	100π	110π	Δ % /S	140π	200π	Δ % /S
Total piston pin joint force	S	18150	17950	0,	15880	15400	-31,	13340	9230	+17,
maximums [N] DISPARATE	C	18150	17500	-3	10880	9355	-39	15600	30330	+229
Total crank pin joint force	S	18150	17400	+100,	9745	10320	+123,	17420	34820	+79,
maximums [N]	C	36300	35000	+101	21760	18710	+81	31200	60660	+74
Total main pin joint force	S	18150	17400	+100,	9745	10320	+123,	17420	34820	+79,
maximums [N]	C	36300	35000	+101	21760	18710	+81	31200	60660	+74
Total crankshaft torque	S	191	192	-11,	211	216	-21,	245	295	+34,
maximums [Nm]	C	170	161	-16	166	196	-9	328	624	+111

Variables		ZBA = 4·ZAA0, ZAA0 = 0.04 m, ZBA = 0.16 m, "titanium" rod in the cardan gear, otherwise steel links, compression ratio 12 :1, standard atmospheric pressure 1.01325·10^5 Pa, polytropic exponent γ = 1.4, cylinder filling 107 %, piston diameter = 2·ZAA0, displacement 402 cm³, AIR PUMP								
Angular acceleration αAA0 [rad/s²]		0			0			200π		
Initial angular velocity ωAA00 [rad/s]		3π	30π	Δ % /S	100π	110π	Δ % /S	140π	200π	Δ % /S
Total piston pin joint force	S	18150	17950	0,	15880	15400	-14,	13340	9230	-25,
maximums [N] DISPARATE	C	18150	17750	-1	13610	12650	-18	9960	19170	+108
Total crank pin joint force	S	18150	17400	+100,	9745	10320	+179,	17420	34820	+14,
maximums [N]	C	36300	35490	+104	27220	25310	+145	19920	38330	+10
Total main pin joint force	S	18150	17400	+100,	9745	10320	+179,	17420	34820	+14,
maximums [N]	C	36300	35490	+104	27220	25310	+145	19920	38330	+10
Total crankshaft torque	S	191	192	-11,	211	216	-47,	245	295	-13,
maximums [Nm]	C	171	165	-14	111	130	-40	214	399	+35

S = slider-crank   C = cardan gear

Variables		ZBA = 2.33·ZAA0, ZAA0 = 0.06 m, ZBA = 0.14 m, steel links, equal masses, compression ratio 12 :1, standard atmospheric pressure 1.01325·10^5 Pa, polytropic exponent γ = 1.4, cylinder filling 107 %, piston diameter = 2·ZAA0, maximum combustion pressure 12 MPa, gasoline combustion, displacement 1357 cm^3, FOUR-STROKE ENGINE								
Angular acceleration αAA0 [rad/s^2]		0			0			0		
Initial angular velocity ωAA00 [rad/s]		3π	30π	Δ % /S	100π	110π	Δ % /S	140π	200π	Δ % /S
Total piston pin joint force	S	1.357	1.355	+1,	1.331	1.326	-3,	1.307	1.254	-6,
maximums [·10^5 N] DISPARATE	C	1.371	1.364	+1	1.297	1.282	-3	1.226	1.076	-14
Total crank pin joint force	S	1.364	1.356	+101,	1.275	1.256	+104,	1.190	1.013	+106,
maximums [·10^5 N]	C	2.742	2.729	+101	2.595	2.564	+104	2.453	2.152	+113
Total main pin joint force	S	1.364	1.356	+101,	1.275	1.256	+104,	1.190	1.013	+106,
maximums [·10^5 N]	C	2.742	2.729	+101	2.595	2.564	+104	2.453	2.152	+113
Total crankshaft torque	S	3453	3451	-22,	3427	3421	-27,	3402	3348	-31,
maximums [Nm]	C	2701	2683	-22	2502	2468	-28	2346	2014	-40
Angular acceleration αAA0 [rad/s^2]		30π			100π			200π		
Initial angular velocity ωAA00 [rad/s]		3π	30π	Δ % /S	100π	110π	Δ % /S	140π	200π	Δ % /S
Total piston pin joint force	S	1.357	1.355	+1,	1.330	1.325	-3,	1.304	1.252	-6,
maximums [·10^5 N] DISPARATE	C	1.370	1.364	+1	1.294	1.279	-3	1.220	1.070	-15
Total crank pin joint force	S	1.363	1.355	+101,	1.271	1.252	+104,	1.182	1.005	+106,
maximums [·10^5 N]	C	2.740	2.727	+101	2.588	2.557	+104	2.440	2.139	+113
Total main pin joint force	S	1.363	1.355	+101,	1.271	1.252	+104,	1.182	1.005	+106,
maximums [·10^5 N]	C	2.740	2.727	+101	2.588	2.557	+104	2.440	2.139	+113
Total crankshaft torque	S	3448	3446	-22,	3411	3405	-27,	3370	3316	-32,
maximums [Nm]	C	2694	2676	-22	2482	2447	-28	2305	1973	-41

S = slider-crank C = cardan gear

Variables		ZBA = 2.33·ZAA0, ZAA0 = 0.06 m, ZBA = 0.14 m, "titanium" rod in the cardan gear, otherwise steel links, compression ratio 12 :1, standard atmospheric pressure 1.01325·10^5 Pa, polytropic exponent γ = 1.4, cylinder filling 107 %, piston diameter = 2·ZAA0, maximum combustion pressure 12 MPa, gasoline combustion, displacement 1357 cm³, FOUR-STROKE ENGINE								
Angular acceleration αAA0 [rad/s²]		0			0			0		
Initial angular velocity ωAA00 [rad/s]		3π	30π	Δ % /S	100π	110π	Δ % /S	140π	200π	Δ % /S
Total piston pin joint force	S	1.357	1.355	+1,	1.331	1.326	-0.5,	1.307	1.254	-2,
maximums [·10^5 N] DISPARATE	C	1.371	1.367	+1	1.325	1.315	-1	1.281	1.187	-5
Total crank pin joint force	S	1.364	1.356	+101,	1.275	1.256	+108,	1.190	1.013	+115,
maximums [·10^5 N]	C	2.742	2.734	+102	2.650	2.631	+109	2.561	2.373	+134
Total main pin joint force	S	1.364	1.356	+101,	1.275	1.256	+108,	1.190	1.013	+115,
maximums [·10^5 N]	C	2.742	2.734	+102	2.650	2.631	+109	2.561	2.373	+134
Total crankshaft torque	S	3453	3451	-22,	3427	3421	-25,	3402	3348	-28,
maximums [Nm]	C	2701	2690	-22	2573	2547	-26	2466	2258	-33
Angular acceleration αAA0 [rad/s²]		30π			100π			200π		
Initial angular velocity ωAA00 [rad/s]		3π	30π	Δ % /S	100π	110π	Δ % /S	140π	200π	Δ % /S
Total piston pin joint force	S	1.357	1.355	+1,	1.330	1.325	-0.5,	1.304	1.252	-2,
maximums [·10^5 N] DISPARATE	C	1.370	1.366	+1	1.230	1.313	-1	1.277	1.183	-6
Total crank pin joint force	S	1.363	1.355	+101,	1.271	1.252	+108,	1.182	1.005	+116,
maximums [·10^5 N]	C	2.741	2.733	+102	2.646	2.627	+110	2.554	2.365	+135
Total main pin joint force	S	1.363	1.355	+101,	1.271	1.252	+108,	1.182	1.005	+116,
maximums [·10^5 N]	C	2.741	2.733	+102	2.646	2.627	+110	2.554	2.365	+135
Total crankshaft torque	S	3448	3446	-22,	3411	3405	-25,	3370	3316	-28,
maximums [Nm]	C	2695	2684	-22	2554	2527	-26	2430	2222	-33

S = slider-crank   C = cardan gear

Variables		ZBA = 3·ZAA0, ZAA0 = 0.05 m, ZBA = 0.15 m, steel links, equal masses, compression ratio 12 :1, standard atmospheric pressure 1.01325·10^5 Pa, polytropic exponent γ = 1.4, cylinder filling 107 %, piston diameter = 2·ZAA0, maximum combustion pressure 12 MPa, gasoline combustion, displacement 785 cm³, FOUR-STROKE ENGINE								
Angular acceleration αAA0 [rad/s²]		0			0			200π		
Initial angular velocity ωAA00 [rad/s]		3π	30π	Δ % /S	100π	110π	Δ % /S	140π	200π	Δ % /S
Total piston pin joint force	S	0.9425	0.9403	+1,	0.9183	0.9132	-5,	0.8929	0.8435	-11,
maximums [·10⁵ N] DISPARATE	C	0.9499	0.9433	+0.3	0.8759	0.8603	-6	0.7985	0.6473	-23
Total crank pin joint force	S	0.9453	0.9377	+101,	0.8599	0.8420	+104,	0.7719	0.6072	+107,
maximums [·10⁵ N]	C	1.900	1.887	+101	1.752	1.721	+104	1.597	1.295	+113
Total main pin joint force	S	0.9453	0.9377	+101,	0.8599	0.8420	+104,	0.7719	0.6072	+107,
maximums [·10⁵ N]	C	1.900	1.887	+101	1.752	1.721	+104	1.597	1.295	+113
Total crankshaft torque	S	1897	1897	-18,	1899	1900	-26,	1887	1893	-34,
maximums [Nm]	C	1559	1544	-19	1402	1374	-27	1247	970	-49

Variables		ZBA = 3·ZAA0, ZAA0 = 0.05 m, ZBA = 0.15 m, "titanium" rod in the cardan gear, otherwise steel links, compression ratio 12 :1, standard atmospheric pressure 1.01325·10^5 Pa, polytropic exponent γ = 1.4, cylinder filling 107 %, piston diameter = 2·ZAA0, maximum combustion pressure 12 MPa, gasoline combustion, displacement 785 cm³, FOUR-STROKE ENGINE								
Angular acceleration αAA0 [rad/s²]		0			0			200π		
Initial angular velocity ωAA00 [rad/s]		3π	30π	Δ % /S	100π	110π	Δ % /S	140π	200π	Δ % /S
Total piston pin joint force	S	0.9425	0.9403	+1,	0.9183	0.9132	-2,	0.8929	0.8435	-4,
maximums [·10⁵ N] DISPARATE	C	0.9499	0.9458	+1	0.9037	0.8939	-2	0.8553	0.7608	-10
Total crank pin joint force	S	0.9453	0.9377	+101,	0.8599	0.8420	+110,	0.7719	0.6072	+122,
maximums [·10⁵ N]	C	1.900	1.892	+102	1.807	1.788	+112	1.711	1.522	+151
Total main pin joint force	S	0.9453	0.9377	+101,	0.8599	0.8420	+110,	0.7719	0.6072	+122,
maximums [·10⁵ N]	C	1.900	1.892	+102	1.807	1.788	+112	1.711	1.522	+151
Total crankshaft torque	S	1897	1897	-18,	1899	1900	-23,	1887	1893	-28,
maximums [Nm]	C	1560	1550	-18	1454	1436	-24	1352	1178	-38

S = slider-crank   C = cardan gear

Variables		ZBA = 4·ZAA0, ZAA0 = 0.04 m, ZBA = 0.16 m, steel links, equal masses, compression ratio 12 :1, standard atmospheric pressure 1.01325·10^5 Pa, polytropic exponent γ = 1.4, cylinder filling 107 %, piston diameter = 2·ZAA0, maximum combustion pressure 12 MPa, gasoline combustion, displacement 402 cm³, FOUR-STROKE ENGINE								
Angular acceleration αAA0 [rad/s²]		0			0			200π		
Initial angular velocity ωAA00 [rad/s]		3π	30π	Δ % /S	100π	110π	Δ % /S	140π	200π	Δ % /S
Total piston pin joint force	S	0.6032	0.6012	+1,	0.5815	0.5769	-8,	0.5588	0.5144	-17,
maximums [·10^5 N] DISPARATE	C	0.6067	0.6004	-0.1	0.5361	0.5213	-10	0.4623	0.3187	-38
Total crank pin joint force	S	0.6042	0.5971	+101,	0.5262	0.5101	+104,	0.4473	0.3539	+107,
maximums [·10^5 N]	C	1.213	1.201	+101	1.072	1.043	+104	0.9246	0.6375	+80
Total main pin joint force	S	0.6042	0.5971	+101,	0.5262	0.5101	+104,	0.4473	0.3539	+107,
maximums [·10^5 N]	C	1.213	1.201	+101	1.072	1.043	+104	0.9246	0.6375	+80
Total crankshaft torque	S	925	926	-14,	941	944	-27,	951	984	-40,
maximums [Nm]	C	797	785	-15	682	661	-30	569	668	-32

Variables		ZBA = 4·ZAA0, ZAA0 = 0.04 m, ZBA = 0.16 m, "titanium" rod in the cardan gear, otherwise steel links, compression ratio 12 :1, standard atmospheric pressure 1.01325·10^5 Pa, polytropic exponent γ = 1.4, cylinder filling 107 %, piston diameter = 2·ZAA0, maximum combustion pressure 12 MPa, gasoline combustion, displacement 402 cm³, FOUR-STROKE ENGINE								
Angular acceleration αAA0 [rad/s²]		0			0			200π		
Initial angular velocity ωAA00 [rad/s]		3π	30π	Δ % /S	100π	110π	Δ % /S	140π	200π	Δ % /S
Total piston pin joint force	S	0.6032	0.6012	+1,	0.5815	0.5769	-3,	0.5588	0.5144	-8,
maximums [·10^5 N] DISPARATE	C	0.6068	0.6028	+0.3	0.5626	0.5534	-4	0.5165	0.4264	-17
Total crank pin joint force	S	0.6042	0.5971	+101,	0.5262	0.5101	+114,	0.4473	0.3539	+131,
maximums [·10^5 N]	C	1.214	1.206	+102	1.125	1.107	+117	1.033	0.8528	+141
Total main pin joint force	S	0.6042	0.5971	+101,	0.5262	0.5101	+114,	0.4473	0.3539	+131,
maximums [·10^5 N]	C	1.214	1.206	+102	1.125	1.107	+117	1.033	0.8528	+141
Total crankshaft torque	S	925	926	-14,	941	944	-23,	951	984	-32,
maximums [Nm]	C	797	790	-15	721	708	-25	648	516	-48

S = slider-crank   C = cardan gear

Appendix 11.4.2

Comparison of the summed lossless Newtonian dynamics:
Total torques, works and powers
Pumps and four-stroke engines

Variables		ZBA = 2.33·ZAA0, ZAA0 = 0.06 m, ZBA = 0.14 m, steel links, equal masses, compression ratio 12 : 1, 1 atm = 1.01325·10^5 Pa, γ = 1.4, cylinder filling 107 %, piston diameter = 2·ZAA0, displacement 1357 cm³, cycle = 4π rad, AIR PUMP							
Angular acceleration αAA0 [rad/s²]		100π				200π			
Initial angular velocity ωAA00 [rad/s]		3π	30π	200π	Δ % /S	3π	30π	200π	Δ % /S
Maximum total torque [Nm]	S	698	696	707	-16, -18, +42	712	710	731	-17, -19, +41
	C	583	576	1001		591	576	1030	
Mean total torque [Nm]	S	126	126	126	-1	141	141	141	-2
	C	125	125	125		139	139	139	
Total work consumption / cycle [J]	S	1589	1589	1589	-1	1777	1777	1777	-2
	C	1571	1571	1571		1740	1740	1740	
Maximum total power consumption [kW]	S	61.27	89.20	448	-18, -20, +42	88.09	110	467	-19, -21, +41
	C	50.41	71.69	634		71.02	86.57	657	
Mean total power consumption [kW]	S	8.913	14.82	79.13	-2	13.82	19.23	89.24	-3
	C	8.743	14.57	77.94		13.41	18.68	86.79	

Variables		ZBA = 2.33·ZAA0, ZAA0 = 0.06 m, ZBA = 0.14 m, "titanium" rod in the cardan gear, otherwise steel links, compression ratio 12 :1, 1 atm = 1.01325·10^5 Pa, γ = 1.4, cylinder filling 107 %, piston diameter = 2·ZAA0, displacement 1357 cm³, cycle = 4π rad, AIR PUMP							
Angular acceleration αAA0 [rad/s²]		100π				200π			
Initial angular velocity ωAA00 [rad/s]		3π	30π	200π	Δ % /S	3π	30π	200π	Δ % /S
Maximum total torque [Nm]	S	698	696	707	-16, -17, -7	712	710	731	-16, -17, -7
	C	585	576	655		595	586	677	
Mean total torque [Nm]	S	126	126	126	-1	141	141	141	-2
	C	125	125	125		138	138	138	
Total work consumption / cycle [J]	S	1589	1589	1589	-1	1777	1777	1777	-2
	C	1571	1571	1571		1740	1740	1740	
Maximum total power consumption [kW]	S	61.27	89.20	448	-17, -18, -8	88.09	110	467	-18, -19, -8
	C	50.87	73.17	414		72.33	89.18	432	
Mean total power consumption [kW]	S	8.913	14.82	79.13	-2, -2, -1	13.82	19.23	89.24	-3
	C	8.751	14.59	78.02		13.44	18.71	86.96	

S = slider-crank C = cardan gear

Variables		ZBA = 3·ZAA0, ZAA0 = 0.05 m, ZBA = 0.15 m, steel links, equal masses, compression ratio 12 : 1, 1 atm = 1.01325·10^5 Pa, γ = 1.4, cylinder filling 107 %, piston diameter = 2·ZAA0, displacement 785 cm³, cycle = 4π rad, AIR PUMP							
Angular acceleration αAA0 [rad/s²]		100π				200π			
Initial angular velocity ωAA00 [rad/s]		3π	30π	200π	Δ % /S	3π	30π	200π	Δ % /S
Maximum total torque [Nm]	S	391	391	448	-14, -18, +82	398	398	460	-16, -19, +82
	C	334	322	817		336	323	836	
Mean total torque [Nm]	S	71.90	71.90	71.90	-2	79.33	79.33	79.33	-3
	C	70.70	70.70	70.70		76.88	76.88	76.88	
Total work consumption / cycle [J]	S	904	904	904	-2	997	997	997	-3
	C	888	888	888		966	966	966	
Maximum total power consumption [kW]	S	34.07	49.85	283	-16, -19, +83	49.06	61.59	294	-19, -22, +82
	C	28.71	40.26	517		39.80	47.80	533	
Mean total power consumption [kW]	S	5.077	8.433	45.02	-2	7.779	10.80	50.08	-4
	C	4.956	8.238	44.01		7.471	10.37	48.03	

Variables		ZBA = 3·ZAA0, ZAA0 = 0.05 m, ZBA = 0.15 m, "titanium" rod in the cardan gear, otherwise steel links, compression ratio 12 :1, 1 atm = 1.01325·10^5 Pa, γ = 1.4, cylinder filling 107 %, piston diameter = 2·ZAA0, displacement 785 cm³, cycle = 4π rad, AIR PUMP							
Angular acceleration αAA0 [rad/s²]		100π				200π			
Initial angular velocity ωAA00 [rad/s]		3π	30π	200π	Δ % /S	3π	30π	200π	Δ % /S
Maximum total torque [Nm]	S	391	391	448	-14, -16, +17	398	398	460	-15, -17, +18
	C	336	329	526		339	332	540	
Mean total torque [Nm]	S	71.90	71.90	71.90	-2	79.33	79.33	79.33	-3
	C	70.69	70.69	70.70		76.88	76.88	76.88	
Total work consumption / cycle [J]	S	904	904	904	-2	997	997	997	-3
	C	888	888	888		966	966	966	
Maximum total power consumption [kW]	S	34.07	49.85	283	-15, -17, +18	49.06	61.59	294	-17, -19, +17
	C	29.10	41.50	333		40.89	49.98	345	
Mean total power consumption [kW]	S	5.077	8.433	45.02	-2	7.779	10.80	50.08	-4
	C	4.962	8.251	44.08		7.490	10.39	48.17	

S = slider-crank C = cardan gear

Variables		ZBA = 4·ZAA0, ZAA0 = 0.04 m, ZBA = 0.16 m, steel links, equal masses, compression ratio 12 : 1, 1 atm = $1.01325 \cdot 10^5$ Pa, γ = 1.4, cylinder filling 107 %, piston diameter = 2·ZAA0, displacement 402 cm³, cycle = 4π rad, AIR PUMP							
Angular acceleration αAA0 [rad/s²]		100π				200π			
Initial angular velocity ωAA00 [rad/s]		3π	30π	200π	Δ % /S	3π	30π	200π	Δ % /S
Maximum total torque [Nm]	S	194	196	290	-13, -18, +111	198	199	295	-15, -20, +111
	C	169	160	612		168	159	624	
Mean total torque [Nm]	S	36.39	36.39	36.39	-3	39.76	39.76	39.75	-5
	C	35.46	35.46	35.46		37.88	37.88	37.88	
Total work consumption / cycle [J]	S	457	457	457	-3	500	500	500	-5
	C	446	446	446		476	476	476	
Maximum total power consumption [kW]	S	16.87	24.90	184	-15, -21, +111	24.42	30.92	189	-20, -26, +111
	C	14.37	19.69	387		19.46	22.79	398	
Mean total power consumption [kW]	S	2.572	4.270	22.80	-3	3.910	5.425	25.13	-6
	C	2.488	4.126	22.02		3.688	5.099	23.56	

Variables		ZBA = 4·ZAA0, ZAA0 = 0.04 m, ZBA = 0.16 m, "titanium" rod in the cardan gear, otherwise steel links, compression ratio 12 :1, 1 atm = $1.01325 \cdot 10^5$ Pa, γ = 1.4, cylinder filling 107 %, piston diameter = 2·ZAA0, displacement 402 cm³, cycle = 4π rad, AIR PUMP							
Angular acceleration αAA0 [rad/s²]		100π				200π			
Initial angular velocity ωAA00 [rad/s]		3π	30π	200π	Δ % /S	3π	30π	200π	Δ % /S
Maximum total torque [Nm]	S	194	196	290	-12, -16, +35	198	199	295	-14, -17, +35
	C	171	165	390		171	165	399	
Mean total torque [Nm]	S	36.39	36.39	36.38	-3	39.76	39.76	39.75	-5
	C	35.46	35.46	35.46		37.88	37.88	37.88	
Total work consumption / cycle [J]	S	457	457	457	-3	500	500	500	-5
	C	446	446	446		476	476	476	
Maximum total power consumption [kW]	S	16.87	24.90	184	-13, -17, +34	24.42	30.92	189	-17, -21, +35
	C	14.67	20.63	247		20.29	24.45	254	
Mean total power consumption [kW]	S	2.572	4.270	22.80	-3	3.910	5.425	25.13	-5, -6, -6
	C	2.493	4.136	22.07		3.702	5.120	23.67	

S = slider-crank C = cardan gear

Variables		ZBA = 2.33·ZAA0, ZAA0 = 0.06 m, ZBA = 0.14 m, steel links, equal masses, compression ratio 12 : 1, 1 atm = $1.01325 \cdot 10^5$ Pa, γ = 1.4, cylinder filling 107 %, maximum combustion pressure 12 MPa, gasoline combustion, piston diameter = 2·ZAA0, displacement 1357 cm³, cycle = 4π rad, FOUR-STROKE ENGINE							
Angular acceleration αAA0 [rad/s²]		100π				200π			
Initial angular velocity ωAA00 [rad/s]		3π	30π	200π	Δ % /S	3π	30π	200π	Δ % /S
Maximum total torque [Nm]	S	3437	3435	3332	-22, -23,	3421	3419	3316	-22, -23,
	C	2678	2660	1994	-40	2655	2637	1973	-40
Mean total torque [Nm]	S	101	101	101	-14	86.25	86.25	86.25	-14
	C	87.33	87.33	87.33		73.82	73.82	73.82	
Total work output / cycle [J]	S	1273	1273	1273	-14	1084	1084	1084	-14
	C	1097	1097	1097		928	928	928	
Maximum total power output [kW]	S	225	393	2105	-21, -22,	315	449	2105	-21, -22,
	C	177	305	1259	-40	247	349	1253	-41
Mean total power output [kW]	S	7.964	12.19	63.13	-8, -11,	9.955	12.54	54.01	-7, -10,
	C	7.339	10.81	54.76	-13	9.244	11.29	46.85	-13

Variables		ZBA = 2.33·ZAA0, ZAA0 = 0.06 m, ZBA = 0.14 m, "titanium" rod in the cardan gear, otherwise steel links, compression ratio 12 :1, 1 atm = $1.01325 \cdot 10^5$ Pa, γ = 1.4, cylinder filling 107 %, maximum combustion pressure 12 MPa, gasoline combustion, piston diameter = 2·ZAA0, displacement 1357 cm³, cycle = 4π rad, FOUR-STROKE ENGINE							
Angular acceleration αAA0 [rad/s²]		100π				200π			
Initial angular velocity ωAA00 [rad/s]		3π	30π	200π	Δ % /S	3π	30π	200π	Δ % /S
Maximum total torque [Nm]	S	3437	3435	3332	-22, -22,	3421	3419	3316	-22, -22,
	C	2682	2670	2240	-33	2662	2651	2222	-33
Mean total torque [Nm]	S	101	101	101	-14	86.25	86.25	86.25	-14
	C	87.33	87.33	87.33		73.82	73.82	73.82	
Total work output / cycle [J]	S	1273	1273	1273	-14	1084	1084	1084	-14
	C	1097	1097	1097		928	928	928	
Maximum total power output [kW]	S	225	393	2105	-21, -22,	315	449	2105	-21, -22,
	C	178	307	1415	-33	248	350	1411	-33
Mean total power output [kW]	S	7.964	12.19	63.13	-8, -11	9.955	12.54	54.01	-7, -10,
	C	7.331	10.79	54.67	-13	9.222	11.26	46.69	-14

S = slider-crank C = cardan gear

Variables		ZBA = 3·ZAA0, ZAA0 = 0.05 m, ZBA = 0.15 m, steel links, equal masses, compression ratio 12 : 1, 1 atm = $1.01325 \cdot 10^5$ Pa, γ = 1.4, cylinder filling 107 %, maximum combustion pressure 12 MPa, gasoline combustion, piston diameter = 2·ZAA0, displacement 785 cm³, cycle = 4π rad, FOUR-STROKE ENGINE							
Angular acceleration αAA0 [rad/s²]		100π				200π			
Initial angular velocity ωAA00 [rad/s]		3π	30π	200π	Δ % /S	3π	30π	200π	Δ % /S
Maximum total torque [Nm]	S	1889	1890	1900	-18, -19, -48	1882	1883	1893	-19, -19, -49
	C	1546	1530	982		1532	1516	970	
Mean total torque [Nm]	S	57.52	57.52	57.52	-10	50.09	50.09	50.09	-8
	C	52.04	52.04	52.04		45.86	45.86	45.86	
Total work output / cycle [J]	S	723	723	723	-10	629	629	629	-8
	C	654	654	654		576	576	576	
Maximum total power output [kW]	S	124	216	1200	-17, -19, -48	173	247	1202	-18, -19, -49
	C	102	176	620		143	200	616	
Mean total power output [kW]	S	4.561	6.943	35.85	-5, -7, -9	5.798	7.299	31.35	-3, -5, -7
	C	4.340	6.432	32.70		5.626	6.958	29.23	

Variables		ZBA = 3·ZAA0, ZAA0 = 0.05 m, ZBA = 0.15 m, "titanium" rod in the cardan gear, otherwise steel links, compression ratio 12 : 1, 1 atm = $1.01325 \cdot 10^5$ Pa, γ = 1.4, cylinder filling 107 %, maximum combustion pressure 12 MPa, gasoline combustion, piston diameter = 2·ZAA0, displacement 785 cm³, cycle = 4π rad, FOUR-STROKE ENGINE							
Angular acceleration αAA0 [rad/s²]		100π				200π			
Initial angular velocity ωAA00 [rad/s]		3π	30π	200π	Δ % /S	3π	30π	200π	Δ % /S
Maximum total torque [Nm]	S	1889	1890	1900	-18, -19, -37	1882	1883	1893	-18, -19, -38
	C	1548	1539	1188		1537	1528	1178	
Mean total torque [Nm]	S	57.52	57.52	57.52	-10	50.09	50.09	50.09	-8
	C	52.05	52.05	52.05		45.86	45.86	45.86	
Total work output / cycle [J]	S	723	723	723	-10	629	629	629	-8
	C	654	654	654		576	576	576	
Maximum total power output [kW]	S	124	216	1200	-17, -18, -37	173	247	1202	-17, -18, -38
	C	103	177	751		143	202	748	
Mean total power output [kW]	S	4.561	6.943	35.85	-5, -8, -9	5.798	7.299	31.35	-3, -5, -7
	C	4.333	6.420	32.63		5.607	6.930	29.09	

S = slider-crank C = cardan gear

Variables		ZBA = 4·ZAA0, ZAA0 = 0.04 m, ZBA = 0.16 m, steel links, equal masses, compression ratio 12 : 1, 1 atm = $1.01325 \cdot 10^5$ Pa, γ = 1.4, cylinder filling 107 %, maximum combustion pressure 12 MPa, gasoline combustion, piston diameter = 2·ZAA0, displacement 402 cm³, cycle = 4π rad, FOUR-STROKE ENGINE							
Angular acceleration αAA0 [rad/s²]		100π				200π			
Initial angular velocity ωAA00 [rad/s]		3π	30π	200π	Δ % /S	3π	30π	200π	Δ % /S
Maximum total torque [Nm]	S	923	924	986	-15, -16, -33	920	922	984	-15, -17, -32
	C	788	777	663		780	768	668	
Mean total torque [Nm]	S	28.89	28.89	28.89	-5	25.52	25.51	25.52	-2
	C	27.33	27.33	27.33		24.90	24.90	24.90	
Total work output / cycle [J]	S	363	363	363	-5	321	321	321	-2
	C	343	343	343		313	313	313	
Maximum total power output [kW]	S	60.40	106	623	-14, -16, -33	84.75	121	625	-14, -16, -32
	C	52.22	89.19	419		72.70	102	425	
Mean total power output [kW]	S	2.309	3.496	17.99	-2, -3, -4	2.966	3.725	15.95	+2, +1, +0.1
	C	2.266	3.378	17.22		3.011	3.762	15.96	

Variables		ZBA = 4·ZAA0, ZAA0 = 0.04 m, ZBA = 0.16 m, "titanium" rod in the cardan gear, otherwise steel links, compression ratio 12 :1, 1 atm = $1.01325 \cdot 10^5$ Pa, γ = 1.4, cylinder filling 107 %, maximum combustion pressure 12 MPa, gasoline combustion, piston diameter = 2·ZAA0, displacement 402 cm³, cycle = 4π rad, FOUR-STROKE ENGINE							
Angular acceleration αAA0 [rad/s²]		100π				200π			
Initial angular velocity ωAA00 [rad/s]		3π	30π	200π	Δ % /S	3π	30π	200π	Δ % /S
Maximum total torque [Nm]	S	923	924	986	-14, -15, -47	920	922	984	-15, -16, -48
	C	791	783	521		784	777	516	
Mean total torque [Nm]	S	28.89	28.89	28.89	-5	25.52	25.51	25.52	-2
	C	27.33	27.33	27.33		24.90	24.90	24.90	
Total work output / cycle [J]	S	363	363	363	-5	321	321	321	-2
	C	343	343	343		313	313	313	
Maximum total power output [kW]	S	60.40	106	623	-13, -15, -47	84.75	121	625	-14, -15, -48
	C	52.37	89.95	329		73.12	103	328	
Mean total power output [kW]	S	2.309	3.496	17.99	-2, -4, -5	2.966	3.725	15.95	+1, +0.4 -0.6
	C	2.261	3.369	17.16		2.997	3.741	15.85	

S = slider-crank C = cardan gear

Appendix 11.6.1

Comparison of the operational torques, powers and mechanical efficiencies Dynamic tooth loads of the cardan wheels Pumps and four-stroke engines

Variables S = slider-crank C = cardan gear		ZBA = 2.33·ZAA0, ZAA0 = 0.06 m, ZBA = 0.14 m, steel links, equal masses, compression ratio 12 :1, standard atmospheric pressure 1.01325·10^5 Pa, polytropic exponent γ = 1.4, cylinder filling 107 %, piston diameter = 2·ZAA0, displacement 1357 cm³, AIR PUMP								
Angular acceleration αAA0 [rad/s²]		0			0			0		
Initial angular velocity ωAA00 [rad/s]		3π	30π	Δ % /S	100π	110π	Δ % /S	140π	200π	Δ % /S
Dynamic tooth load of the cardan wheel [N]		48380	49010	- -	55380	56990	- -	62730	79310	- -
Mean torque need [Nm]	S	118	118	-0.07,	127	129	-7,	136	157	-12,
	C	118	117	-1.2	118	119	-8	120	125	-20
Mean power loss [kW]	S	0.072	0.797	-2.2,	5.398	6.639	-52,	11.65	29.28	-61,
	C	0.070	0.660	-17	2.602	3.002	-55	4.506	9.582	-67
Mean power need [kW]	S	1.108	11.16	-0.07,	39.95	44.65	-7,	60.03	98.39	-12,
	C	1.108	11.04	-1.2	37.19	41.04	-8	52.92	78.75	-20
Mechanical efficiency	S	0.935	0.929	+0.18,	0.865	0.851	+8,	0.806	0.702	+14,
	C	0.937	0.941	+1.2	0.930	0.927	+9	0.915	0.879	+25
Angular acceleration αAA0 [rad/s²]		30π			100π			200π		
Initial angular velocity ωAA00 [rad/s]		3π	30π	Δ % /S	100π	110π	Δ % /S	140π	200π	Δ % /S
Dynamic tooth load of the cardan wheel [N]		48550	49170	- -	55880	57350	- -	63860	80510	- -
Mean torque need [Nm]	S	122	123	-0.80,	143	145	-8,	167	187	-11,
	C	121	121	-1.6	132	132	-9	148	153	-19
Mean power loss [kW]	S	0.282	0.866	-8,	5.634	6.888	-52,	12.25	30.08	-62,
	C	0.259	0.706	-18	2.678	3.078	-55	4.673	9.809	-67
Mean power need [kW]	S	4.908	12.59	-1.5,	45.95	51.04	-8,	75.48	119	-12,
	C	4.837	12.36	-1.8	42.38	46.56	-9	66.17	96.55	-19
Mechanical efficiency	S	0.900	0.894	+0.91,	0.773	0.762	+8,	0.659	0.588	+14,
	C	0.909	0.910	+1.7	0.836	0.833	+9	0.748	0.723	+23

Variables S = slider-crank C = cardan gear		ZBA = 2.33·ZAA0, ZAA0 = 0.06 m, ZBA = 0.14 m, "titanium" rod in the cardan gear, otherwise steel links, compression ratio 12 :1, standard atmospheric pressure 1.01325·10^5 Pa, polytropic exponent γ = 1.4, cylinder filling 107 %, piston diameter = 2·ZAA0, displacement 1357 cm³, AIR PUMP								
Angular acceleration αAA0 [rad/s²]		0			0			0		
Initial angular velocity ωAA00 [rad/s]		3π	30π	Δ % /S	100π	110π	Δ % /S	140π	200π	Δ % /S
Dynamic tooth load of the cardan wheel [N]		48370	48800	- -	53030	54010	- -	57730	68430	- -
Mean torque need [Nm]	S	118	118	-0.07,	127	129	-8,	136	157	-22,
	C	118	117	-1.2	118	118	-9	119	122	-13
Mean power loss [kW]	S	0.072	0.797	-2.2,	5.398	6.639	-56,	11.65	29.28	-67,
	C	0.070	0.657	-18	2.393	2.713	-59	3.856	7.330	-75
Mean power need [kW]	S	1.108	11.16	-0.07,	39.95	44.65	-8,	60.03	98.39	-22,
	C	1.108	11.03	-1.2	36.98	40.76	-9	52.27	76.50	-13
Mechanical efficiency	S	0.935	0.929	+0.18,	0.865	0.851	+8,	0.806	0.702	+15,
	C	0.937	0.941	+1.3	0.936	0.934	+10	0.927	0.904	+29
Angular acceleration αAA0 [rad/s²]		30π			100π			200π		
Initial angular velocity ωAA00 [rad/s]		3π	30π	Δ % /S	100π	110π	Δ % /S	140π	200π	Δ % /S
Dynamic tooth load of the cardan wheel [N]		48500	48910	- -	53380	54360	- -	58190	69230	- -
Mean torque need [Nm]	S	122	123	-0.80,	143	145	-8,	167	187	-13,
	C	121	121	-1.6	131	131	-9	146	149	-21
Mean power loss [kW]	S	0.282	0.866	-8,	5.634	6.888	-56,	12.25	30.08	-68,
	C	0.258	0.703	-19	2.455	2.775	-60	3.980	7.478	-75
Mean power need [kW]	S	4.908	12.59	-1.4,	45.95	51.04	-8,	75.48	119	-13,
	C	4.838	12.37	-1.8	42.20	46.31	-9	65.60	94.38	-21
Mechanical efficiency	S	0.900	0.894	+0.91,	0.773	0.762	+9,	0.659	0.588	+15,
	C	0.909	0.910	+1.7	0.840	0.839	+10	0.756	0.741	+26

Variables S = slider-crank C = cardan gear		ZBA = 3·ZAA0, ZAA0 = 0.05 m, ZBA = 0.15 m, steel links, equal masses, compression ratio 12 : 1, standard atmospheric pressure 1.01325·10^5 Pa, polytropic exponent γ = 1.4, cylinder filling 107 %, piston diameter = 2·ZAA0, displacement 785 cm³, AIR PUMP								
Angular acceleration αAA0 [rad/s²]		0			0			0		
Initial angular velocity ωAA00 [rad/s]		3π	30π	Δ % /S	100π	110π	Δ % /S	140π	200π	Δ % /S
Dynamic tooth load of the cardan wheel [N]		37640	38290	- -	44890	46500	- -	52530	69580	- -
Mean torque need [Nm]	S	68.25	68.93	+0.43,	75.95	77.58	-8,	83.45	99.68	-14,
	C	68.54	68.31	-0.90	69.62	69.99	-10	71.45	76.15	-24
Mean power loss [kW]	S	0.043	0.496	+5,	3.858	4.808	-52,	8.702	22.63	-61,
	C	0.046	0.434	-12	1.857	2.173	-55	3.407	7.818	-65
Mean power need [kW]	S	0.643	6.497	+0.43,	23.86	26.81	-8,	36.70	62.63	-14,
	C	0.646	6.438	-0.90	21.87	24.19	-10	31.43	47.85	-24
Mechanical efficiency	S	0.933	0.924	-0.34,	0.838	0.821	+9,	0.763	0.639	+17,
	C	0.930	0.933	+0.99	0.915	0.910	+11	0.892	0.837	+31
Angular acceleration αAA0 [rad/s²]		30π			100π			200π		
Initial angular velocity ωAA00 [rad/s]		3π	30π	Δ % /S	100π	110π	Δ % /S	140π	200π	Δ % /S
Dynamic tooth load of the cardan wheel [N]		37820	38450	- -	45260	46980	- -	53730	70460	- -
Mean torque need [Nm]	S	70.58	71.26	-0.52,	83.70	85.33	-10,	98.96	115	-15,
	C	70.21	70.17	-1.5	75.87	76.25	-11	83.98	88.72	-23
Mean power loss [kW]	S	0.168	0.540	0,	4.036	4.999	-53,	9.164	23.27	-61,
	C	0.168	0.465	-14	1.916	2.234	-55	3.548	8.021	-66
Mean power need [kW]	S	2.829	7.285	-1.1,	26.97	30.11	-10,	44.64	73.30	-16,
	C	2.800	7.159	-1.7	24.34	26.79	-11	37.58	56.01	-24
Mechanical efficiency	S	0.903	0.894	+0.60,	0.762	0.747	+10,	0.645	0.554	+18,
	C	0.908	0.909	+1.6	0.841	0.837	+12	0.760	0.720	+30

Variables S = slider-crank C = cardan gear		ZBA = 3·ZAA0, ZAA0 = 0.05 m, ZBA = 0.15 m, "titanium" rod in the cardan gear, otherwise steel links, compression ratio 12 :1, standard atmospheric pressure 1.01325·10^5 Pa, polytropic exponent γ = 1.4, cylinder filling 107 %, piston diameter = 2·ZAA0, displacement 785 cm³, AIR PUMP								
Angular acceleration αAA0 [rad/s²]		0			0			0		
Initial angular velocity ωAA00 [rad/s]		3π	30π	Δ % /S	100π	110π	Δ % /S	140π	200π	Δ % /S
Dynamic tooth load of the cardan wheel [N]		37640	38080	- -	42320	43400	- -	47250	58320	- -
Mean torque need [Nm]	S	68.25	68.93	+0.42,	75.95	77.58	-9,	83.45	99.68	-16,
	C	68.54	68.29	-0.93	69.00	69.23	-11	70.09	72.81	-27
Mean power loss [kW]	S	0.043	0.496	+5,	3.858	4.808	-57,	8.702	22.63	-68,
	C	0.046	0.432	-13	1.664	1.908	-60	2.807	5.719	-75
Mean power need [kW]	S	0.643	6.497	+0.42,	23.86	26.81	-9,	36.70	62.63	-16,
	C	0.646	6.436	-0.93	21.68	23.92	-11	30.83	45.75	-27
Mechanical efficiency	S	0.933	0.924	-0.34,	0.838	0.821	+10,	0.763	0.639	+19,
	C	0.930	0.933	+1.0	0.924	0.921	+12	0.909	0.875	+37
Angular acceleration αAA0 [rad/s²]		30π			100π			200π		
Initial angular velocity ωAA00 [rad/s]		3π	30π	Δ % /S	100π	110π	Δ % /S	140π	200π	Δ % /S
Dynamic tooth load of the cardan wheel [N]		37770	38180	- -	42680	43660	- -	47970	59130	- -
Mean torque need [Nm]	S	70.58	71.26	-0.52,	83.70	85.33	-10,	98.96	115	-17,
	C	70.21	70.14	-1.6	75.22	75.45	-12	82.54	85.28	-26
Mean power loss [kW]	S	0.168	0.540	0,	4.036	4.999	-58,	9.164	23.27	-68,
	C	0.168	0.462	-15	1.711	1.955	-61	2.906	5.847	-75
Mean power need [kW]	S	2.829	7.285	-1.0,	26.97	30.11	-10,	44.64	73.30	-17,
	C	2.801	7.160	-1.7	24.17	26.55	-12	37.03	53.97	-26
Mechanical efficiency	S	0.903	0.894	+0.60,	0.762	0.747	+11,	0.645	0.554	+20,
	C	0.908	0.909	+1.7	0.848	0.845	+13	0.773	0.749	+35

Variables S = slider-crank C = cardan gear		ZBA = 4·ZAA0, ZAA0 = 0.04 m, ZBA = 0.16 m, steel links, equal masses, compression ratio 12 : 1, standard atmospheric pressure 1.01325·10^5 Pa, polytropic exponent γ = 1.4, cylinder filling 107 %, piston diameter = 2·ZAA0, displacement 402 cm³, AIR PUMP								
Angular acceleration αAA0 [rad/s²]		0			0			0		
Initial angular velocity ωAA00 [rad/s]		3π	30π	Δ % /S	100π	110π	Δ % /S	140π	200π	Δ % /S
Dynamic tooth load of the cardan wheel [N]		27960	28590	- -	35040	36690	- -	42550	59080	- -
Mean torque need [Nm]	S	35.21	35.72	+0.83,	40.95	42.17	-11,	46.57	58.72	-18,
	C	35.51	35.41	-0.85	36.58	36.90	-13	38.14	42.11	-28
Mean power loss [kW]	S	0.025	0.294	+11,	2.623	3.308	-53,	6.142	16.41	-60,
	C	0.027	0.264	-10	1.245	1.480	-55	2.430	5.962	-64
Mean power need [kW]	S	0.332	3.366	+0.83,	12.87	14.57	-11,	20.48	36.90	-18,
	C	0.335	3.338	-0.85	11.49	12.75	-13	16.78	26.46	-28
Mechanical efficiency	S	0.926	0.913	-0.76,	0.796	0.773	+12,	0.700	0.555	+22,
	C	0.919	0.921	+0.93	0.892	0.884	+14	0.855	0.775	+40
Angular acceleration αAA0 [rad/s²]		30π			100π			200π		
Initial angular velocity ωAA00 [rad/s]		3π	30π	Δ % /S	100π	110π	Δ % /S	140π	200π	Δ % /S
Dynamic tooth load of the cardan wheel [N]		28150	28750	- -	35620	37260	- -	43700	59980	- -
Mean torque need [Nm]	S	36.30	36.80	-0.43,	44.57	45.79	-12,	53.81	65.97	-20,
	C	36.14	36.15	-1.7	39.06	39.39	-14	43.14	47.13	-29
Mean power loss [kW]	S	0.095	0.321	+5,	2.751	3.444	-53,	6.480	16.88	-61,
	C	0.100	0.282	-12	1.288	1.526	-56	2.541	6.126	-64
Mean power need [kW]	S	1.452	3.761	-0.87,	14.36	16.16	-13,	24.27	41.97	-21,
	C	1.439	3.685	-2	12.50	13.81	-15	19.23	29.65	-29
Mechanical efficiency	S	0.899	0.886	+0.48,	0.732	0.713	+14,	0.607	0.495	+25,
	C	0.903	0.903	+1.9	0.836	0.829	+16	0.757	0.694	+40

Variables S = slider-crank C = cardan gear		ZBA = 4·ZAA0, ZAA0 = 0.04 m, ZBA = 0.16 m, "titanium" rod in the cardan gear, otherwise steel links, compression ratio 12 :1, standard atmospheric pressure 1.01325·10^5 Pa, polytropic exponent γ = 1.4, cylinder filling 107 %, piston diameter = 2·ZAA0, displacement 402 cm³, AIR PUMP								
Angular acceleration αAA0 [rad/s²]		0			0			0		
Initial angular velocity ωAA00 [rad/s]		3π	30π	Δ % /S	100π	110π	Δ % /S	140π	200π	Δ % /S
Dynamic tooth load of the cardan wheel [N]		27960	28390	- -	32590	33620	- -	37440	48280	- -
Mean torque need [Nm]	S	35.21	35.72	+0.83,	40.95	42.17	-12,	46.57	58.72	-21,
	C	35.51	35.39	-0.92	36.06	36.25	-14	36.99	39.32	-33
Mean power loss [kW]	S	0.025	0.294	+11,	2.623	3.308	-59,	6.142	16.41	-69,
	C	0.027	0.261	-11	1.082	1.257	-62	1.923	4.209	-74
Mean power need [kW]	S	0.332	3.366	+0.83,	12.87	14.57	-12,	20.48	36.90	-21,
	C	0.335	3.335	-0.92	11.33	12.53	-14	16.27	24.70	-33
Mechanical efficiency	S	0.926	0.913	-0.76	0.796	0.773	+14,	0.700	0.555	+26,
	C	0.919	0.922	+1.0	0.905	0.900	+16	0.882	0.830	+49
Angular acceleration αAA0 [rad/s²]		30π			100π			200π		
Initial angular velocity ωAA00 [rad/s]		3π	30π	Δ % /S	100π	110π	Δ % /S	140π	200π	Δ % /S
Dynamic tooth load of the cardan wheel [N]		28100	28490	- -	32820	33920	- -	38210	48840	- -
Mean torque need [Nm]	S	36.30	36.80	-0,43	44.57	45.79	-14,	53.81	65.97	-23,
	C	36.14	36.12	-1.9	38.52	38.72	-15	41.92	44.27	-33
Mean power loss [kW]	S	0.095	0.321	+5,	2.751	3.444	-59,	6.480	16.88	-69,
	C	0.100	0.279	-13	1.115	1.290	-63	1.998	4.312	-74
Mean power need [kW]	S	1.452	3.761	-0.81,	14.36	16.16	-14,	24.27	41.97	-22,
	C	1.440	3.685	-2	12.36	13.60	-16	18.76	27.94	-33
Mechanical efficiency	S	0.899	0.886	+0.49	0.732	0.713	+16,	0.607	0.495	+28,
	C	0.903	0.904	+1.9	0.848	0.843	+18	0.779	0.738	+49

Variables S = slider-crank C = cardan gear		ZBA = 2.33·ZAA0, ZAA0 = 0.06 m, ZBA = 0.14 m, steel links, equal masses, compression ratio 12 :1, standard atmospheric pressure 1.01325·10^5 Pa, polytropic exponent γ = 1.4, cylinder filling 107 %, piston diameter = 2·ZAA0, maximum combustion pressure 12 MPa, gasoline combustion, displacement 1357 cm³, FOUR-STROKE ENGINE								
Angular acceleration αAA0 [rad/s²]		0			0			0		
Initial angular velocity ωAA00 [rad/s]		3π	30π	Δ % /S	100π	110π	Δ % /S	140π	200π	Δ % /S
Dynamic tooth load of the cardan wheel [N]		119100	119900	- -	126900	128500	- -	134300	149900	- -
Mean output torque [Nm]	S	99.27	98.43	-16,	89.76	87.75	-5,	80.53	60.64	+4,
	C	83.29	85.11	-14,	85.13	84.88	-3	83.76	79.79	+32
Mean power loss [kW]	S	0.147	1.547	+5,	7.881	9.364	-42,	15.10	34.06	-54,
	C	0.154	1.364	-12	4.541	5.081	-46	6.960	22.44	-63
Mean output power [kW]	S	0.936	9.277	-16,	28.20	30.32	-5,	35.42	38.10	+4,
	C	0.785	8.022	-14	26.74	29.33	-3	36.84	50.13	+32
Mechanical efficiency	S	0.864	0.857	-3,	0.782	0.764	+9,	0.701	0.528	+20,
	C	0.836	0.855	-0.28	0.855	0.852	+12	0.841	0.802	+52
Angular acceleration αAA0 [rad/s²]		30π			100π			200π		
Initial angular velocity ωAA00 [rad/s]		3π	30π	Δ % /S	100π	110π	Δ % /S	140π	200π	Δ % /S
Dynamic tooth load of the cardan wheel [N]		119300	120000	- -	127200	128900	- -	135000	150600	- -
Mean output torque [Nm]	S	94.65	93.81	-15,	74.34	72.33	-4,	49.68	29.79	+14,
	C	80.33	81.10	-14	71.57	71.32	-1.4	56.60	52.58	+77
Mean power loss [kW]	S	0.557	1.661	-3,	8.162	9.655	-43,	15.75	34.90	-55,
	C	0.539	1.449	-13	4.646	5.184	-46	7.162	12.68	-64
Mean output power [kW]	S	4.228	9.709	-9,	24.12	25.68	-3,	22.70	19.17	+16,
	C	3.842	8.491	-13	23.42	25.51	-0.63	26.26	34.23	+79
Mechanical efficiency	S	0.858	0.850	-2.0,	0.745	0.725	+12,	0.588	0.355	+33,
	C	0.841	0.849	-0.15	0.832	0.829	+14	0.781	0.727	+105

Variables S = slider-crank C = cardan gear		ZBA = 2.33·ZAA0, ZAA0 = 0.06 m, ZBA = 0.14 m, "titanium" rod in the cardan gear, otherwise steel links, compression ratio 12 :1, standard atmospheric pressure 1.01325·10^5 Pa, polytropic exponent γ = 1.4, cylinder filling 107 %, piston diameter = 2·ZAA0, maximum combustion pressure 12 MPa, gasoline combustion, displacement 1357 cm^3, FOUR-STROKE ENGINE								
Angular acceleration αAA0 [rad/s^2]		0			0			0		
Initial angular velocity ωAA00 [rad/s]		3π	30π	Δ % /S	100π	110π	Δ % /S	140π	200π	Δ % /S
Dynamic tooth load of the cardan wheel [N]		119100	119700	- -	124300	125400	- -	129300	139700	- -
Mean output torque	S	99.27	98.43	-16,	89.76	87.75	-5,	80.53	60.64	+6,
[Nm]	C	83.29	85.14	-14	85.59	85.50	-3	84.96	82.79	+37
Mean power loss	S	0.147	1.547	+5,	7.881	9.364	-44,	15.10	34.06	-57,
[kW]	C	0.154	1.362	-12	4.396	4.867	-48	6.431	10.55	-69
Mean output power	S	0.936	9.277	-16,	28.20	30.32	-5,	35.42	38.10	+6,
[kW]	C	0.785	8.024	-14	26.89	29.55	-3	37.37	52.02	+37
Mechanical efficiency	S	0.864	0.857	-3,	0.782	0.764	+10,	0.701	0.528	+22,
	C	0.836	0.855	-0.25	0.860	0.859	+12	0.853	0.832	+57
Angular acceleration αAA0 [rad/s^2]		30π			100π			200π		
Initial angular velocity ωAA00 [rad/s]		3π	30π	Δ % /S	100π	110π	Δ % /S	140π	200π	Δ % /S
Dynamic tooth load of the cardan wheel [N]		119300	119800	- -	124600	125700	- -	129700	140100	- -
Mean output torque	S	94.65	93.81	-15,	74.34	72.33	-3,	49.68	29.79	+16,
[Nm]	C	80.34	81.13	-14	72.07	71.97	-0.50	57.87	55.67	+87
Mean power loss	S	0.557	1.661	-3,	8.162	9.655	-45,	15.75	34.90	-58,
[kW]	C	0.539	1.447	-13	4.489	4.955	-49	6.593	10.72	-69
Mean output power	S	4.228	9.709	-9,	24.12	25.68	-2,	22.70	19.17	+18,
[kW]	C	3.841	8.489	-13	23.53	25.70	+0.08	26.72	36.02	+88
Mechanical efficiency	S	0.858	0.850	-2,	0.745	0.725	+12,	0.588	0.355	+36,
	C	0.841	0.849	-0.11	0.838	0.837	+15	0.799	0.769	+117

Variables S = slider-crank C = cardan gear		ZBA = 3·ZAA0, ZAA0 = 0.05 m, ZBA = 0.15 m, steel links, equal masses, compression ratio 12 : 1, standard atmospheric pressure 1.01325·10^5 Pa, polytropic exponent γ = 1.4, cylinder filling 107 %, piston diameter = 2·ZAA0, maximum combustion pressure 12 MPa, gasoline combustion, displacement 785 cm³, FOUR-STROKE ENGINE								
Angular acceleration αAA0 [rad/s²]		0			0			0		
Initial angular velocity ωAA00 [rad/s]		3π	30π	Δ % /S	100π	110π	Δ % /S	140π	200π	Δ % /S
Dynamic tooth load of the cardan wheel [N]		86590	87410	- -	94420	96030	- -	101800	117500	- -
Mean output torque	S	55.96	55.29	-15,	48.32	46.70	-0.08,	40.88	24.82	+15,
[Nm]	C	47.69	48.72	-12	48.29	48.00	+3,	46.85	42.96	+73
Mean power loss	S	0.077	0.834	+20,	4.969	6.025	-42,	10.23	24.70	-54,
[kW]	C	0.092	0.827	-0.75	2.897	3.283	-46	4.686	9.136	-63
Mean output power	S	0.527	5.211	-15,	15.18	16.14	-0.08,	17.98	15.60	+15,
[kW]	C	0.449	4.592	-12	15.17	16.59	+3	20.60	26.99	+73
Mechanical efficiency	S	0.873	0.862	-5,	0.753	0.728	+11,	0.638	0.387	+28,
	C	0.829	0.847	-1.7	0.840	0.835	+15	0.815	0.748	+93
Angular acceleration αAA0 [rad/s²]		30π			100π			200π		
Initial angular velocity ωAA00 [rad/s]		3π	30π	Δ % /S	100π	110π	Δ % /S	140π	200π	Δ % /S
Dynamic tooth load of the cardan wheel [N]		86830	87510	- -	94770	96380	- -	102500	118200	- -
Mean output torque	S	53.64	52.96	-13,	40.57	38.95	+4,	25.37	9.305	+35,
[Nm]	C	46.47	46.89	-11	42.04	41.76	+7	34.34	30.42	+227
Mean power loss	S	0.292	0.898	+11,	5.167	6.234	-42,	10.72	25.35	-55,
[kW]	C	0.325	0.880	-2	2.972	3.357	-46	4.841	9.335	-63
Mean output power	S	2.420	5.490	-8,	13.17	13.84	+5,	11.62	6.048	+38,
[kW]	C	2.223	4.912	-11	13.78	14.97	+8	16.00	19.94	+230
Mechanical efficiency	S	0.867	0.856	-4,	0.716	0.688	+14,	0.517	0.193	+47,
	C	0.835	0.843	-1.5	0.820	0.814	+18	0.762	0.677	+251

Variables S = slider-crank C = cardan gear		ZBA = 3·ZAA0, ZAA0 = 0.05 m, ZBA = 0.15 m, "titanium" rod in the cardan gear, otherwise steel links, compression ratio 12 :1, standard atmospheric pressure 1.01325·10^5 Pa, polytropic exponent γ = 1.4, cylinder filling 107 %, piston diameter = 2·ZAA0, maximum combustion pressure 12 MPa, gasoline combustion, displacement 785 cm³, FOUR-STROKE ENGINE								
Angular acceleration αAA0 [rad/s²]		0			0			0		
Initial angular velocity ωAA00 [rad/s]		3π	30π	Δ % /S	100π	110π	Δ % /S	140π	200π	Δ % /S
Dynamic tooth load of the cardan wheel [N]		86590	87180	- -	91850	92930	- -	96780	107200	- -
Mean output torque	S	55.96	55.29	-15,	48.32	46.70	+0.92,	40.88	24.82	+17,
[Nm]	C	47.69	48.74	-12	48.76	48.63	+4	48.00	45.82	+85
Mean power loss	S	0.077	0.834	+20,	4.969	6.025	-45,	10.23	24.70	-59,
[kW]	C	0.092	0.825	-1.0	2.745	3.067	-49	4.177	7.338	-70
Mean output power	S	0.527	5.211	-15,	15.18	16.14	+0.92,	17.98	15.60	+17,
[kW]	C	0.449	4.594	-12	15.32	16.80	+4	21.11	28.79	+85
Mechanical efficiency	S	0.873	0.862	-5,	0.753	0.728	+13,	0.638	0.387	+31,
	C	0.829	0.848	-1.7	0.848	0.846	+16	0.835	0.798	+106
Angular acceleration αAA0 [rad/s²]		30π			100π			200π		
Initial angular velocity ωAA00 [rad/s]		3π	30π	Δ % /S	100π	110π	Δ % /S	140π	200π	Δ % /S
Dynamic tooth load of the cardan wheel [N]		86790	87250	- -	92080	93160	- -	97240	107700	- -
Mean output torque	S	53.64	52.96	-13,	40.57	38.95	+5,	25.37	9.305	+40,
[Nm]	C	46.47	46.91	-11	42.56	42.41	+9	35.56	33.36	+259
Mean power loss	S	0.292	0.898	+11,	5.167	6.234	-46,	10.72	25.35	-60,
[kW]	C	0.325	0.877	-2	2.808	3.128	-50	4.295	7.472	-71
Mean output power	S	2.420	5.490	-8,	13.17	13.84	+6,	11.62	6.048	+42,
[kW]	C	2.222	4.911	-11	13.91	15.16	+10	16.45	21.66	+258
Mechanical efficiency	S	0.867	0.856	-4,	0.716	0.688	+16,	0.517	0.193	+52,
	C	0.835	0.843	-1.5	0.830	0.827	+20	0.789	0.741	+284

Variables S = slider-crank C = cardan gear		ZBA = 4·ZAA0, ZAA0 = 0.04 m, ZBA = 0.16 m, steel links, equal masses, compression ratio 12 : 1, standard atmospheric pressure 1.01325·10^5 Pa, polytropic exponent γ = 1.4, cylinder filling 107 %, piston diameter = 2·ZAA0, maximum combustion pressure 12 MPa, gasoline combustion, displacement 402 cm³, FOUR-STROKE ENGINE								
Angular acceleration αAA0 [rad/s²]		0			0			0		
Initial angular velocity ωAA00 [rad/s]		3π	30π	Δ % /S	100π	110π	Δ % /S	140π	200π	Δ % /S
Dynamic tooth load of the cardan wheel [N]		59140	59970	- -	66650	68200	- -	73700	88680	- -
Mean output torque [Nm]	S	27.85	27.35	-14,	22.15	20.94	+8,	16.58	4.544	+36,
	C	24.03	24.53	-10	23.88	23.61	+13	22.58	19.16	+322
Mean power loss [kW]	S	0.038	0.425	+34,	3.049	3.773	-43,	6.717	17.16	-55,
	C	0.050	0.457	+8	1.730	1.993	-47	2.992	6.421	-63
Mean output power [kW]	S	0.263	2.578	-14,	6.958	7.236	+8,	7.293	2.855	+36,
	C	0.226	2.312	-10	7.501	8.16	+13	9.931	12.04	+322
Mechanical efficiency	S	0.874	0.859	-6,	0.695	0.657	+17,	0.521	0.143	+48,
	C	0.818	0.835	-3	0.813	0.804	+22	0.769	0.654	+357
Angular acceleration αAA0 [rad/s²]		30π			100π			200π		
Initial angular velocity ωAA00 [rad/s]		3π	30π	Δ % /S	100π	110π	Δ % /S	140π	200π	Δ % /S
Dynamic tooth load of the cardan wheel [N]		59420	60070	- -	66990	68530	- -	74370	89340	- -
Mean output torque [Nm]	S	26.77	26.27	-12,	18.53	17.32	+15,	9.347	(-2.702)	+88,
	C	23.62	23.81	-9	21.40	21.14	+22	17.61	14.16	- -
Mean power loss [kW]	S	0.143	0.459	+24,	3.184	3.917	-44,	7.064	17.64	-56,
	C	0.178	0.486	+6	1.780	2.044	-48	3.106	6.580	-63
Mean output power [kW]	S	1.221	2.728	-7,	6.026	6.163	+17,	4.307	(-1.652)	+92,
	C	1.132	2.498	-8	7.043	7.609	+23	8.278	9.414	- -
Mechanical efficiency	S	0.868	0.852	-5,	0.652	0.609	+22,	0.376	(-0.102)	+91,
	C	0.824	0.831	-2	0.794	0.785	+29	0.719	0.581	- -

Variables S = slider-crank C = cardan gear		ZBA = 4·ZAA0, ZAA0 = 0.04 m, ZBA = 0.16 m, "titanium" rod in the cardan gear, otherwise steel links, compression ratio 12 :1, standard atmospheric pressure 1.01325·10⁵ Pa, polytropic exponent γ = 1.4, cylinder filling 107 %, piston diameter = 2·ZAA0, maximum combustion pressure 12 MPa, gasoline combustion, displacement 402 cm³, FOUR-STROKE ENGINE								
Angular acceleration αAA0 [rad/s²]		0			0			0		
Initial angular velocity ωAA00 [rad/s]		3π	30π	Δ % /S	100π	110π	Δ % /S	140π	200π	Δ % /S
Dynamic tooth load of the cardan wheel [N]		59140	59750	- -	64210	65230	- -	68900	78890	- -
Mean output torque [Nm]	S	27.85	27.35	-14,	22.15	20.94	+10,	16.58	4.544	+42,
	C	24.03	24.55	-10	24.31	24.17	+15	23.58	21.63	+376
Mean power loss [kW]	S	0.038	0.425	+34,	3.049	3.773	-48,	6.717	17.16	-62,
	C	0.050	0.455	+7	1.592	1.801	-52	2.552	4.873	-72
Mean output power [kW]	S	0.263	2.578	-14,	6.958	7.236	+10,	7.293	2.855	+42,
	C	0.226	2.314	-10	7.638	8.352	+15	10.37	13.59	+376
Mechanical efficiency	S	0.874	0.859	-6,	0.695	0.657	+19,	0.521	0.143	+54,
	C	0.818	0.836	-3	0.828	0.823	+25	0.803	0.737	+414
Angular acceleration αAA0 [rad/s²]		30π			100π			200π		
Initial angular velocity ωAA00 [rad/s]		3π	30π	Δ % /S	100π	110π	Δ % /S	140π	200π	Δ % /S
Dynamic tooth load of the cardan wheel [N]		59380	59820	- -	64430	65460	- -	69350	79330	- -
Mean output torque [Nm]	S	26.77	26.27	-12,	18.53	17.32	+18,	9.347	(-2.702)	+100,
	C	23.62	23.83	-9	21.86	21.71	+25	18.66	16.69	- -
Mean power loss [kW]	S	0.143	0.459	+24,	3.184	3.917	-49,	7.064	17.64	-63,
	C	0.178	0.484	+5	1.633	1.841	-53	2.634	4.975	-72
Mean output power [kW]	S	1.221	2.728	-7,	6.026	6.163	+19,	4.307	(-1.652)	+101,
	C	1.132	2.497	-8	7.163	7.783	+26	8.675	10.91	- -
Mechanical efficiency	S	0.868	0.852	-5,	0.652	0.609	+24,	0.376	(-0.102)	+103,
	C	0.824	0.832	-2	0.811	0.806	+32	0.762	0.683	- -

Variables S = slider-crank C = cardan gear		ZBA = 2.78·ZAA0, ZAA0 = 0.03780 m, ZBA = 0.105 m, steel links, compression ratio 12 :1, standard atmospheric pressure 1.01325·10⁵ Pa, polytropic exponent γ = 1.4, cylinder filling 107 %, piston diameter = 2·ZAA0, maximum combustion pressure 12 MPa, gasoline combustion, displacement 339 cm³, FOUR-STROKE ENGINE								
Angular acceleration αAA0 [rad/s²]		0			0			0		
Initial angular velocity ωAA00 [rad/s]		3π	30π	Δ % /S	100π	110π	Δ % /S	140π	200π	Δ % /S
Dynamic tooth load of the cardan wheel [N]		53880	54150	- -	54980	55170	- -	55860	57720	- -
Mean output torque [Nm]	S	23.87	23.81	-15,	23.14	22.99	-10,	22.44	20.94	-7,
	C	20.24	20.71	-13	20.89	20.90	-9	20.89	20.76	-0.83
Mean power loss [kW]	S	0.039	0.393	+12,	1.520	1.725	-18,	2.437	4.424	-29,
	C	0.043	0.391	-0.54	1.246	1.368	-21	1.742	2.572	-42
Mean output power [kW]	S	0.225	2.244	-15,	7.269	7.943	-10,	9.868	13.16	-7,
	C	0.191	1.951	-13	6.563	7.221	-9	9.189	13.05	-0.83
Mechanical efficiency	S	0.853	0.851	-5,	0.827	0.822	+1.6,	0.802	0.748	+5,
	C	0.814	0.833	-2	0.840	0.841	+2	0.841	0.835	+12
Angular acceleration αAA0 [rad/s²]		30π			100π			200π		
Initial angular velocity ωAA00 [rad/s]		3π	30π	Δ % /S	100π	110π	Δ % /S	140π	200π	Δ % /S
Dynamic tooth load of the cardan wheel [N]		54080	54160	- -	55020	55220	- -	55940	57810	- -
Mean output torque [Nm]	S	23.25	23.19	-14,	21.07	20.92	-10,	18.30	16.80	-7,
	C	19.94	20.14	-13	18.97	18.98	-9	17.05	16.92	+0.68
Mean power loss [kW]	S	0.145	0.420	+6,	1.560	1.764	-19,	2.514	4.506	-29,
	C	0.153	0.415	-1.1	1.270	1.391	-21	1.779	2.602	-42
Mean output power [kW]	S	1.047	2.402	-9,	6.829	7.419	-10,	8.323	10.74	-6,
	C	0.955	2.107	-12	6.177	6.758	-9	7.806	10.86	+1.2
Mechanical efficiency	S	0.850	0.847	-3,	0.813	0.807	+1.8,	0.766	0.704	+6,
	C	0.821	0.830	-2	0.827	0.828	+3	0.812	0.805	+14

Variables S = slider-crank C = cardan gear		ZBA = 2.78·ZAA0, ZAA0 = 0.03780 m, ZBA = 0.105 m, steel links, compression ratio 14 :1, standard atmospheric pressure 1.01325·10^5 Pa, polytropic exponent γ = 1.4, cylinder filling 107 %, piston diameter = 2·ZAA0, maximum combustion pressure 12 MPa, gasoline combustion, displacement 339 cm³, FOUR-STROKE ENGINE								
Angular acceleration αAA0 [rad/s²]		0			0			0		
Initial angular velocity ωAA00 [rad/s]		3π	30π	Δ % /S	100π	110π	Δ % /S	140π	200π	Δ % /S
Dynamic tooth load of the cardan wheel [N]		52440	52680	- -	53340	53490	- -	54040	55530	- -
Mean output torque	S	23.08	23.01	-16,	22.34	22.19	-10,	21.64	20.14	-7,
[Nm]	C	19.49	19.90	-14	20.06	20.06	-10	20.05	19.89	-1.2
Mean power loss	S	0.036	0.366	+13,	1.429	1.625	-17,	2.309	4.241	-28,
[kW]	C	0.041	0.369	+0.91	1.181	1.298	-20	1.659	2.468	-42
Mean output power	S	0.217	2.169	-16,	7.019	7.668	-10,	9.518	12.66	-7,
[kW]	C	0.184	1.876	-14	6.302	6.933	-10	8.818	12.50	-1.2
Mechanical efficiency	S	0.858	0.856	-5,	0.831	0.825	+1.4,	0.805	0.749	+5,
	C	0.818	0.836	-2	0.842	0.842	+2	0.842	0.835	+12
Angular acceleration αAA0 [rad/s²]		30π			100π			200π		
Initial angular velocity ωAA00 [rad/s]		3π	30π	Δ % /S	100π	110π	Δ % /S	140π	200π	Δ % /S
Dynamic tooth load of the cardan wheel [N]		52620	52690	- -	53370	53530	- -	54100	55590	- -
Mean output torque	S	22.46	22.39	-15,	20.28	20.12	-11,	17.51	16.01	-7,
[Nm]	C	19.16	19.34	-14	18.14	18.14	-10	16.21	16.05	+0.24
Mean power loss	S	0.134	0.391	+7,	1.467	1.662	-18,	2.383	4.321	-29,
[kW]	C	0.144	0.392	+0.40	1.205	1.320	-21	1.694	2.498	-42
Mean output power	S	0.987	2.311	-10,	6.563	7.129	-10,	7.949	10.22	-7,
[kW]	C	0.892	2.014	-13	5.898	6.453	-9	7.407	10.30	+0.74
Mechanical efficiency	S	0.855	0.852	-4,	0.816	0.810	+1.5,	0.768	0.702	+6,
	C	0.824	0.832	-2	0.829	0.829	+2	0.812	0.804	+14

Variables S = slider-crank C = cardan gear		ZBA = 3·ZAA0, ZAA0 = 0.02654 m, ZBA = 0.08 m, steel links, compression ratio 12 :1, standard atmospheric pressure 1.01325·10⁵ Pa, polytropic exponent γ = 1.4, cylinder filling 107 %, piston diameter = 3.4·ZAA0, maximum combustion pressure 12 MPa, gasoline combustion, displacement 339 cm³, FOUR-STROKE ENGINE								
Angular acceleration αAA0 [rad/s²]		0			0			0		
Initial angular velocity ωAA00 [rad/s]		3π	30π	Δ % /S	100π	110π	Δ % /S	140π	200π	Δ % /S
Dynamic tooth load of the cardan wheel [N]		62400	63720	- -	63970	64030	- -	64240	64810	- -
Mean output torque [Nm]	S	23.87	23.86	-17,	23.70	23.67	-14,	23.54	23.20	-13,
	C	19.77	20.23	-15	20.45	20.47	-14	20.50	20.55	-11
Mean power loss [kW]	S	0.036	0.363	+32,	1.258	1.396	+10,	1.832	2.831	+4,
	C	0.048	0.424	+20	1.379	1.511	+8	1.907	2.699	-5
Mean output power [kW]	S	0.225	2.249	-17,	7.446	8.178	-14,	10.35	14.58	-13,
	C	0.186	1.907	-15	6.425	7.073	-14	9.018	12.91	-11
Mechanical efficiency	S	0.862	0.861	-8,	0.855	0.854	-4,	0.850	0.837	-3,
	C	0.796	0.815	-5	0.823	0.824	-4	0.825	0.827	-1.2
Angular acceleration αAA0 [rad/s²]		30π			100π			200π		
Initial angular velocity ωAA00 [rad/s]		3π	30π	Δ % /S	100π	110π	Δ % /S	140π	200π	Δ % /S
Dynamic tooth load of the cardan wheel [N]		63690	63720	- -	63990	64050	- -	64270	64840	- -
Mean output torque [Nm]	S	23.73	23.71	-16,	23.21	23.17	-14,	22.55	22.21	-13,
	C	19.90	20.11	-15	19.99	20.01	-14	19.58	19.62	-12
Mean power loss [kW]	S	0.135	0.387	+26,	1.286	1.422	+9,	1.876	2.868	+4,
	C	0.170	0.461	+19	1.405	1.535	+8	1.945	2.725	-5
Mean output power [kW]	S	1.064	2.455	-11,	7.514	8.211	-14,	10.23	14.17	-13,
	C	0.952	2.103	-14	6.496	7.111	-13	8.919	12.55	-11
Mechanical efficiency	S	0.861	0.860	-6,	0.853	0.851	-4,	0.844	0.831	-3,
	C	0.806	0.814	-5	0.820	0.821	-4	0.819	0.821	-1.3

Variables S = slider-crank C = cardan gear		ZBA = 4·ZAA0, ZAA0 = 0.06 m, ZBA = 0.24 m, steel links, compression ratio 12 :1, standard atmospheric pressure 1.01325·10^{5} Pa, polytropic exponent γ = 1.4, cylinder filling 107 %, piston diameter = ZAA0, maximum combustion pressure 12 MPa, gasoline combustion, displacement 339 cm³, FOUR-STROKE ENGINE								
Angular acceleration αAA0 [rad/s²]		0			0			0		
Initial angular velocity ωAA00 [rad/s]		3π	30π	Δ % /S	100π	110π	Δ % /S	140π	200π	Δ % /S
Dynamic tooth load of the cardan wheel [N]		51610	53170	- -	68910	72540	- -	86300	125200	- -
Mean output torque	S	23.02	21.30	-12,	3.512	(-0.639)	+369,	(-15.58)	(-56.84)	- -
[Nm]	C	20.26	20.51	-4	16.46	15.36	- -	11.09	(-2.306)	
Mean power loss	S	0.036	0.526	+17,	7.341	9.509	-64,	18.67	52.60	-68,
[kW]	C	0.043	0.404	-23	2.617	3.260	-66	6.026	17.03	-68
Mean output power	S	0.217	2.007	-12,	1.103	(-0.221)	+369,	(-6.850)	(-35.71)	- -
[kW]	C	0.191	1.933	-4	5.171	5.307	- -	4.878	(-1.449)	
Mechanical efficiency	S	0.856	0.792	-5,	0.131	(-0.023)	+408,	(-0.579)	(-2.11)	- -
	C	0.817	0.827	+4	0.665	0.621	- -	0.450	(-0.085)	
Angular acceleration αAA0 [rad/s²]		30π			100π			200π		
Initial angular velocity ωAA00 [rad/s]		3π	30π	Δ % /S	100π	110π	Δ % /S	140π	200π	Δ % /S
Dynamic tooth load of the cardan wheel [N]		51860	53410	- -	69700	73330	- -	88110	127100	- -
Mean output torque	S	17.72	16.00	-7,	(-14.15)	(-18.31)	- -	(-50.93)	(-92.22)	- -
[Nm]	C	16.45	16.42	+3	2.73	1.619		(-16.44)	(-29.92)	
Mean power loss	S	0.144	0.584	+4,	7.740	9.945	-65,	19.77	54.16	-68,
[kW]	C	0.150	0.433	-26	2.736	3.389	-66	6.365	17.56	-68
Mean output power	S	0.864	1.682	-2,	(-4.481)	(-6.386)	- -	(-22.82)	(-58.55)	- -
[kW]	C	0.845	1.760	+5	1.252	0.966		(-6.441)	(-17.75)	
Mechanical efficiency	S	0.813	0.735	-2,	(-1.35)	(-1.76)	- -	(-5.92)	(-12.4)	- -
	C	0.794	0.793	+8	0.256	0.159		(-6.36)	(-13.3)	

Variables S = slider-crank C = cardan gear		ZBA = 5·ZAA0, ZAA0 = 0.04579 m, ZBA = 0.229 m, steel links, compression ratio 12 :1, standard atmospheric pressure 1.01325·10^5 Pa, polytropic exponent γ = 1.4, cylinder filling 107 %, piston diameter = 1.5·ZAA0, maximum combustion pressure 12 MPa, gasoline combustion, displacement 339 cm³, FOUR-STROKE ENGINE								
Angular acceleration αAA0 [rad/s²]		0			0			0		
Initial angular velocity ωAA00 [rad/s]		3π	30π	Δ % /S	100π	110π	Δ % /S	140π	200π	Δ % /S
Dynamic tooth load of the cardan wheel [N]		51560	52650	- -	63080	65480	- -	74080	98630	- -
Mean output torque	S	23.08	22.21	-12,	13.25	11.16	+42,	3.629	(-17.23)	+345,
[Nm]	C	20.25	20.62	-7	18.81	18.26	+64	16.15	9.257	- -
Mean power loss	S	0.031	0.395	+36,	4.133	5.269	-55,	10.02	27.41	-62,
[kW]	C	0.043	0.391	-1.1	1.871	2.246	-57	3.786	9.741	-64
Mean output power	S	0.217	2.093	-12,	4.162	3.855	+42,	1.596	(-10.82)	+345,
[kW]	C	0.191	1.943	-7	5.908	6.311	+64	7.104	5.817	- -
Mechanical efficiency	S	0.874	0.841	-6,	0.502	0.423	+51,	0.138	(-0.651)	+374,
	C	0.818	0.833	-1.0	0.760	0.738	+75	0.654	0.378	- -
Angular acceleration αAA0 [rad/s²]		30π			100π			200π		
Initial angular velocity ωAA00 [rad/s]		3π	30π	Δ % /S	100π	110π	Δ % /S	140π	200π	Δ % /S
Dynamic tooth load of the cardan wheel [N]		51780	52810	- -	63600	66000	- -	75120	99830	- -
Mean output torque	S	21.17	20.30	-9,	6.880	4.787	+110,	(-9.119)	(-29.99)	- -
[Nm]	C	19.23	19.33	-5	14.44	13.89	+190	7.377	0.422	
Mean power loss	S	0.121	0.433	+24,	4.343	5.496	-55,	10.58	28.21	-62,
[kW]	C	0.150	0.416	-4	1.941	2.320	-58	3.971	10.03	-64
Mean output power	S	0.985	2.115	-5,	2.272	1.740	+114,	(-4.017)	(-19.01)	- -
[kW]	C	0.934	2.039	-4	4.860	5.119	+194	3.846	0.936	
Mechanical efficiency	S	0.860	0.825	-5,	0.340	0.239	+107,	(-0.606)	(-2.03)	- -
	C	0.819	0.824	-0.20	0.706	0.679	+185	0.461	0.039	

Appendix 11.7.1

Comparison of the summed lossless Newtonian dynamics:
Special applications
Pumps and four-stroke engines

Table part 1 Variables	ZBA = 4·ZAA0, ZAA0 = 0.06 m, ZBA = 0.24 m, angular acceleration 100 rad/s², initial angular velocity 100 rad/s, steel links, equal medium masses, compression ratio 12 :1, standard atmospheric pressure $1.01325 \cdot 10^5$ Pa, polytropic exponent γ = 1.4, cylinder filling 107 %, piston diameter = ZAA0, displacement 339 cm³, cycle = 4π rad, AIR PUMP and FOUR-STROKE ENGINE		
	Slider-crank machine	Cardan gear machine	Δ and Δ % /S
Maximum piston position difference ΔZBA0 [mm]	- -	- -	+7.618 mm +3 %
Maximum piston velocity vBA0 [m/s]	20.07	19.49	-0.572 m/s -3 %
Maximum piston acceleration aBA0 [m/s²]	7994	6396	-1599 m/s² -20 %
Connecting rod maximum velocity vPA0 [m/s]	19.71	19.49	-0.217 m/s -1 %
Connecting rod maximum acceleration aPA0 [m/s²]	7195	6396	-799 m/s² -11 %
Inertial work consumption / cycle [J]	211	170	-41.53 J -20 %
Mean inertial torque [Nm]	16.83	13.52	-3.305 Nm -20 %
Mean inertial power consumption [kW]	5.434	4.044	-1.390 kW -26 %

Table part 2 Variables	ZBA = 4·ZAA0, ZAA0 = 0.06 m, ZBA = 0.24 m, angular acceleration 100 rad/s², initial angular velocity 100 rad/s, steel links, equal medium masses, compression ratio 12 :1, standard atmospheric pressure 1.01325·10^5 Pa, polytropic exponent γ = 1.4, cylinder filling 107 %, piston diameter = ZAA0, displacement 339 cm³, cycle = 4π rad, AIR PUMP		
	Slider-crank machine	Cardan gear machine	Δ and Δ % /S
Maximum isothermal compression pressure [MPa]	1.216	1.216	0 0 %
Maximum polytropic compression pressure [MPa]	3.612	3.612	0 0 %
Compression work consumption / cycle [J]	350	350	0 0 %
Mean compression torque [Nm]	27.86	27.87	+0.013 Nm +0.05 %
Mean compression power consumption [kW]	8.873	8.876	+0.003 kW +0.03 %
Total work consumption / cycle [J]	562	520	-41.37 J -7 %
Mean total torque [Nm]	44.68	41.39	-3.292 Nm -7 %
Mean total power consumption [kW]	14.31	12.92	-1.388 kW -10 %
Maximum piston pin total joint force [N] DISPARATE!	8319	20630	+12310 N +148 %
Maximum crank pin and main pin total joint force [N]	23440	41260	+17810 N +76 %
Maximum total torque [Nm]	317	646	+328 Nm +103 %

Table part 3 Variables	ZBA = 4·ZAA0, ZAA0 = 0.06 m, ZBA = 0.24 m, angular acceleration 100 rad/s², initial angular velocity 100 rad/s, steel links, equal medium masses, compression ratio 12 :1, standard atmospheric pressure $1.01325 \cdot 10^5$ Pa, polytropic exponent γ = 1.4, cylinder filling 107 %, piston diameter = ZAA0, gasoline combustion, displacement 339 cm³, cycle = 4π rad, FOUR-STROKE ENGINE		
	Slider-crank machine	Cardan gear machine	Δ and Δ % /S
Maximum combustion pressure [MPa]	12	12	0 0 %
Combustion work / cycle [J]	342	315	-26.56 J -8 %
Mean combustion torque [Nm]	27.22	25.10	-2.114 Nm -8 %
Mean combustion power [kW]	8.693	8.032	-0.662 kW -8 %
Total work output / cycle [J]	131	146	+14.97 J +11 %
Mean total torque output [Nm]	10.39	11.58	+1.191 Nm +11 %
Mean total power output [kW]	3.260	3.988	+0.728 kW +22 %
Maximum piston pin total joint force [N] DISPARATE!	25930	21500	-4421 N -17 %
Maximum crank pin and main pin total joint force [N]	24370	43010	+18640 N +76 %
Maximum total torque [Nm]	747	658	-89.04 Nm -12 %

Table part 1 Variables	ZBA = 3·ZAA0, ZAA0 = 0.02654 m, ZBA = 0.08 m, angular acceleration 3 rad/s², initial angular velocity 30 rad/s, steel links, equal medium masses, compression ratio 12 :1, standard atmospheric pressure $1.01325 \cdot 10^5$ Pa, polytropic exponent γ = 1.4, cylinder filling 107 %, piston diameter = 3.4·ZAA0, displacement 339 cm³, cycle = 4π rad, AIR PUMP and FOUR-STROKE ENGINE		
	Slider-crank machine	Cardan gear machine	Δ and Δ % /S
Maximum piston position difference ΔZBA0 [mm]	- -	- -	+4.527 mm +6 %
Maximum piston velocity vBA0 [m/s]	2.668	2.529	-0.138 m/s -5 %
Maximum piston acceleration aBA0 [m/s²]	322	242	-80.27 m/s² -25 %
Connecting rod maximum velocity vPA0 [m/s]	2.573	2.529	-0.043 m/s -2 %
Connecting rod maximum acceleration aPA0 [m/s²]	282	242	-40.13 m/s² -14 %
Inertial work consumption / cycle [J]	0.184	0.174	-0.010 J -5 %
Mean inertial torque [Nm]	0.015	0.014	-0.001 Nm -5 %
Mean inertial power consumption [kW]	0.0014	0.0013	-0.0001 kW -7 %

Table part 2 Variables	ZBA = 3·ZAA0, ZAA0 = 0.02654 m, ZBA = 0.08 m, angular acceleration 3 rad/s², initial angular velocity 30 rad/s, steel links, equal medium masses, compression ratio 12 :1, standard atmospheric pressure $1.01325 \cdot 10^5$ Pa, polytropic exponent γ = 1.4, cylinder filling 107 %, piston diameter = 3.4·ZAA0, displacement 339 cm³, cycle = 4π rad, AIR PUMP		
	Slider-crank machine	Cardan gear machine	Δ and Δ % /S
Maximum isothermal compression pressure [MPa]	1.216	1.216	0 0 %
Maximum polytropic compression pressure [MPa]	3.612	3.612	0 0 %
Compression work consumption / cycle [J]	350	350	0 0 %
Mean compression torque [Nm]	27.85	27.87	+0.017Nm +0.06 %
Mean compression power consumption [kW]	2.616	2.617	+0.001 kW +0.05 %
Total work consumption / cycle [J]	350	350	0 0 %
Mean total torque [Nm]	27.87	27.88	+0.01 Nm +0.1 %
Mean total power consumption [kW]	2.617	2.618	+0.001 kW +0.05 %
Maximum piston pin total joint force [N] DISPARATE!	23080	23060	-16.23 N -0.07 %
Maximum crank pin and main pin total joint force [N]	23050	46120	+23070 N +100 %
Maximum total torque [Nm]	166	144	-21.92 Nm -13 %

Table part 3 Variables	ZBA = 3·ZAA0, ZAA0 = 0.02654 m, ZBA = 0.08 m, angular acceleration 3 rad/s², initial angular velocity 30 rad/s, steel links, equal medium masses, compression ratio 12 :1, standard atmospheric pressure $1.01325 \cdot 10^5$ Pa, polytropic exponent γ = 1.4, cylinder filling 107 %, piston diameter = 3.4·ZAA0, gasoline combustion, displacement 339 cm³, cycle = 4π rad, FOUR-STROKE ENGINE		
	Slider-crank machine	Cardan gear machine	Δ and Δ % /S
Maximum combustion pressure [MPa]	12	12	0 0 %
Combustion work / cycle [J]	352	316	-36.27 J -10 %
Mean combustion torque [Nm]	28.04	25.15	-2.886 Nm -10 %
Mean combustion power [kW]	2.635	2.366	-0.269 kW -10 %
Total work output / cycle [J]	352	316	-36.26 J -10 %
Mean total torque output [Nm]	28.03	25.14	-2.885 Nm -10 %
Mean total power output [kW]	2.634	2.364	-0.269 kW -10 %
Maximum piston pin total joint force [N] DISPARATE!	76700	77300	+593 N +0.8 %
Maximum crank pin and main pin total joint force [N]	76920	154600	+77670 N +101 %
Maximum total torque [Nm]	819	673	-145 Nm -18 %

Table part 1 Variables	ZBA = 3·ZAA0, ZAA0 = 0.02654 m, ZBA = 0.08 m, angular acceleration 100 rad/s², initial angular velocity 100 rad/s, steel links, equal medium masses, compression ratio 12 :1, standard atmospheric pressure $1.01325 \cdot 10^5$ Pa, polytropic exponent γ = 1.4, cylinder filling 107 %, piston diameter = 3.4·ZAA0, displacement 339 cm³, cycle = 4π rad, AIR PUMP and FOUR-STROKE ENGINE		
	Slider-crank machine	Cardan gear machine	Δ and Δ % /S
Maximum piston position difference ΔZBA0 [mm]	- -	- -	+4.527 mm +6 %
Maximum piston velocity vBA0 [m/s]	9.098	8.621	-0.477 m/s -5 %
Maximum piston acceleration aBA0 [m/s²]	3767	2828	-938 m/s² -25 %
Connecting rod maximum velocity vPA0 [m/s]	8.772	8.621	-0.151 m/s -2 %
Connecting rod maximum acceleration aPA0 [m/s²]	3298	2828	-469 m/s² -14 %
Inertial work consumption / cycle [J]	6.133	5.806	-0.327 J -5 %
Mean inertial torque [Nm]	0.488	0.462	-0.026 Nm -5 %
Mean inertial power consumption [kW]	0.157	0.146	-0.011 kW -7 %

Table part 2 Variables	ZBA = 3·ZAA0, ZAA0 = 0.02654 m, ZBA = 0.08 m, angular acceleration 100 rad/s², initial angular velocity 100 rad/s, steel links, equal medium masses, compression ratio 12 :1, standard atmospheric pressure 1.01325·10^5 Pa, polytropic exponent γ = 1.4, cylinder filling 107 %, piston diameter = 3.4·ZAA0, displacement 339 cm³, cycle = 4π rad, AIR PUMP		
	Slider-crank machine	Cardan gear machine	Δ and Δ % /S
Maximum isothermal compression pressure [MPa]	1.216	1.216	0 0 %
Maximum polytropic compression pressure [MPa]	3.612	3.612	0 0 %
Compression work consumption / cycle [J]	350	350	0 0 %
Mean compression torque [Nm]	27.85	27.87	+0.017 Nm +0.06 %
Mean compression power consumption [kW]	8.872	8.875	+0.003 kW +0.04 %
Total work consumption / cycle [J]	356	356	0 0 %
Mean total torque [Nm]	28.34	28.33	-0.009 Nm -0.03 %
Mean total power consumption [kW]	9.029	9.021	-0.008 kW -0.09 %
Maximum piston pin total joint force [N] DISPARATE!	22940	22750	-190 N -0.8 %
Maximum crank pin and main pin total joint force [N]	22670	45500	22820 N +101 %
Maximum total torque [Nm]	166	141	-24 Nm -15 %

Table part 3 Variables	ZBA = 3·ZAA0, ZAA0 = 0.02654 m, ZBA = 0.08 m, angular acceleration 100 rad/s², initial angular velocity 100 rad/s, steel links, equal medium masses, compression ratio 12 :1, standard atmospheric pressure $1.01325 \cdot 10^5$ Pa, polytropic exponent γ = 1.4, cylinder filling 107 %, piston diameter = 3.4·ZAA0, gasoline combustion, displacement 339 cm³, cycle = 4π rad, FOUR-STROKE ENGINE		
	Slider-crank machine	Cardan gear machine	Δ and Δ % /S
Maximum combustion pressure [MPa]	12	12	0 0 %
Combustion work / cycle [J]	352	316	-36.27 J -10 %
Mean combustion torque [Nm]	28.04	25.15	-2.886 Nm -10 %
Mean combustion power [kW]	8.951	8.047	-0.904 kW -10 %
Total work output / cycle [J]	346	310	-35.94 J -10 %
Mean total torque output [Nm]	27.55	24.69	-2.860 Nm -10 %
Mean total power output [kW]	8.795	7.901	-0.893 kW -10 %
Maximum piston pin total joint force [N] DISPARATE!	76580	77010	+428 N +0.6 %
Maximum crank pin and main pin total joint force [N]	76580	154000	+77430 N +101 %
Maximum total torque [Nm]	818	669	-148 Nm -18 %

Table part 1 Variables	ZBA = 2.78·ZAA0, ZAA0 = 0.03780 m, ZBA = 0.105 m, angular acceleration 100 rad/s², initial angular velocity 100 rad/s, steel links, equal medium masses, compression ratio 12 : 1, standard atmospheric pressure $1.01325 \cdot 10^5$ Pa, polytropic exponent $\gamma = 1.4$, cylinder filling 107 %, piston diameter = 2·ZAA0, displacement 339 cm³, cycle = 4π rad, AIR PUMP and FOUR-STROKE ENGINE		
	Slider-crank machine	Cardan gear machine	Δ and Δ % /S
Maximum piston position difference ΔZBA0 [mm]	- -	- -	+7.036 mm +7 %
Maximum piston velocity vBA0 [m/s]	13.08	12.28	-0.795 m/s -6 %
Maximum piston acceleration aBA0 [m/s²]	5479	4029	-1450 m/s² -26 %
Connecting rod maximum velocity vPA0 [m/s]	12.54	12.28	-0.264 m/s -2 %
Connecting rod maximum acceleration aPA0 [m/s²]	4754	4029	-725 m/s² -15 %
Inertial work consumption / cycle [J]	25.58	24.11	-1.470 J -6 %
Mean inertial torque [Nm]	2.036	1.919	-0.117 Nm -6 %
Mean inertial power consumption [kW]	0.654	0.605	-0.049 kW -7 %

Table part 2 Variables	ZBA = 2.78·ZAA0, ZAA0 = 0.03780 m, ZBA = 0.105 m, angular acceleration 100 rad/s², initial angular velocity 100 rad/s, steel links, equal medium masses, compression ratio 12 : 1, standard atmospheric pressure $1.01325 \cdot 10^5$ Pa, polytropic exponent $\gamma = 1.4$, cylinder filling 107 %, piston diameter = 2·ZAA0, displacement 339 cm³, cycle = 4π rad, AIR PUMP		
	Slider-crank machine	Cardan gear machine	Δ and Δ % /S
Maximum isothermal compression pressure [MPa]	1.216	1.216	0 0 %
Maximum polytropic compression pressure [MPa]	3.612	3.612	0 0 %
Compression work consumption / cycle [J]	350	350	0 0 %
Mean compression torque [Nm]	27.85	27.87	+0.019 Nm +0.07 %
Mean compression power consumption [kW]	8.872	8.876	+0.004 kW +0.04 %
Total work consumption / cycle [J]	376	374	-1.233 J -0.3 %
Mean total torque [Nm]	29.89	29.79	-0.098 Nm -0.3 %
Mean total power consumption [kW]	9.526	9.481	-0.045 kW -0.5 %
Maximum piston pin total joint force [N] DISPARATE!	15710	15110	-600 N -4 %
Maximum crank pin and main pin total joint force [N]	14850	30220	+15380 N +104 %
Maximum total torque [Nm]	166	132	-34.82 Nm -21 %

Table part 3 Variables	ZBA = 2.78·ZAA0, ZAA0 = 0.03780 m, ZBA = 0.105 m, angular acceleration 100 rad/s², initial angular velocity 100 rad/s, steel links, equal medium masses, compression ratio 12 : 1, standard atmospheric pressure $1.01325 \cdot 10^5$ Pa, polytropic exponent γ = 1.4, cylinder filling 107 %, piston diameter = 2·ZAA0, gasoline combustion, displacement 339 cm³, cycle = 4π rad, FOUR-STROKE ENGINE		
	Slider-crank machine	Cardan gear machine	Δ and Δ % /S
Maximum combustion pressure [MPa]	12	12	0 0 %
Combustion work / cycle [J]	356	316	-39.76 J -11 %
Mean combustion torque [Nm]	28.33	25.17	-3.164 Nm -11 %
Mean combustion power [kW]	9.044	8.053	-0.992 kW -11 %
Total work output / cycle [J]	330	292	-38.29 J -12 %
Mean total torque output [Nm]	26.30	23.25	-3.047 Nm -12 %
Mean total power output [kW]	8.390	7.447	-0.943 kW -11 %
Maximum piston pin total joint force [N] DISPARATE!	53400	53290	-109 N -0.2 %
Maximum crank pin and main pin total joint force [N]	52830	106600	+53760 N +102 %
Maximum total torque [Nm]	827	654	-173 Nm -21 %

Table part 1 Variables	ZBA = 2.78·ZAA0, ZAA0 = 0.03780 m, ZBA = 0.105 m, angular acceleration 100 rad/s², initial angular velocity 100 rad/s, steel links, equal medium masses, compression ratio 14 : 1, standard atmospheric pressure 1.01325·10^5 Pa, polytropic exponent γ = 1.4, cylinder filling 107 %, piston diameter = 2·ZAA0, displacement 339 cm³, cycle = 4π rad, AIR PUMP and FOUR-STROKE ENGINE		
	Slider-crank machine	Cardan gear machine	Δ and Δ % /S
Maximum piston position difference ΔZBA0 [mm]	- -	- -	+7.036 mm +7 %
Maximum piston velocity vBA0 [m/s]	13.08	12.28	-0.795 m/s -6 %
Maximum piston acceleration aBA0 [m/s²]	5479	4029	-1450 m/s² -26 %
Connecting rod maximum velocity vPA0 [m/s]	12.54	12.28	-0.264 m/s -2 %
Connecting rod maximum acceleration aPA0 [m/s²]	4754	4029	-725 m/s² -15 %
Inertial work consumption / cycle [J]	25.58	24.11	-1.470 J -6 %
Mean inertial torque [Nm]	2.036	1.919	-0.117 Nm -6 %
Mean inertial power consumption [kW]	0.654	0.605	-0.049 kW -7 %

Table part 2 Variables	ZBA = 2.78·ZAA0, ZAA0 = 0.03780 m, ZBA = 0.105 m, angular acceleration 100 rad/s², initial angular velocity 100 rad/s, steel links, equal medium masses, compression ratio 14 : 1, standard atmospheric pressure 1.01325·10^5 Pa, polytropic exponent γ = 1.4, cylinder filling 107 %, piston diameter = 2·ZAA0, displacement 339 cm³, cycle = 4π rad, AIR PUMP		
	Slider-crank machine	Cardan gear machine	Δ and Δ % /S
Maximum isothermal compression pressure [MPa]	1.419	1.419	0 0 %
Maximum polytropic compression pressure [MPa]	4.482	4.482	0 0 %
Compression work consumption / cycle [J]	380 (380.232)	381 (380.526)	+0.294 J +0.08 %
Mean compression torque [Nm]	30.26	30.28	+0.023 Nm +0.08 %
Mean compression power consumption [kW]	9.640	9.645	+0.005 kW +0.05 %
Total work consumption / cycle [J]	406	405	-1.176 J -0.3 %
Mean total torque [Nm]	32.29	32.20	-0.094 Nm -0.3 %
Mean total power consumption [kW]	10.29	10.25	-0.044 kW -0.4 %
Maximum piston pin total joint force [N] DISPARATE!	19620	19020	-600 N -3 %
Maximum crank pin and main pin total joint force [N]	18750	38030	+19280 N +103 %
Maximum total torque [Nm]	192	153	-38.38 Nm -20 %

Table part 3 Variables	ZBA = 2.78·ZAA0, ZAA0 = 0.03780 m, ZBA = 0.105 m, angular acceleration 100 rad/s², initial angular velocity 100 rad/s, steel links, equal medium masses, compression ratio 14 : 1, standard atmospheric pressure $1.01325 \cdot 10^5$ Pa, polytropic exponent γ = 1.4, cylinder filling 107 %, piston diameter = 2·ZAA0, gasoline combustion, displacement 339 cm³, cycle = 4π rad, FOUR-STROKE ENGINE		
	Slider-crank machine	Cardan gear machine	Δ and Δ % /S
Maximum combustion pressure [MPa]	12	12	0 0 %
Combustion work / cycle [J]	342	303	-39.12 J -11 %
Mean combustion torque [Nm]	27.23	24.12	-3.113 Nm -11 %
Mean combustion power [kW]	8.684	7.708	-0.977 kW -11 %
Total work output / cycle [J]	317	279	-37.65 J -12 %
Mean total torque output [Nm]	25.20	22.20	-2.996 Nm -12 %
Mean total power output [kW]	8.031	7.102	-0.928 kW -12 %
Maximum piston pin total joint force [N] DISPARATE!	53400	53380	-25.84 N -0.05 %
Maximum crank pin and main pin total joint force [N]	52830	106800	+53930 N +102 %
Maximum total torque [Nm]	796	630	-166 Nm -21 %

Table part 1 Variables	ZBA = 5·ZAA0, ZAA0 = 0.04579 m, ZBA = 0.229 m, angular acceleration 200 rad/s², initial angular velocity 100 rad/s, steel links, equal medium masses, compression ratio 12 : 1, standard atmospheric pressure $1.01325 \cdot 10^5$ Pa, polytropic exponent γ = 1.4, cylinder filling 107 %, piston diameter = 1.5·ZAA0, displacement 339 cm³, cycle = 4π rad, AIR PUMP and FOUR-STROKE ENGINE		
	Slider-crank machine	Cardan gear machine	Δ and Δ % /S
Maximum piston position difference ΔZBA0 [mm]	- -	- -	+4.623 mm +2 %
Maximum piston velocity vBA0 [m/s]	15.65	15.35	-0.299 m/s -2 %
Maximum piston acceleration aBA0 [m/s²]	6290	5242	-1048 m/s² -17 %
Connecting rod maximum velocity vPA0 [m/s]	15.47	15.35	-0.12 m/s -0.8 %
Connecting rod maximum acceleration aPA0 [m/s²]	5766	5242	-524 m/s² -9 %
Inertial work consumption / cycle [J]	149	107	-42.02 J -28 %
Mean inertial torque [Nm]	11.88	8.536	-3.344 Nm -28 %
Mean inertial power consumption [kW]	3.929	2.488	-1.440 kW -37 %

Table part 2 Variables	ZBA = 5·ZAA0, ZAA0 = 0.04579 m, ZBA = 0.229 m, angular acceleration 200 rad/s², initial angular velocity 100 rad/s, steel links, equal medium masses, compression ratio 12 : 1, standard atmospheric pressure $1.01325 \cdot 10^5$ Pa, polytropic exponent $\gamma = 1.4$, cylinder filling 107 %, piston diameter = 1.5·ZAA0, displacement 339 cm³, cycle = 4π rad, AIR PUMP		
	Slider-crank machine	Cardan gear machine	Δ and Δ % /S
Maximum isothermal compression pressure [MPa]	1.216	1.216	0 0 %
Maximum polytropic compression pressure [MPa]	3.612	3.612	0 0 %
Compression work consumption / cycle [J]	350	350	0 0 %
Mean compression torque [Nm]	27.86	27.87	+0.010 Nm +0.04 %
Mean compression power consumption [kW]	9.098	9.099	+0.004 kW +0.005 %
Total work consumption / cycle [J]	499	457	-41.89 J -8 %
Mean total torque [Nm]	39.74	36.40	-3.333 Nm -8 %
Mean total power consumption [kW]	13.03	11.59	-1.440 kW -11 %
Maximum piston pin total joint force [N] DISPARATE!	7513	14660	+7144 N +95 %
Maximum crank pin and main pin total joint force [N]	15870	29310	+13450 N +85 %
Maximum total torque [Nm]	202	356	+154 Nm +76 %

Table part 3 Variables	ZBA = 5·ZAA0, ZAA0 = 0.04579 m, ZBA = 0.229 m, angular acceleration 200 rad/s², initial angular velocity 100 rad/s, steel links, equal medium masses, compression ratio 12 : 1, standard atmospheric pressure $1.01325 \cdot 10^5$ Pa, polytropic exponent γ = 1.4, cylinder filling 107 %, piston diameter = 1.5·ZAA0, displacement 339 cm³, cycle = 4π rad, FOUR-STROKE ENGINE		
	Slider-crank machine	Cardan gear machine	Δ and Δ % /S
Maximum combustion pressure [MPa]	12	12	0 0 %
Combustion work / cycle [J]	336	315	-20.88 J -6 %
Mean combustion torque [Nm]	26.74	25.08	-1.662 Nm - 6 %
Mean combustion power [kW]	8.784	8.259	-0.052 kW -6 %
Total work output / cycle [J]	187	208	+21.14 J +11 %
Mean total torque output [Nm]	14.86	16.54	+1.682 Nm +11 %
Mean total power output [kW]	4.855	5.770	+0.916 kW +19 %
Maximum piston pin total joint force [N] DISPARATE!	39150	31200	-7943 N -20 %
Maximum crank pin and main pin total joint force [N]	30150	62410	+32260 N +107 %
Maximum total torque [Nm]	754	427	-327 Nm -43 %

ACTA UNIVERSITATIS LAPPEENRANTAENSIS

256. RAUMA, KIMMO. FPGA-based control design for power electronic applications. 2006. Diss.

257. HIRVONEN, MARKUS. On the analysis and control of a linear synchronous servomotor with a flexible load. 2006. Diss.

258. LIU, JUNHONG. On the differential evolution algorithm and its application to training radial basis function networks. 2006. Diss.

259. LAITINEN, RISTO. Development of LC-MS and extraction methods for the analyses of AKD, ASA, and rosin sizes in paper products. 2006. Diss.

260. KUISMA, PETRI. Seinärakenteen infrapunakontrastin pienentäminen käyttäen ilmajäähdytystä ja säteilysuojausta. 2007. Diss.

261. ELLONEN, HANNA-KAISA. Exploring the strategic impact of technological change – studies on the role of Internet in magazine publishing. 2007. Diss.

262. SOININEN, AURA. Patents in the information and communications technology sector – development trends, problem areas and pressures for change. 2007. Diss.

263. MATTILA, MERITA. Value processing in organizations – individual perceptions in three case companies. 2007. Diss.

264. VARTIAINEN, JARKKO. Measuring irregularities and surface defects from printed patterns. 2007. Diss.

265. VIRKKI-HATAKKA. TERHI. Novel tools for changing chemical engineering practice. 2007. Diss.

266. SEKKI, ANTTI. Successful new venturing process implemented by the founding entrepreneur: A case of Finnish sawmill industry. 2007. Diss.

267. TURKAMA, PETRA. Maximizing benefits in information technology outsourcing. 2007. Diss.

268. BUTYLINA, SVETLANA. Effect of physico-chemical conditions and operating parameters on flux and retention of different components in ultrafiltration and nanofiltration fractionation of sweet whey. 2007. Diss.

269. YOUSEFI, HASSAN. On modelling, system identification and control of servo-systems with a flexible load. 2007. Diss.

270. QU, HAIYAN. Towards desired crystalline product properties: In-situ monitoring of batch crystallization. 2007. Diss.

271. JUSSILA, IIRO. Omistajuus asiakasomisteisissa osuuskunnissa. 2007. Diss.

272. 5th Workshop on Applications of Wireless Communications. Edited by Jouni Ikonen, Matti Juutilainen and Jari Porras. 2007.

273. 11th NOLAMP Conference in Laser Processing of Materials Lappeenranta, August 20-22, 2007. Ed. by Veli Kujanpää and Antti Salminen. 2007.

274. 3rd JOIN Conference Lappeenranta, August 21-24, 2007. International Conference on Total Welding Management in Industrial Applications. Ed. by Jukka Martikainen. 2007.

275. SOUKKA, RISTO. Applying the principles of life cycle assessment and costing in process modeling to examine profit-making capability. 2007. Diss.

276. TAIPALE, OSSI. Observations on software testing practice. 2007. Diss.

277. SAKSA, JUHA-MATTI. Organisaatiokenttä vai paikallisyhteisö: OP-ryhmän strategiat institutionaalisten ja kilpailullisten paineiden ristitulessa. 2007. Diss.

278. NEDEOGLO, NATALIA. Investigation of interaction between native and impurity defects in ZnSe. 2007. Diss.

279. KÄRKKÄINEN, ANTTI. Dynamic simulations of rotors during drop on retainer bearings. 2007. Diss.

280. KARPOVA, TATJANA. Aqueous photocatalytic oxidation of steroid estrogens. 2007. Diss.

281. SHIPILOVA, OLGA. Particle transport method for convection-diffusion-reaction problems. 2007. Diss.

282. ILONEN, JARMO. Supervised local image feature detection. 2007. Diss.

283. BOTAR-JID, CLAUDIU CRISTIAN. Selective catalytic reduction of nitrogen oxides with ammonia in forced unsteady state reactors. Case based and mathematical model simulation reasoning. 2007. Diss.

284. KINNUNEN, JANNE. Direct-on-line axial flux permanent magnet synchronous generator static and dynamic performance. 2007. Diss.

285. VALTONEN, MIKKO. Performance characteristics of an axial-flux solid-rotor-core induction motor. 2007. Diss.

286. PUNNONEN, PEKKA. Impingement jet cooling of end windings in a high-speed electric machine. 2007. Diss.

287. KÄRRI, TIMO. Timing of capacity change: Models for capital intensive industry. 2007. Diss.

288. TUPPURA, ANNI. Market entry order and competitive advantage of the firm. 2007. Diss.

289. TARKIAINEN, ANSSI. Field sales management control: Towards a multi-level theory. 2007. Diss.

290. HUANG, JUN. Analysis of industrial granular flow applications by using advanced collision models. 2007. Diss.

291. SJÖMAN, ELINA. Purification and fractionation by nanofiltration in dairy and sugar and sweetener industry applications. 2007. Diss.

292. AHO, TUOMO. Electromagnetic design of a solid steel rotor motor for demanding operation environments. 2007. Diss.

293. PURHONEN, HEIKKI. Experimental thermal hydraulic studies on the enhancement of safety of LWRs. 2007. Diss.

294. KENGPOL, ATHAKORN. An evaluation of ICTs investment using decision support systems: Case applications from distributor´s and end user´s perspective group decision. 2007. Diss.

295. LASHKUL, ALEXANDER. Quantum transport phenomena and shallow impurity states in CdSb. 2007. Diss.

296. JASTRZĘBSKI, RAFAŁ PIOTR. Design and implementation of FPGA-based LQ control of active magnetic bearings. 2007. Diss.

297. GRÖNLUND, TANJA. Development of advanced silicon radiation detectors for harsh radiation environment. 2007. Diss.

298. RUOKONEN, MIKA. Market orientation in rapidly internationalizing small companies – evidence from the software industry. 2008. Diss.